UPGRADING SOUTH AUSTRALIAN

LIGNITES BY

HIGH-TEMPERATURE PRE-TREATMENT

A thesis submitted for the degree of

Doctor of Philosophy

by

David John DUNNE B.E.(Hons.)

August, 1988

Department of Chemical Engineering,

The University of Adelaide.

DECLARATION

This thesis contains no material which has been accepted for the award of any other degree or diploma in any University and, to the best of the author's knowledge and belief, the thesis contains no material previously published or written by another person, except where due reference is made in the text or where common knowledge is assumed.

(David J. Dunne)

ACKNOWLEDGEMENTS

My sincere thanks are due to Professor J.B. Agnew for his foresight, guidance and supervision throughout this research project. I also wish thank to Mr. Leigh Francis for his invaluable contribution to this project. Dr. P.K. Agarwal's supervision during Professor Agnew's sabbatical leave is also greatly appreciated.

I wish to acknowledge the financial assistance for this project provided by the University of Adelaide and a grant funded by The State Energy Research Advisory Committee. The award of a Postgraduate Energy Scholarship by the South Australian Department of Mines and Energy is also greatly appreciated. I am grateful to Dr. E. Williams and Mrs A. Hounslow for NMR analysis of coal samples.

Thanks are warmly extended to the workshop, laboratory and department staff for their constant support and friendship throughout this project. I wish to thank Andy Zwahlen and other postgraduate students for their friendship, and the illuminating discussions which were initiated on any subject during tea breaks.

I wish to thank my parents for their support during the course of this study. Finally, I thank my wife for her unfailing love, support and encouragement, even when times became a little difficult.

SUMMARY

Low rank South Australian coals contain substantial amounts of moisture, sodium, chlorine and sulphur. High-temperature pre-treatment is a process which has the potential to reduce these impurities and enhance the value of these coals as sources of fuel. The process uses high temperature and pressure to modify the structure of the coal.

The primary aim of this project was to examine high-temperature, high-pressure pre-treatment of Bowmans coal under controlled conditions in microautoclaves in order to determine the extent of removal of unwanted constituents and to establish the kinetics of water removal and devolatilization. Investigations were also undertaken to shed light on the chemistry and mechanisms of the process.

The results of high temperature pre-treatment experiments on Bowmans coal using microautoclaves are presented. Temperatures of between 250°C and 350°C were studied for residence times up to 1 hour, and the extents of moisture and impurity removal for a coal to water ratio of 1:1 were determined. It was found that up to 80% moisture, 60% of both sodium and chlorine, 50% oxygen and 40% organic sulphur was removed from coal during processing. The reduction of m.a.f coal due to decarboxylation and pyrolysis reactions results in the loss of 33% of the volatile matter as a low calorific value gas, while there is 30% less ash from combustion of dewatered coal. The net energy loss from this process through devolatilization reactions is only about 3%, while there is an increase in energy available for combustion, caused by water removal, of about 8%. The energy required to heat the coal slurry to reaction temperature is about 5% of the energy in raw coal.

IV

The leaching characteristics of coal were examined as an aid to determining mechanisms of mineral matter removal during dewatering. The extents of sodium and chlorine removal during hot water dewatering were comparable to that found during leaching experiments, while magnesium, calcium and sulphate ions appeared to be retained. While 40% of the organic sulphur was removed from the coal during dewatering, only 24% of total sulphur was removed and sulphate sulphur appeared to increase. This may be due to precipitation of magnesium/calcium sulphate during dewatering. The use of methanol as an additive in the slurry to enhance dewatering was not successful, although further work should be performed on fresh Bowmans coal to confirm this result.

In later tests there was a marked reduction in the efficiency of dewatering; this was attributed to oxidation of the coal surface over a long period. It was also found that slower heating to reaction temperature slightly improved dewatering.

The kinetics of devolatilization and water removal were studied using time-temperature equivalence and distributed-activation-energy models. Both models fitted experimental results adequately. The removal of various gaseous species from coal during dewatering was modelled using distributed activation energy kinetics.

Investigations of FT-IR and NMR spectroscopic methods of analysis have been carried out on raw and dewatered coal samples. NMR spectra of Bowmans coal show an unusually low carbon aromaticity which increases following dewatering. A general decrease in carboxyl functional groups as a result of dewatering was observed using both of these methods. Na NMR indicated that there is much less sodium present as sodium chloride in dried coal than expected from extraction analysis and also indicated the presence of an unidentified sodium compound.

The filtration characteristics of dewatered coal slurries showed a marked improvement over untreated coal-water slurries; cloth binding would no longer be a problem.

Analysis of the aqueous effluent from high-temperature dewatering showed that it is a strong organic wastewater, with high dissolved solids content and high sulphide content.

TABLE OF CONTENTS

1. INTRODUCTION

The need to develop South Australian energy resources has heightened interest in utilizing local reserves of poor quality brown coal as sources of fuel. These coals are high in moisture, salt and sulphur content (see Table 1.1) - properties which militate against their use in pulverized-fuel furnaces. It is beyond current technology to utilize the more easily recoverable deposits of South Australian lignites directly in conventional boilers, which would require extensive modification to avoid problems such as slagging, fouling and corrosion. Bowmans coal in particular is very difficult to burn, and has therefore been considered for use in gasification/combined cycle power generation. However, most gasification processes require a low moisture coal, and problems may still occur within the plant as a result of high levels of sodium, sulphur and chlorine. Therefore, the economical reduction of these impurities would greatly enhance the value of South Australian coals as sources of fuel.

Drying by conventional evaporative techniques requires high energy input to vaporize the water, while impurities such as sodium and chlorine remain as the water is removed. Therefore although the moisture content is reduced, problems in utilizing the coal would still exist as all the inorganic impurities remain in the coal. Alternative drying processes, such as "Fleissner", "Evans-Siemon", and "Hot Water" thermal dewatering use chemical and physical changes in the coal structure to remove moisture as well as some of the inorganic

impurities. These processes are more thermally efficient and are better suited to low rank coals than evaporative methods. They leave a product which is substantially reduced in water, sodium, chlorine and oxygen, while partly reducing the sulphur content.

In this project Bowmans coal was subjected to high-temperature pre-treatment in order to remove impurities such as water, sodium, chlorine and sulphur. This pre-treatment process utilitizes the principles of hot water dewatering, a process developed by the University of North Dakota Energy Research Center to produce coal/water slurries suitable for direct combustion.

Hot water dewatering is a process which has potential to upgrade the lignite in simple and economic processing steps (Baria et al., 1983; Paulson and Wiltsee, 1982). In this process the coal is heated as a slurry with water at high pressure to prevent vaporization of the water. The coal structure is chemically modified by the destruction of water-binding functional groups, and water exudes from the coal pores as the coal structure changes. Very little water is reabsorbed on cooling, as the water holding capacity of the coal is permanently reduced. The coal surface changes from hydrophilic to hydrophobic in nature as a result of decarboxylation reactions and the filtering characteristics of the coal are very much improved. Energy can be recovered by countercurrent heat exchange with the feed stream, making the process thermally efficient. Reduction of sodium, sulphate and chlorine ions occurs by water leaching and the thermal cracking of the coal structure removes organic sulphur as hydrogen sulphide.

Although this process has been studied quantitatively, the mechanisms, kinetics and structural changes occurring during the dewatering reaction have yet to be established for Bowmans coal. Problems of rapidly heating and quenching large autoclaves of high thermal mass make them unsatisfactory for carrying out kinetic studies. Therefore the kinetic study of the removal of impurities from coal during dewatering was conducted using microautoclaves.

The objectives of this project were:-

1) To carry out experimental high-temperature pre-treatment investigations on Bowmans Lignite under controlled short residence times in microautoclaves.

2) To examine the extent of water, sodium, chlorine and sulphur removal.

3) To formulate quantitative kinetic expressions for water, sodium, chlorine and sulphur removal.

4) To examine structural changes taking place in coal during treatment.

5) To propose mechanisms for removal of water, sulphur and sodium under the conditions of the experiments.

6) To examine the effects of added solvents (eg. methanol) in improving water removal and upgrading generally.

7) To develop a conceptual design for a continuous processing plant from the results obtained.

TABLE 1.1

Analyses of South Australian Lignites

Deposit	Moisture %	Volatile Matter % d.b.	Fixed Carbon % d.b.	Ash % d.b.	Total Sulphur % d.b.	Chlorine % d.b.	Sodium-in-ash %
Bowmans	56	50	38	12	5.0	1.14	14
Lochiel	61	49	36	15	2.8	-	6
Kingston	53	47	38	15	3.2	0.23	6
Sedan	58	45	34	21	5.5	0.19	3

2. REVIEW OF THERMAL DEWATERING TECHNOLOGY

There have been a number of thermal dewatering processes developed for beneficiating lignite based on the investigations of Fleissner in the 1920's (Fleissner, 1927 and 1928). He demonstrated that water could be removed from coal by heating the coal to moderate temperatures in a saturated steam environment which inhibited the vaporization of water from the coal. The batch process Fleissner developed has been used to upgrade low grade lignite in a number of European countries. This process, steam thermal dewatering, consisted of a number of large reactor vessels operating sequentially, removing moisture from the coal in a saturated steam environment.

Comprehensive studies of steam thermal dewatering were undertaken by the University of North Dakota and the Grand Forks Energy Technology Center since the 1930's by a number of workers. Results of Lavine, Gauger and Mann (1930) showed that North Dakota Lignite was suited for this process, while Cooley and Lavine (1933) found that the use of certain oils in the dewatering process was beneficial to the physical properties of the coal. Extensive studies of steam dewatering various of lignites and subbituminous coals are presented by Harrington, Parry and Koth (1942) and by Oppelt, Ellman and Ongstad (1955). The sorption isotherms of thermally treated coal were reported by Kobe (1957), while the effect of increasing the process pressure to 1500 psig was examined by Oppelt, Kube and Kamps (1959).

In 1944 the first studies were conducted in Australia to upgrade Leigh Creek subbituminous coal using a pilot plant of 80 kg capacity at Osborne, South Australia (Harrison, 1945; Harrod and Milne, 1948; Bainbridge, 1949). It was found that the Fleissner process was technically and economically feasible, and it would overcome problems with fouling of Leigh Creek coal in pulverised fuel boilers.

Work at University of Melbourne in Victoria also began in 1944 to evaluate steam thermal dewatering as a process to beneficiate high moisture Victorian brown coals. Bainbridge and Satchwell (1947) and Eisenklam (1947) reported data on the dewatering characteristics of coal samples from Latrobe and Yallourn seams. The evaluation of Fleissner drying was continued by the State Electricity Commission and the Brown Coal Research Laboratory. Interest was concerned with developing this process to reduce the high salt content in Morwell coal which was causing fouling of boilers. However, most of this work has not been published. Reviews of Steam Dewatering are presented by Allardice (1973) and Stanmore, Baria and Paulson (1982).

Unfortunately batch processing is not as thermally efficient as continuous processing, and much energy is wasted by the Fleissner process in heating and cooling reactor vessels. Work at Melbourne University in the late 1960's showed that a similar quantity of moisture can be removed from the coal by drying in water, oil or an inert gas medium (Evans and Siemon, 1968 and 1970; Murray and Evans, 1972). The Evans-Siemon process (Evans and Siemon, 1971) was developed from this research. An advantage of using a water medium to dewater the coal is that it simplifies the type of equipment required to feed coal to the reactors and greatly improves the energy efficiency. However the coal must be separated from the water before the reaction temperature and pressure are lowered in order to inhibit water reabsorption in the coal.

There has been extensive research into the Evans-Siemon processes by the University of Melbourne and the State Electricity Commission of Victoria. Again much of the research

was not formally reported. A review of the development of the Evans-Siemon process was presented by Higgins and Allardice (1973), while a summary of the SECV studies was presented by Allardice (1976). Studies to dewater South Australian coals using this process have been undertaken by Tuffley (1982).

The Saskatchewen Power Corporation in 1979 undertook an investigation to develop a steam/hot water dewatering process for beneficiating Canadian Coal (Mourits and Kybett, 1980; Szladow, Granatstein and Champagne, 1983). Results from their study were generally favourable, and they were able to produce a coal considerably reduced in sulphur and alkali metals.

In 1983 the University of North Dakota Energy Research Center began studies using water as a dewatering medium to make a coal-water slurry fuel. Initial studies of hot water drying of North Dakota Lignite were performed by Maas (1983) and Joseph (1984). The University of North Dakota Energy Research Center developed a process to dewater coal at temperatures slightly higher than that used in the Evans-Siemon process to produce a coal product able to resist water reabsorption. Hot Water Slurry Dewatering produces a coal-water slurry fuel suitable for combustion (Paulson and Wiltsee, 1982; Baria, Maas and Paulson, 1983). A continuous processing unit (45 kg/hr) was built to solve problems with process operation. The results of dewatering a suite of 15 different low rank coals from various deposits in North America and overseas (including one from Morwell in Australia) were presented by Sears, Baker and Maas (1985).

Other variations of the thermal dewatering process have also been developed. These include the Koppelman process (Phillips, Koppelman and Murray, 1978), the Shell process (Ruyter, van Raam and van der Poel, 1984), the DK process (Kamei, Ono, Komai, Wakabayashi and Itoh, 1985) and the Kaymr Process (Kamyr Inc., 1983a). A number of these processes are described in more detail in the following sections.

2.1   FLEISSNER STEAM THERMAL DEWATERING

The first commercial plant which used this process to upgrade lignite was built in Austria in 1927, and ran successfully until it was closed in the 1960's (Stanmore et al., 1982). It consisted of a number of autoclaves where the coal was treated in a semi-batch cycle. These autoclaves were vertical cylinders 2 m in diameter and were 12 m^3 in capacity. They were capable of treating lump sizes up to 200 mm; coal smaller than 10 mm had to be removed by preliminary screening to prevent high pressure drops in autoclaves.

The autoclaves operated sequentially, using the blowdown from one unit to preheat a fresh charge for another unit. Saturated steam at 13 atmospheres heated the coal to 192°C, and the coal was held at that temperature until thermal dewatering was completed. Blowing the autoclave with air after depressurizing assisted in cooling and helped removal of water.

The initial water removed from the coal in this process as a liquid was 40% at 192°C, although further water was removed during depressurization by blowing with air. Typical residual water in the lignite was 10% to 20%.

A typical heating cycle was (Bainbridge, 1949):-

Process	Time (mins)
Filling and closing	5
Preheating	20
Steaming	60-80
Depressurization	20
Air blowing	20-40
Emptying	15
Total cycle time	140-180

A number of process schemes have been developed from this process to make the operation continuous. These are based on using lock hoppers and two-stage reactor systems, and generally are not envisaged with an air blowing cycle. The air blowing cycle introduces inefficiencies into the system as the sensible heat of the coal is used to evaporate the moisture from the coal. The temperatures of operating modern dewatering reactors have been increased to 250°C, which results in the same amount of water being removed as can be achieved by air blowing the coal.

2.2 EVANS-SIEMON THERMAL DEWATERING

The Evans-Siemon process is a more recent development from the University of Melbourne in the 1960's, and utilizes a liquid medium instead of saturated steam to dewater the coal. The coal must be separated from the water before cooling and depressurization to prevent water reabsorption. Using a liquid medium greatly increases the efficiency of

the process over the Fleissner process, as heat can be easily recovered. The initial concept proposed the use of screw extruders to feed the coal to the reactor vessel (Evans and Siemon, 1968), although further development by Davy McKee Pacific have modified the reactor vessel to feed coal via lock hoppers in a suspension with water. The current status of the Evans-Siemon process is described in a report by Davy McKee Pacfic (1984).

The Evans-Siemon process is a semi-continuous process which uses lock hoppers to feed and remove the coal from the reactors. Coal of particle size greater than 6 mm must be used as the reactor feed so that separation of the coal and water is less of a problem. If small coal particle sizes are used, the filtration equipment (eg centrifuges or belt filters) would need to be completely encased to withstand the high pressure of the process. This would make the cost of such a plant prohibitive.

The reactor vessel is a water-filled, narrow vertical vessel built to facilitate heat transfer between descending coal and a rising steam water mixture. High pressure steam at 40-86 bar, 250-300°C, is injected to heat the vessel, and cold water is withdrawn from the top. The coal of 40 mm to 6 mm is fed via lock hoppers in a water suspension to the reactor, while coal is separated from waste water in discharge lock hoppers. The waste water is flashed and used to preheat the coal feed.

The final moisture content of the coal is claimed to be between 20-23%. Drying efficiency may be lower than expected due to natural convection occurring inside the reaction vessel (Stanmore et al., 1982).

2.3 KOPPELMAN STEAM THERMAL DEWATERING

The Koppelman process has been developed to beneficiate lignite, wood or peat, and is claimed to produce a product with little moisture and a heating value of 28 MJ/kg (Phillips,

Koppelman and Murray, 1978; Chemical Engineering, 1978; Parkinson, 1978). In this continuous process, coal is fed to the reactor as a slurry and steam is used as the drying medium. The coal is pumped in 25 mm lumps into the cool end of the 100 atm reactor, and a temperature of about 540°C is reached near the discharge end through counter-current heat exchange. Residence time in the reactor is 10 mins. The coal is discharged at 320°C through lock hoppers to a water cooling system which cools the coal to 65-70°C. The commercial size reactor for 50,000 ton/year plant would measure 400 mm in diameter and would be 10 m long.

The process is claimed to be 90-92% efficient, and would utilize the energy obtained from the recovery of gases driven off in the reaction. As the final reactor temperature is 540°C, the coal would be substantially pyrolysed (Stanmore et al., 1982). Therefore the coal product may not be satisfactory for some purposes.

2.4 KAMYR HOT WATER DEWATERING

This process has been proposed by Kamyr Inc. to utilize the principles employed to dewater pulp and paper in industry (Kamyr Inc., 1983a) These principles are very similar to the thermal dewatering of coal, and the process would require little adaptation to coal dewatering. The advantage with the process is that most of the equipment required has already been proven by the paper industry.

The process would use continuous rotary lock chambers to transfer low pressure coal slurry to high pressure and using high pressure water (Kamyr Inc., 1983b). The temperature of processing is 260°C at pressures of about 50 bar. The coal is fed to the dehydrator at this temperature, and exits the vessel at 137°C. The heat is recovered from the product stream, and is used to preheat the feed in the heat exchange vessel. The coal particle size used is less than 25 mm, and the product moisture is claimed to be 20-23%.

2.5 HOT WATER DEWATERING (UNDERC)

Hot water dewatering utilizes higher temperatures than the Evans-Siemon process to produce a coal slurry product able to resist water reabsorption (Baria et al., 1983; Paulson and Wiltsee, 1982). The coal is dewatered in a water medium, and is pressurized and fed to the reactors by using slurry pumps instead of lock hoppers. Because the coal is pumped to high pressure as a slurry a small particle size is required. The product from this process may be a slurry for pipeline transportation and used as a coal-water fuel, or it may be filtered to use as a dry coal feed. The conceptual design of this plant is shown in figure 2.1.

A slurry of 30% solids is first pumped to a pressure above saturation pressure at the process temperature. The coal passes through a counter-current heat exchanger and is then heated in the reactor vessel to about 320°C for about 5 to 10 mins. The product slurry is cooled by counter-current heat exchange with the feed stream, and lowered in pressure without flashing. The slurry is then filtered and the dry coal recovered for combustion, or concentrated for pipeline transport and combusted as a slurry fuel. Coal size in the feed would be less than 150 μm to produce a stable and homogeneous slurry product.

A process scheme and process demonstration unit have been developed by the University of North Dakota to utilize this technology (Sears et al., 1985).

The North Dakota process has been developed primarily to produce coal-water fuel slurries for combustion or pipeline transport. Therefore a fine coal particle size will ensure that there is a homogeneous and stable suspension of coal and water. However, it is unlikely that utilizing a coal-water slurry made from Bowmans coal would be possible, as the dewatered product liquor contains many impurities which would have to be removed before combustion. Therefore the basic concepts of Hot Water Dewatering will need to be modified to produce a dry coal product suitable for gasification or direct combustion.

To produce a dry coal product a coal-water filtration stage must be included in the process scheme. If larger particle sizes of up to about 4mm could be used in a processing plant it would mean coal pre-treatment and filtering stages would be of more basic design. The size of coal particle used in the process is constrained by the kinetics of impurity removal and method of feeding the slurry to the reactor.

While this process is essentially similar to the Evans-Siemon process, it differs fundamentally in the coal-water separation stage. In the Evans-Siemon process the coal must be separated from the water environment at the processing temperature and pressure to retard water reabsorption as the temperature is lowered. As Hot Water Dewatering produces a product which is able to resist water reabsorption by using slightly higher processing temperatures, coal-water separation can be carried out after the coal has been cooled and the pressure reduced.
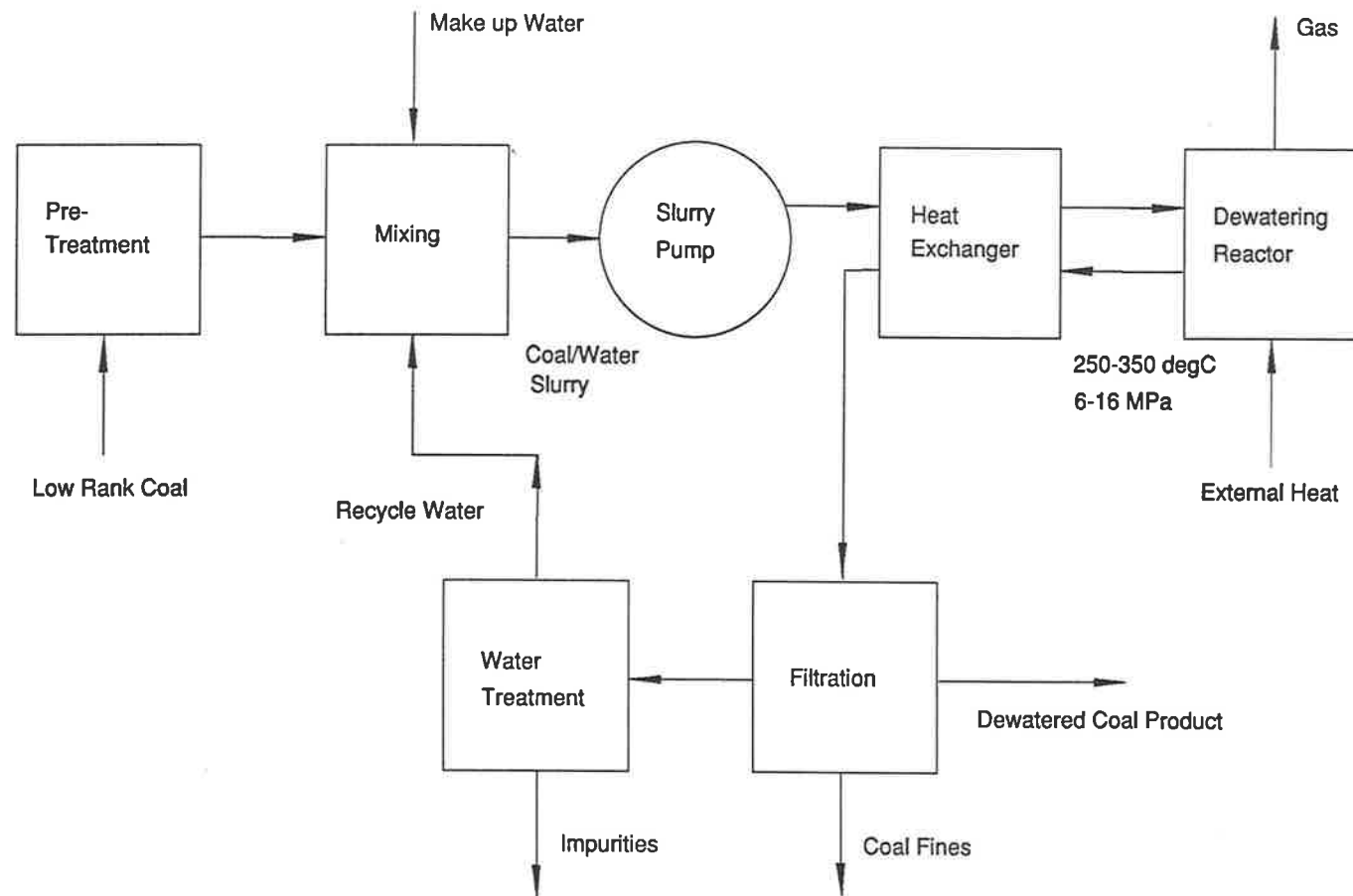
Figure 2.1   Hot Water Dewatering Process

3.   EXPERIMENTAL SYSTEM

To establish the kinetics of the dewatering reaction a method of rapidly heating and quenching a slurry of coal and water under high pressure must be used. Work in the past used large, slow heating autoclaves of high thermal mass, which proved inadequate for carrying out kinetic studies. A technique developed by Exxon (Maa, Neavel and Vernon, 1984) to carry out coal liquefaction studies used microautoclaves or tube bombs to replace these large autoclaves. Although these tube bombs use a small sample size, they show excellent characterization of liquefaction reactions.

In this study, the design of the microautoclaves used in the liquefaction studies was slightly modified and used to characterise the high-temperature pre-treatment reaction. The tube bomb setup requires a heated fluidized sand bath for heating the tube bombs to reaction temperature, and water bath to rapidly quench the tube bombs and stop the reaction. It also requires a peripheral gas charging system and tube bomb volume measuring apparatus.

The design of the tube bombs which were used in these tests is shown in figure 3.1. These bombs were constructed of 316 stainless steel tubing and swagelok tube fittings. The main reactor is made from 3/4 inch, 14 gauge stainless steel tube. It has a swagelok end cap at one end, and a reducing union connected to a stem of 1/4 inch, 20 gauge tube at the other. These fittings can be removed to allow charging and removing the reactants. The long stem

minimizes heat conduction to a pressure transducer which is placed on a fitting on top of the stem. A sheathed 1mm diameter chromel-alumel (type K) thermocouple passes through the stem and extends half way into the reactor tube. The thermocouple and a pressure transducer (0-5000psig) are attached to a chart recorder.

The microautoclave test facility is shown in figure 3.2. This system contains a heated fluidized sand bath used to quickly heat the tube bombs to reaction temperature, and a water bath to quench the bombs and stop the reaction. A lever mechanism can move the bombs between the sand bath and the water bath. Two bombs were used in each test, and were agitated at a frequency of about 100 cycles per minute during the test by a double acting air cylinder coupled with a variable impulse generator. The stroke of the air cylinder was about 2cm. The temperature of the fluidized sand bath was controlled by a simple PID controller connected to a K type thermocouple inserted at the bottom of the bath. A temperature probe was used to check the temperature throughout the depth of the sand bath before each test. There was generally a 1 degree gradient through from the top to the bottom of the sand bath. The top of the sand bath was extended, and connected to an air exhaust system to prevent entrained sand from spreading about the laboratory.

The tube bomb was first filled with a coal water mixture and pre-pressurized using an inert gas, nitrogen. It was then lowered into the fluidized sand bath held at reaction temperature, and agitated for the required time. As the temperature increases within the tube bomb, the coal water mixture expands and autogenously builds up the necessary reaction pressure. A chart recorder was used to record the pressure and temperature of one of the tube bombs used in the experiment.

When the microautoclave was then removed from the sand bath it was immediately quenched in the water bath. Pressure was then released, and the reaction products removed for analysis. The kinetic rate data was obtained for moisture and impurity reduction at various reaction temperatures and residence times. Analysis of the product liquor and gas

was performed using atomic absorption spectrometry and gas chromatography respectively. Proximate and ash analysis of the product coal was performed in the Chemical Engineering Department, while ultimate and sulphur analysis was done by the AMDEL laboratories.

Peripheral equipment for gas charging and finding the internal volume of the tube bombs are shown in figures 3.2 and 3.3. The gas charging system was also used for calibrating the tube bomb pressure transducers, and discharging the product gas through activated carbon to remove the pungent hydrogen sulphide odour. It consisted of a nitrogen cylinder attached to a high pressure regulator, which was used to fill the bombs with high purity nitrogen. The 0-2000psi pressure gauge was used to calibrate the pressure transducers and to ensure that the bombs were filled to the correct initial pressure of nitrogen.

The volume of the tube bombs was required to calculate the quantity of coal and water which can be loaded on the tube bomb. As the pressure is created autogenously, this volume is needed so that over or under pre-pressurization of tube bombs will not occur. The volume was measured by pressurizing the tube bomb with air to 200 kPa, and then discharging the gas to atmospheric pressure through an Orsat apparatus measuring burette. The volume displaced in the burette is proportional to the internal volume of the bomb. Approximate internal volumes of the tube bombs are 50 ml.

Thermocouple
Type K

Needle
Valve

Quick
Connect

Pressure
Transducer
0-5000 psig

STEM
1/4" 316 SS
Tube

300mm

3/4" to 1/4"
Reducing Union

REACTOR
3/4" 316 SS
Tube

200mm

3/4" End Cap
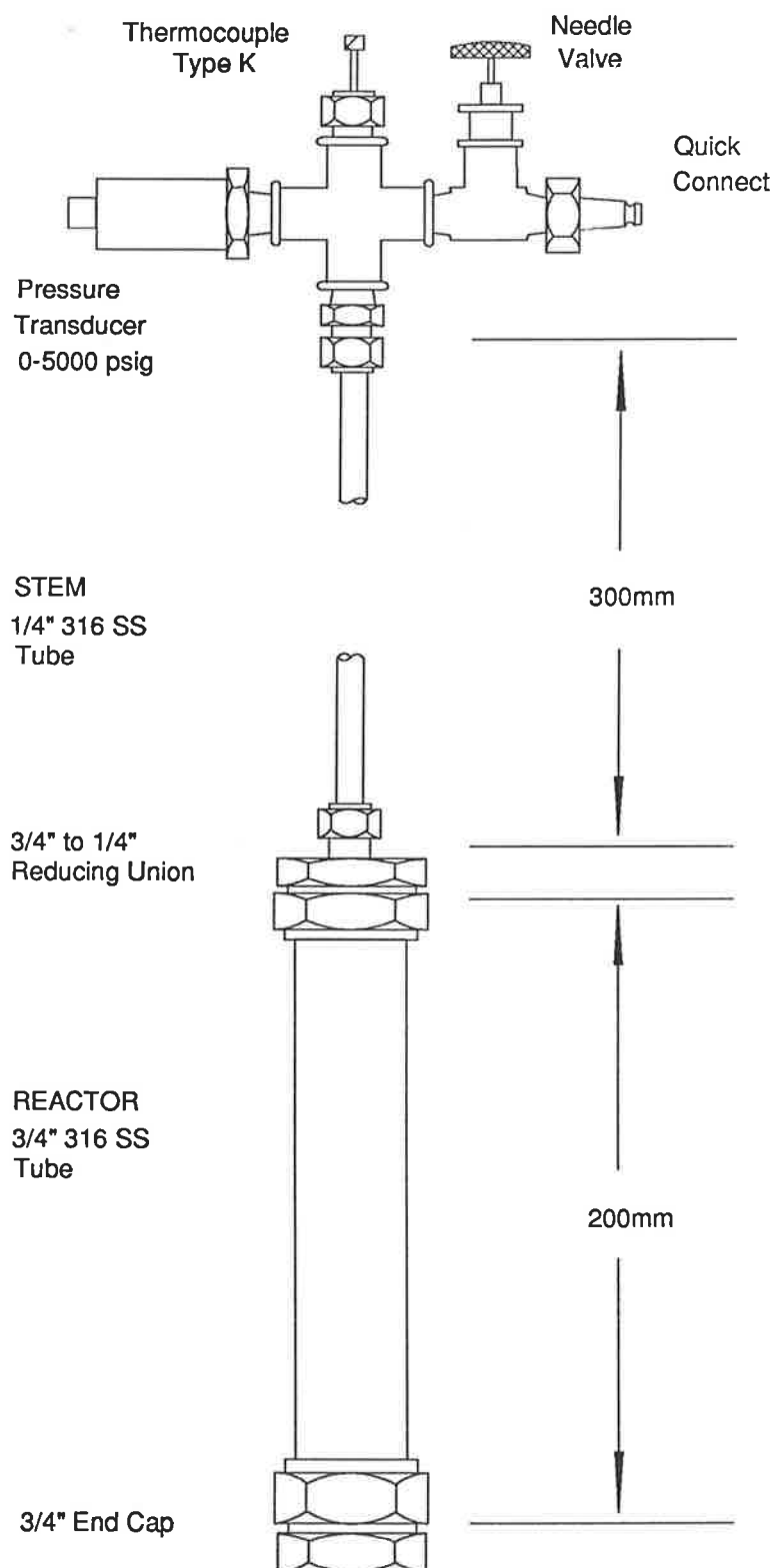
Figure 3.1   Microautoclave or Tube Bomb
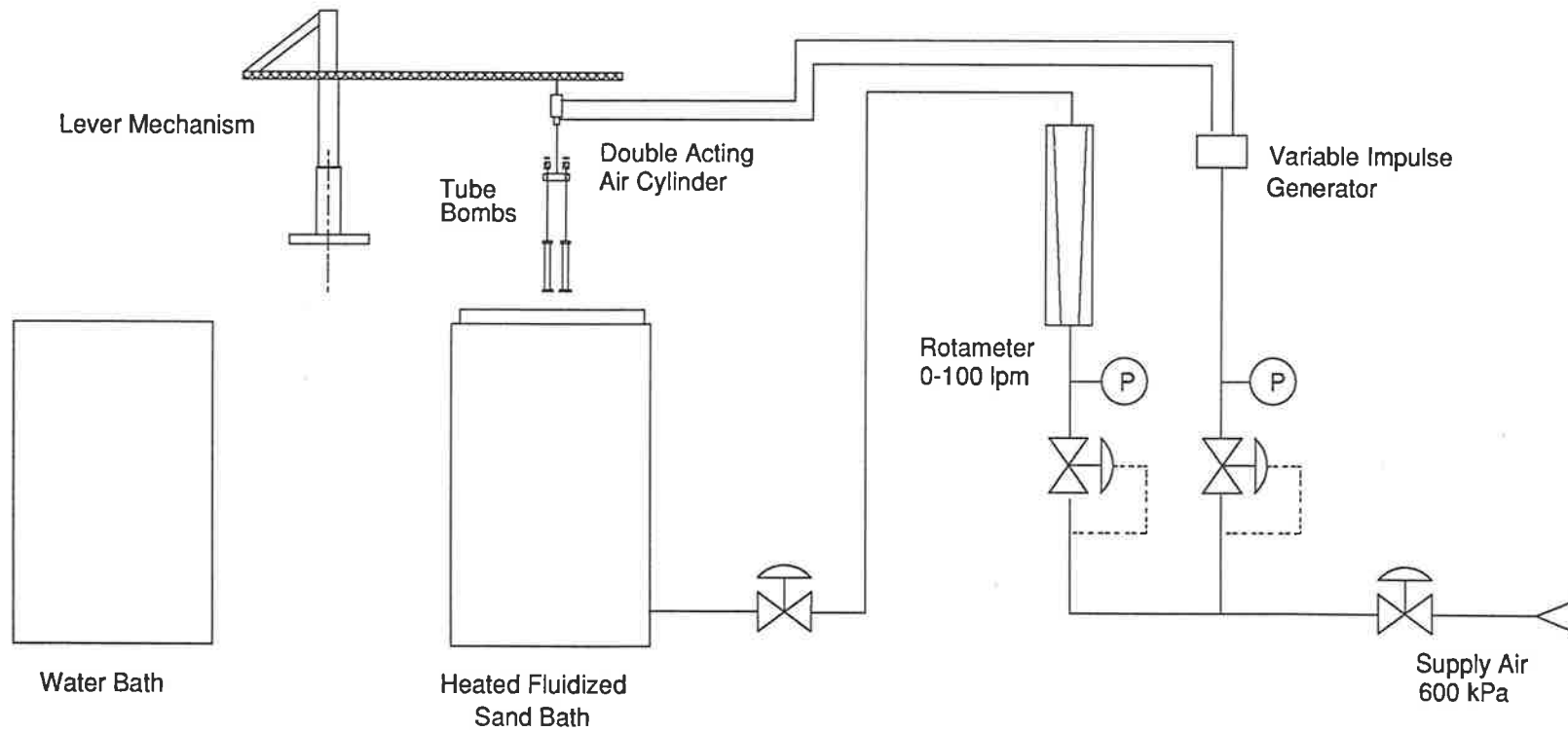
Figure 3.2   Experimental System
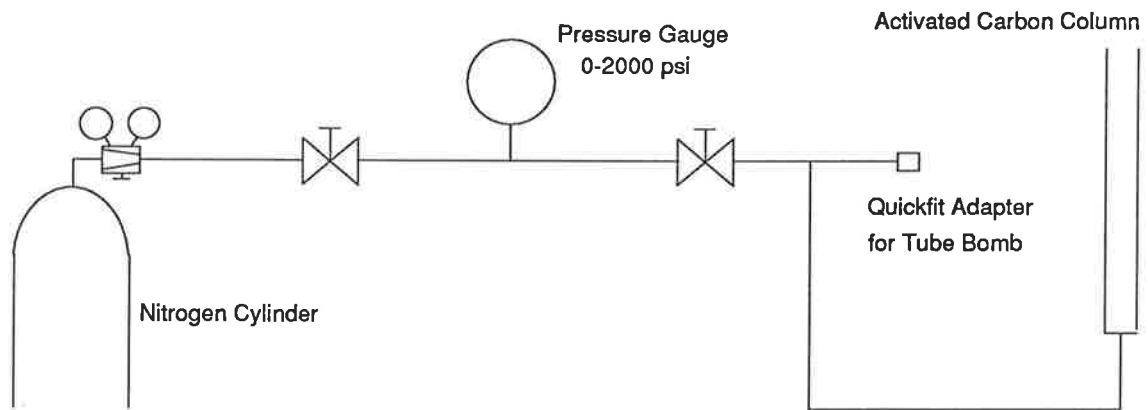
Figure 3.3   Gas Charging and Venting System
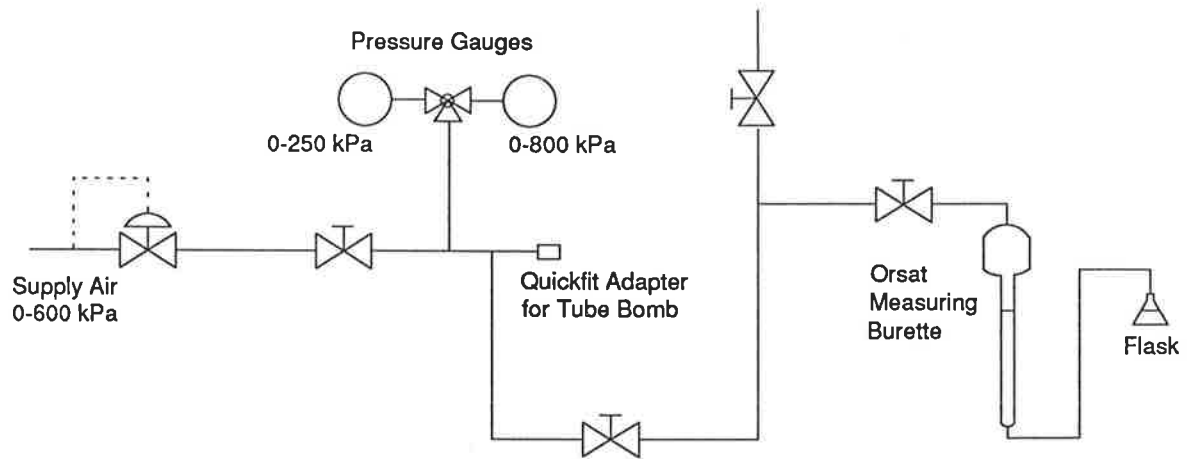
Figure 3.4   Volume Measuring Equipment

4. EXPERIMENTAL PROCEDURE

4.1   USE OF THE TUBE BOMB REACTOR

Before the tube bombs are used for an experiment they must first be examined to ensure they will hold the necessary reaction pressure. They are checked for possible wear and leaks by assembling and pressure testing with nitrogen to about 6 MPa. A soap solution is used around the Swagelok fittings to ensure that they are not leaking. If the tube bomb does not leak the reducing union is removed and the bomb prepared for dewatering experiments. The tube bombs generally require replacement after 6 tests.

The coal used in this study was crushed to less than 4mm in size, and stored in large plastic bags sealed in a 200 litre drum. When required for each series of experiments, the coal was removed from this store and sieved to the size fraction required. It was then placed in plastic bags to prevent moisture removal, and used when necessary. A number of dewatering experiments were performed using coal specially mixed, riffled and split into discrete samples. This did not appear to make any difference to results obtained in the experiments, and, as it would have further dried the coal by the exposure to air, it was not done for most dewatering experiments. In the kinetic experiments a quantity of coal from the drum was crushed to less than 1mm in size to ensure the coal used was representative of the whole sample.

Two tube bombs were used for each test. Each bomb used was filled with 15 grams of coal and an equal quantity of distilled water. After filling the tube bombs the slurry was stirred to ensure complete mixing and the reducing union replaced. The bomb was then purged and pre-pressurized with nitrogen to 4 MPa. The high pressure ensures that the

reaction temperature is reached without evaporating the water inside the bomb. The tube bomb was then left before each experiment for 30 minutes to allow most of the ions to leach from the coal (see Chapter 8). This will minimize the effect soluble ion removal may have on the extent of dewatering.

When ready the bomb was clamped to a holder attached to the double acting air cylinder and connected to the thermocouple and pressure transducer leads. It is then lowered into the heated fluidized sand bath which was controlled to reaction temperature +/- 1°C. The tube bomb was vibrated at a rate of about 100 cycles/minute so that some mixing occurred during the dewatering reaction. Although two bombs could be loaded into the sand bath for each test, only one could be connected to the chart recorder. The temperature and pressure of each bomb was seen as an electrical signal output. After the test was completed the bomb was quickly removed and lowered in the water bath to quench and stop the dewatering reaction.

After the tube bomb cooled, it was removed from the water and the gas was released in a fume hood or into the activated carbon column. Some of the gas was collected in air tight gas syringes for analysis using Gas Chromatography. The reducing union was then removed and the reaction mixture poured into a Buchner funnel. The liquor separated from the coal was collected for analysis, after which the coal adhering to the sides of the bomb was collected by rinsing with distilled water.

The moisture-holding capacity of coal is often reported as the moisture content of coal in equilibrium with a relative humidity of 96% at 30°C. This would not realistically be a measure of the residual moisture in a dewatering plant designed for Bowmans coal, as the coal would need to be filtered to remove the water before further treatment. Therefore an alternative method was used to determine the residual moisture content of dewatered coal. Moisture content was determined by filtering the coal slurry on the Buchner funnel until the bulk water was no longer discernable on the coal surface, and then allowing a further

minute for bulk water to drain from the coal. While this method is dependent on the operator technique and the filtration characteristics of the coal, the results from these determinations are more meaningful for the design of a continuous processing plant.

The product coal which was recovered from the Buchner funnel was stored in plastic bags until analysed for moisture, volatile matter, fixed carbon, ash and equilibrium moisture content.

4.2   PROXIMATE ANALYSIS

The proximate analysis method used in these tests varied slightly, although not significantly, from the Australian Standard Method 2434. This was because of the equipment available and the small sample size used. The moisture content of coal was determined by placing about 3 grams of sample into a nitrogen oven and heated to a temperature of $107^{O}C$ until the coal reached constant weight (generally 3-4 hours). High purity nitrogen was vented through the oven at a rate sufficient to change the atmosphere about 30 times per hour. The dried coal was then removed from the oven. The coal sample was placed in a desiccator for it to reach ambient temperature before weighing.

The quantity of volatile matter in the coal was determined by pyrolysing nitrogen-dried coal at high temperatures. For each determination about 2 grams of coal was put into a silica crucible, over which a lid was placed to prevent coal oxidizing on contact with air. Up to 9 crucibles could be used in each test. The crucibles were transferred to a nitrogen purged furnace which was heated to $950^{O}C$. After 7 minutes the crucibles were removed and placed in a desiccator to cool before they were weighed.

The ash content of coal was determined by removing the lids from these crucibles, and placing the devolatilized coal samples in a furnace held at a temperature of $750^{O}C$. Oxygen

was passed through the furnace to assist in oxidizing the coal and combusting the fixed carbon. Coal was removed when no further weight loss was recorded (generally about 4 hours).

4.3 EQUILIBRIUM MOISTURE

The equilibrium moisture content of the coal at 96-97% relative humidity was determined according to the ASTM D-1412 method. For each determination about 3 grams of dewatered coal was placed in a sample bottle and put into a desiccator. The humidity in the desiccator was attained by using a saturated potassium sulphate solution and evacuating the desiccator to about 3 kPa. To keep the desiccator at a constant temperature it was placed in a water bath and held at $30^{\circ}C$ for 3 days. It was then removed the bath, and the sample bottles were carefully removed. Samples were dried in a nitrogen oven at $107^{\circ}C$ for 3 hours to obtain the coal moisture content. During the tests it was found that droplets of condensate fell from the lid of the desiccator. A fluted filter paper was inverted and placed over the top of the sample bottles to prevent droplets from falling on the coal and interfering with results.

4.4 LIQUOR ANALYSIS

Flame Atomic Absorption Spectroscopy was used to analyse for sodium, magnesium, calcium, potassium and iron in the product liquor. A single beam Varian Atomic Absorption Spectrophotometer, model AA-1275, was used for the analysis. An air-acetylene flame was used for sodium and potassium ions, while a nitrous oxide-acetylene flame was used for the other ions. Care was taken to minimize interferences.

The chlorine content of the product liquor was determined using the standard Mohr titration method. As the liquor tended to darken as it aged, the analysis had to be performed soon after the dewatering test was completed, as the dark colour of the liquor made determination of the titration end point difficult.

A number of techniques were used to analyse sulphate in the product liquor with varying success. A gravimetric method, ASTM D-516 method A, appeared to give the best results. This analysis was performed as soon as possible after completion of dewatering to prevent a black precipitate, which formed in the liquor on contact with air, from interfering with results.

4.5   GAS ANALYSIS

A Shimadzu GC-4A Gas Chromatograph was used to analyse the product gas for carbon dioxide, carbon monoxide, hydrogen sulphide, methane and light hydrocarbon gases up to propene. The output signal was connected to a Varian 4290 integrator to calculate peak areas of the gases. The thermal conductivity detector of the gas chromatograph was used as some of these gases are difficult to detect using a flame ionization detector.

Two columns were used for each analysis. They were an 80/100 mesh carbosphere column of 3mm diameter and 2m in length, and a porapack Q column of 3mm diameter and 1m length. Helium was used as the carrier gas, and a flow rate of 20 ml/min was used in both columns. Temperature of the oven was $70^{\circ}C$, while temperature of the thermal conductivity detector was $80^{\circ}C$. The carbosphere column was able to separate the permanent gases and methane (N_2, CO_2, CO and CH_4), while the porapack Q column separated mainly hydrogen sulphide and the light hydrocarbons. Nitrogen was used as an internal standard.

5 RESULTS AND DISCUSSION

5.1 INTRODUCTION

Various experiments were performed on Bowmans coal to determine its dewatering characteristics for the design of a processing plant. These included an initial study to determine the effect of increasing processing temperature, and a more comprehensive study to obtain kinetic data used to model the dewatering reaction. Results from the initial studies include the proximate analysis of dewatered coal, as well as ultimate, sulphur and ash analysis of dewatered coal. Comprehensive studies of impurity removal using Atomic Absorption Spectrometry and Gas Chromatography, as well as the proximate analysis and the equilibrium moisture contents of the coal were performed on the series of kinetic experiments.

While most of the experiments were performed to gain kinetic information, a number of experiments were undertaken to study various characteristics of high-temperature pre-treatment. These experiments also ensured that the experimental system used did not influence the experimental results. The effect mixing within the tube bombs may have upon the dewatering characteristics was studied by loading various amounts of coal in the tube bombs. The rate of heating a coal/water slurry and the effect of particle size on dewatering was also studied. The effect of adding methanol to the slurry to enhance the dewatering ability of coal was also investigated.

Experiments were undertaken to determine the ratio of water and carbon dioxide formed by the breakdown of carboxylate groups during dewatering. This result was required for use in the kinetic study of this process to calculate quantities of gaseous components removed from the coal.

The thermal efficiency of the high-temperature pre-treatment of Bowmans coal and the net energy available for combustion were calculated from the calorific value of raw and dewatered coal. An eight week study on the long term moisture reabsorption characteristics of dewatered coal is also reported. The effectiveness of dewatering as the coal aged is discussed.

5.2 THE EFFECT OF TEMPERATURE

Initial tests were undertaken to study the extent of impurity removal from Bowmans coal for dewatering temperatures between 250°C and 350°C. These results formed the basis for a CHEMECA conference paper presented in Perth in 1985 (Dunne, 1985). These experiments were the first series of results obtained for dewatering Bowmans coal, and it was found that the product coal showed a much lower residual moisture content than observed in later tests. It was observed over the period of this study that the effectiveness of dewatering appeared to decrease with the age of the coal. The possible reasons for this are discussed in a later section.

For this series of tests coal of particle size less than 495 μm in diameter was heated for 20 minutes in the tube bombs to temperatures of 250, 275, 300, 325 and 350°C. The results of the proximate analysis of the raw and dewatered coal are shown in table 5.1. Ultimate and sulphur analysis of the coal were performed at AMDEL, and these results are shown in table 5.2. The quantity of various components removed from the coal during

dewatering are shown in tables 5.3 and 5.4. The ash analyses of raw and dewatered coal are shown in table 5.5, while the percentages of soluble ions removed from the coal in the wastewater are reported in table 5.6.

The dewatered coal physically appeared much different from the raw coal. It was slightly brown in colour and seemed to be lightly bonded together when removed from the bomb. Some of the coal particles appeared plastically deformed and bloated, while other particles stuck to the sides of the tube bombs and proved difficult to remove. Plastic deformation and bloating of coal particles during thermal treatment has also been found to occur during steam dewatering of North Dakota lignite at high temperatures (Oppelt, Kube and Kamps, 1959).

The filtration characteristics of the dewatered coal were very much improved compared with raw coal. The product gas smelt strongly of hydrogen sulphide, and the product liquor was yellow in colour and frothed when the tube bombs were first opened. Deposited in discrete lumps throughout the dewatered coal was a red substance which was shown to be organic in origin by simple chemical analysis. This compound darkened and became very hard after contact with air. A flaky off-white compound was also deposited throughout the dewatered coal product and was tentatively identified by SEM analysis performed by the South Australian Institute of Technology as a form of calcium/magnesium sulphate.

As it was difficult to recover all the products of the dewatering reaction from the tube bombs, the removal of various components from the coal were calculated using a mass balance of the proximate analysis of the raw and dewatered coal. Two assumptions were made in this mass balance. They were:-

(1) fixed carbon remained constant throughout dewatering.

(2) that there was no loss of inorganic matter during proximate analysis of volatile matter in coal.

The first assumption can be justified by considering the definition of fixed carbon; the quantity of coal which remains after devolatilization in an inert atmosphere at temperatures of 950°C. During high-temperature pre-treatment the coal is in an inert environment (as it is slurried in water), and the temperatures used are less severe. Therefore unless water leaches fixed carbon or products of the dewatering reaction it is unlikely that fixed carbon is removed from the coal.

While assumption two is not strictly valid as it is likely that some inorganic matter will be volatilized during the proximate analysis of coal, it was assumed that this loss would be minimal and would not affect the mass balance to a large extent.

From tables 5.1 and 5.3 it can be seen that the total moisture in the coal following dewatering has dropped from 51.7% to between 40 to 20.6%, which corresponds to a 40-80% decrease in water based on the initial moisture content of raw dry coal.

There has also been a decrease in coal volatile matter, due to the destruction of oxygenated hydrophilic functional groups. Although up to 30% of the coal is lost through devolatilization reactions, the compounds removed are heavily oxygenated and have little calorific value. The removal of these functional groups greatly enhances the filtering characteristics of the coal (see Chapter 9).

From table 5.2 it can be seen that there is a general increase in carbon content in the coal. On a moisture-and-ash-free basis the carbon content has increased from 62.3% to 72.1%. Therefore other components in the coal are removed in a greater ratio than carbon. The percentage of hydrogen and total sulphur in the coal have changed little from raw to dewatered coal, although there is a general decrease in these elements due to devolatilization

of the coal. In table 5.3 it can be seen that sulphur and hydrogen are removed in approximately the same percentage as total dry coal, whereas oxygen is removed in much higher proportion.

Table 5.2 also shows that the atomic H/C ratio decreases during dewatering. This indicates that condensation is occurring in the aliphatic structure of the coal, probably caused by cleavage of oxygenated functional groups such as ethers. Hydrogen is removed from the coal as water (due to carboxyl group breakdown), hydrogen sulphide gas, light hydrocarbon gases and as organics in the wastewater.

The results showing the percentage of various sulphur groups removed from raw coal are presented in table 5.4. Up to 45% of the organic sulphur and 24% of the total sulphur is removed. Therefore, while overall sulphur reduction is in proportion to the removal of volatile matter in total dry coal during dewatering, the removal of organic sulphur is in higher proportion. It can be deduced that most, or possibly all of the organic sulphur in the coal is present in the coal volatile matter, as organic sulphur groups are being destroyed in a higher ratio than the general breakdown of the coal. The sulphur would be removed as hydrogen sulphide gas, or in the liquor as a sulphate ion.

While the quantity of organic sulphur is decreasing in dewatered coal, the amount of sulphate sulphur and pyritic sulphur are increasing. The increase in pyritic sulphur would probably have little effect on the chemical properties of the coal as it is in minor quantity. However it is obvious that there is a reaction taking place which causes pyritic sulphur to form, probably through the reverse reaction between hydrogen sulphide and iron. The increase in sulphate in the coal is likely due to a precipitation of a non-soluble sulphate compound in the coal during dewatering. This would inhibit the leaching of this ion from the coal.

Table 5.5 shows the ash analysis of coal. It must be noted that the quantity of sulphate in the ash is not reported in this analysis, therefore the percentages of elements in the ash are higher than would be expected from a full analysis. Also as the coal:water ratio used was only 1:1, it would be expected that more of these elements would be removed if the coal to water ratio is increased. Up to 30% of the ash is removed during dewatering at a 1:1 coal:water ratio. The ash analysis shows that the percentage of sodium in the ash has decreased from about 20% to between 2-6%. This indicates the coal is probably suitable for conventional combustion without major fouling problems.

The percentage of soluble ions removed from the coal in the product wastewater is shown in table 5.6. It can be seen that the main constituents removed from the coal during dewatering are sodium, chlorine, calcium and magnesium. Up to 60% of the soluble sodium and chlorine is removed from the coal for a coal:water ratio of 1:1. For most of these elements there appears to be a general increase in the quantity removed from the coal as the temperature increases. However magnesium removal decreases as temperature increases, which suggests that there is a reaction which occurs during dewatering that suppresses the removal of magnesium. This is probably the formation of a form of magnesium sulphate.

A series of plots showing the percentage removal of various impurities as a function of reaction temperature are shown in figures 5.1 to 5.8. All of these figures show that the extent of impurity removal increases with temperature except the plot for magnesium ion removal. Also, most of these plots appear to be straight lines, showing a linear relationship for impurity removal with temperature. However, the rate of volatile matter and sulphur removal appears to decrease as temperature increases. This trend was not expected for volatile matter removal, and is not apparent in latter kinetic studies. The rate change of sulphur removal with temperature, however, may be due to the fixation of sulphur compounds in the coal during treatment.

TABLE 5.1

Proximate Analysis of Raw and Dewatered Coal

Coal Particle Size   0.0 - 495 μm

Coal Water Ratio   1:1

Reaction Time   20 mins

	Weight Percent %					
	Raw Coal	Processing Temperature				
		250°C	275°C	300°C	325°C	350°C
Moisture (wet basis)	51.7	39.7	35.1	31.0	28.0	20.6
Volatile Matter d.b.*	52.4	52.2	47.1	45.8	44.0	44.6
Fixed carbon d.b.	35.6	38.5	42.6	44.3	45.3	45.5
Ash d.b.	12.0	9.3	10.3	9.9	10.7	9.9

*d.b. = dry basis

TABLE 5.2

Ultimate and Sulphur Analysis of Raw and Dewatered Coal

	Weight Percent %					
	Raw Coal	Processing Temperature				
		250°C	275°C	300°C	325°C	350°C
Carbon daf*	62.3	64.3	65.7	67.6	69.7	72.1
Hydrogen daf	5.4	5.2	5.3	5.2	5.3	5.1
Nitrogen daf	1.6	0.9	2.0	1.5	1.0	1.5
Total Sulphur daf	5.9	5.5	5.6	5.7	5.8	5.6
Oxygen daf by difference	24.8	24.1	21.4	20.0	18.2	15.7
Atomic H/C Ratio	1.04	0.98	0.97	0.93	0.92	0.85
Pyritic Sulphur daf	0.05	0.06	0.08	0.09	0.17	0.19
Sulphate Sulphur daf	1.86	1.91	2.18	2.59	2.87	2.46
Organic Sulphur daf	4.00	3.53	3.38	2.99	2.73	2.97

*daf = dry ash free coal

TABLE 5.3

Removal of Coal Constituents Based on 100 units of Dry Raw Coal

	Weight % in Raw Coal d.b.	% Removed at				
		250°C	275°C	300°C	325°C	350°C
Total Dry Coal	100.0	7.8	16.4	21.1	21.4	21.6
Moisture	107.3	43.4	58.0	66.9	71.5	81.1
VolatileMatter	52.4	8.3	24.9	32.2	34.0	33.3
Ash	12.0	28.6	28.3	34.8	29.9	34.7
Carbon	54.8	1.9	10.2	12.3	10.8	7.1
Hydrogen	4.7	7.8	16.4	21.9	21.5	24.0
Nitrogen	1.3	37.7	-	24.6	47.8	25.4
Oxygen	21.9	7.9	26.5	34.8	41.5	49.3
Sulphur	5.2	11.7	18.9	22.5	22.1	23.9
Atomic O/C Ratio		3.0	2.0	2.1	2.8	5.2

TABLE 5.4

Removal of Sulphur Compounds Based on 100 units of Dry Raw Coal

	Weight % in Raw Coal d.b.	% Removed at				
		250°C	275°C	300°C	325°C	350°C
Sulphur Total	5.2	11.7	18.9	22.5	22.1	23.9
Pyritic	0.04	-15.0*	-46.2*	-57.5*	-195.6*	-233.2*
Sulphate	1.64	2.7	0.6	-12.2*	-22.6*	-5.7*
Organic	3.52	16.2	28.1	39.7	45.5	40.5

* = % of Constituent increased after Dewatering

TABLE 5.5

Ash Analysis of Raw and Dewatered Coal

	Weight Percent %					
	Raw Coal	Processing Temperature				
		250°C	275°C	300°C	325°C	350°C
SiO_2	38.4	43.0	43.8	39.8	41.7	36.9
Al_2O_3	2.8	3.9	4.3	4.8	5.2	3.4
Fe_2O_3	15.0	20.9	22.6	25.4	22.3	19.4
CaO	6.9	8.7	6.8	8.1	8.2	8.2
MgO	16.5	15.8	20.4	17.2	19.0	14.4
Na_2O	19.8	6.9	1.8	3.9	3.1	5.8
K_2O	0.4	0.6	0.1	0.4	0.2	0.8
BaO	0.2	0.3	0.2	0.2	0.2	0.2

TABLE 5.6

Removal of Inorganics Based on Analysis of Product Liquor

	Weight % in Raw Coal d.b.	% Removed at				
		250°C	275°C	300°C	325°C	350°C
Aluminium	0.16	0.1	0.1	0.2	0.2	0.2
Calcium	0.54	7.5	7.2	8.4	8.7	11.5
Chlorine	1.37	53.1	43.6	53.7	57.6	60.4
Iron	1.16	0.1	0.0	0.1	0.1	0.0
Magnesium	1.09	17.3	14.2	12.7	9.0	6.1
Potassium	0.4	36.0	33.0	36.3	40.8	42.3
Silicon	1.97	0.6	1.2	0.7	1.0	0.9
Sodium	1.31	46.9	45.7	55.4	59.0	60.7

Figure 5.1   Percentage of Water Removed

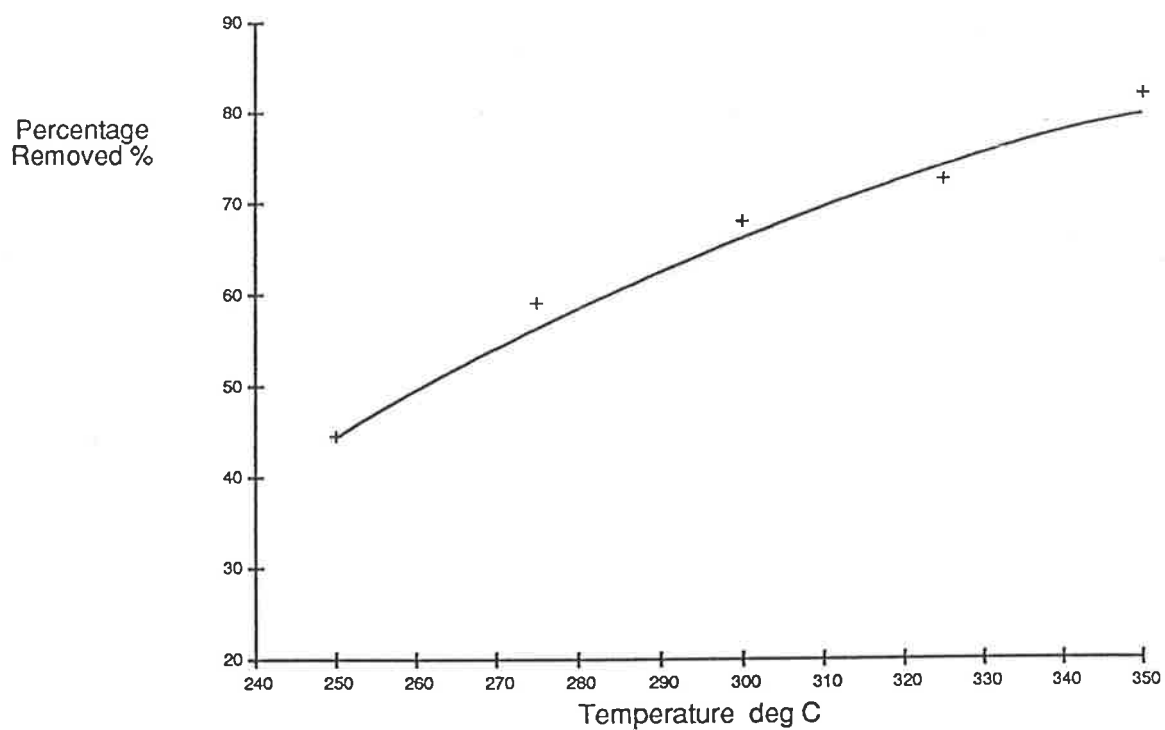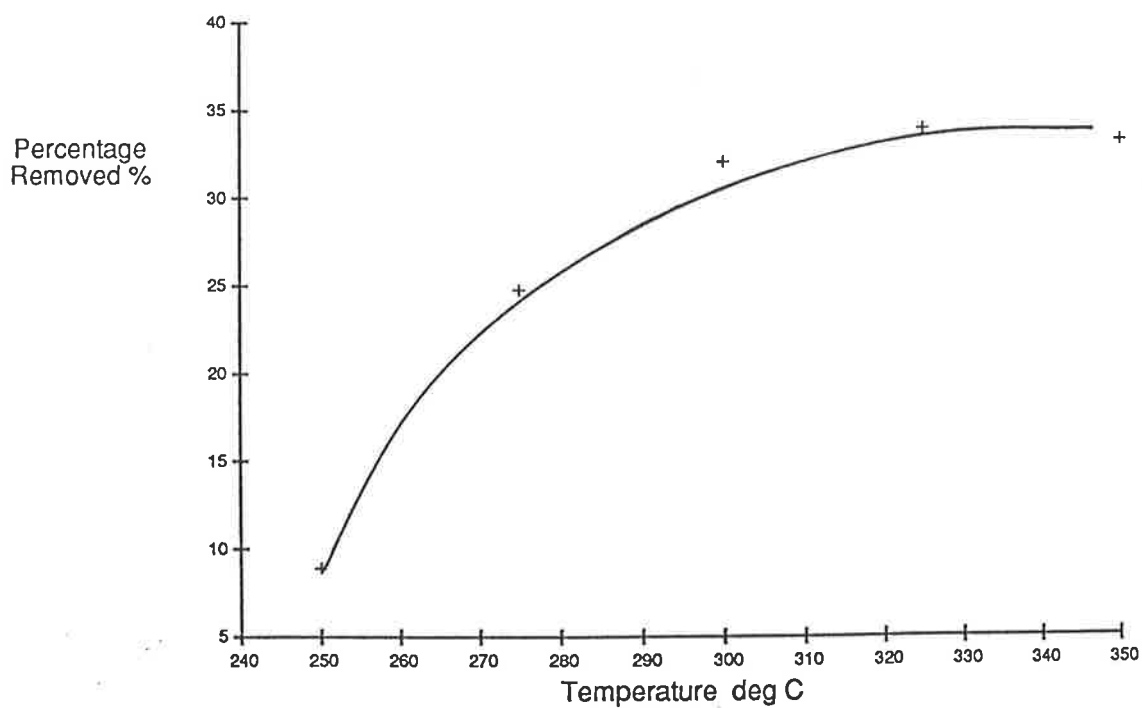Figure 5.2 Percentage of Volatile Matter Removed
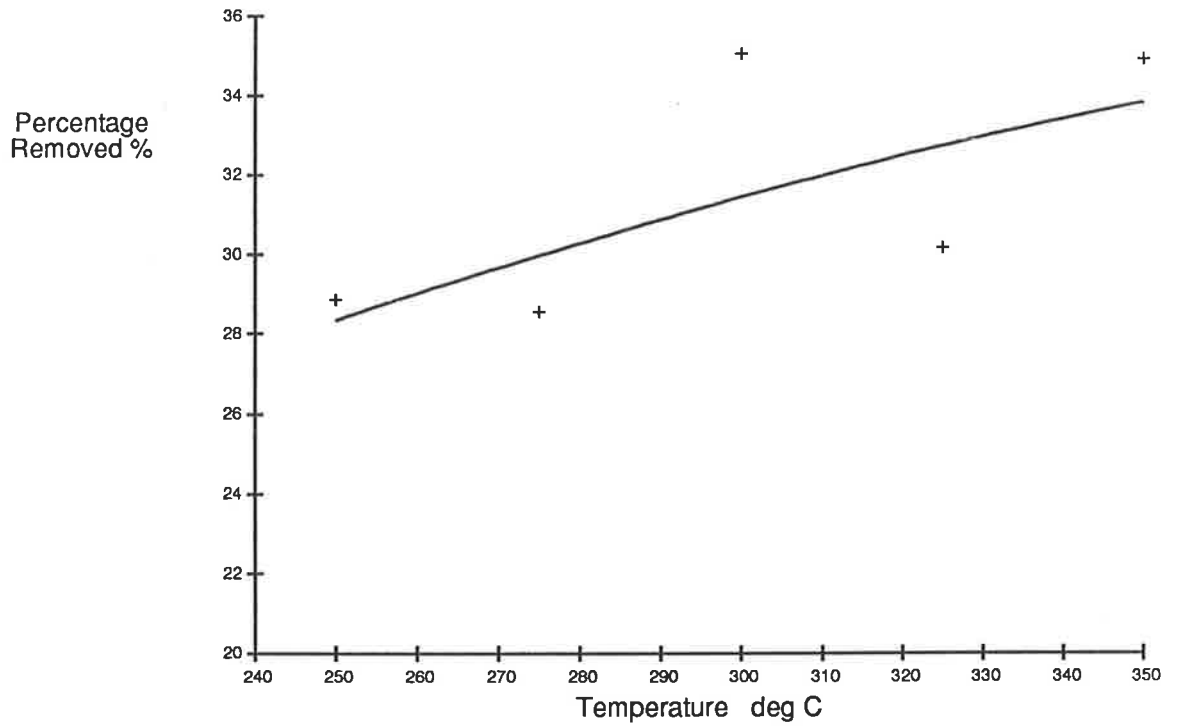
Figure 5.3   Percentage of Ash Removed

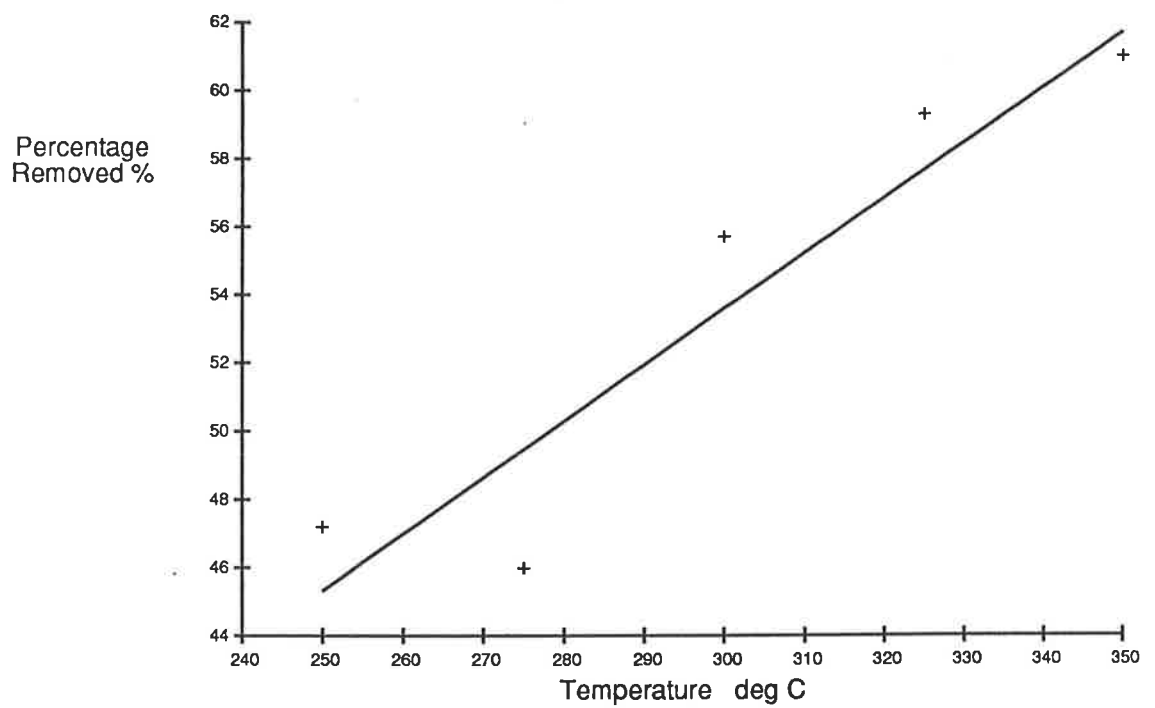Figure 5.4   Percentage of Sodium Removed
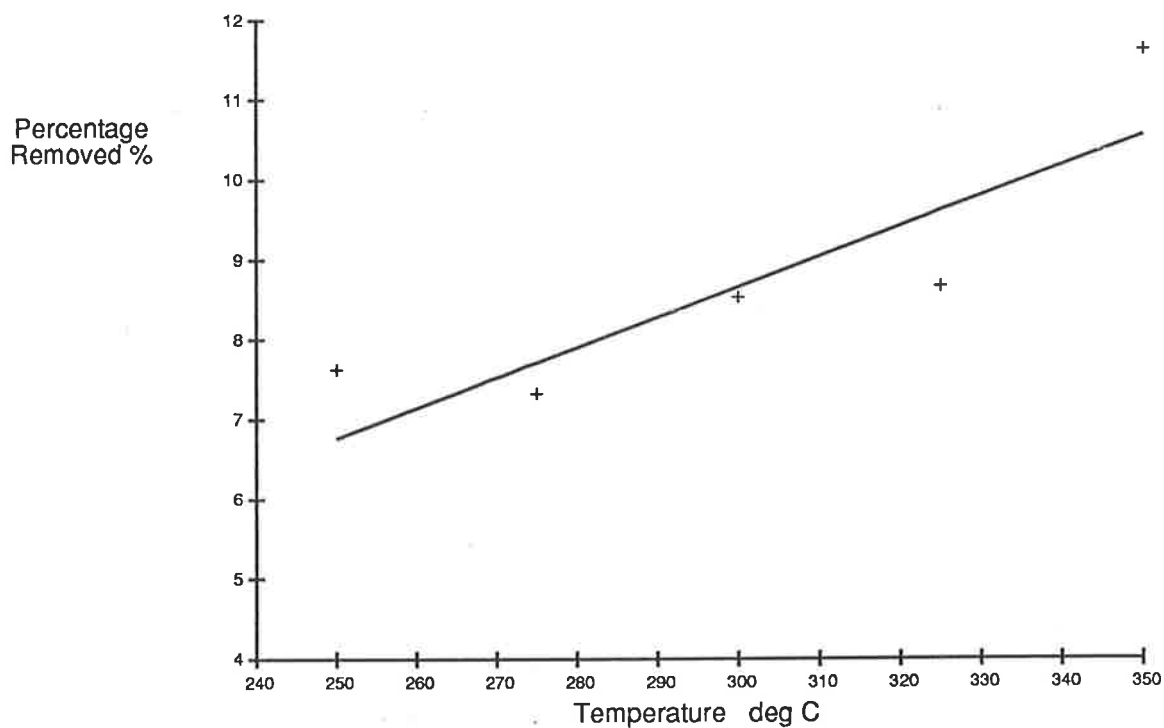
Figure 5.5   Percentage of Calcium Removed
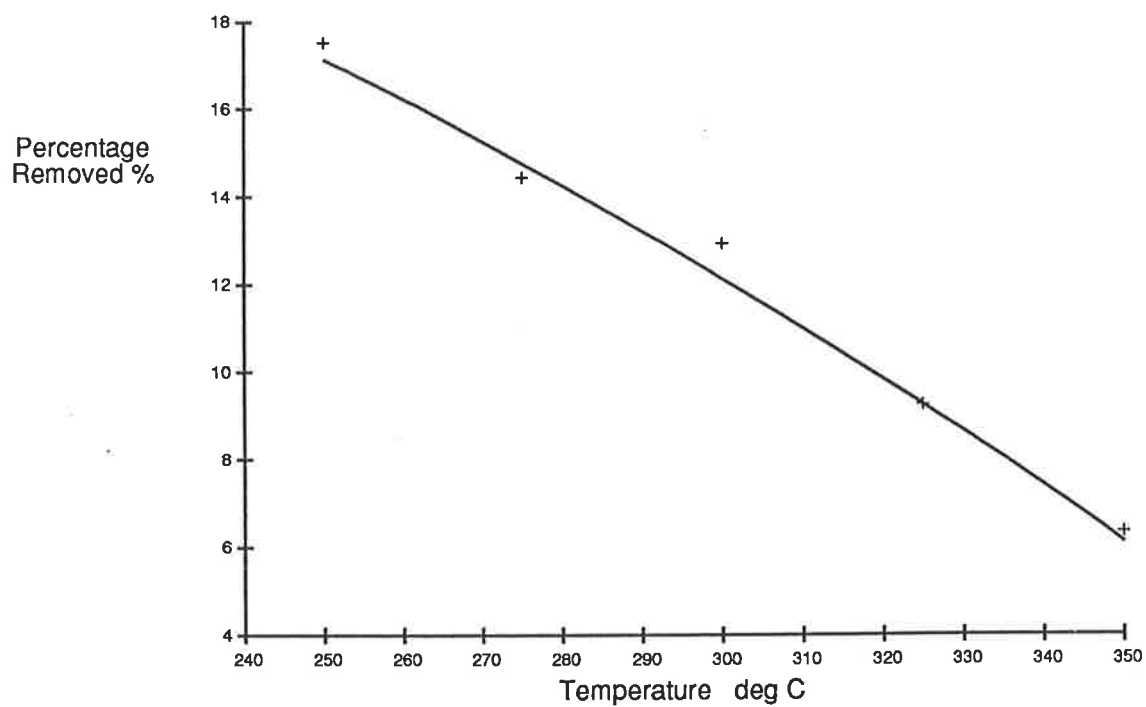

Figure 5.6   Percentage of Magnesium Removed

Figure 5.7   Percentage of Chlorine Removed

Percentage
Removed %

Temperature   deg C
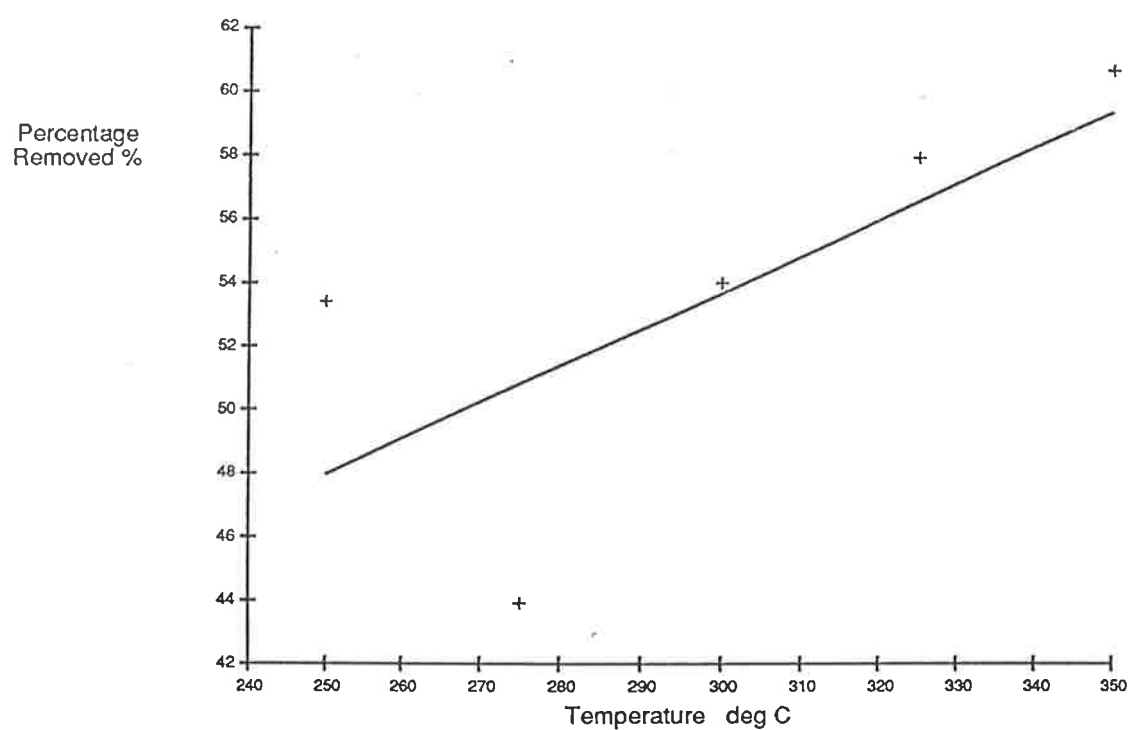
Figure 5.8   Percentage of Sulphur Removed

Percentage
Removed %

Temperature   deg C
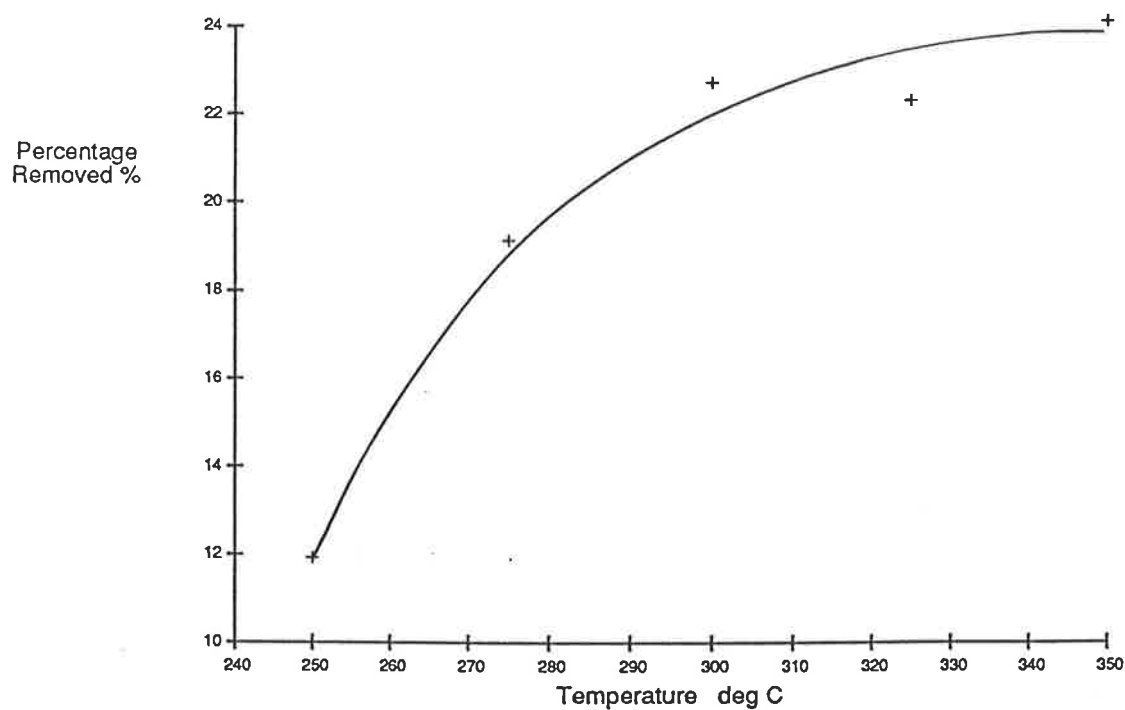
5.3   ALTERING THE EXPERIMENTAL CONDITIONS

5.3.1   Varying Tube Bomb Loading

A series of experiments were carried out to establish whether the amount of coal loaded in the tube bombs had any effect on the dewatering characteristics of Bowmans coal. If there is less coal in the tube bombs then the coal may be better mixed in the slurry during the reaction, and therefore ions may be more effectively leached from the coal. This may change the dewatering characteristics of the coal. These tests were carried out using similar experimental conditions used in earlier studies. Tests differed because less coal was added to the tube bombs and therefore a correspondingly greater initial charge of nitrogen was needed to build up the necessary reaction pressure.

The results for loading from 2 to 15 grams of coal at ratios of coal to water between 1:1 to 1:5 are shown in table 5.7. Coal was dewatered at $325^{\circ}C$ for 20 minutes. As can be seen from these results there was no definite trend which can be noted. The variation in the residual moisture in the coal from 29% to 36% has occurred in other tests, and cannot be considered peculiar to these results. There would generally be lower moisture contents as less coal is loaded, as filtering small quantities of coal on a Buchner funnel would enhance moisture reduction. When 2 grams of coal is used the residual moisture content does not appear to have improved, while for 5 or 10 grams of coal the moisture content appears to be lower. Therefore, while the variation in coal quality makes it difficult to interpret these results, it is unlikely that the degree of mixing in the tube bombs or leaching of the ions from the coal will influence the residual moisture content of dewatered coal.

The anomalous variation of equilibrium moisture contents makes it equally difficult to determine any changes to coal surface properties from these effects. Therefore no change in the equilibrium moisture content could be detected as the coal to water ratio increases.

A preliminary study of the effect of inorganic content in the coal on water removal for some South Australian Coals was undertaken by Buckley (1986). He found that there was no conclusive evidence to show that removing the inorganics from coal by aqueous leaching before dewatering changes the residual moisture content of the coal. While the variation of the coal to water ratio does not appear to influence the quantity of moisture removed during dewatering, an increase in coal:water ratio will enable more inorganic impurities to be leached from the coal.

TABLE 5.7

The effect of varying the mass of coal
loaded into the tube bombs

Mass of Coal in Tube Bomb g	Coal/Water Ratio	Moisture Content %	Equilibrium Moisture %
2	1:1	35.1	15.5
5	1:1	31.4	10.5
10	1:1	32.9	13.7
15	1:1	36.4	12.3
2	1:2	35.7	19.1
5	1:2	29.1	15.1
10	1:2	35.1	14.0
2	1:5	35.8	19.8
5	1:5	32.4	8.9

5.3.2 Rate of Heating

The effect of heating rate on the dewatering characteristics of the coal was investigated. Three tests were performed on Bowmans coal, the first test was performed by heating the coal slurry slowly and holding it at reaction temperature for 2 hours. The slower heating rate of $4^{\circ}C$ per minute was obtained by immersing the microautoclave in the fluidized sand bath while the bath was still being heated. In the second and third tests the tube bombs were heated rapidly to $300^{\circ}C$, and held it at this temperature for 20 mins and 2 hours respectively. Coal greater than 4 mm in diameter was used in these tests, as this particle size simplifies the estimation of residual moisture content by diminishing the effect of surface moisture during filtration. Although two tube bombs were used for each experiment and the moisture contents for each experimental condition averaged, tests were repeated to verify the trends obtained.

The results from these experiments are shown in table 5.8. From this table it appears the coal's propensity to dewater improves when heated slowly to reaction temperature. While this trend could be due to coal variability, slowly heating the coal to reaction temperature consistantly resulted in lower moisture contents than the faster heated counterpart.

TABLE 5.8

Rate of Heating Coal

Condition	Heating Rate Time Constant	Residence Time mins	Moisture Content %
Slow Heating	45 mins	120	32.4
Rapid Heating	1 min	20	35.6
Rapid Heating	1 min	120	36.0

5.3.3   Particle Size

A number of dewatering experiments were performed to investigate the effect of coal particle size on dewatering at a temperature of 325°C and a heating time of 20 minutes. Four ranges of particle size were investigated viz: <200, <1000, 2000-4000 and 4000-8000 um. A 1:1 coal water ratio was used.

From the results (Table 5.9) it appears that the smaller coal particle size did not dewater as effectively as larger particle sizes. This can most likely be attributed to the reduced filtration characteristics and greater surface area of small particle sizes. While thermal dewatering mechanisms such as coal shrinkage and pore collapse may not be affected by small particle sizes, the filtration characteristics of the coal slurry may cause a significant increase in residual moisture as coal particle size decreases. No detectable change in residual moisture content was shown for coal above 1000 um. Coal of large particle size would therefore be desirable in a continuous processing facitity.

While the smaller coal particle had a higher residual moisture content, the equilibrium moisture content of this coal was lower than for larger coal. Sears (1985) found that while particle size had minimal effect on dewatering, smaller coal particles showed increased pyrolysis and decarboxylation. This was thought to be due to the greater surface area and exposed pore volume of small particles. Therefore, there would be less water binding functional groups in the coal and the equilibrium moisture content would be lower.

As coal particle size decreased, the extent of water removal by thermal dewatering mechanisms such as coal shrinkage and pore collapse could not be determined from these experiments. The increase in residual moisture as coal particle size decreases was thought to be due to reduced filtration characteristics and increased surface area. The maximum coal size used in high-temperature pre-treatment would therefore be dictated by the constraints of process equipment.

TABLE 5.9
The effect of Coal Particle Size

Particle Size um	Moisture Content %	Equilibrium Moisture %
<200	40.6	10.7
<1000	36.0	19.5
2000-4000	36.5	12.8
4000-8000	35.6	-

5.3.4 Effect of Adding Methanol

The effect of adding methanol to the coal as an additive to enhance the dewatering characteristics of lignite was examined.

Tests were carried out using 1% and 10 % solutions of methanol added to the water in the slurry, and dewatering was carried out at a temperature of $325^{\circ}C$ for 20 minutes. The coal slurries were placed on a filtration cell and held at a vacuum of 10in Hg for 6 minutes. The residual moisture contents of the filtered and dewatered coal are shown in table 5.10. From these results the addition of methanol did not appear to have had any effect on dewatering. However, as the coal used in the study had been stored for a long period (see Chapter 5.8), the results may have been affected by surface oxidation of the coal and are therefore not conclusive.

TABLE 5.10

Adding Methanol to the Coal/Water Slurry

Additive	Moisture Content	
	Leached	Dewatered
H_2O	60.2	39.5
1% Methanol	60.2	38.0
10% Methanol	59.3	41.3

5.4 DECOMPOSITION OF CARBOXYL GROUPS

5.4.1 Introduction

During high-temperature pre-treatment the carboxyl groups in coal will break down to carbon dioxide and water. The ratio of carbon dioxide to water evolved is dependent on whether carboxyl groups are present in the acid or the salt form in the coal, and is therefore a function of every coal tested. Reported values for other coals could not be assumed to apply for Bowmans coal. The yields of products from the pyrolysis of Bowmans coal at temperatures between 520 and 650°C (Allen, 1981c) showed ratios of carbon dioxide to water in a range between 0.8 to 1.5, with an average value of 1.34.

As the experimental facilities available were not capable of accurate determination of this ratio, a simplified method of analysis was used. The results were compared with those from a more rigorous study by Schafer (1981) performed on Yallourn coal at low temperatures. Although the technique used in this study was somewhat crude, results appeared to compare favourably with ratios found in other coals.

5.4.1 Experimental Technique

A known mass of dry coal (oven-dried in nitrogen for 3 hrs at 107°C) was loaded into a tube bomb and purged with nitrogen. The bomb was sealed at atmospheric pressure and accurately weighed. It was then placed in a fluidized sand bath held at temperature for 1 hr. Temperatures examined were 250, 300 and 350°C. The bomb was then cooled in a water bath for an hour, dried and then reweighed to ensure no gas had escaped during the thermal treatment.

The gas (built up from pyrolysis reactions) was then released from the bomb and the tube bomb was reweighed. The difference between initial and final masses of the bomb was assumed to be equivalent to the amount of gaseous volatile matter released. The gas removed by this treatment was assumed to have the same composition as product gas obtained by dewatering the coal at the corresponding temperature. The tube bomb stem was then removed and the main body of the bomb was placed in an oven under nitrogen atmosphere at $107^{\circ}C$ until a constant weight was obtained. The resulting mass loss was considered to be the amount of water evolved on decomposition.

5.4.3 Results

The masses of water and carbon dioxide evolved from Bowmans Coal at temperatures up to $350^{\circ}C$ are shown in table 5.11 and are plotted in figure 5.9. In figure 5.10 these results are compared to the relation between water of decomposition and carbon dioxide evolved on pyrolysis of the acid and sodium form of Yallourn coal for temperatures up to $600^{\circ}C$ (Schafer, 1979).

From these limited results it appears that there is a good correlation between water and carbon dioxide evolved for Bowmans coal. The ratio of carbon dioxide to water evolved was 1.35:1, which compares favourably with that reported by Allen (1981c). Figure 5.10 shows that the plot of water and carbon dioxide evolved on pyrolysis of Bowmans coal lies between the values reported for pyrolysis of both the acid and sodium carboxylate forms in Yallourn coal. However, this is not a rigorous study, and much more work using more accurate equipment would be required to establish a dependable correlation.

TABLE 5.11

Carbon Dioxide and Water removed from Bowmans Coal
by the breakdown of Carboxylate Groups

	Mass of Component Removed g/100g daf coal		
	250°C	300°C	350°C
Mass Volatile Matter	7.2	11.0	19.3
Mass Fraction CO_2 in Volatile Matter*	0.96	0.94	0.90
Mass CO_2	6.9	10.3	17.4
Mass H_2O	4.7	7.6	13.1
Total Mass Removed	11.6	17.7	30.5
Mass Removed during Dewatering*	11.3	16.8	26.5

*From High-Temperature Pre-Treatment Experiments.

Figure 5.9 Decomposition of Carboxylate Groups

Carbon Dioxide and Water Evolved on Heating
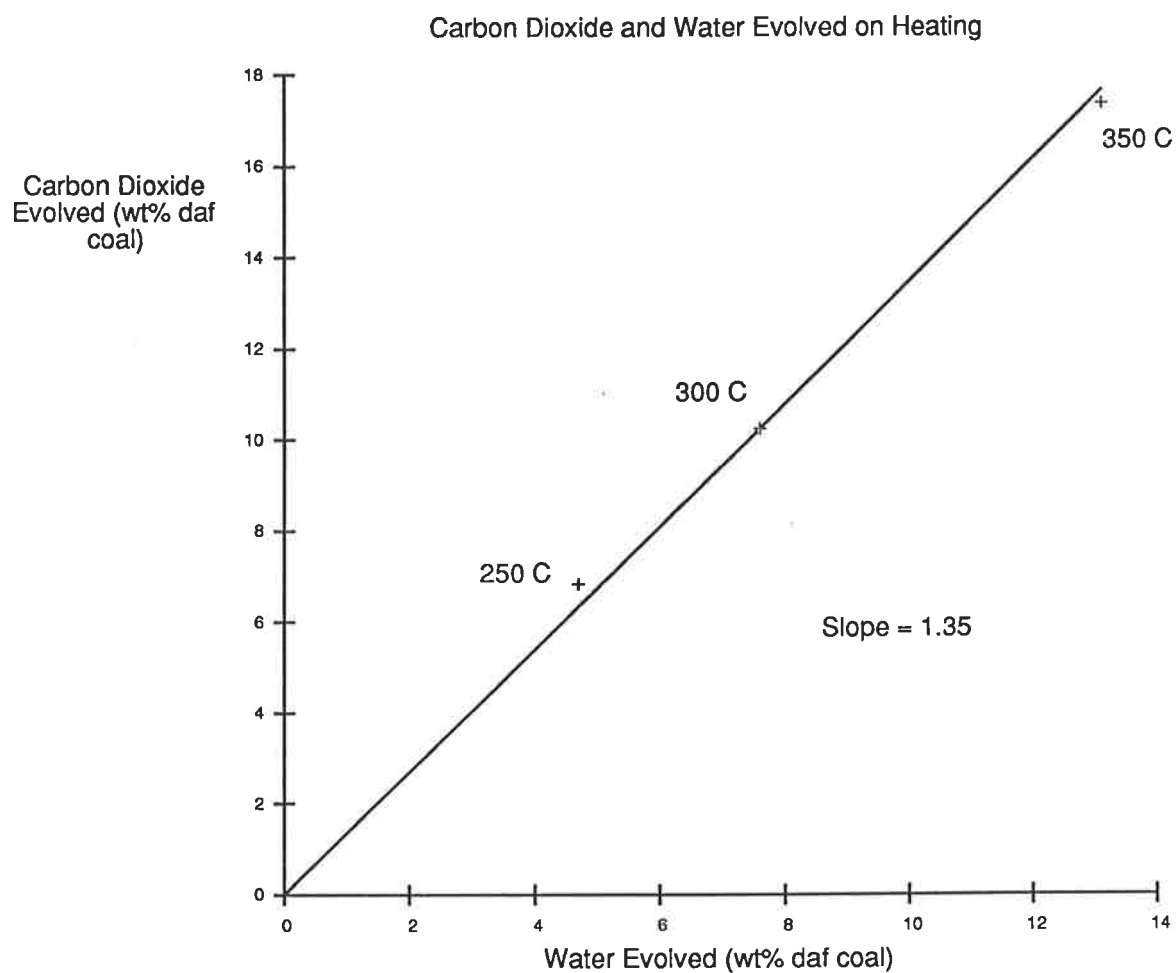
Figure 5.10   Decomposition of Carboxylate Groups

Comparison between Bowmans and Yallourn Coal
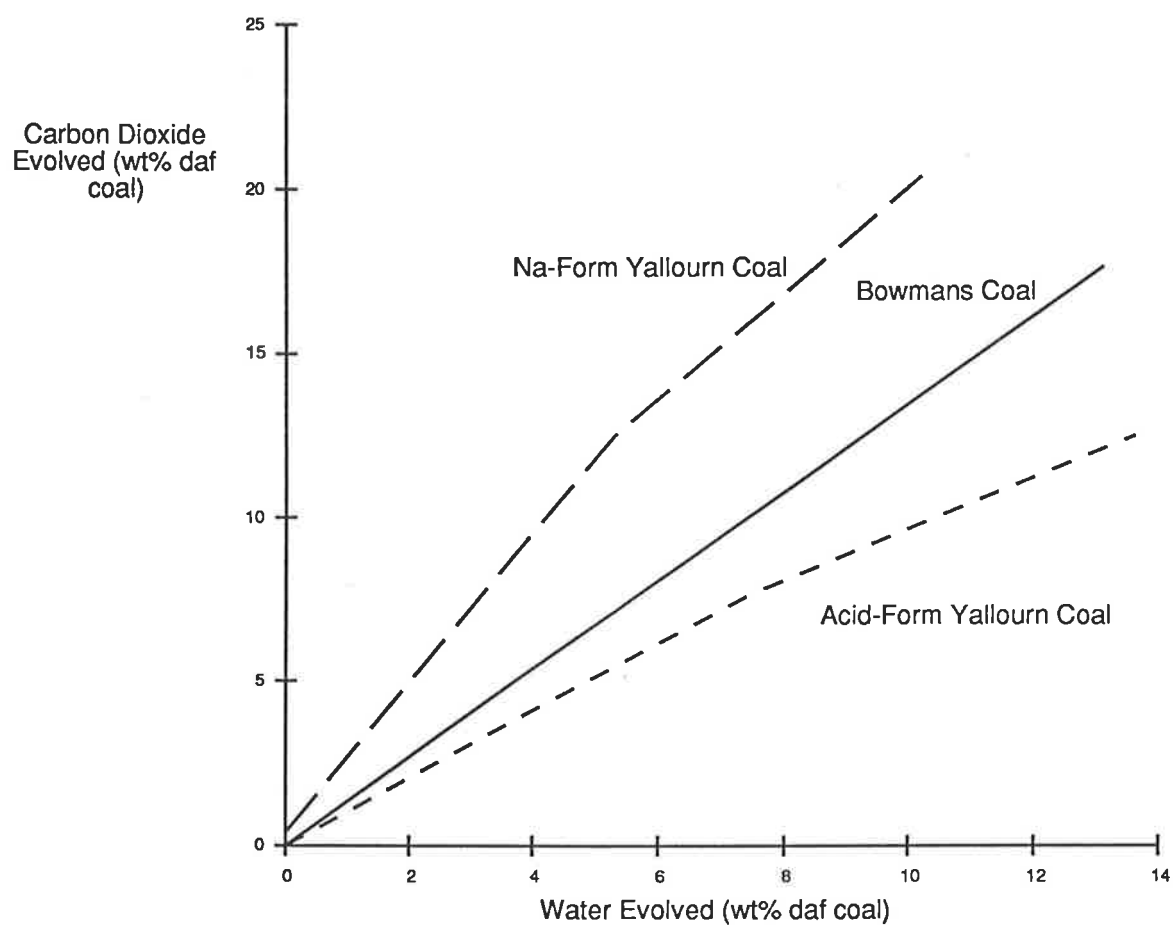
5.5   KINETICS EXPERIMENTS

Tests were undertaken to study the kinetics of impurity removal for temperatures between 250 to 350°C at 5, 10, 15, 20 and 60 minute intervals. Coal was crushed to a particle size <1mm to ensure a representative sample, and slurried with a 1:1 coal/water ratio. Results from these tests formed the basis for modelling the rate of volatile matter and moisture removal from coal during dewatering.

A number of analyses of the reaction products were performed, including the determination of the soluble ions in the waste water and the constituents in the product gas. The quantity of impurity removal was calculated for each test.

5.5.1   Proximate Analysis

Table 5.12 shows results of the proximate analysis and equilibrium moisture contents of dewatered coal, while table 5.13 shows the extent of coal constituent removal. The coal used in this series of tests had been stored for two years longer than that used in the earlier experiments, and it was found that the efficiency of dewatering had decreased. Residual moisture contents were much higher than had been reported in previous tests. Unfortunately most coal from the Bowmans coal deposit could only be obtained from a test pit dug in 1982. As this was the only source of coal available for these experiments, fresh coal samples could not be used.

Two tests were performed at temperatures of 150 and 200°C to determine if dewatering was apparent at lower temperatures. As coal slurried with water and filtered without dewatering shows a moisture content of about 60%, it was clear that slight

dewatering occurs for Bowmans coal at temperatures as low as 150°C. This may be due to either the improved filtering characteristics of the coal following devolatilization, or shrinkage of the coal structure lowering its water holding capacity.

The equilibrium moisture content of coal provides an indication of the hydrophilic character of the coal, and therefore will decrease as the water binding functional groups are removed during dewatering. Reduction of the equilibrium moisture content of the coal is likely due to the loss of hydrophilic functional groups, and the lessening of the surface area for wetting as it becomes coated with coal tars and waxes which repel the water. As expected, the experimental results show that the equilibrium moisture content for each temperature generally decreases over time. However some equilibrium moisture contents are higher than would be expected as the reaction temperature increases. For coal dewatered at 325°C equilibrium moisture contents of between 9 to 20% have been determined in various other experiments. This variation is probably caused by the coal age. In these experiments, tests at each temperature were performed at about the same time, and used the same source of coal to try to achieve consistent results.

The quantity of moisture removed from the coal was based on the moisture content of as mined coal of about 57% total moisture (133g/100g dry coal). This was done to give a realistic figure which would be necessary for the design of a processing plant.

TABLE 5.12

Proximate Analysis of Dewatered Coal
following Kinetics Experiments

TIME min	MOISTURE Total % in Coal	VOLATILE MATTER % d.b.*	FIXED CARBON % d.b.	ASH % d.b.	EQUILIBRIUM MOISTURE %
RAW	49.3	49.7	39.1	11.2	44.0
T=150°C					
20	54.6	50.4	41.6	8.0	43.0
T=200°C					
20	48.9	49.0	42.7	8.3	36.3
T=250°C					
5	46.6	46.6	45.3	8.1	26.0
10	44.1	47.1	45.2	7.7	23.8
15	44.6	47.0	44.3	8.7	22.8
20	44.5	46.1	45.3	8.6	22.7
60	43.3	45.0	44.3	10.7	19.5
T=275°C					
5	45.1	45.3	45.6	9.1	33.9
10	45.6	45.0	45.8	9.2	26.0
15	39.5	45.0	46.0	9.0	24.0
20	40.8	45.0	46.0	9.0	24.0
60	40.6	43.6	47.0	9.4	23.7

*d.b. = dry basis

TABLE 5.12 (cont)

Proximate Analysis of Dewatered Coal
following Kinetics Experiments

TIME min	MOISTURE Total % in Coal	VOLATILE MATTER % d.b.*	FIXED CARBON % d.b.	ASH % d.b.	EQUILIBRIUM MOISTURE %
T=300°C					
5	40.9	45.7	45.9	8.4	28.2
10	37.2	44.4	45.5	10.1	23.4
15	39.8	44.5	46.8	8.7	17.9
20	36.8	44.3	46.6	9.1	20.4
60	36.6	42.4	47.5	10.1	17.1
T=325°C					
5	41.2	44.5	46.3	9.2	21.5
10	38.4	43.3	47.1	9.6	23.6
15	34.3	42.3	47.0	10.7	27.4
20	33.5	43.6	47.1	9.3	19.5
60	34.9	40.2	49.0	10.8	23.8
T=350°C					
5	35.0	41.7	48.6	9.7	10.7
10	33.5	39.9	50.0	10.1	8.6
15	33.3	40.7	49.8	9.5	13.3
20	30.5	37.9	51.0	11.1	8.9
60	30.4	35.9	53.3	10.8	9.9

* d.b. = dry basis

TABLE 5.13

Removal of Coal Constituents

TIME min	CONSTITUENT REMOVED g/100g dry coal			
	COAL	WATER	V.M.	ASH
T=150°C				
20	6.0	19.6	2.3	3.7
T=200°C				
20	8.4	45.0	4.8	3.6
T=250°C				
5	13.7	57.3	9.5	4.2
10	13.5	64.4	9.0	4.5
15	11.7	61.5	8.2	3.5
20	13.7	63.4	9.9	3.8
60	11.7	65.2	10.0	1.8
T=275°C				
5	14.3	62.2	10.9	3.4
10	14.6	61.0	11.3	3.4
15	15.0	77.1	11.5	3.6
20	15.0	74.0	11.5	3.6
60	16.8	75.7	13.4	3.4

TABLE 5.13 (cont)

Removal of Coal Constituents

TIME min	CONSTITUENT REMOVED g/100g dry coal			
	COAL	WATER	V.M.	ASH
T=300°C				
5	14.8	73.6	10.7	4.0
10	14.1	81.7	11.6	2.5
15	16.5	77.4	12.5	3.9
20	16.1	83.7	12.5	3.6
60	17.7	85.1	14.8	2.9
T=325°C				
5	15.6	73.4	12.1	3.5
10	17.0	80.9	13.8	3.2
15	16.8	89.2	14.5	2.3
20	17.0	90.8	13.5	3.5
60	20.2	89.8	17.6	2.6
T=350°C				
5	19.5	89.3	16.2	3.4
10	21.8	93.2	18.5	3.3
15	21.5	93.4	17.7	3.7
20	23.3	99.0	20.6	2.7
60	26.6	100.6	23.4	3.3

5.5.2 Ion Removal

Tables 5.14 and 5.15 show the analysis of the soluble ions in the product wastewater following dewatering and the quantity of these ions removed from coal. From these analyses it can be seen that there are substantial quantities of sodium, chlorine and sulphate removed from the coal. However the quantities of sulphate and magnesium removed appear to decrease as the temperature increases, suggesting that reactions occur during dewatering which retard the extent of removal of these elements.

There are a number of mechanisms which will influence ion removal during high-temperature pre-treatment. The major mechanisms are

1) Leaching of ions when the coal is slurried with water.
2) Expulsion of ions as the coal shrinks and water is exuded from coal pores.
3) Chemical reaction.
4) The release of chemically bonded ions from the coal surface.

Leaching starts to influence the kinetics of ion removal as soon as the coal is slurried with water before dewatering commences. Therefore it masks the possible influence of the other mechanisms on the kinetics of ion removal during dewatering.

As aqueous leaching is the major mechanism by which ions are released from the coal this phenomenon has been made the subject of a separate study. By using information gained from this study and comparing results to those obtained for ion removal during high-temperature pre-treatment, it was possible to infer effects which occur in the dewatering reactor.

Before each experiment the coal was slurried with water and left for 1/2 hour to allow most of the ions to leach from the coal. After this time the coal was thermally treated and

the liquor analysed for ion removal. From the conditions of the test, the quantity of ions which would have been leached from the coal if no thermal treatment had taken place could be roughly calculated. A comparison between the quantity of ions removed by aqueous leaching and the actual quantity removed indicates whether mechanisms other than leaching influence the extent of ion removal during high-temperature pre-treatment.

While there was little difference in the quantity of chlorine and sodium which could be removed from the coal, there does appear to be some mechanisms which retards the extent of calcium, magnesium and sulphate removed from the coal. Much less soluble calcium was removed by dewatering than could be leached from the coal under similar conditions. Removal was slightly improved at higher temperatures, which may be due to variation and anomalies in coal quality. Magnesium and sulphate are similarly removed in much lower concentration than could be obtained at similar coal/water ratios during leaching experiments. As time and temperature increases the extent of removal of both of these elements decreases.

The retardation of these elements in coal during dewatering was observed in earlier studies, and also appeared to occur over long periods at lower temperatures during aqueous leaching experiments. An off-white flakey precipitate was found in some dewatered coal samples and was tentatively identified as a form of calcium and magnesium sulphate. It is very probable that calcium/magnesium sulphate precipitates out of solution and is retained in the coal. It may be possible to stop this precipitate from forming by using an additive, thereby enhancing the removal of magnesium and sulphate during dewatering.

TABLE 5.14

Ion Analysis of Product Liquor

TIME min	DISSOCIATED IONS ppm						
	Na^+	K^+	Mg^{++}	Ca^{++}	Fe^{++}	$SO_4^=$	Cl^-
T=150°C							
20	1770	22	510	80	17	2710	2180
T=200°C							
20	1690	17	460	170	20	2700	2320
T=250°C							
5	2860	35	890	160	21	3850	3910
10	3200	40	975	220	18	4430	4330
15	3140	38	740	140	9	3440	3970
20	3210	37	830	210	8	3800	3900
60	3140	46	830	190	7	3130	3730
T=275°C							
5	2225	32	530	150	12	3300	2560
10	2580	24	500	110	21	2490	3120
15	2820	61	590	160	2.0	2343	3546
20	2560	35	590	125	2.1	1830	3160
60	2570	37	490	90	0.9	1910	3050

TABLE 5.14   (cont)

Ion Analysis of Product Liquor

| TIME | DISSOCIATED IONS | | | | | | |
| min | ppm | | | | | | |
	Na^+	K^+	Mg^{++}	Ca^{++}	Fe^{++}	$SO_4^=$	Cl^-
T=300°C							
5	2200	33	430	140	5.3	2250	2810
10	3210	44	560	210	2.8	3620	3950
15	2820	24	320	170	1.9	1780	2390
20	3490	41	490	225	1.9	2720	3953
60	2890	24	360	225	1.6	2075	3260
T=325°C							
5	3450	43	260	275	1.8	2800	3960
10	3360	45	200	260	1.1	2000	3850
15	3260	46	175	300	1.3	2080	3680
20	3330	43	190	300	1.2	1870	3800
60	3425	45	240	260	-	2140	3740
T=350°C							
5	4020	45	560	400	13	3600	4630
10	3100	45	390	300	10	3000	4000
15	3000	42	310	325	2.1	2100	3170
20	3050	35	280	250	1.0	4500	4000
60	2735	32	190	260	2.0	1366	3119

TABLE 5.15

Quantity of Soluble Ions Removed from Dewatered Coal
in the Wastewater

TIME min	REMOVAL OF SOLUBLE IONS FROM COAL g/100g dry coal				
	Na^+	Mg^{++}	Ca^{++}	$SO_4^=$	Cl^-
T=150°C					
20	0.197	0.057	0.009	0.301	0.242
T=200°C					
20	0.212	0.058	0.021	0.338	0.291
T=250°C					
5	0.384	0.119	0.021	0.517	0.525
10	0.440	0.134	0.030	0.609	0.595
15	0.426	0.100	0.019	0.466	0.538
20	0.441	0.114	0.029	0.523	0.536
60	0.435	0.115	0.026	0.433	0.516
T=275°C					
5	0.306	0.073	0.021	0.454	0.352
10	0.354	0.069	0.015	0.341	0.428
15	0.410	0.086	0.023	0.340	0.515
20	0.368	0.085	0.018	0.263	0.454
60	0.375	0.071	0.013	0.278	0.445

TABLE 5.15   (cont)

Quantity of Soluble Ions Removed from Dewatered Coal
in the Wastewater

TIME min	REMOVAL OF SOLUBLE IONS FROM COAL g/100g dry coal				
	Na^+	Mg^{++}	Ca^{++}	$SO_4^=$	Cl^-
T=300°C					
5	0.315	0.062	0.020	0.322	0.402
10	0.474	0.083	0.031	0.534	0.583
15	0.412	0.047	0.025	0.260	0.349
20	0.521	0.073	0.034	0.406	0.590
60	0.437	0.054	0.034	0.314	0.493
T=325°C					
5	0.496	0.037	0.040	0.403	0.570
10	0.499	0.030	0.039	0.297	0.572
15	0.499	0.027	0.046	0.318	0.563
20	0.511	0.029	0.046	0.287	0.583
60	0.532	0.037	0.040	0.332	0.581
T=350°C					
5	0.462	0.086	0.062	0.555	0.714
10	0.488	0.061	0.047	0.472	0.630
15	0.471	0.049	0.051	0.330	0.498
20	0.493	0.045	0.040	0.727	0.646
60	0.449	0.031	0.043	0.224	0.511

5.5.3 Gas Removal

The analysis of the product gas from dewatering of the coal and the percentage removal of the gas components are shown in tables 5.16 and 5.17. Results show that mainly carbon dioxide is produced. However there are also substantial quantities of hydrogen sulphide, carbon monoxide and methane. Other light hydrocarbons were removed, although not in significant quantities. These compounds were often difficult to detect and therefore the concentrations reported in the product gas are not highly accurate.

It was also apparent that the concentration of carbon monoxide in the product gas was decreasing over time at each reaction temperature. The reason for this is not apparent, as oxidation of the carbon monoxide in the product gas would be unlikely. However, carbon monoxide may react with oxygen functional groups in the coal structure.

There is a significant quantity of hydrogen sulphide removed from the coal during dewatering, due to the destruction of organic sulphur from the volatile matter in the coal. While this will improve the quality of the product coal for combustion, it will necessitate the treatment of the product gas. It also dissolves in the product liquor, giving it an unpleasant odour.

TABLE 5.16

Composition of Product Gas

TIME mins	GAS COMPOSITION							
	CO_2 %	H_2S %	CO %	CH_4 %	C_2H_4 ppm	C_2H_6 ppm	C_3H_6 ppm	C_3H_8 ppm
T=150°C								
20	100							
T=200°C								
20	99.3		0.7					
T=250°C								
5	98.0	1.5	0.4			670		
10	92.6	3.1	3.5	0.8		150		170
15	93.3	3.3	2.3	1.1	30	275		280
20	93.5	3.2	2.5	0.8		220		
60	93.8	3.1	1.7	1.2		520	430	700
T=275°C								
5	96.6	1.2	1.9	0.3		3		
10	94.8	1.9	2.5	0.7		310		570
15	96.3	1.5	1.5	0.7		30		
20	97.1	1.5	0.7	0.7		280	40	60
60	97.8	1.3	0.3	0.6		90		10

TABLE 5.16   (cont)

Composition of Product Gas

TIME mins	GAS COMPOSITION							
	CO_2 %	H_2S %	CO %	CH_4 %	C_2H_4 ppm	C_2H_6 ppm	C_3H_6 ppm	C_3H_8 ppm
T=300°C								
5	89.6	3.9	5.8	0.7				
10	89.8	4.1	5.1	0.9		580		
15	91.8	3.9	3.6	0.5		880	570	1050
20	93.6	4.4	1.0	1.0		460		
60	91.7	5.0	1.2	1.9	430	1070		1760
T=325°C								
5	87.1	8.4	3.7	0.4	1190	1512	330	1330
10	88.0	9.4	1.5	0.8	980	990	540	420
15	87.1	10.2	1.4	0.8	810	940	1320	2050
20	86.7	8.3	3.1	1.4	330	920	2460	1880
60	86.1	8.6	2.7	1.8	430	1070	2500	3200
T=350°C								
5	89.2	4.8	4.9	1.0	260	610		
10	86.4	8.4	3.3	1.6	370	1150		1170
15	85.6	7.9	3.1	2.8	310	2620		3170
20	86.1	8.6	2.9	2.0	530	920	840	1640
60	84.9	8.4	2.3	3.3	900	3540	1880	5170

TABLE 5.17

Removal of Constituents in the Volatile Matter

TIME mins	REMOVAL OF CONSTITUENTS FROM PYROLYSIS REACTIONS g/100g coal d.b.					
	H_2O	GAS	CO_2	H_2S	CO	CH_4
T=150°C						
20	0.99	1.34	1.34	0.000	0.000	0.000
T=200°C						
20	2.04	2.78	2.76	0.019	0.019	0.000
T=250°C						
5	3.98	5.49	5.38	0.082	0.022	0.000
10	3.64	5.31	4.92	0.165	0.186	0.042
15	3.35	4.86	4.53	0.160	0.112	0.053
20	4.05	5.86	5.47	0.187	0.146	0.047
60	4.09	5.89	5.53	0.183	0.100	0.071
T=275°C						
5	4.52	6.33	6.11	0.076	0.120	0.019
10	4.65	6.63	6.28	0.126	0.166	0.046
15	4.76	6.68	6.44	0.100	0.100	0.047
20	4.79	6.66	6.47	0.100	0.047	0.047
60	5.64	7.78	7.62	0.101	0.023	0.047

TABLE 5.17   (cont)

Removal of Constituents in the Volatile Matter

TIME mins	REMOVAL OF CONSTITUENTS FROM PYROLYSIS REACTIONS g/100g coal d.b.					
	H_2O	GAS	CO_2	H_2S	CO	CH_4
T=300°C						
5	4.29	6.47	5.80	0.252	0.375	0.045
10	4.61	6.93	6.23	0.284	0.354	0.062
15	5.06	7.45	6.84	0.291	0.268	0.037
20	5.13	7.40	6.93	0.326	0.074	0.074
60	5.98	8.81	8.08	0.441	0.106	0.167
T=325°C						
5	4.75	7.37	6.42	0.619	0.273	0.029
10	5.42	8.33	7.33	0.783	0.125	0.067
15	5.69	8.82	7.68	0.900	0.123	0.071
20	5.28	8.22	7.13	0.683	0.255	0.115
60	6.86	10.70	9.26	0.925	0.291	0.194
T=350°C						
5	6.42	9.75	8.67	0.467	0.477	0.097
10	7.21	11.28	9.75	0.947	0.372	0.180
15	6.88	10.86	9.30	0.858	0.337	0.304
20	8.03	12.60	10.85	1.084	0.366	0.252
60	9.02	14.34	12.18	1.205	0.330	0.473

5.6 THERMAL EFFICIENCY

A number of analyses of calorific value using an adiabatic bomb calorimeter were performed to determine the thermal efficiency of high-temperature pre-treatment. Unfortunately, although duplicate analysis were performed, most of these tests proved to be unreliable. This was probably due to the variability of small coal samples used and, to a lesser extent, the poor accuracy of the bomb calorimeter available for use in these tests.

However, a series of analyses performed on raw and coal dewatered at 325°C for 20 mins appeared to be more reliable. There was only small variation in the number of repeat analyses, and while it would unwarranted to place absolute confidence in these results, they can be considered reasonably accurate. The results at these processing conditions were used to calculate the thermal efficiency of dewatering. The calorific values of raw and coal dewatered at various processing conditions are shown in table 5.18.

To evaluate the effectiveness of the high-temperature pre-treatment process a number of parameters will be defined. The percentage of energy recovered is a measure of the energy removed by pyrolysis reactions during the dewatering process. The percentage increase in net energy available from combustion accounts for the removal of water from the coal by non-evaporative means and compares the effective energy available from combustion of dewatered coal. The percentage energy penalty is defined as the percentage of the HHV of raw coal required to heat the coal/water slurry to reaction temperature .

The energy recovered from the process is defined as:

$$\% \text{ Energy Recovery} = \left(\frac{\text{HHV dewatered coal x yield of maf coal}}{\text{HHV raw coal}} \right) \times 100 \qquad ...(5.1)$$

Table 5.19 shows the value of energy recovery based on an 80% yield of coal dewatered at 325°C for 20 mins is 97.7%. This shows that most of the coal lost through devolatilization reactions is from oxygenated carbon compounds of calorific value less than 3% of the total calorific value of the coal.

As the devolatilization of coal is slightly endothermic, the efficiency of the dewatering process can be verified using an energy balance using the products of the dewatering reaction. Energy is lost through the removal of carbon and hydrogen in the product gas and organics in the waste water. From a calculation of the calorific values of the gaseous and liquid products it was found that the energy loss from these components is similar to that reported above, approximately 2%. Values of energy recovery reported by Sears et al (1985) for a suite of 15 coals from various deposits ranged between 92 to 99%; the average being 96.9%; the energy recovery reported for Morwell Coal was 97.4%.

While the energy recovery gives some indication of amount of energy removed during dewatering and therefore the efficiency of the process, the energy saved by reduction of water in the coal using non-evaporative processes was not considered. The effect of the increase in calorific value due to the reduction in moisture content is given by:

$$\text{\% Net Energy Available from Combustion} = \left(\frac{\text{HHV dewatered coal} - \left(\frac{\text{g water}}{\text{g maf coal}}\right) \times H_{vap}\text{water}}{\text{HHV raw coal} - \left(\frac{\text{g water}}{\text{g maf coal}}\right) \times H_{vap}\text{water}} \right) \quad \text{...(5.2)}$$
$$\times \text{ yield of coal maf } \times 100$$

To calculate this parameter it was assumed that the moisture content of as mined coal was 57%, while the dewatered coal had a moisture content of 34%. Table 5.19 shows that, while there is an energy reduction from pyrolysis reactions, the net energy available for combustion when the effect of removing water by non-evaporative methods is taken into account has increase the calorific value of the coal by about 9%. This efficiency may be

greater when other factors are considered, for example the increase in efficiency within the boilers from the increase in coal quality and a reduction in sodium and chlorine levels in the coal.

However it is not possible to recover all the thermal energy from the dewatering reactor and energy must be used to heat the coal/water slurry to the required reaction temperature. The amount of energy input into the process depends on the quantity of energy which can be recovered from the feed stream. The heat input to the system can be expressed in terms of a percentage of HHV of the feed. It is given by:

$$\% \text{ Energy Penalty} = \left(\frac{\Delta H_{Feed} - \Delta H_{Product}}{HHV \text{ raw coal}} \right) \times 100 \qquad ...(5.3)$$

To calculate an approximate value for the energy required for dewatering it was assumed that to heat the slurry from $20^{\circ}C$ to $325^{\circ}C$ only energy between $320^{\circ}C$ and $65^{\circ}C$ could be recovered from the product stream. Pumping energy was calculated assuming the plant would be operating at a pressure of 12.5 MPa, and that the efficiency of electrical power generation would be 32%. A coal/water ratio of 1:1 and a specific heat for coal of 1.5 kJ/kg was assumed (see chapter 11.6 for energy balance calculations).

The energy penalty for processing under these conditions is shown in table 5.19. Approximately 4.4% of the HHV of the coal is required as thermal energy to dewater the coal. This value does not include crushing, filtering or wastewater treatment energy requirements. These factors are very dependent on the type of plant equipment installed, and, as these items would need electrical power, the efficiency of power generation.

Energy flow diagrams for direct combustion and dewatering followed by combustion of Bowmans coal are shown in figure 5.11. These diagrams show that there appears to be some thermodynamic justification to dewater the coal before combustion, which may be augmented by feeding the product gas to the boiler for combustion. A more detailed analysis

would take account of the energy required for associated pumping, filtering and wastewater treatment, and the reduced capital cost of the boiler and associated equipment for the upgraded coal feed.

TABLE 5.18

Calorific Values of Dewatered Coal Samples

Time (mins)	Calorific Value kJ/g	Moisture %	Ash %	HHV kJ/g
Raw*	10.9	50.0	12.0	24.0
T=325°C				
5	19.1	35.1	7.5	26.9
10	18.7	37.7	9.0	27.4
15	25.0	33.8	9.9	34.8
20*	18.0	33.5	8.1	29.3

TABLE 5.19

Efficiency of Dewatering at 325°C for 20 minutes.

% Energy recovery	97.7%
% Net Energy Available from Combustion	108.9%
% Energy Penalty	4.4%

DIRECT COMBUSTION

3.4 MJ

Energy Required to
Vaporize Water in Coal

Raw Coal — 24.0 MJ → COMBUS-TION — 20.6 MJ → Energy Available from Combustion

DEWATERING FOLLOWED BY COMBUSTION

0.7 MJ   1.0 MJ

Energy in
Gas Removed

Energy Required to
Vaporize Water in Coal

24.0 MJ → DEWATER-ING — 23.3 MJ → COMBUS-TION — 21.1 MJ →

Raw Coal

1.2 MJ
Energy Required for
Heating and Pumping

Energy Available
from Combustion
(21.9 MJ if Gas
Combusted)

Energy Required
to Remove Water
Non-Evaporatively

1.2 MJ

Figure 5.11   Energy Flow Diagram for Combustion of
Raw and Dewatered Coal
Basis 1 Kg of daf coal

5.7   LONG TERM MOISTURE REABSORPTION

If the dewatered coal were to be stored for a considerable time as a slurry, or pipeline transported from the mine site to a power station, the long term moisture reabsorption characteristics would need to be known. A series of tests was therefore undertaken to determine these characteristics on three separate coal samples dewatered at 300°C for 20 minutes.

About 5 grams of 4 mm dewatered coal was carefully weighed and placed in a beaker filled with distilled water. The coal was then periodically removed from the water and filtered in a Buchner funnel until the surface water was no longer visible in the funnel. It was then left for a further minute. The coal was then reweighed and the moisture absorbed was calculated. Samples were then replaced in the distilled water. After the tests were completed after 8 weeks the coal was analysed for moisture content.

Calculations of water reabsorption were based on the average weight of coal measured after the first 5 minutes, as water initially absorbed was considered to be due to the experimental method. Coal of greater than 4 mm in diameter was used in these tests to decrease the effect of surface moisture when the coal was filtered. A mass balance showed that this technique worked adequately.

The percentage increase in moisture content over time is shown in table 5.20, while the average increase is plotted in figure 5.12. It can be seen the average water reabsorption from these tests after 8 weeks was approximately 8%. The average initial moisture contents of the dewatered coal was 36%; after 8 weeks the average moisture content had increased to about 39%. It was found that water reabsorbed slowly over the first few weeks before reaching a reasonably constant moisture content.

TABLE 5.20

Long Term Moisture Reabsorption Characteristics

Coal Dewatered at 300°C for 20 minutes

| Time | Moisture Absorbed in Coal Percentage Increase | | | |
days	Sample 1	Sample 2	Sample 3	Average
Initial Moisture Content %	33.2	38.2	37.0	36.1
1hr	0.5	0.2	0.0	0.3
3hr	1.2	0.0	0.0	0.4
18hr	3.4	1.3	2.2	2.4
2	4.0	1.9	1.9	2.7
3	4.6	1.9	1.9	2.9
7	8.3	4.9	5.3	6.2
21	10.2	6.3	7.5	8.0
56	9.6	6.3	7.5	7.9

Figure 5.12   Water Reabsorption Characteristics

Average Increase in Moisture Content
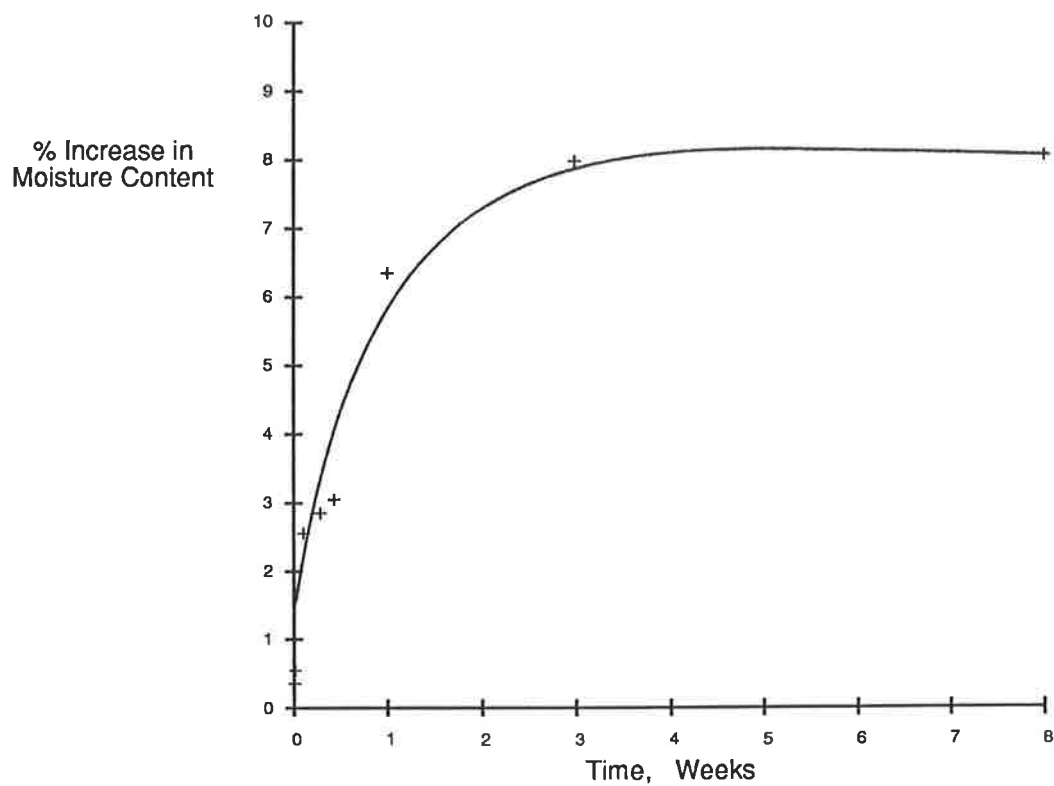
5.8 DISCUSSION ON THE EFFECT OF COAL AGE

During the course of the high-temperature pre-treatment experiments it was noticed that the efficiency of the dewatering process decreased as a function of time. The changes in dewatering characteristics are shown in table 5.21. It can be seen the preliminary results showed that the moisture content in the coal was reduced to 28% when coal was dewatered at 325°C for 20 mins, while in latter test the moisture content of dewatered coal increased up to 40%. While this is a reduction in the effectiveness of dewatering, there is still a significant quantity of water removed as the moisture content is based on a higher quality and more condensed coal particle.

A number of factors which may have caused this variation were investigated, including the effect of coal water ratio, coal size, filtration characteristics and the quantity of coal loaded into the tube bombs. It was found that these effects did not overly influence the extent of dewatering, and they would not cause the large variation in moisture content. Therefore, while the differences may in part be due to the variability of the coal used and to experimental error, it is likely that as coal ages a reaction occurs which retards the extent of dewatering.

The test samples which were used for Bowmans coal was obtained from coal which was removed from a test pit in May, 1982 and sealed in 44 gallon drums. It was subsequently crushed in 1984 for these tests, when the drum was first opened. While the coal first used from this source showed excellent dewatering characteristics, the effectiveness of dewatering appeared to steadily deteriorate over time. Unfortunately as no source of fresh Bowmans coal was available, results had to be based on this coal.

This reduced effectiveness of dewatering coal which had been stored for some period was reported by researchers studying the steam/hot water drying of Canadian lignite for

temperatures up to 400°C. They suspected that oxidation of the run-of-mine coal was the cause. In these tests, the obvious deterioration of dewatering effectiveness after the coal storage drum was opened confirms that oxidation would be the most likely cause.

The physical characteristics of coal dewatered in latter tests also appeared much different from that observed in earlier tests. In the earlier studies coal dewatered at 325°C the coal had a dry surface, and was lightly bonded together - in some instances in large lumps the diameter of the tube bomb. Some lumps of the coal appeared to be bloated or plastically deformed. The coal appeared to be much more brown in colour, and the product liquor yellow. The liquor frothed markedly when the tube bombs were first opened, and the coal adhered to the sides of the tube bomb and was difficult to remove.

Coal in more recent studies appeared to be slightly wet on the surface. While the coal had agglomerated to some extent, it was not bonded together in large lumps, did not appear bloated and did not stick to the sides of the bombs. The coal was black in colour and the product liquor less yellow. The filtering characteristics were very different. While obviously better than raw coal, the dewatered coal slurries in earlier tests appeared to filter more rapidly.

TABLE 5.21

Effect of Coal Age
Dewatered at 325°C for 20 minutes.

Date	Moisture Content %
Oct. 1984*	28
May 1985*	32-36
Nov. 1985*	34-38
Aug. 1986#	32-36
March 1987#	43-45
May 1987^	33-34
Aug. 1987^	36
Nov. 1987^	39-41

*#^ Using sample removed from the
same sealed plastic bag

6. KINETICS OF DEWATERING

6.1 INTRODUCTION

To establish the kinetics of the high-temperature pre-treatment process two models will be fitted to experimental results; a time-temperature equivalence model and a distributed activation energy model. These models will be used to determine the devolatilization kinetics of dewatering. The relationship between moisture and volatile matter removed from the coal during dewatering can be used to establish the kinetics of water removal.

During high-temperature pre-treatment low rank brown coal is transformed into a higher-rank product by processes such as decarboxylation, polymerization and condensation. There are several thermal-dewatering processes that have been the topic of studies concerned mainly with the quantity of water removed and the quality of the coal obtained. However the rates of these processes have not been extensively studied and reported, mainly because the large autoclaves commonly used are not satisfactory for kinetic studies.

It is difficult to establish a mechanism for the chemical kinetics of these processes as there are many reactions taking place. In terms of overall process kinetics these reactions may be modelled by measuring the rate of removal of oxygen (as CO_2 and H_2O) as volatile matter from the coal. While the rate of devolatilization can be modelled, it is difficult to use a kinetic model to study the rate at which water exudes from coal pores as no simple chemical

reaction can be defined for this process. Therefore the rate at which water is removed from coal must be related to a reaction which occurs during dewatering and then kinetically modelling this reaction.

There have been two major studies of the kinetics of thermal dewatering. Boyd (1976) and Stanmore and Boyd (1978) looked at steam thermal dewatering characteristics using lumps of Morwell coal. These results showed that the bulk of dewatering occurs rapidly within the first few minutes of heating; a slow heating rate for large lumps of coal will allow sufficient time for the dewatering mechanisms to occur and water to drain from the coal. In fact, Harrison (1946) and Bainbridge and Satchell (1947) showed that excessive steaming may increase the moisture content of the coal.

Therefore it appears that the rate controlling step for processes such as steam dewatering or the Evans-Siemon process is the heating rate of large lumps of coal. Boyd modelled the heating rates of extruded cylinders of coal, and developed a model based on the heat transfer through these cylinders. In this study it was found that although most of the reaction took place within a very short time, further reaction will take place over much longer time periods. In contrast to steam thermal dewatering where water removal does not appear to continue once process temperature is attained, water removed during high-temperature pre-treatment continues as long as devolatilization occurs until a maximum quantity of water expressed from the coal is reached. Therefore, although the heating rate of coal particles will influence the rate of dewatering, a model which includes the effect of chemical reaction should be developed for the high-temperature pre-treatment process.

Ruyter (1982) studied the kinetics of the hydrothermal coalification process (heat treatment in an autoclave with water) for temperatures from 120°C to 390°C and residence periods from 1 min to 6 months. Hydrothermal coalification can be considered to be similar to Hot Water Dewatering, where coal is slurried with water and heated at saturated steam pressure to prevent the vaporization of water. Ruyter used electrically heated autoclaves

which required some time to reach reaction temperature because of the thermal inertia of the metal mass. Therefore the time for reaction at certain temperatures was corrected for this effect; the residence time at reaction temperature included residence times at lower temperatures as the autoclave was heated.

To model the coalification of low rank material Ruyter used the Steitz and Balazs (1968) solution to basic reaction kinetics by integrating at a certain point in time the reaction rate and the Arrhenius equation. The Steitz and Balazs solution uses the principle of time-temperature equivalence of polymers to predict long term behaviour; this principle means that a short time at a high temperature is equivalent to a long time at low temperature for the same conversion. It is given by:

$$\ln\frac{x_R}{x} = A\,\ln\frac{t}{t_R} + B\left(\frac{1}{T_R} - \frac{1}{T}\right) \qquad \ldots(6.1)$$

where x is the chosen measure of conversion and R the reference conversion. If t_R, T_R, A and B are constants then $\ln t$ is proportional to $1/T$ for the same conversion x. This is the principle of time-temperature equivalence.

In Ruyter's model the oxygen content was used as a variable reflecting conversion, with 'complete' conversion defined as the difference between oxygen in the feed and sub-bituminous coal. By manipulation of equation (6.1) and using data from a number of studies the following equation was developed:

$$f = 50t^{0.2}e^{-\frac{3500}{T}} \qquad \ldots(6.2)$$

where f is conversion, t time (s) and T temperature (K).

While this model adequately describes the behaviour of crystalline polymers by time-temperature equivalence, a model which can describe the actual reaction mechanisms of devolatilization may be more applicable. The thermal decomposition of coal during high-temperature pre-treatment is closely related to conditions which occur when coal is pyrolysed in inert conditions at low temperatures. Therefore the kinetic models which predict the removal of gas from coal during pyrolysis are ideally suited to modelling volatile matter removal during Hydrothermal treatment.

There are a number of methods which have been used to model coal decomposition during coal pyrolysis, generally by using first or nth order kinetics. Recent work on devolatilization in fluidized beds by Agarwal (1984) used the distributed activation energy kinetics of Anthony et al. (1975) and treated overall coal decomposition as a large number of independent, parallel first order processes. In conjunction with heat transfer kinetics this method was found to predict the pyrolysis behaviour of coal very well. The distributed activation energy model uses a pre-exponential factor in the Arrhenius rate expression, and the activation energies of the large number pyrolysis reactions are represented as a Gaussian distribution. The following expressions are used for a non-isothermal particle:

$$\frac{V^o - V}{V^o} = \int_o^\infty \exp\left(-\left(\int_o^t k_o\, e^{-\frac{E}{RT}}\, dt\right)\right) f(E)\, dE \qquad \ldots(6.3)$$

where:

$$f(E) = [\,\sigma(2\pi)^{1/2}\,]^{-1} \exp\left(-\frac{(E - E_o)^2}{2\sigma^2}\right) \qquad \ldots(6.4)$$

This model and the time-temperature equivalence model (equation (6.2)) are used to correlate the dewatering characteristics of Bowmans coal. This model is also used to model the removal of gaseous species from coal during dewatering.

6.2 MODELLING HEATING RATES FOR TUBE BOMBS

Before the dewatering kinetics can be studied adequately, the heating rates of the tube bombs must first be modelled. Although the tube bombs rapidly reach reaction temperature after they are placed in the fluidized sand bath, dewatering occurs as the tube bombs are heated. Therefore the heating rate of the bombs will influence the kinetics of dewatering.

The rate of heating tube bombs in a fluidized sand bath was modelled using a single-capacity lumped system. This model is based on the expectation of a reasonably uniform temperature distribution in the bombs; resistance to heat transfer within the bomb is negligible in comparison to convection resistance at the surface. This can be justified as the coal/water slurry would have a high heat transfer coefficient compared to the coefficient between the sand and stainless steel. Also the mass of the tube bomb is much greater than the reactor contents, and would probably be rate limiting. The mathematical solution to this system is given by the equation:-

$$\frac{T - T_\infty}{T_o - T_\infty} = e^{-\left(\frac{hA}{\rho C_p V}\right)\tau} \qquad ...(6.5)$$

where the time constant is given by:

$$\tau = \frac{\rho C_p V}{hA} \qquad ...(6.6)$$

The time constant (τ) of the system for each temperature was found by a least squares fit of the temperature history of the tube bombs obtained from the chart recorder. Results of this fit are shown in table 6.1, and a plot of the variation of time constant with temperature is shown in figure 6.1. These results shows that the time constant increases as the temperature, therefore it was correlated to a simple first order equation.

$$\tau = BT + C \qquad \qquad ...(6.7)$$

Where B = 0.14

C = 28.7

As the stainless steel in the bombs is approx 10 times the mass of the coal/water slurry, its properties will have greater influence on the time constant. The increase of specific heat in stainless steel with temperature probably causes the variation of the time constant. The fit of this model to the temperature history of a tube bomb, placed in the fluidized sand bath at 300°C, is shown in figure 6.2.

6.3   RESULTS AND DISCUSSION

The equation for the heating rate of the tube bombs was substituted for coal temperature into both model expressions (equations (6.2) and (6.3)). Data used to model the volatile removal from Bowmans coal was obtained from table 5.13.

As the coefficients used by Ruyter in the time-temperature equivalence model were based on conversion of the oxygen in the coal rather than volatile matter, they were recalculated using a Nelder-Mead non-linear parameter estimation program. The equation with calculated parameters for the devolatilization of Bowmans coal were:

$$\frac{V - V^o}{V^o} = 5.5t^{0.12}e^{-\frac{2200}{T}} \qquad \qquad ...(6.8)$$

The results of this fit are shown in fig 6.3. As can be seen this model provides a good fit with experimental results.

Figure 6.4 shows the results of the distributed activation energy kinetic model (equation (6.3)). Again this model gives a reasonable fit with the experimental results. The mean activation energy (E_o) and the standard deviation of activation energy (σ) were optimized for best fit, and the values obtained (as well as those used in other studies) are shown in Table 1. The mean activation energy was found to be slightly lower than those reported for pyrolysis studies on Bowmans Coal. This is probably because at lower temperatures the "easier" devolatilization reactions would occur, and these would be at lower activation energies. While the optimized value of the standard deviation of the activation energy distribution factor was slightly higher than that reported in the other studies, a lower value could have been used without a significant change in the accuracy of the fit.

While both models appear to fit results well, the variation in coal quality and the non-isothermal behaviour of the reactor system makes it difficult to determine which model fits results best. The ability of either model to follow the experimental trends does not justify the validity of the assumptions made to develop the kinetic equations without more fundamental research. Both equations (equation (6.2) and (6.3)) have the same number of adjustable parameters which can be optimized to fit experimental results. However the distributed activation model appeared to be less sensitive the variation in parameters. While the time-temperature equivalence model is simpler, statistically the square of errors between predicted and experimental values are slightly lower in the distributed activation energy model.

Devolatilization is important in modelling the kinetics dewatering, not only because of the production of water by reaction, but also because of the consequent change in surface properties. Heat treating the coal causes shrinkage and pore collapse which results in water exuding from coal pores. Eisenklam (1947) found that there was a linear correlation between water expressed form Victorian brown coals with both the amount of carbon dioxide and the shrinkage of the coal during steam dewatering. Therefore it may be relevant to examine the relationship between devolatilization and the quantity of water removed during high-temperature pre-treatment. This is shown in fig 6.5. As there is a strong relationship between volatile matter and water removed from the coal, it was correlated with a simple 2nd order function:

$$\text{Moisture Removed} = 4.2 \times \text{V.M} - 0.043 \times (\text{V.M.})^2 \qquad ...(6.9)$$
$$(\text{g/g coal d.b.})$$

When fitting this equation it was assumed that it should pass through the origin; ie. if no devolatilization occurs then no moisture is removed. It was also apparent that there is a lower proportion of water removed at higher temperatures although more volatile matter is removed. The maximum quantity of water seems to occur after 50% of the volatile matter is removed. Therefore there may be little value in heating the coal above 350°C to remove more moisture from the coal.

The devolatilization model can be used in conjunction with this correlation to find the rate of water removal from Bowmans coal during high-temperature pre-treatment. A plot of water removal vs reaction time for temperatures between 250 to 350°C using the dissociated activation energy model is shown in fig 6.6. This plot was obtained by first calculating the devolatilization of coal at each reaction temperature, and then finding the corresponding quantity water removed by using equation 6.9. As expected, this method fits the rate of water removed reasonably well within the limits of experimental error.

6.4   PARAMETRIC STUDY OF THE DISTRIBUTED ACTIVATION ENERGY MODEL

It was found that the distributed activation energy was less sensitive to the variation of parameters than the time-temperature equivalence model (which can fit almost any shaped exponential curve). While the parameters for each model were optimized for best fit, the ability of the model to fit the data with only slight variation of the parameters gives some validity to the model. This was done using the distributed activation energy model by varying the standard deviation of the activated energy (σ) and optimizing the mean activation energy by using a Nelder-Mead optimizing program. This is shown in figures 6.7 and 6.8.

These figures show that when the standard deviation is increased the mean activation energy must also increase to achieve a viable fit of the data. This is because devolatilization is less rapid when the activation energy increases, therefore the standard deviation of the activation energy must increase to encompass lower activation energies. The extent of devolatilization with temperature decreases as the activation energy increases.

Also shown in figures 6.9 and 6.10 are the effects of varying the pre-exponential factor in the Arrhenius rate expression. The standard deviation and the mean of the activation energy was least squares fitted to the experimental data using the Nelder-Mead optimization program. The increase in the pre-exponential factor does not appear to influence the fit greatly, and appears to increase the mean activation energy while the standard deviation of the activation energy remains constant. The value of k_o of 1.67×10^{13} is preferred as it is estimated from on theoretical grounds from transition-state theory (Anthony et al., 1975).

The standard deviation of the fit using the various parameters in the distributed activation energy model and experimental data are shown in table 6.3.

6.5   KINETICS OF GAS REMOVAL

The evolution of the various gaseous species from Bowmans coal during thermal dewatering was modelled using the distributed activation energy kinetic model. This model was used in preference to time-temperature equivalence kinetics as it was noticed that there are proportionally more individual components (mainly hydrogen sulphide and methane) removed at high temperatures than at low temperatures, which would invalidate the principle of time-temperature equivalence.

To model the removal of the gaseous species using the distributed activation energy model, the equation was slightly modified for each individual component removed during devolatilization.

$$X = \frac{V^o_{species} - V_{species}}{V^o_{species}} = \int_o^\infty \exp -\left(\int_o^t k_o e^{\frac{-E}{RT}} dt \right) f(E) dE \qquad ...(6.10)$$

where X is the fraction of total species removed in the volatile matter, and $V^o_{species}$ is the total quantity of each species removed during devolatilization. The Gaussian distribution factor is given by

$$f(E) = [\sigma(2\pi)^{1/2}]^{-1} \exp\left(-\frac{(E - E_o)^2}{2\sigma^2} \right) \qquad ...(6.4)$$

The above equation can be further modified to account for contributions from different clustered sources

$$X_{avg} = \sum_{i=1}^n V^*_i X \qquad ...(6.12)$$

where V_i^* is the fractional maximum yield of the ith cluster of sources in the volatile matter. While the assumption of clusters is useful to kinetically model the removal of components during pyrolysis reactions, it does not appear to be necessary for dewatering.

The total quantity of each species evolved during devolatilization has not been determined for Bowmans coal, therefore a value for use in the model was estimated. The estimations were based on results of pyrolysis studies at temperatures up to 700°C (AMDEL, 1981), and a number of assumptions. The major assumptions made were:

1) All the organic sulphur in the coal is removed from the coal as hydrogen sulphide.

2) There would be only slight increase in the quantity of carbon dioxide evolved at temperatures above 700°C.

3) The water evolved during devolatilization is only due to decarboxylation reactions; and the ratio of water to carbon dioxide is 1.0:1.35.

4) The ratio of carbon monoxide and methane evolved from the coal does not change at temperatures above 700°C.

5) The yields of light hydrocarbons, with the exception of methane, are insignificant.

While these assumptions are obviously not totally accurate, they will enable the estimation of yields of species during devolatilization with reasonable accuracy. These results will be used to indicate whether the distributed activation model can fit the dewatering kinetics adequately, or whether further study is warranted to accurately determine yields of species during devolatilization. A table showing the estimated maximum yields of the major components evolved during devolatilization is shown in Table 6.4.

The activation energy and the standard deviation of the Gaussian activation energy distribution were optimized for best fit using the experimental data and the maximum yield of

each gas. The pre-exponential factor used was the same as used for devolatilization modelling. The values obtained for dewatering is shown in table 6.5, while plots showing the fit of this model to experimental data are shown in figures 6.11 to 6.14.

These results show that the distributed activation energy kinetics satisfactorily model the removal of carbon dioxide (and associated water from this reaction), methane and hydrogen sulphide. Unfortunately, the evolution of carbon monoxide during dewatering decreased with time, and therefore could not be fitted to the kinetic model. The values of the activation energies for these compounds are consistent with those found in other studies. However, as results in other studies were based on devolatilization at much higher temperatures, the parameters obtained for dewatering are, as expected, slightly different.

6.6   CONCLUSIONS

Both proposed models, time-temperature equivalence and distributed activation energy, adequately fit the devolatilization characteristics of Bowmans Coal during high-temperature pre-treatment. While the experimental results were not accurate enough to determine which equation fitted the data more accurately, the distributed activation energy model was less sensitive to the adjustable parameters and provided a slightly better fit. It is significant that this model uses similar values for its adjustable parameters when applied to the study of pyrolysis reactions. This equation is able to model volatile evolution from coal for temperatures well above the dewatering reaction temperatures.

It is also significant that there appears to be a strong correlation between the volatile matter and water removed during dewatering. This relationship enables the modelling of the rate of water removal using devolatilization kinetics.

The distributed activation energy kinetic model was able to satisfactorily model the evolution of most of the gaseous species from the coal during dewatering. However, the removal of carbon monoxide was not able to be fitted to any model as its behaviour during dewatering was unusual.

TABLE 6.1

Time Constant at each Temperature

Temperature °C	Time Constant τ sec
150	52.0
200	59.7
250	60.5
275	58.1
300	68.3
325	77.3
350	68.5

TABLE 6.2

Kinetic Parameters used in Distributed Activation Energy Model

	E_o kJ mol^{-1}	σ kJ mol^{-1}	k_o s^{-1}	Reference
Bowmans Lignite	212	53	1.67×10^{13}	Present Study
Bowmans Lignite	240	40	1.67×10^{13}	Wildegger-Gaissmaier (1988)
Mississippi Lignite	192	40	1.67×10^{13}	Agarwal (1984)
Victorian Lignite	220	40	1.67×10^{13}	Agarwal (1984)

TABLE 6.3

Parametric Study

Square of Residuals between the Kinetic Models

and Experimental Data

E_o kJ mol^{-1}	σ kJ mol^{-1}	k_o s^{-1}	Square of Residuals
212	53	1.67×10^{13}	0.014
205	40	1.67×10^{13}	0.025
225	70	1.67×10^{13}	0.021
200	51	1.67×10^{12}	0.015
223	51	1.67×10^{14}	0.014
Time-Temperature Equivalence Model			0.024

TABLE 6.4

Maximum Yield of Species Evolved in the Volatile Matter

Component	Yield g/100g Coal d.b.	% of Total Volatile Matter
CO_2	14.1	28.4
H_2O	10.4	20.9
CO	14.9	30.0
CH_4	6.6	13.3
H_2S	3.7	7.4

Table 6.5

Kinetic Parameters for the Evolution of Gaseous Species
from Bowmans Coal during Thermal Treatment

		Parameters for Pyrolysis of Bowmans Coal Wildegger-Gaissmaier (1988)			Parameters for Dewatering
CO_2	Sources	1	2	3	1
	V_i^*	0.2	0.6	0.2	1.0
	E_o (kJ mole^{-1})	180	236	300	177
	σ (kJ mole^{-1})	16.6	25	27.4	39.5
	$\log_{10} k_o$	14	14	14	13.22
CO	Sources	1	2		-
	V_i^*	0.33	0.66		
	E_o (kJ mole^{-1})	216	300		
	σ (kJ mole^{-1})	28.8	26.7		
	$\log_{10} k_o$	13.22	13.22		
CH_4	Sources	1	2		1
	V_i^*	0.5	0.5		1.0
	E_o (kJ mole^{-1})	230	230		248
	σ (kJ mole^{-1})	12.5	25.0		28.8
	$\log_{10} k_o$	14.23	12.23		13.22
H_2S	Sources		-		1
	V_i^*				1.0
	E_o (kJ mole^{-1})				213.5
	σ (kJ mole^{-1})				27.6
	$\log_{10} k_o$				13.22

Figure 6.1   Lumped-Heat-Capacity Analysis of Tube Bombs

Time Constant vs Temperature
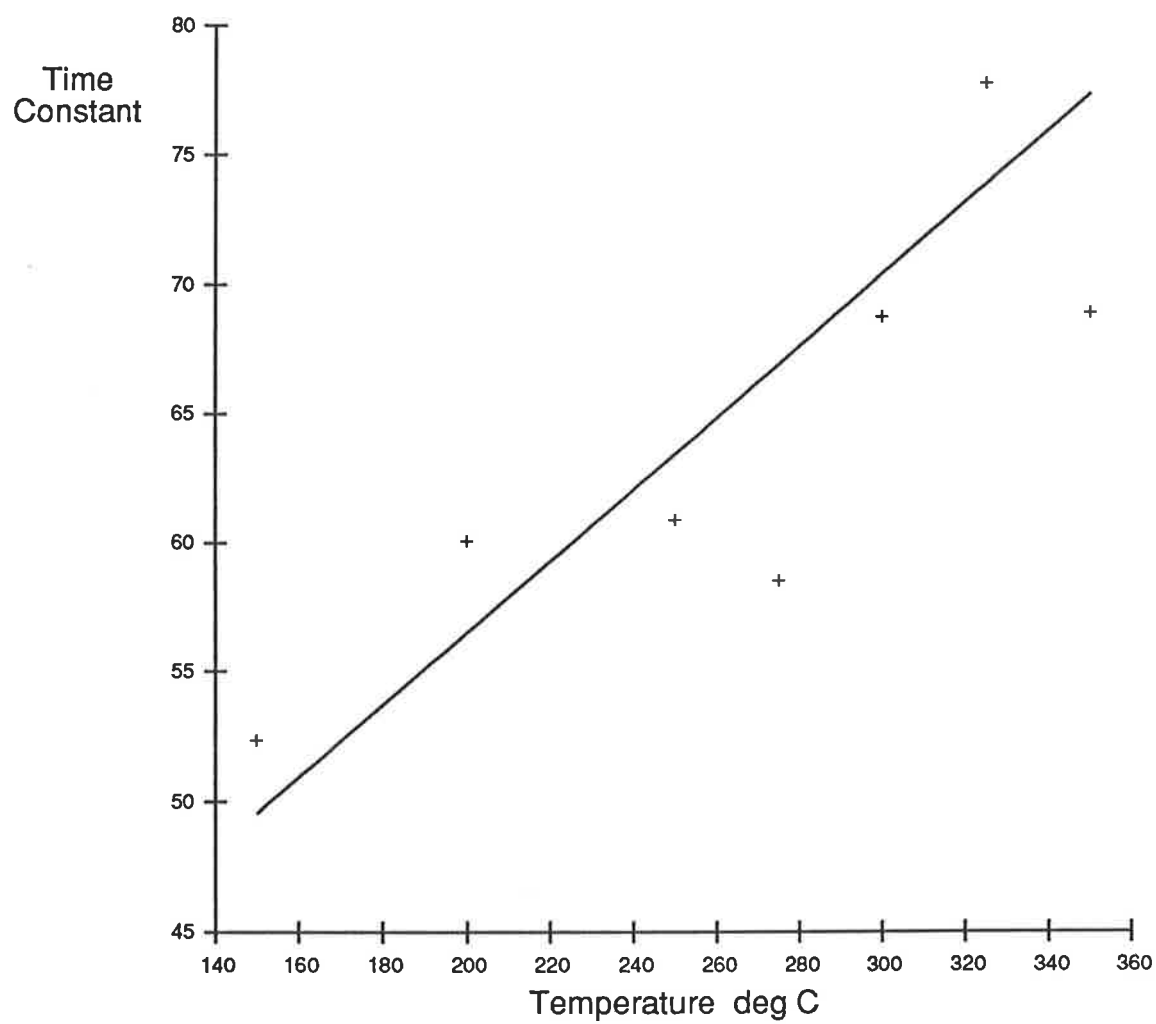
Figure 6.2 Lumped Analysis of Tube Bomb Heating Rate
Temperature 300 deg C
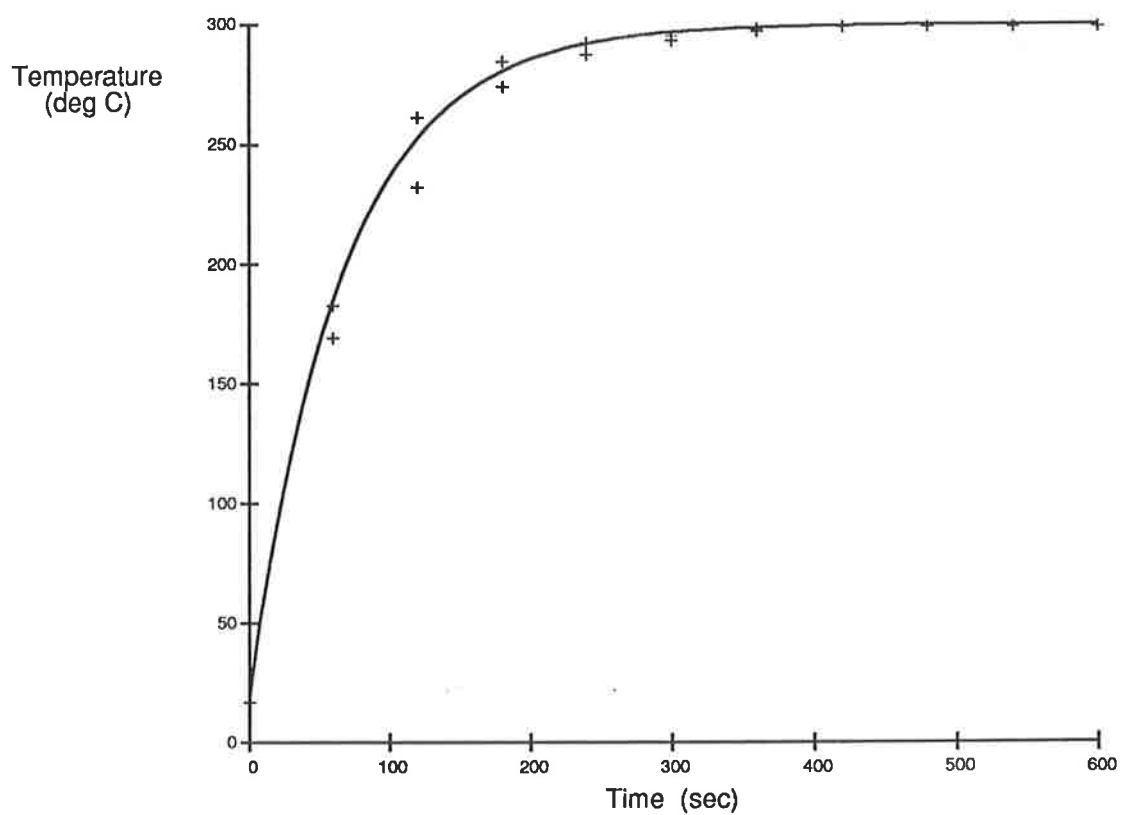
Figure 6.3 Time-Temperature Equivalence Model
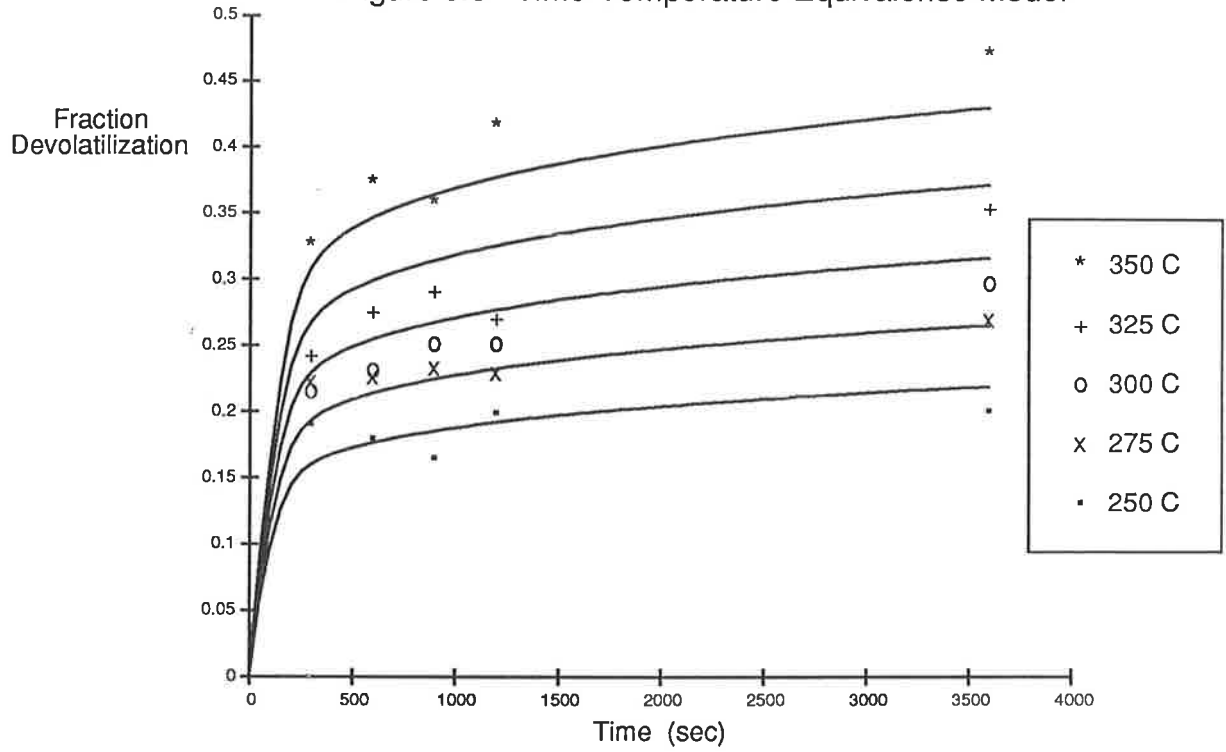
Figure 6.4 Distributed Activation Energy Model
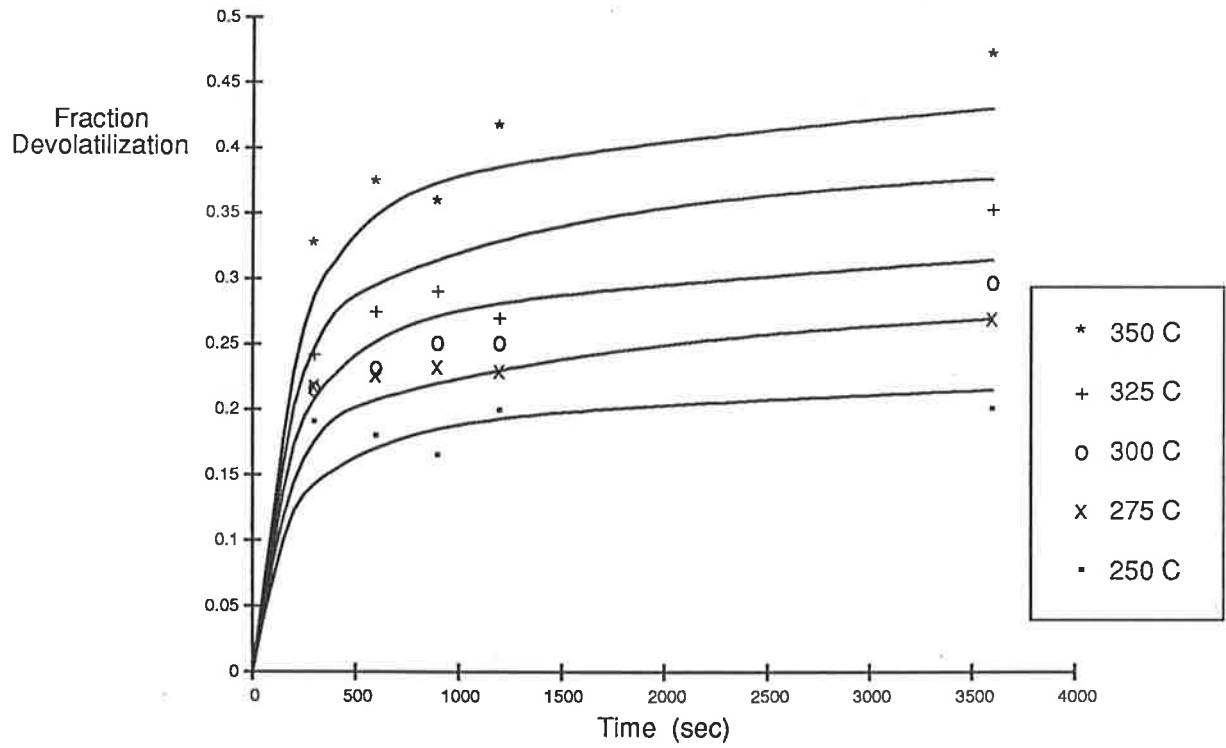
Figure 6.5   Correlation between Moisture and Volatile Matter Removed
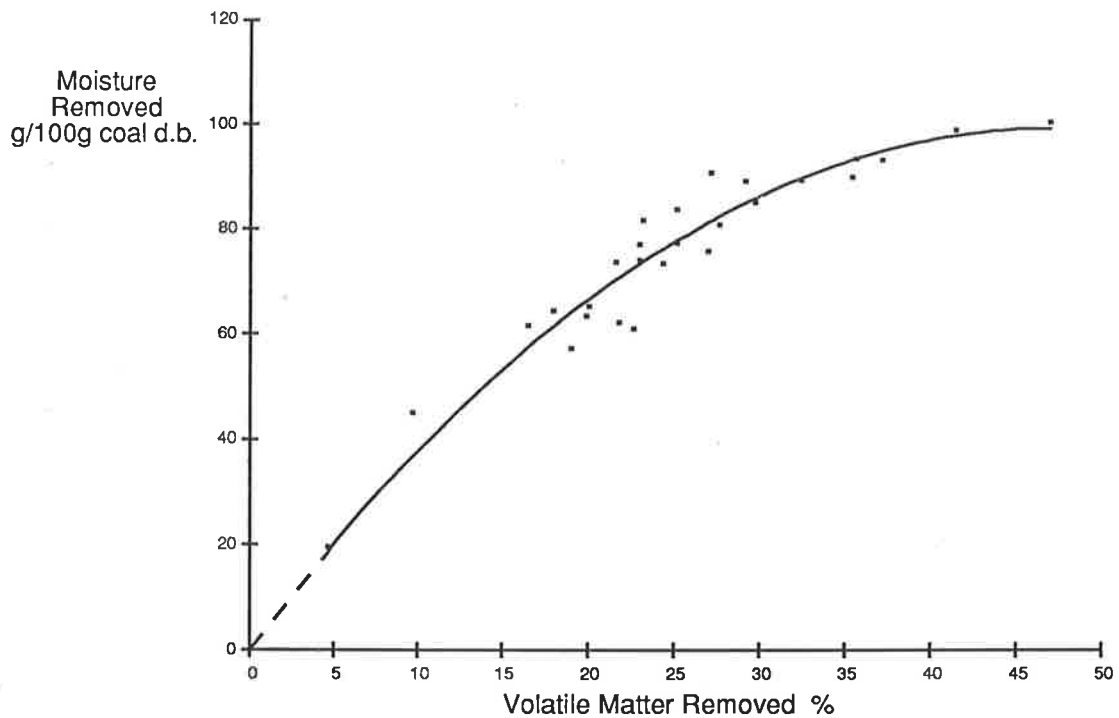
Figure 6.6 Distributed Activation Energy Model used to fit Moisture Removal
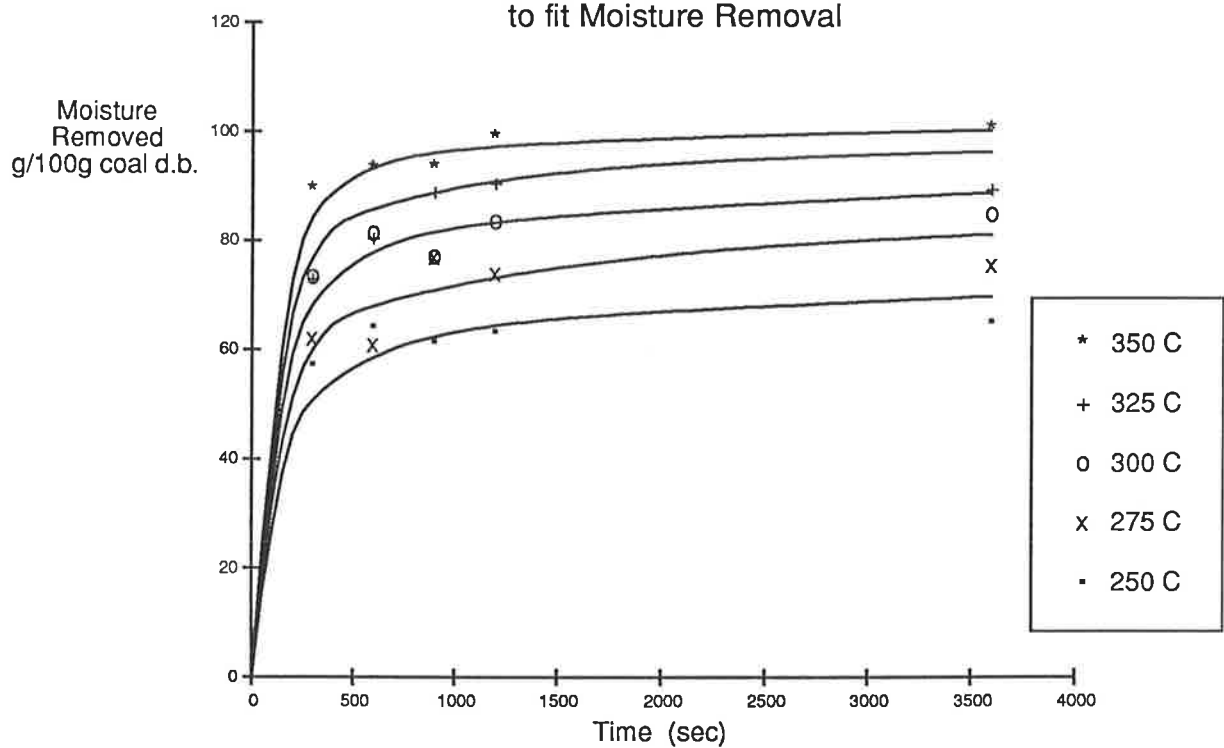
Figure 6.7 Parametric Studies

Fraction Devolatilization

E=205 σ=40 k=1.67E13

*	350 C
+	325 C
o	300 C
x	275 C
·	250 C

Time (sec)
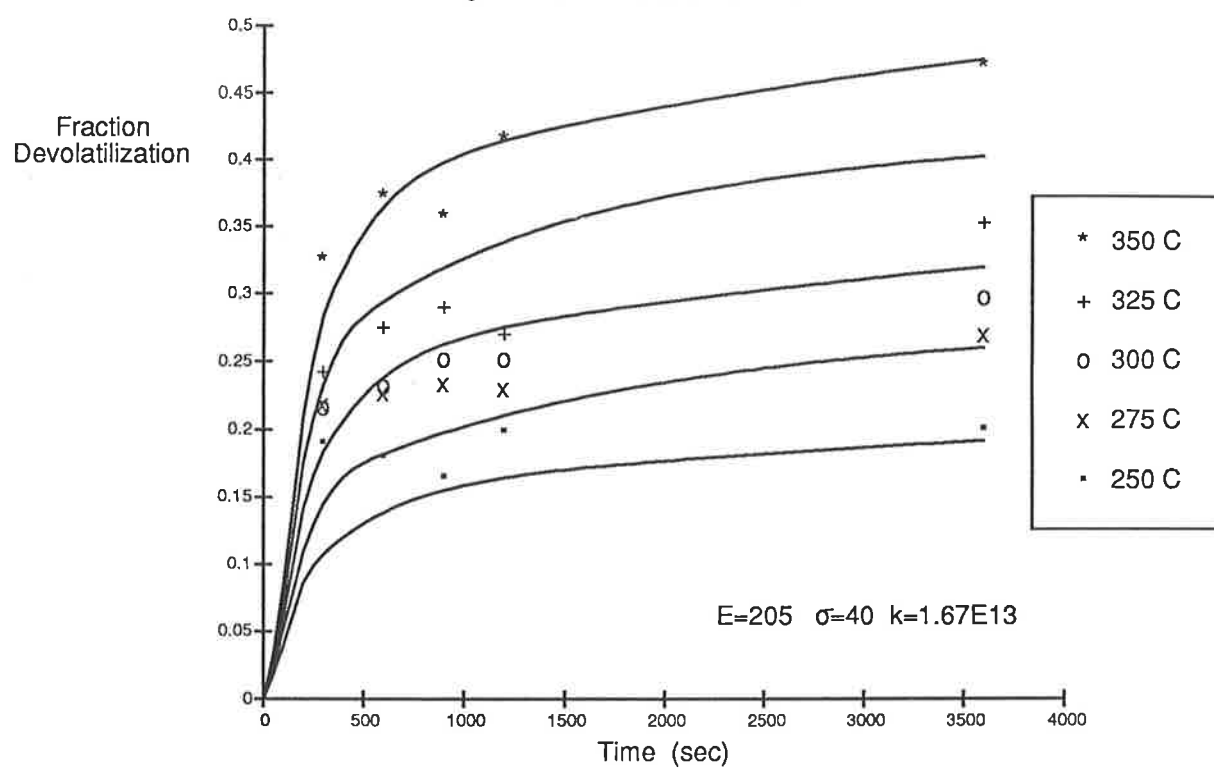
Figure 6.8 Parametric Studies

Fraction Devolatilization

E=225 σ=70 k=1.67E13

*	350 C
+	325 C
o	300 C
x	275 C
·	250 C

Time (sec)
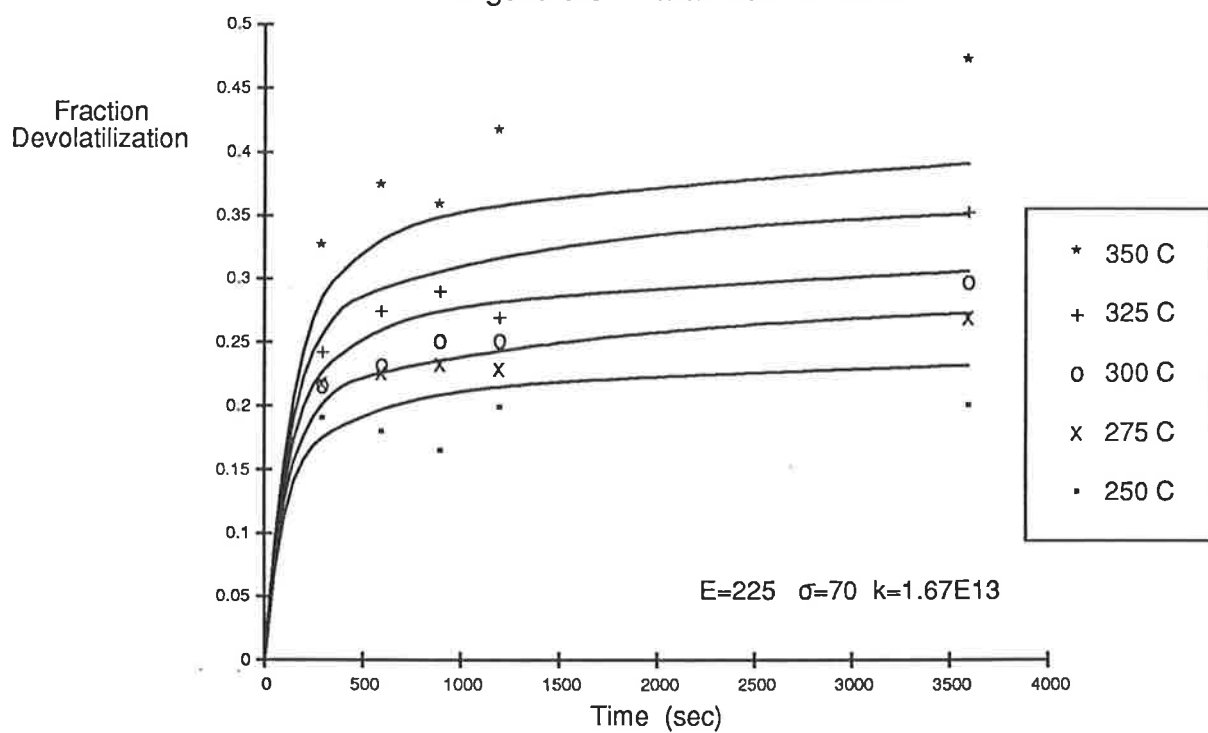
Figure 6.9 Parametric Studies

Fraction Devolatilization

*	350 C
+	325 C
o	300 C
x	275 C
·	250 C

E=200 σ=51 k =1.67E12

Time (sec)
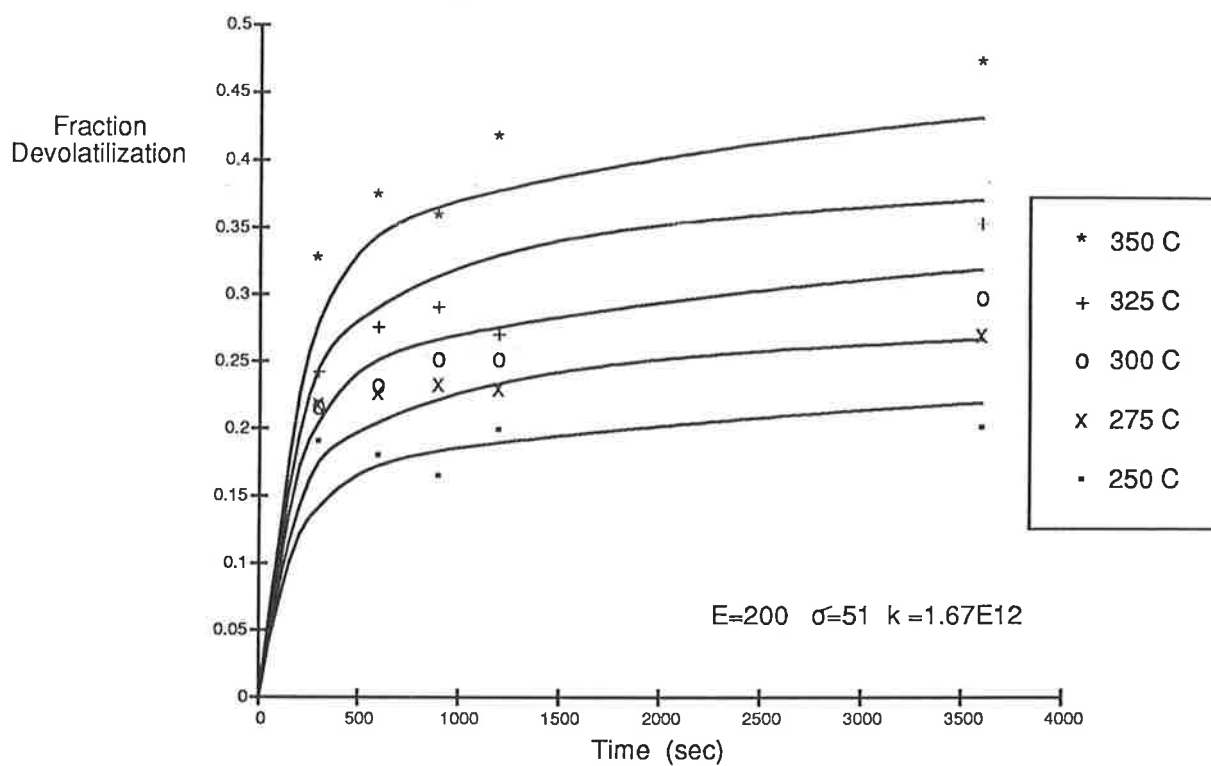
Figure 6.10 Parametric Studies

Fraction Devolatilization

*	350 C
+	325 C
o	300 C
x	275 C
·	250 C

E=220 σ=51 k =1.67E14

Time (sec)
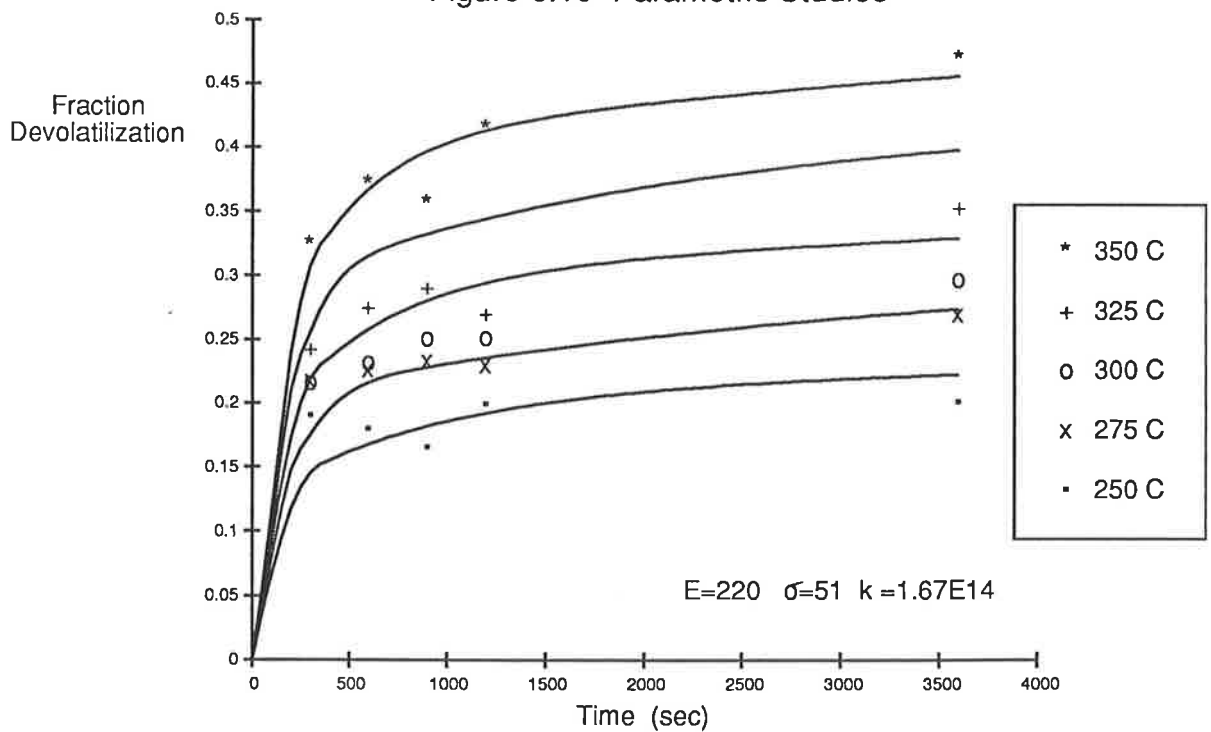
Figure 6.11 Carbon Dioxide Removed

E=177   σ=39.5 k =1.67E13
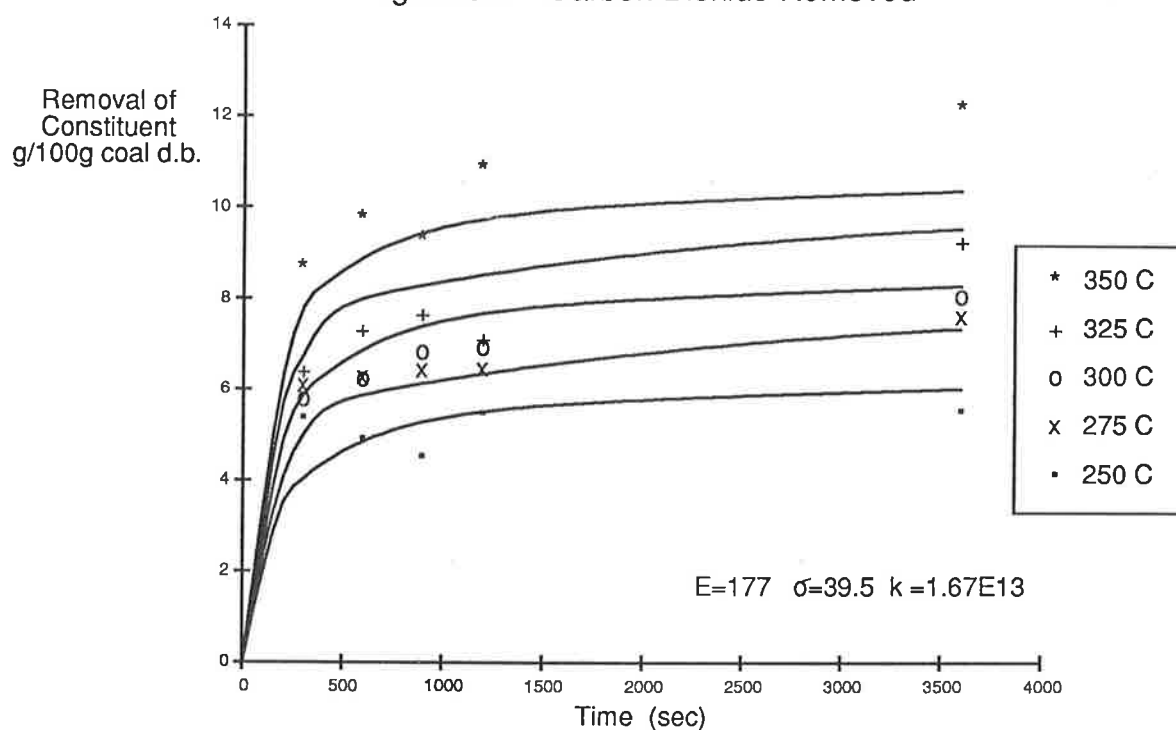
Figure 6.12 Hydrogen Sulphide Removed

E=213.5   σ=27.6 k =1.67E13
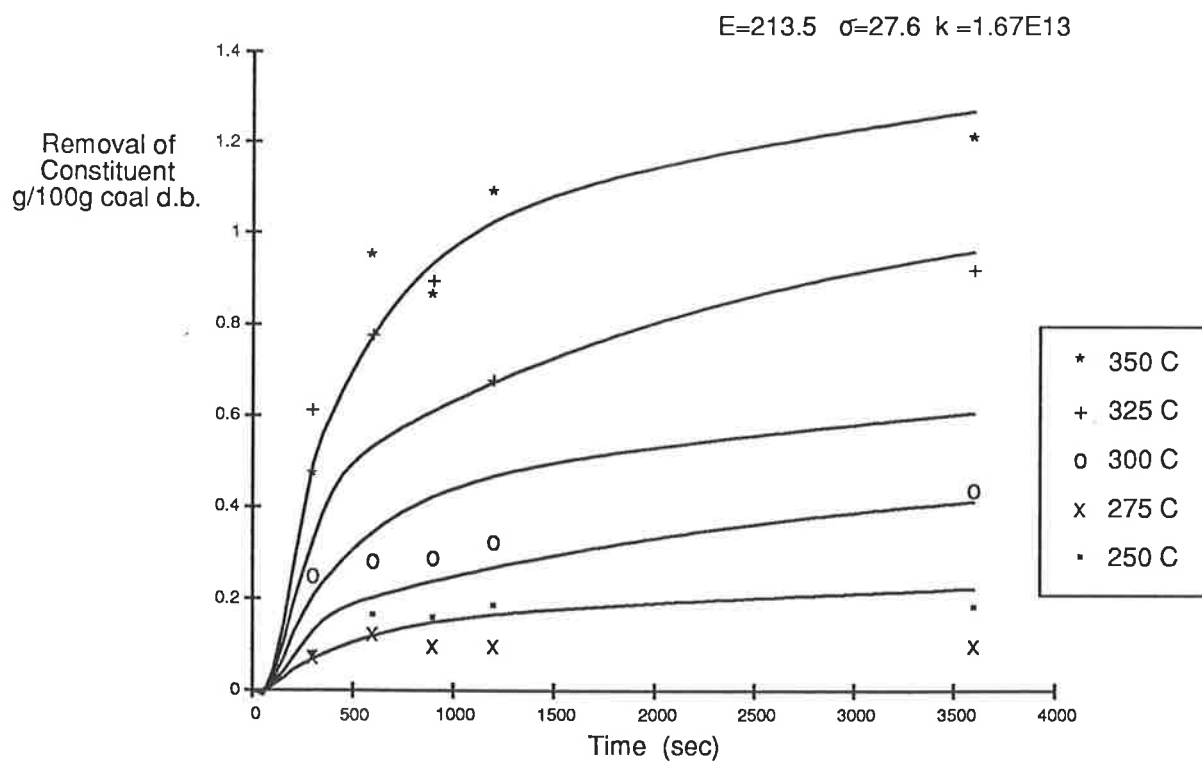
Figure 6.13   Carbon Monoxide Removed
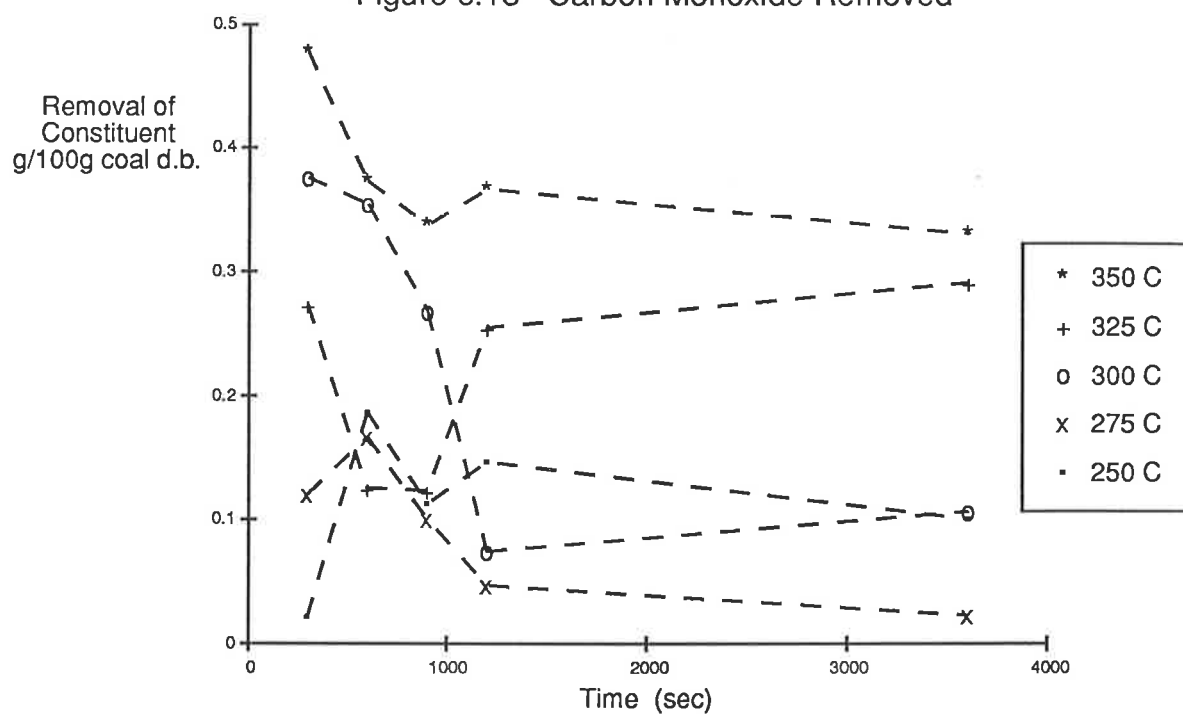
Figure 6.14   Methane Removed

E=248   σ=28.8   k =1.67E13
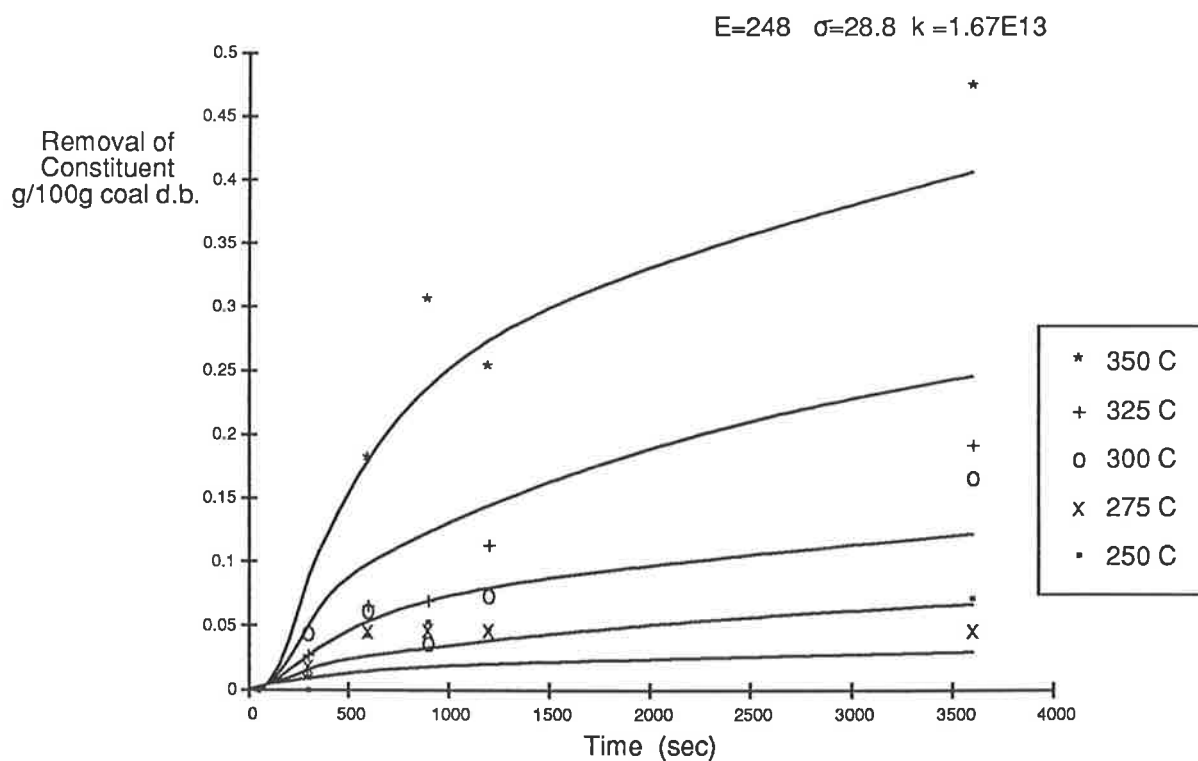
7. MECHANISMS AND STRUCTURAL CHANGES

7.1   INTRODUCTION

The exact mechanisms which occur during high-temperature pre-treatment of lignite have not yet been determined. However, for the expulsion of water while steam dewatering coal, Klein (1930) proposed 5 possible mechanisms:

1.   Coal shrinkage expels water from contracting pores.

2.   Differential expansion of the coal and water causes water to be forced from the pores.

3.   Surface modification changes the coal character from hydrophilic to hydrophobic in nature.

4.   Reduced water viscosity at higher temperatures allows the water to run freely from the coal.

5.   As the carbon dioxide is expelled from the coal it forces water from the pores.

It has been reported that steam thermal dewatering at temperatures up to 300°C will not remove more water after the reaction temperature is reached (Boyd, 1976). Prolonged steaming may actually increase the moisture content of the product (Harrison (1946); Bainbridge and Satchwell (1947). It was also noted by Allardice (1973) that more water was

expressed from the coal by thermal expansion of water during Fleissner processing than can be attributed to shrinkage of the coal. Therefore it can be concluded that coal shrinkage does not play a significant role in the extent of moisture removal during steam thermal dewatering.

In this study of the high-temperature pre-treatment of Bowmans coal it was found that moisture continues to be exuded after the reaction temperature is reached (chapter 5.5.1). Thus the mechanisms governing the extent of moisture removal during steam thermal dewatering are probably not applicable to high-temperature pre-treatment.

The most significant means of removing moisture from the coal during high-temperature pre-treatment is due to the permanent shrinkage of the coal structure. The shrinkage of the coal structure will alter the water holding capacity of the coal, and moisture is not significantly reabsorbed during cooling. There is much controversy as to whether the shrinkage of the coal structure causes the removal of water or is a consequence of it. The mechanisms which cause shrinkage of coal during dewatering at temperatures up to 300°C have been postulated by Murray and Evans (1972) and are discussed in detail in Boyd (1976).

It was also suggested by Willson (1985) that the higher temperatures of Hot Water Dewatering causes a tar or wax to form and block pores which stops water from re-entering the coal. This tar may also coat the coal surface, creating a hydrophobic surface that will aid in water repulsion (Potas, Sears, Maas, Baker and Willson, 1986).

The coal surface turning hydrophobic in nature will influence the filtration characteristics of the coal. A hydrophobic surface will reduce the filter cake resistance of dewatered coal and will therefore lower the residual moisture content of the filter cake.

Modification of the coal surface from hydrophilic to hydrophobic in nature occurs when carboxyl functional groups are destroyed at high temperatures. The carboxyl groups cause

water to bind to the coal surface in micelles due to hydrogen bonding. Decarboxylation, which breaks down these groups, begins at low temperatures (about 180°C) and increases rapidly above this temperature (Murray and Evans, 1972). Sodium, which can be attached to the carboxylate functional group, is released on the breakdown of these groups into the aqueous phase. The degree of association of cations with carboxyl groups in coal influence the equilibrium moisture content of a coal (Schafer, 1972).

It has been reported that more CO_2 can be released from the salt form of carboxylate groups in coal than can be determined by the carboxyl groups present (Schafer, 1979). Therefore it appears that different reactions will occur in coal depending on the nature of carboxyl groups present. Whether the carboxyl groups are in the salt and acid form may influence the dewatering ability of the coal. The involvement of other water-binding functional groups such as phenolic groups has still to be determined. However these groups appear to be stable to temperatures of about 300°C (Drohan, 1977).

In this study the changes to coal structure following dewatering were examined by using Infrared and Nuclear Magnetic Resonance Spectroscopic methods. The sodium environments in the coal and the removal of this element form the coal during dewatering was studied using Sodium Nuclear Magnetic Resonance.

7.2   FOURIER TRANSFORM INFRA-RED SPECTROSCOPY

7.2.1   Introduction

The introduction of computerized Fourier Transform infra-red spectroscopy has renewed interest the in use of infra-red to determine the structural characteristics of coal (Painter et al., 1981; Tooke and Grant, 1982). This is due to the increased resolution possible from co-adding large numbers of interferograms to give markedly better spectra than can be obtained by dispersive instruments. The improved resolution makes FT-IR an important analytical tool to quantitatively determine functional groups such as aromatic, aliphatic, carboxylate and phenolic groups, as well as the mineral matter in coal (Painter et al., 1978, Riesser et al., 1984; Starsinic et al., 1984). This technique has been used to determine changes occurring to coal during liquefaction, pyrolysis, oxidation and carbonization.

Of particular interest in the dewatering reaction is the nature of the carboxyl functional group, either in the acid or salt form. The breakdown of these groups is thought to be a major contributing factor in the dewatering reaction, and its form may determine the quantity of water removed from the coal. It has been determined that more CO_2 is evolved from the coal during pyrolysis when carboxylate groups are in the salt form (Schafer, 1979), and the quantity released can not be related to the destruction of carboxylate groups alone. Obviously a further reaction takes place when carboxylate salts are present, which may determine the propensity of a coal to dewater. Also of interest is the stability of hydrophilic phenoxy groups at dewatering temperatures, as it is not certain whether these groups are involved in the dewatering reaction.

The use of FT-IR to determine functional groups in coal, especially the carboxylic and carboxylate salt forms, and to determine changes which occur to these groups during high-temperature pre-treatment would prove invaluable. The relative ease of detecting

carboxylate groups by FT-IR has shown that traditional methods of analysis have produced erroneous results (Starsinic et al., 1984). This study was undertaken to investigate the possibility of using infra-red spectroscopy to quantitatively determine the carboxylate and other functional groups present in the coal, and to use the results in conjunction with FT-NMR to assist in determining structural changes which takes place in Bowmans coal during thermal treatment.

7.2.2 Experimental

Spectra were obtained using a Digilab Model FTS-15E spectrometer with on line mini computer. Typically either 100 scans or 500 scans were co-added per sample at a resolution of 2 cm⁻¹. As the primary objective of this experiment was to determine functional groups in Bowmans coal on a qualitative basis, the small numbers of scans co-added and the amount of sample used for analysis would not be ideal for a quantitative estimate of functionality in Bowmans coal.

In any study using FT-IR on coal samples it is important to establish reliable methods of preparing samples to get optimum results. Therefore a series of experiments were undertaken to find a reliable method of sample preparation. Two methods of analysis were attempted:-

1) Employing the conventional technique of coal pressed in a halide matrix. The samples for analysis were prepared by dispersing 1.4 mg of coal in 200 mg of KBr.

2) Using diffuse reflectance (DRIFTS) of powdered coal ground with KBr (Anacreon R.E. 1982; Fuller et al., 1982). Initially the spectra were obtained from raw coal, and coal ground with varying percentages of KBr. It was found that about 5% coal in KBr gave the best results.

Raw, air dried and dewatered coal samples were used in this study; the coal was dewatered for 20 minutes at temperatures of between 250°C and 350°C. The spectrum of coal dried in air for 3 days was obtained to investigate changes which may occur to coal when exposed to the atmosphere for long periods of time. The coal particle size used in the samples was reduced from 495 μm by grinding with mortar and pestle for 2 mins.

7.2.3   Results and Discussion

Although the analysis of coal was much quicker and simpler using DRIFTS, it was found that the results obtained using this method did not appear to show as much spectral detail compared to spectra obtained by using pressed disks. Therefore spectra for the series of dewatered coal samples were obtained using pressed halide disks.

The complete interpretation of spectra requires using sophisticated spectral manipulation techniques that a mini-computer is uniquely able to perform. These techniques include methods such as baseline smoothing, spectral subtraction and taking first and second derivatives of spectra. Without these methods some of the less discernible features in spectra can not be seen clearly. Unfortunately many of these techniques were not able to be performed on these spectra. Therefore only a general trend of changes following the dewatering reaction can be observed from the spectra obtained.

Typical band assignments of functional groups that are of importance to this study are shown in table 7.1. The most important regions of the spectra to note in this study are around the 1700 cm^{-1} band, which is due to carboxylic acid COOH groups, the 1700-1600 cm^{-1} region due to C=O carbonyl groups, and the 1560 cm^{-1} peak which corresponds to carboxylate salt COO^{-} groups. Also of interest is the effect of dewatering on phenoxy groups in the 1300 to 1110 cm^{-1} region of the spectra, and the 1100 to 1000 cm^{-1} region of aliphatic ethers and alcohols.

Shown in figure 7.1 is a comparison between the diffuse reflectance spectra of raw coal and coal dewatered at 320°C. It is important to note that each spectrum is at a different scale, therefore no direct comparison can be made of the relative amounts of each component in the coal. However it is obvious that much change has occurred in the coal following thermal treatment, especially in the region of oxygenated functional groups between 1700 to 1000 cm^{-1}. The carboxylic acid characteristic band at 1710 cm^{-1} can easily be seen on the left hand side of the broad 1650 cm^{-1} carbonyl peak. However the carboxylate salt absorbance peak, which would appear to make the broad carbonyl band asymmetric, is not noticeable without spectral manipulation.

As can be seen in the difference spectrum in figure 7.2, the dewatering reaction appears to removes carboxylic groups at 1709.9 cm^{-1}, as well as the carbonyl groups at 1600.9 cm^{-1}. Dewatering also appears to remove many groups in the 1450 to 1200 cm^{-1} region, while the region between 3000 to 1800 cm^{-1} appears to be enhanced. Again the absorbance of carboxylate salts can not be seen in the spectrum.

Figure 7.3 shows the absorbance spectrum of raw coal in pressed KBr disks. Two different coal samples were used to obtain these spectra, and the similarity between separate samples is obvious. Again it must be noted that the scale for each spectrum is different, and comparison between spectra must be made by considering the relative peak heights of each functional group. From the spectra it is obvious that Bowmans coal is heavily oxygenated, as large peaks are present of carbonyl at 1600 cm^{-1}, and ether and alcohol functional groups are present at 1100 cm^{-1}. Both of the carboxyl functional groups can be distinguished overlapping the strong carbonyl peak. The carboxylic acid group is present as a as a shoulder on the carbonyl peak at 1700 cm^{-1}, while the carboxylate salt appears to make the carbonyl peak asymmetric at 1580 cm^{-1}. Note that the presence of absorbed water in the KBr matrix hides an O-H stretching region at 3300 cm^{-1}. Although by drying the KBr disk in an oven for long periods can remove this band, the effect of drying on the functional groups in coal could not be determined with limited use of the FT-IR.

The effect of air drying Bowmans coal can be seen in figure 7.4. The coal has been changed dramatically, with a large increase in carbonyl groups in the 1730-1670 cm^{-1} region of the spectrum, and an increase in ether and alcohol groups in the 1100 to 1000 cm^{-1} regions. Much of the 1400 cm^{-1} region of the spectrum appears to have been removed, perhaps indicating that chain terminating methyl groups have been oxygenated. The large peaks in the 2400 cm^{-1} part of the spectrum may be from carbon dioxide not completely purged from the spectrometer before analysis was taken.

Figures 7.5 to 7.9 show the effect of increasing the dewatering temperature on the FT-IR spectra of Bowmans coal. It must be noted that the following observations made regarding the dewatered coal spectra are made without spectral manipulation techniques, and are therefore very general in nature.

The spectrum of coal dewatered at 250°C, figure 7.5, appears to be only slightly changed from the spectrum of raw coal. The main difference appears to be the 1100 cm^{-1} region of the spectrum where much of the peak has been depleted. It is difficult to assign a particular functional group to this peak, although it is in the aliphatic ether or alcohol region of the spectrum. While it could be silicate absorption in the mineral matter of the coal, it is more likely an aliphatic ether band which is broken as condensation of the aliphatic structures occur. This is likely to be due to devolatilization and shrinkage reactions.

From this spectrum it was noted that the broad band between 2800 cm^{-1} and 3500 cm^{-1} has substantially diminished, perhaps indicating a decrease in hydroxyl concentration in the coal or a decrease in the water present in the KBr matrix. The carbonyl band at 1700 to 1600 cm^{-1} also appears to have diminished, indicating that decarbonisation is taking place in the coal. It is also apparent that methyl groups in the 1375 cm^{-1} region of the spectrum have decreased, indicating that these groups are removed during dewatering.

Figure 7.6 again shows little change compared with the raw coal spectrum following dewatering at 275°C, and appears to be similar to the 250°C spectrum. The broad band at 2800 to 3500 cm^{-1} has increased slightly, while the carbonyl peak at 1600 cm^{-1} now appears to be more symmetrical, perhaps indicating that carboxylate salts have been removed from the coal.

The spectra of dewatered coal from 300°C to 350°C, figures 7.7 to 7.9, exhibit similar characteristics. Generally they show a gradual decrease in the carbonyl group band at 1600 cm^{-1}, the carboxylic acid peak at 1700 cm^{-1}, and the gradual destruction of the 1100 cm^{-1} band.

The mineral bands in Bowmans coal can also be noted in some spectra at 850, 820, 760, 660, 600 and 520 cm^{-1}, as well as a large absorbance in some of the samples at 450 cm^{-1}. Although some of these bands may also correspond to bending in aromatic groups or to water in the coal, the carbon aromaticity in Bowmans coal is low and it is more likely that the strong peaks would be mineral groups. The large absorbance at 450 cm^{-1} would correspond to quartz, while other minerals which could be assigned to these bands are illite, sodium montmorillonite, or gypsum.

7.2.4 Conclusions

From the spectra obtained it is apparent that there is greater change in functionality at higher processing temperatures. At 250 and 275°C, which correspond to the temperatures used in the Evans-Siemon thermal dewatering process, there is little change in carbonyl and carboxylic acid groups, while there appears to be a general decrease in carboxylate salt groups and a decrease in the concentration of an unknown group tentatively identified as a aliphatic ether at 1100 cm^{-1}. As temperatures are increased further, there is much greater decrease in all the oxygen containing functional groups and a termination of methyl groups in the coal structure.

TABLE 7.1

Infra-Red Band Assignments for Functional Groups in Coal

(Painter, Snyder, Starsinic, Coleman, Kuehn and Davis, 1981)

Wavelength cm^{-1}	Functional Group Assignment
3030	Aromatic C-H
2950	CH_3
2920 & 2850	Aliphatic -CH, CH_2, CH_3
1735	C=O, ester
1720-1690	C=O, ketone, aldehyde, -COOH
1650-1630	C=O highly conjugated
1600	Aromatic ring stretching
1590-1560	Carboxyl group in salt form -COO⁻
1490	Aromatic ring stretching
1450	CH_2 and CH_3 bending
1375	CH_3 groups
1300-1110	Phenoxy C-O stretch and O-H bending
1100-1000	Aliphatic ethers, alcohols

WAVENUMBERS
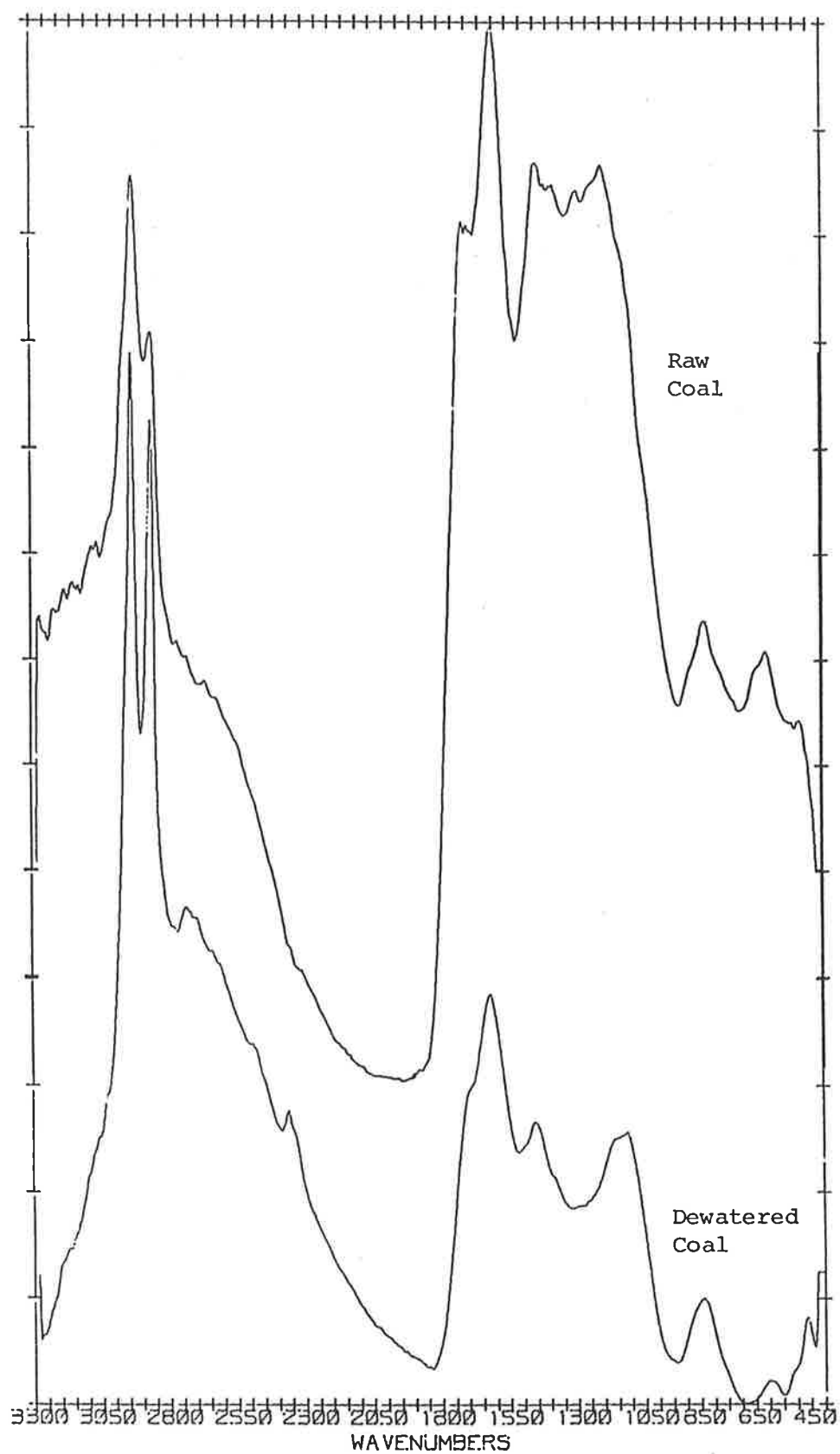
Figure 7.1 "DRIFTS" Spectra of Raw and Dewatered Coal
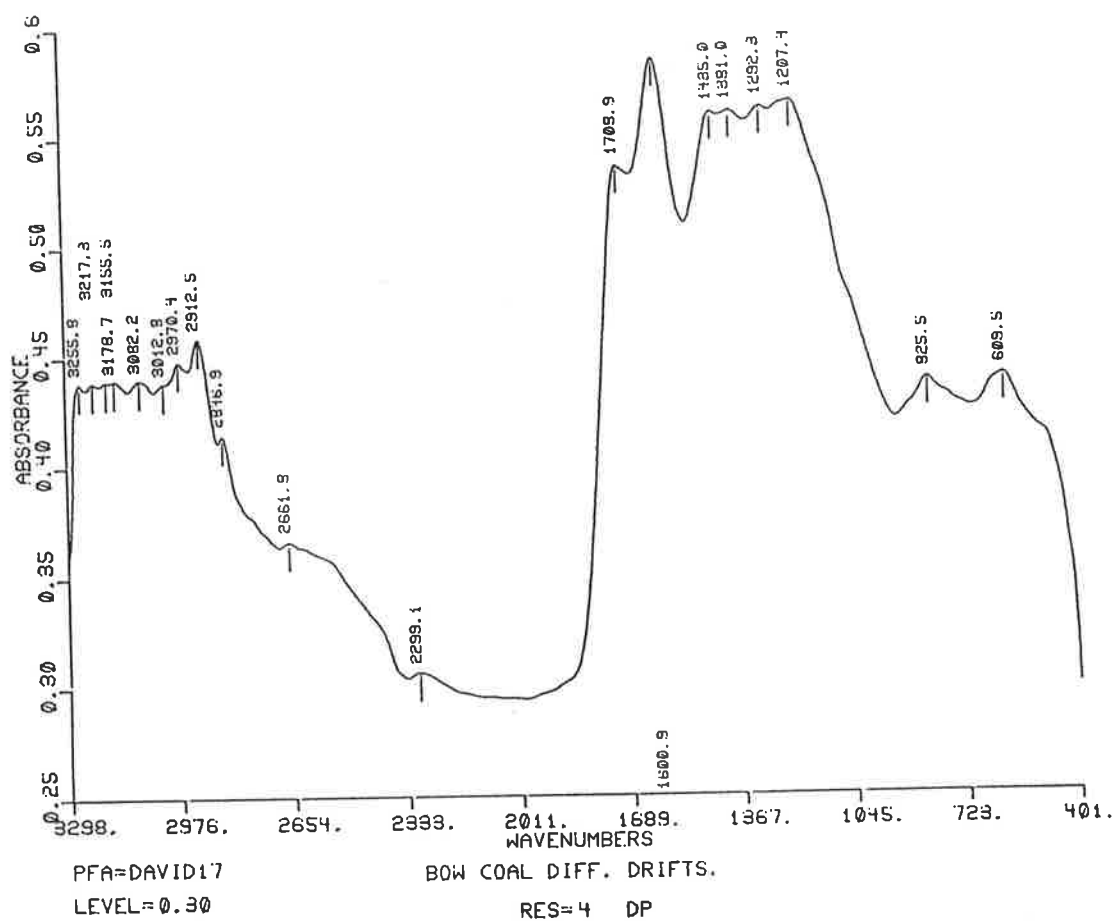
Figure 7.2   Difference Spectra between Raw And Dewatered Coal

WAVENUMBERS

1.4MG RAW COAL IN 200MG OF KBR
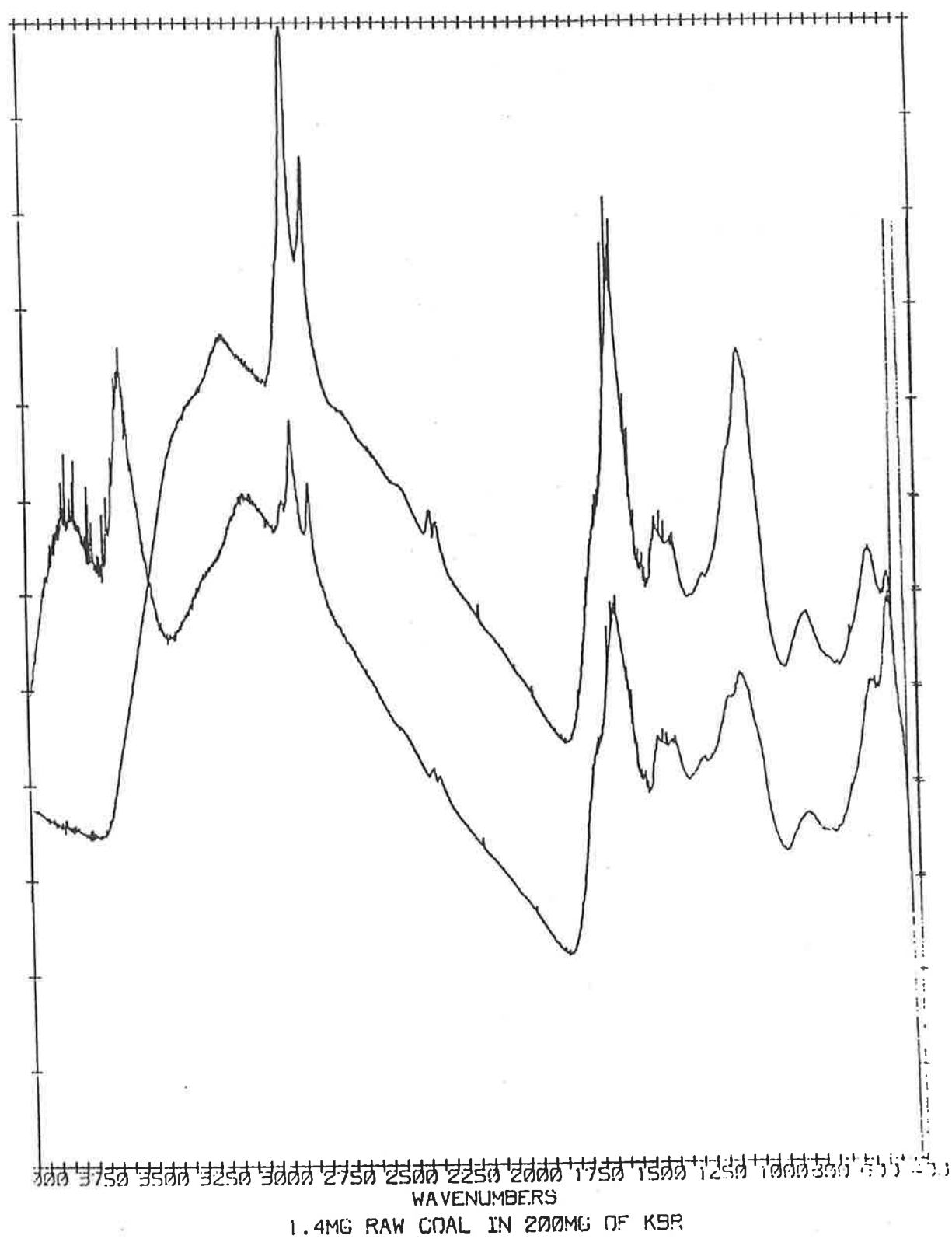
Figure 7.3   Spectra of Raw Coal using Pressed Halide Disk
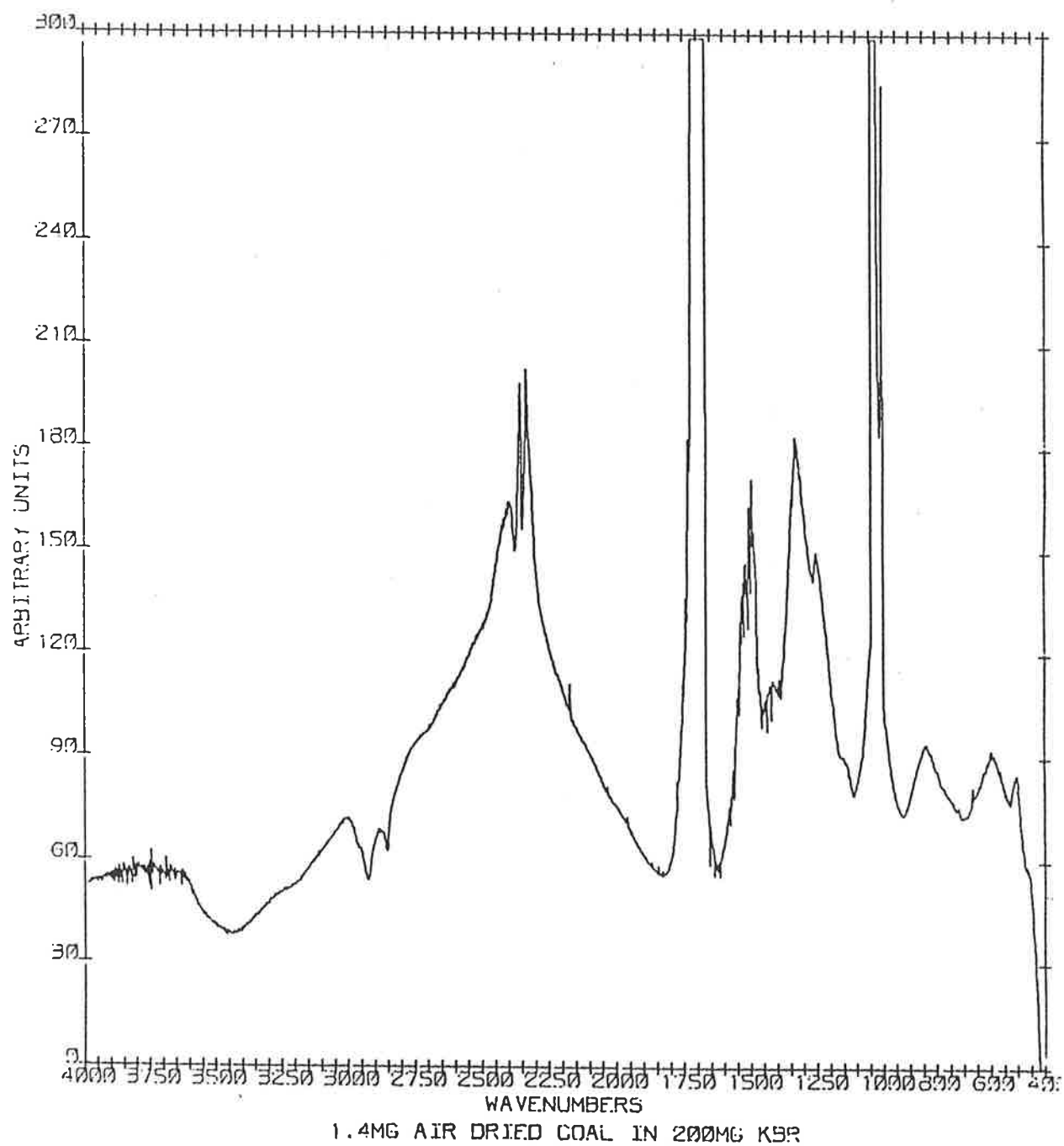
Figure 7.4   Air Dried Coal in Pressed Halide Disk
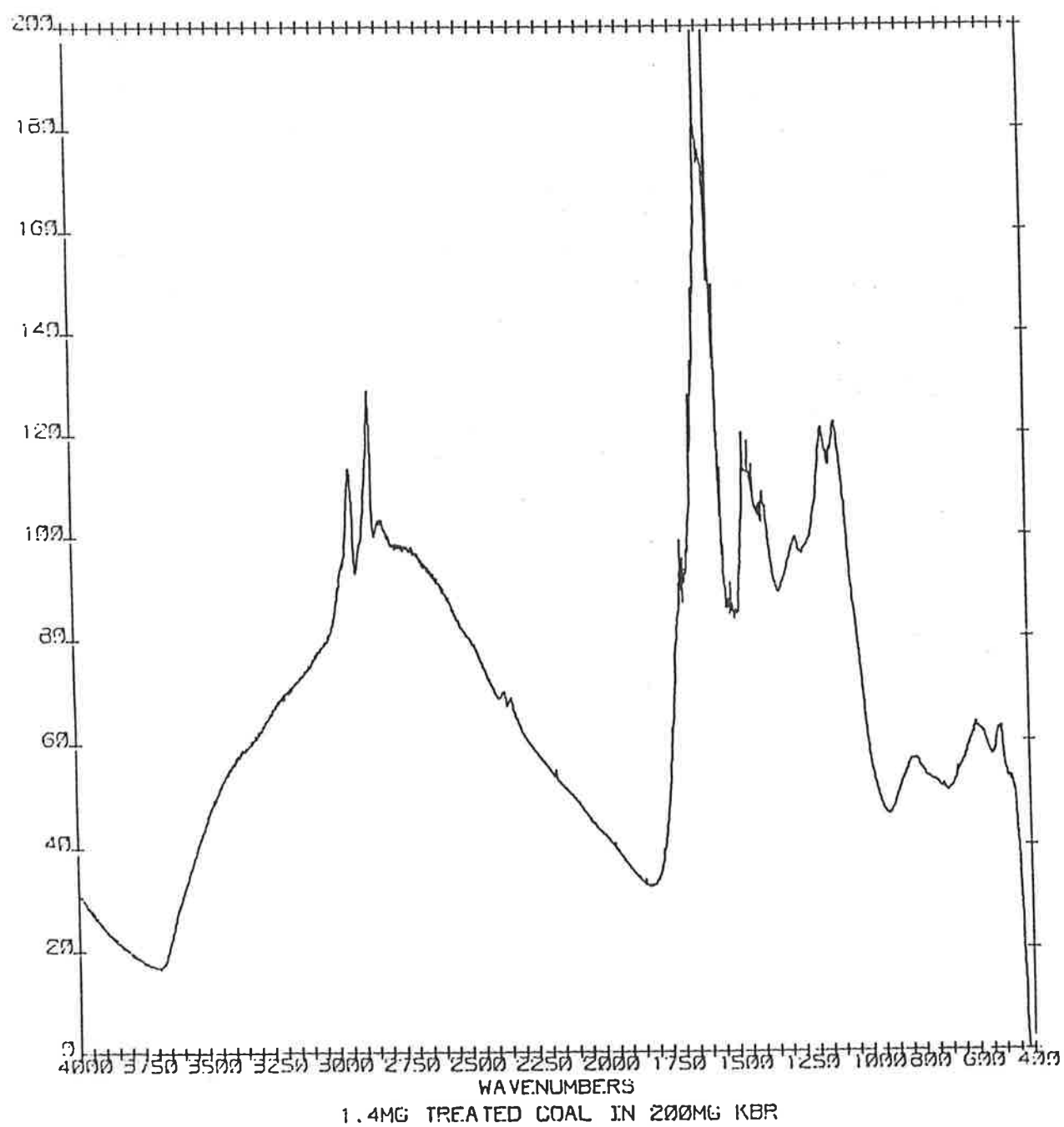
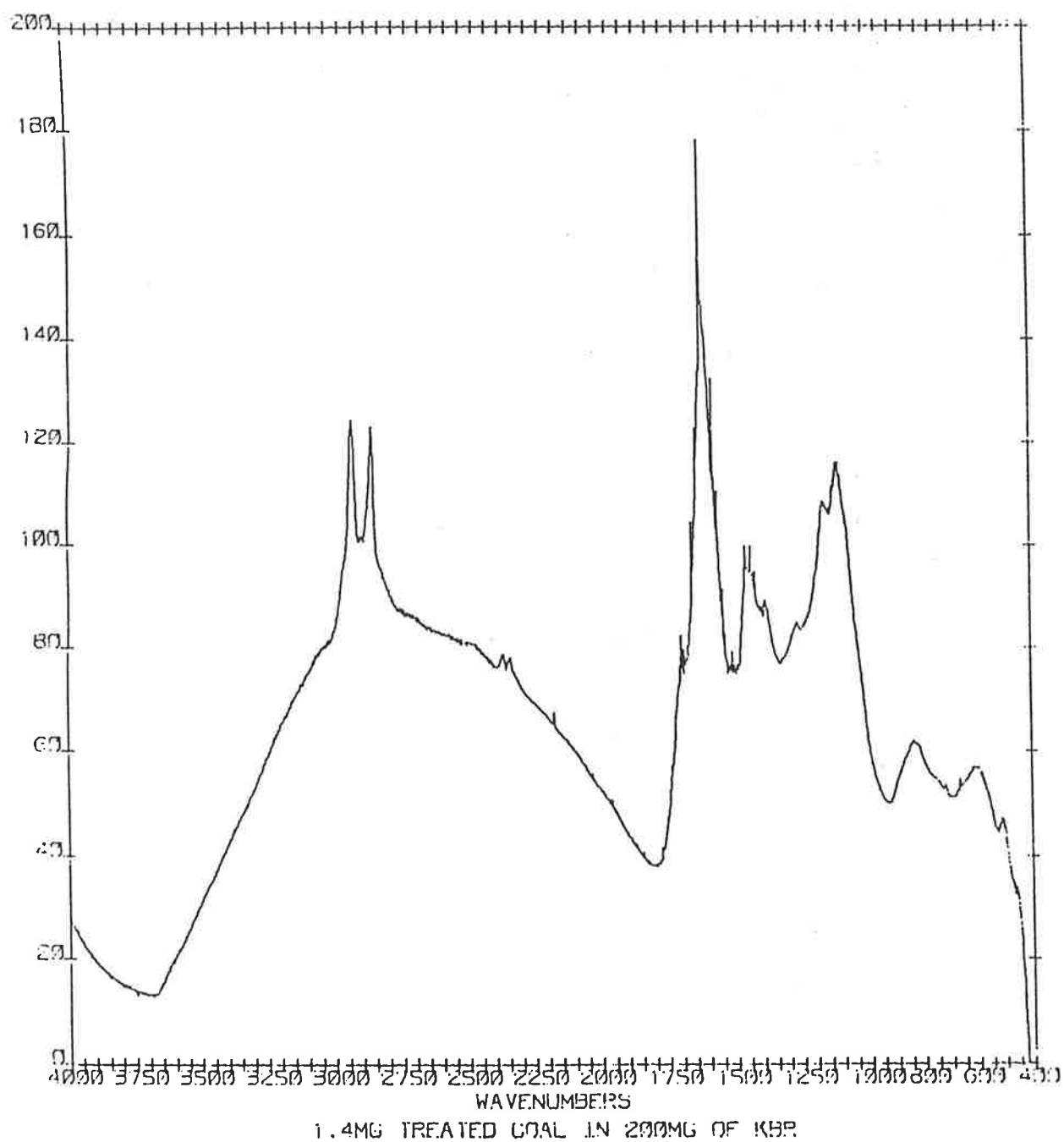Figure 7.5   Coal Dewatered at 250°C in Pressed Halide Disk

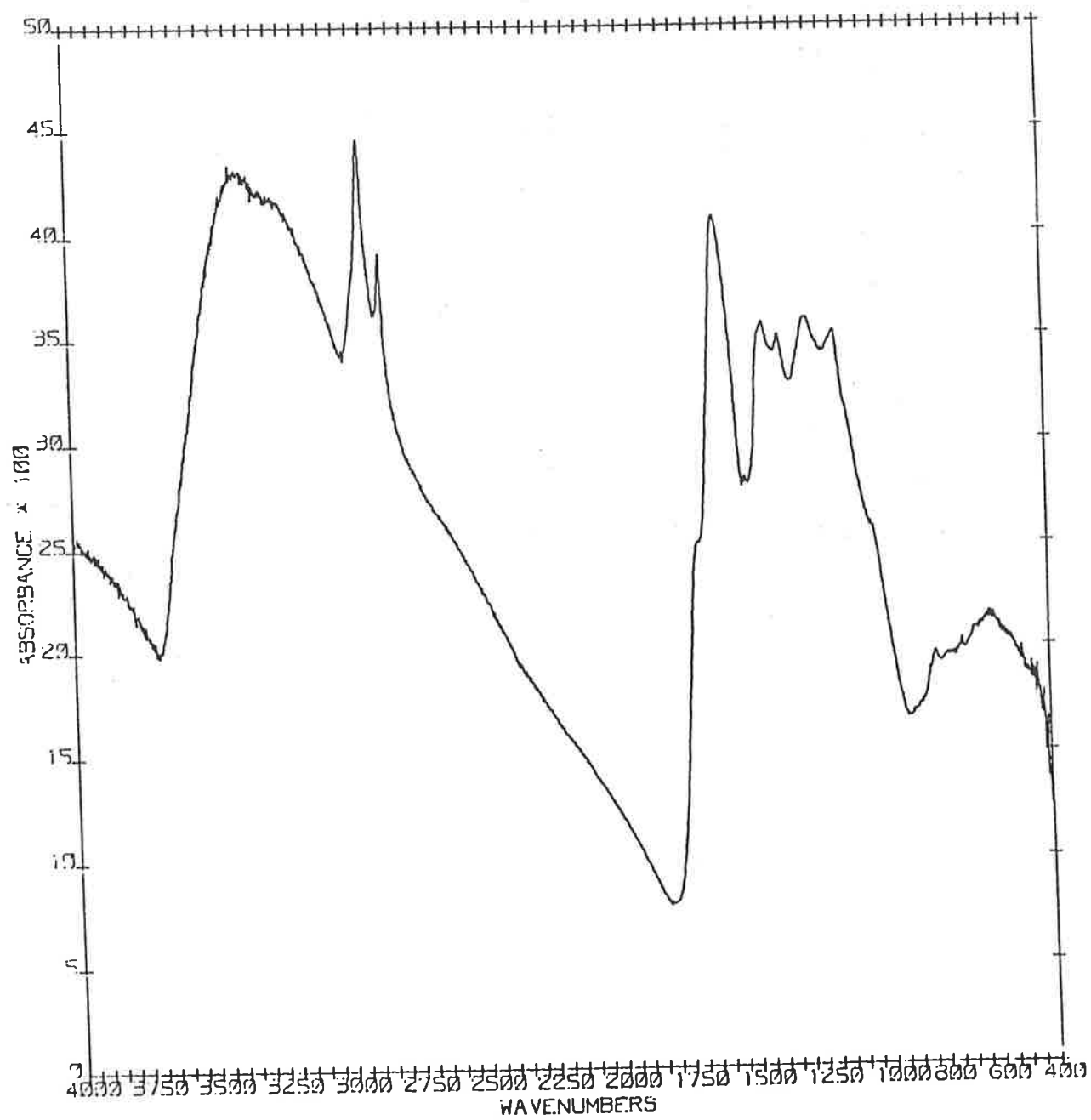Figure 7.6   Coal Dewatered at 275°C in Pressed Halide Disk

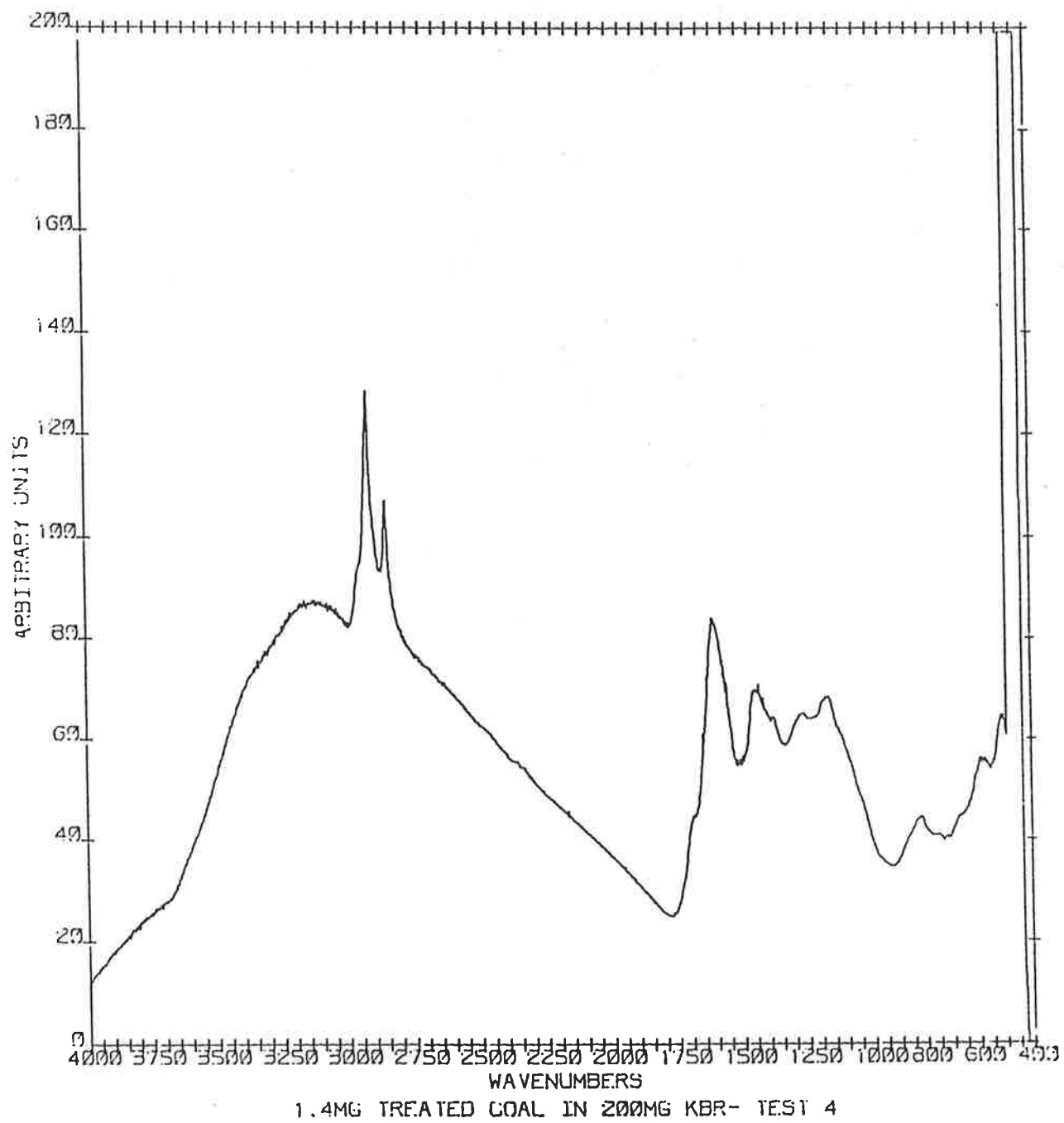Figure 7.7   Coal Dewatered at 300°C in Pressed Halide Disk
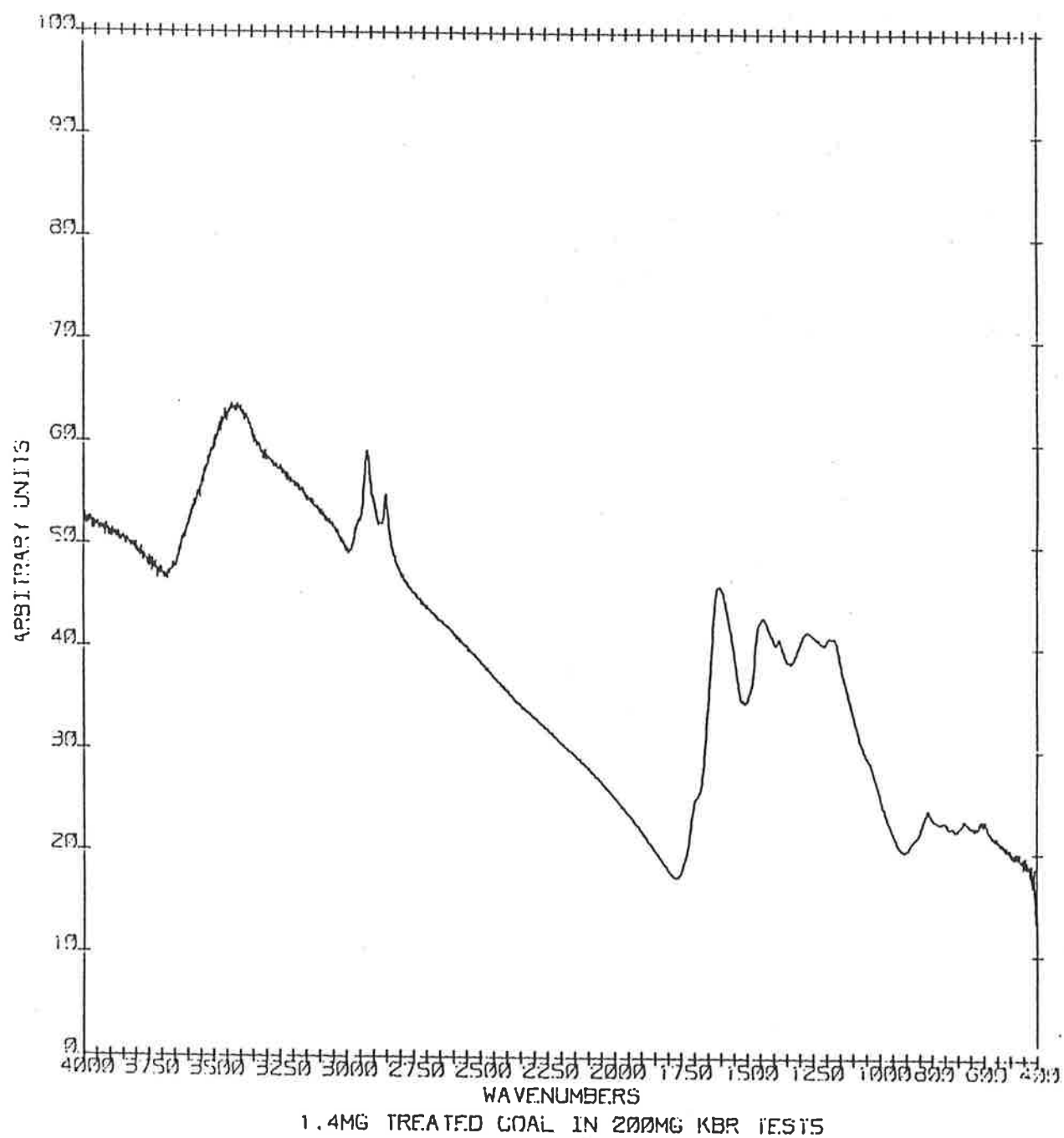
Figure 7.8   Coal Dewatered at 325°C in Pressed Halide Disk

Figure 7.9 Coal Dewatered at 350°C in Pressed Halide Disk

7.3   CARBON NUCLEAR MAGNETIC RESONANCE SPECTROMETRY

7.3.1   Introduction

The introduction of Carbon-13 nuclear magnetic resonance spectrometry with cross polarization and magic angle spinning techniques has proved a powerful method to elucidate the structural characteristics of coal (Pugmire et al., 1981; Maciel et al., 1979; Retcofsky, 1977). As a solid, coal can not be effectively studied by conventional NMR methods. The application of cross polarization and magic angle spinning (CP/MAS) suppresses the broadening which would arise from the anisotropy of solid coal. Therefore by using these techniques it is now possible to directly obtain information about the carbon skeleton of coal.

NMR techniques are applied to gain information about molecular structure and functionality of a coal, and are capable of directly determining the fraction of aromatic carbon in coal. Carbon-13 NMR is now the accepted technique and is extensively used to determine the aromaticity of coal. It has been used to provide information about the usefulness of coal for liquefaction (Yoshida et al., 1982), and to study the effect of mild oxidation (Havens et al., 1983) and heat treatment on coal (Ohtsuka et al., 1984).

In this project ^{13}C NMR has been used to determine the structure and changes to Bowmans coal following high-temperature pre-treatment. It is possible that the thermal dewatering processes may effect the suitability of the coal for various processing and utilization technologies. The reactivity of Bowmans coal for various processes can be evaluated if its chemical nature, and in particular its aromaticity is known. An evaluation of the structural characteristics indigenous to Bowmans coal should be possible if NMR is used in conjunction with FT-IR.

7.3.2 Experimental

To obtain spectra of coal samples a Brukner CXP-300 FT-NMR spectrometer was used operating at 75.47 MHz. A boron nitride rotor was used to magic angle spin at a rate of about 2.6 kHz. Typically 10,000 to 20,000 scans were signal averaged for each sample.

Spectra were obtained of raw, air dried and high-temperature pre-treated samples of Bowmans coal. As the spectra showed a lower coal aromaticity than expected, spectra were also obtained for coal from various other deposits. These were Leigh Creek, Lochiel and Sedan coals from South Australia, and Morwell coal from Victoria. As the aromaticity of Morwell coal has been well documented, a comparison of the spectra obtained from the equipment used in this study would ensure that experimental techniques conformed with methods used elsewhere.

Generally coal of particle size less than 495 μm was used in the tests, and samples were dried in nitrogen for 1 hour at 107°C. Initially a study was undertaken to investigate the effect drying in nitrogen has on coal structure. Spectra were obtained for raw and coal dried in nitrogen for 1 and 3 hours. It was difficult to make a comparison of these spectra because of the variability of Bowmans coal and the low signal to noise ratio. However, there appeared to be little difference in the spectra of coal dried for either 1 or 3 hours in nitrogen, while raw coal showed too much noise for a comparison to be made.

Obtaining a strong signal from the spectrum of untreated Bowmans coal proved to be a major concern. It was found that a large number of scans were required to obtain a low signal to noise ratio for Bowmans coal while for other coals obtaining clearly defined spectra was not difficult. Iron, probably present from crushing the coal, was removed from samples using a magnet as this was thought to cause part of the problem. Drying the coal in nitrogen at

107°C for 1 to 3 hours was found to improve the signal to noise ratio by a significant amount, therefore the presence of free ions in the coal moisture was also thought to cause interference in the NMR signal.

Spectra of low signal to noise ratios were obtained from raw coal leached for long periods in distilled water. Coal leaching was carried out over three days, each day a 1:10 coal to distilled water ratio was used to leach the coal of soluble ions. The leached coal was then thermally treated at 300°C and NMR spectra obtained to study in detail the chemical changes which accompany the dewatering reaction.

7.3.3 Results and Discussion

Figure 7.10 shows characteristic ^{13}C NMR spectral assignments for functional groups in coal. There are two main regions in the spectrum, at about 30 ppm downfield from TMS and 50 ppm wide is a region associated with aliphatic carbon, while at 120 ppm below TMS and about 50 to 70 ppm in width is an area associated with is aromatic, carbonyl and carboxyl functional groups. The carbon aromaticity of a coal can be obtained by comparing the integrated area under each of these regions of the spectrum. The ability to use ^{13}C NMR CP/MAS spectroscopy to study decarboxylation following dewatering is limited, as features in the carboxyl region of the spectrum at about 180 ppm are obscured by the aromatic region of the spectrum.

The typical shapes of spectra which are obtained for various ranks of coals are shown in figure 7.11. From these NMR spectra it can easily be seen that the aromaticity and therefore the aromatic peak of coal decreases as rank decreases from anthracite to peat. Note that peat shows very little aromatic character, while anthracite contains little aliphatic carbon. South Australian lignite is generally lower in rank compared with lignite from other countries, and would be expected to have less aromatic carbon than is shown in figure 7.11 for lignites.

To facilitate comparison between coals it is useful to characterize coal by correlating its chemical properties with carbon aromaticity. Figure 7.12 is a graph which correlates the aromaticity of coal to the atomic H/C ratio. This graph shows there is a strong relationship between these parameters which results in a fairly smooth curve. As the H/C ratio increases the aromaticity decreases until it reaches a low of about 35% total carbon.

Typical spectra of Bowmans coal can be seen in figure 7.13. These spectra were obtained from various raw coal samples representative of those used in the dewatering tests. From these spectra it is obvious that the aromaticity of Bowmans coal is extremely low compared with that reported for other coals. The values of aromaticity, f_a, calculated for these spectra are 28% for figure 7.13a, and about 15% for figures 7.13b and 7.13c. A variation in aromaticity for each coal sample made the determination of aromaticity difficult, and spectra were obtained which showed an almost undetectable level of aromaticity. The spectra in figure 7.13d is a TOSS sequence used to aid in peak assignment and eliminate spinning sidebands. This enhances and therefore can not be used to evaluate aromaticity of coal.

As the aromaticity is low and the spectra look to have a shape similar to peat, it would be expected that the coal is a lignite very close in age to peat, about 2 million years. Bowmans coal has been found to be from the tertiary era of about 50 million years (Department of Mines and Energy, 1987), an age where many coals would have turned sub-bituminous (van Krevelen and Schuyer, 1957). Therefore it appears as though this coal has not gone through a normal coalification process. This may be due to the material from which the coal was formed, or due to the environment where coalification took place.

A comparison of Bowmans coal with other coals in figure 7.12 illustrates its unusually low aromatic nature. Atomic H/C ratios for Bowmans coal for this series of tests is about 1.0. This ratio when plotted against the low aromaticity means that Bowmans coal does not follow the general relationship obtained in figure 7.12. The greater the amount of aromatic material present in coal the less hydrogen can be bonded to the carbon structure, and hence higher

ranked coals generally have a low H/C ratio. This suggests that that the molecular structure of Bowmans coal must contain significant quantity of isolated double bonded and heavily oxygenated carbon. The presence of these functional groups can be seen in the ^{13}C NMR spectra of Bowmans coal, figure 7.13. There are peaks present in the 100 ppm region which would correspond to isolated carbon carbon double bonds, and in the 170 ppm region which shows oxygenated functional groups.

The wide variation in spectra of Bowmans coal also makes it difficult to accurately determine the functionality of this coal. Although this is due in part to the small sample sizes used, the coal generally appears to be very heterogeneous. This variation can be seen by comparing the spectra in figure 7.4. While figures 7.4b and 7.4c show similar aromaticity, figure 7.4b shows more C-O groups in the 70 to 90 ppm region of the spectrum and figure 7.4c appears to show far greater carbonyl and carboxyl groups in the 170 to 190 ppm region in the spectrum.

As the spectra of Bowmans coal showed unusually low aromaticity, spectra were obtained for a number of coal samples to ensure that the methods used to obtain coal spectra were adequate. Figure 7.14 to 7.17 show spectra of Leigh Creek, Morwell, Lochiel and Sedan coals respectively. Table 7.2 shows the aromaticity obtained for these samples. Values obtained for Morwell coal appear to be slightly lower than those reported in other studies (Verheyen et al., 1984).

TABLE 7.2

Aromaticity of Coal from Various Deposits

Coal Deposit	Aromaticity
Bowmans	0-30%
Leigh Creek	52.8%
Morwell	47.9%
Lochiel	36.9%
Sedan	45.3%

Figure 7.18 shows a comparison between the spectra of air dried coal and coal thermally treated at temperatures of 250, 300 and 350°C. Again these spectra demonstrate the variability of Bowmans coal. The spectra of dewatered coal samples shown in figure 7.18 have poor signal strength which, coupled with the variable nature of Bowmans coal, makes it difficult to determine changes to the structure of the coal. The spectrum of air dried coal does not appear to be very different from raw coal. There is no obvious increase in carbonyl functional groups in the 180 ppm region of the spectrum, however it is possible to see some increase in the C-O regions at about 40 to 60 ppm. The spectra of coal dewatered at 300°C was included although it shows no detectable aromaticity to illustrate the variable nature of the coal. Other coal samples dewatered at 300°C showed an aromaticity of about 25%.

To study the changes following the dewatering of Bowmans coal spectra were obtained with low signal to noise ratios. Figure 7.19 shows spectra of coal which was first leached to improve the signal to noise ratio and then dewatered at 300°C. Spectra obtained by co-adding a large number scans of raw and coal dewatered at 300°C are shown in figure 7.20. The better resolution obtained from these spectra enabled a study of changes to the structure and aromaticity of coal following dewatering. Figure 7.21 shows superimposed spectra which facilitates comparison of the results.

A comparison between spectra obtained from the raw and the leached coal shows little difference. Therefore, although the presence of ions in raw coal appear to increase the signal to noise ratio they do not mask spectral detail. Both raw and leached coal increase in aromaticity following dewatering; the leached coal showing greater changes to structure. From the comparison of spectra in figure 7.21 the major change to Bowmans coal following dewatering appears to be a decrease in the 70 to 80 ppm region, which probably corresponds to C-O groups. This could be the effect of scission of ether groups which results in the depolymerization of coal. Small changes in the 170 ppm region of the spectrum are possibly the due to the destruction of the hydrophilic carboxyl groups. The small change to this group may confirm earlier FT-IR work which appeared to show that removal of carboxyl groups appears greater above temperatures of 300°C.

It also can be seen that there is a gradual increase in aromaticity in Bowmans coal following dewatering. There is also a decrease in the H/C ratio as dewatering temperature increases, 1.0 for raw coal, 0.97, 0.93, 0.85 for coal dewatered at 250, 300 and 350°C respectively. The increase in aromaticity may be due to the condensation of the aliphatic structure in coal, and the destruction of methyl/methylene groups. The H/C ratio decreasing while oxygenated functional groups are removed suggests that condensation of aliphatic structures does occur. There is an increase in the 150 to 170 ppm region of the spectrum which corresponds to the aromatic regions of the coal structure, and a corresponding decrease in the region temporarily designated as isolated carbon-carbon double bond material. It is difficult to determine whether there is an increase in methyl groups, or a decrease in methylene groups in the aliphatic regions of the spectra without further investigation.

7.3.4 Conclusions

^{13}C NMR spectra indicates that Bowmans coal contains much less aromatic carbon compared with lignites of similar age. However the coal contains substantial quantities of

isolated carbon carbon double bonded and heavily oxygenated carbon in its structure.

The coal increases in aromaticity following dewatering possibly due to the condensation of the aliphatic structure and the destruction of methyl/methylene groups. Further apparent changes in the spectrum following dewatering are possibly the due to the destruction of the hydrophilic carboxyl groups and the scission of aliphatic ether groups.
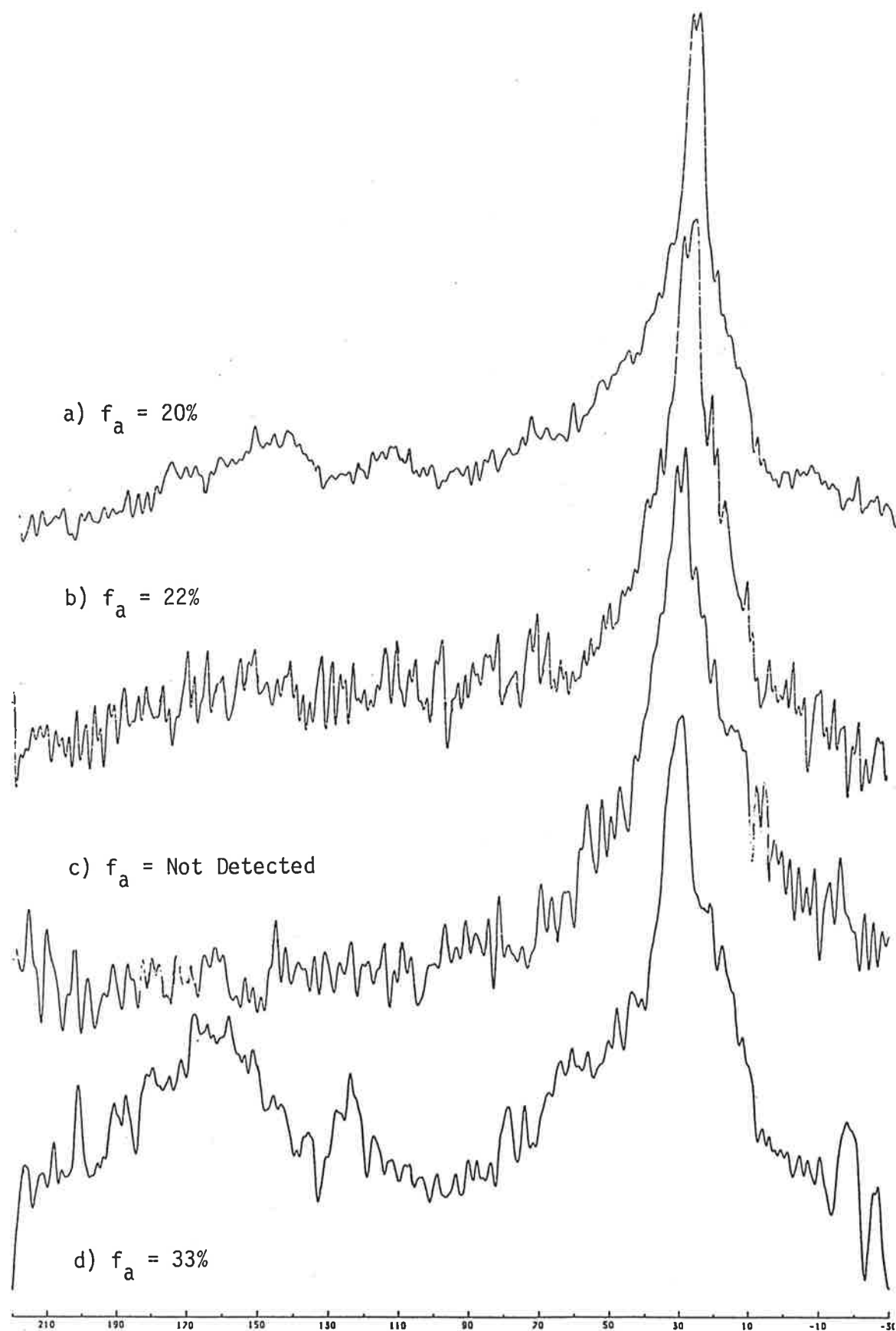
Figure 7.10 Characteristic Groups on NMR
spectra of Coal (Gerstein et al., 1982)

Figure 7.11 General Shapes
of NMR Spectra of various Coal
Types (Davidson, 1980)

Figure 7.12 Aromaticity
of Coal vs H/C ratio
(Jackson et al., 1984)

a) f_a = 20%

b) f_a = 22%

c) f_a = Not Detected

d) f_a = 33%

210   190   170   150   130   110   90   70   50   30   10   -10   -3(

Figure 7.13 ^{13}C NMR Spectra of Various Coal Samples

a), b) and c) raw coal samples

d) raw coal sample using Toss sequence
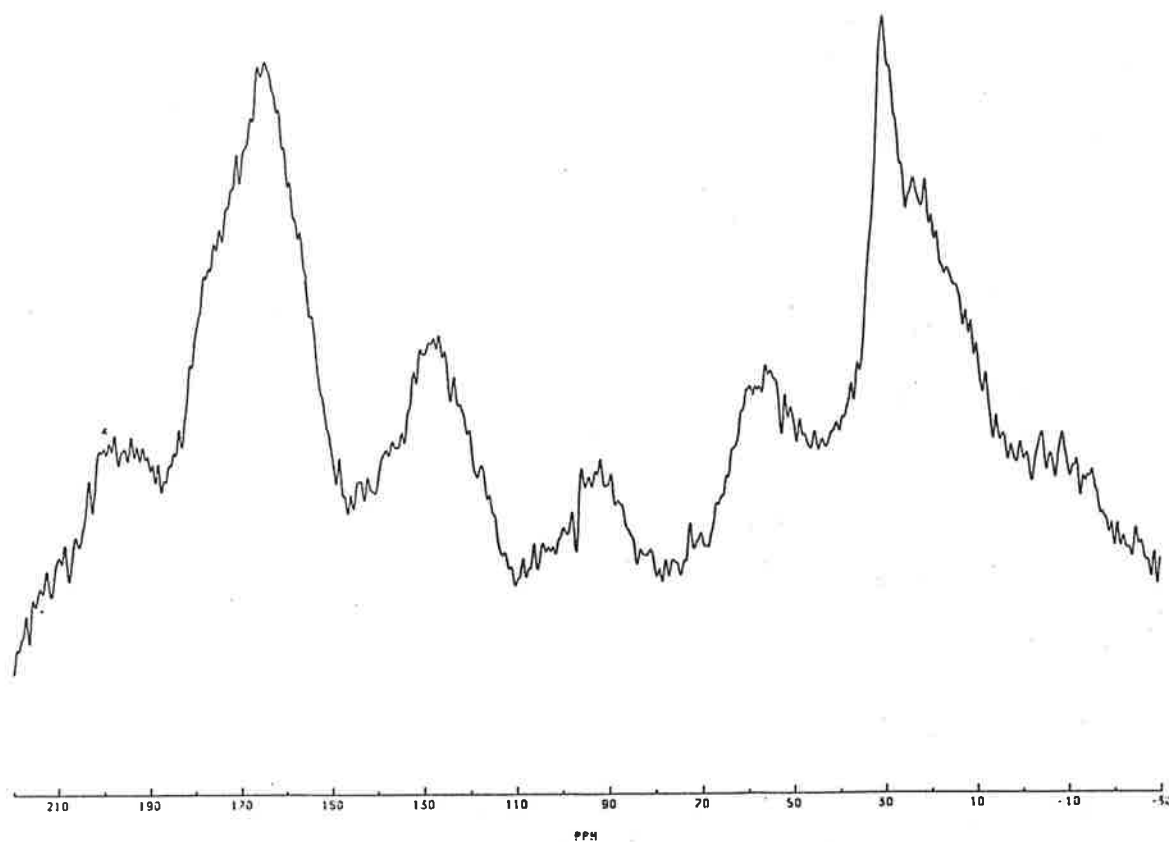
Figure 7.14   Leigh Creek Coal f_a = 52.8%
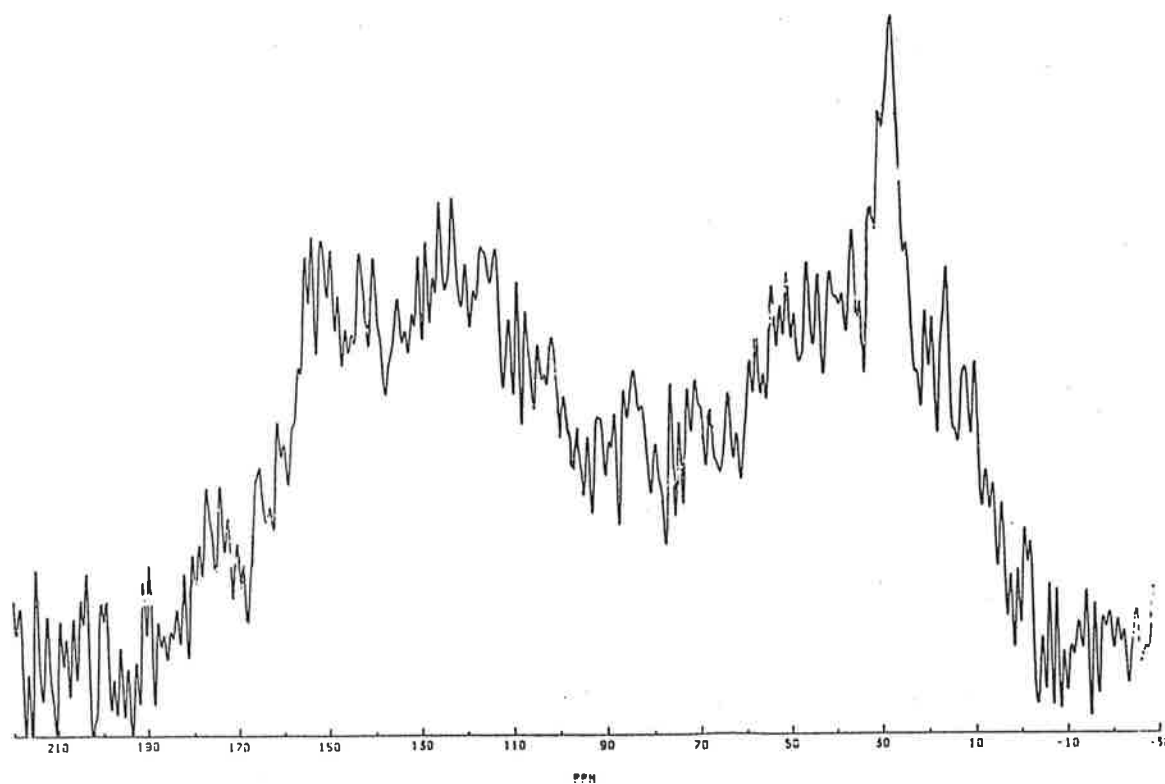
Figure 7.15   Morwell Coal f_a = 48%
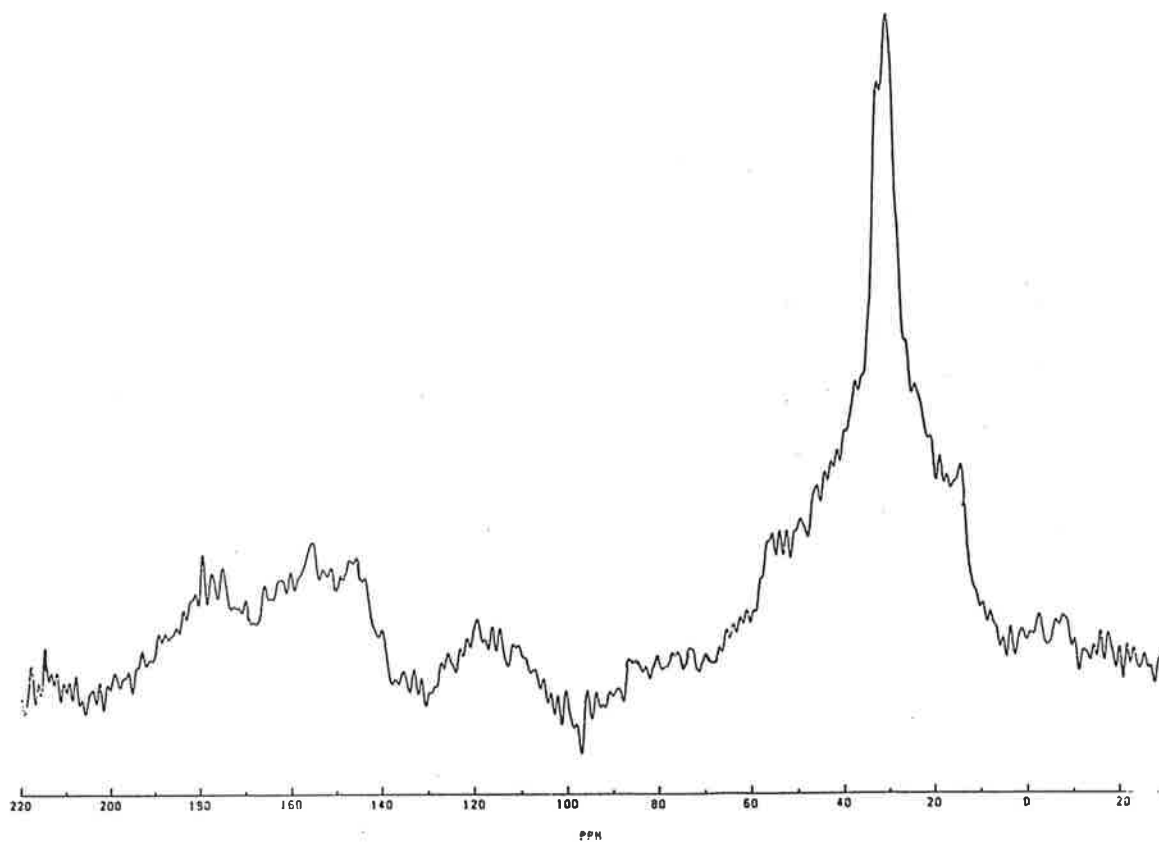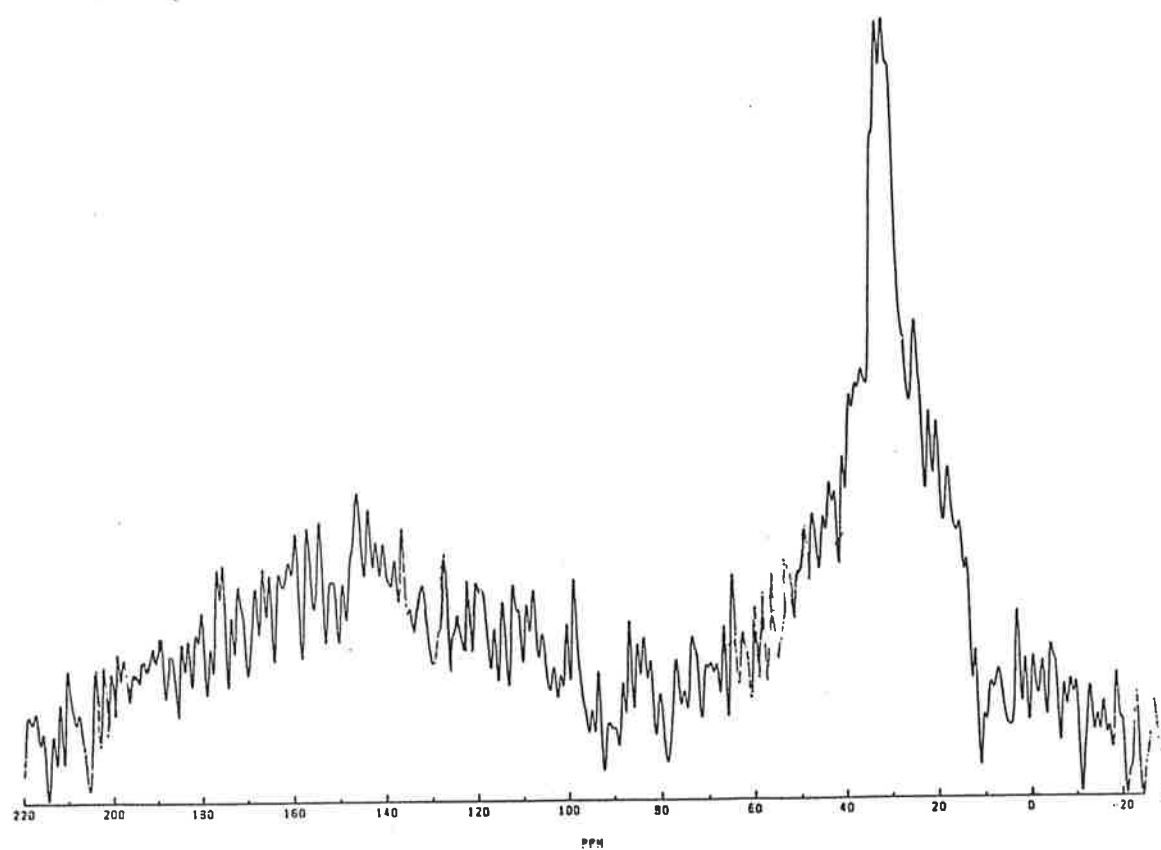
Figure 7.16   Lochiel Coal $f_a = 37\%$

Figure 7.17   Sedan Coal $f_a = 45\%$
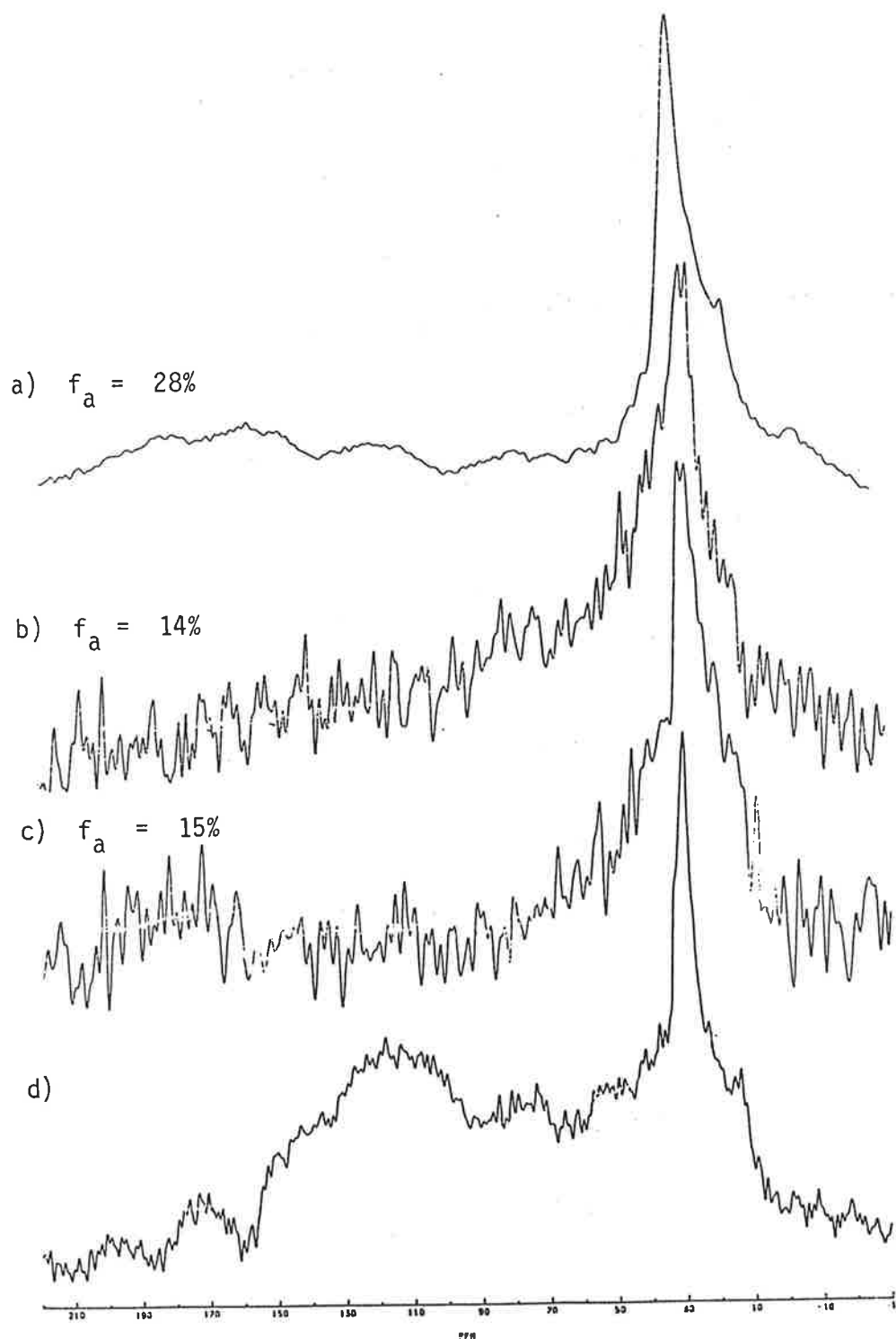
a) f_a = 28%

b) f_a = 14%

c) f_a = 15%

d)

Figure 7.18 a) Air Dried Coal   b) Dewatered Coal 250°C
            c) Dewatered Coal 300°C   d) Dewatered Coal 350°C
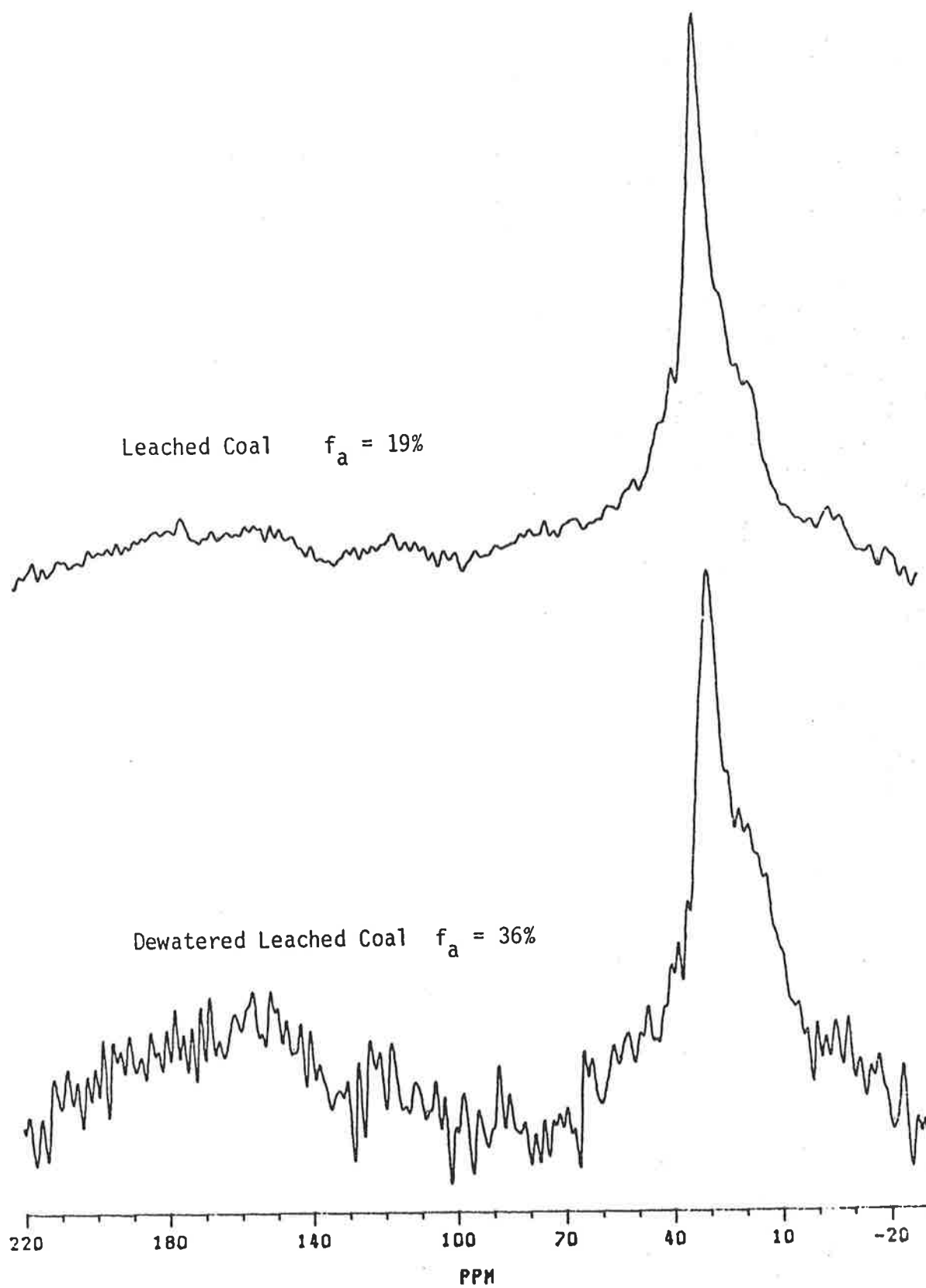
Leached Coal f_a = 19%

Dewatered Leached Coal f_a = 36%

Figure 7.19   Spectra of Leached Coal, and Leached Coal Dewatered at 325°C

Raw Coal f_a = 28%
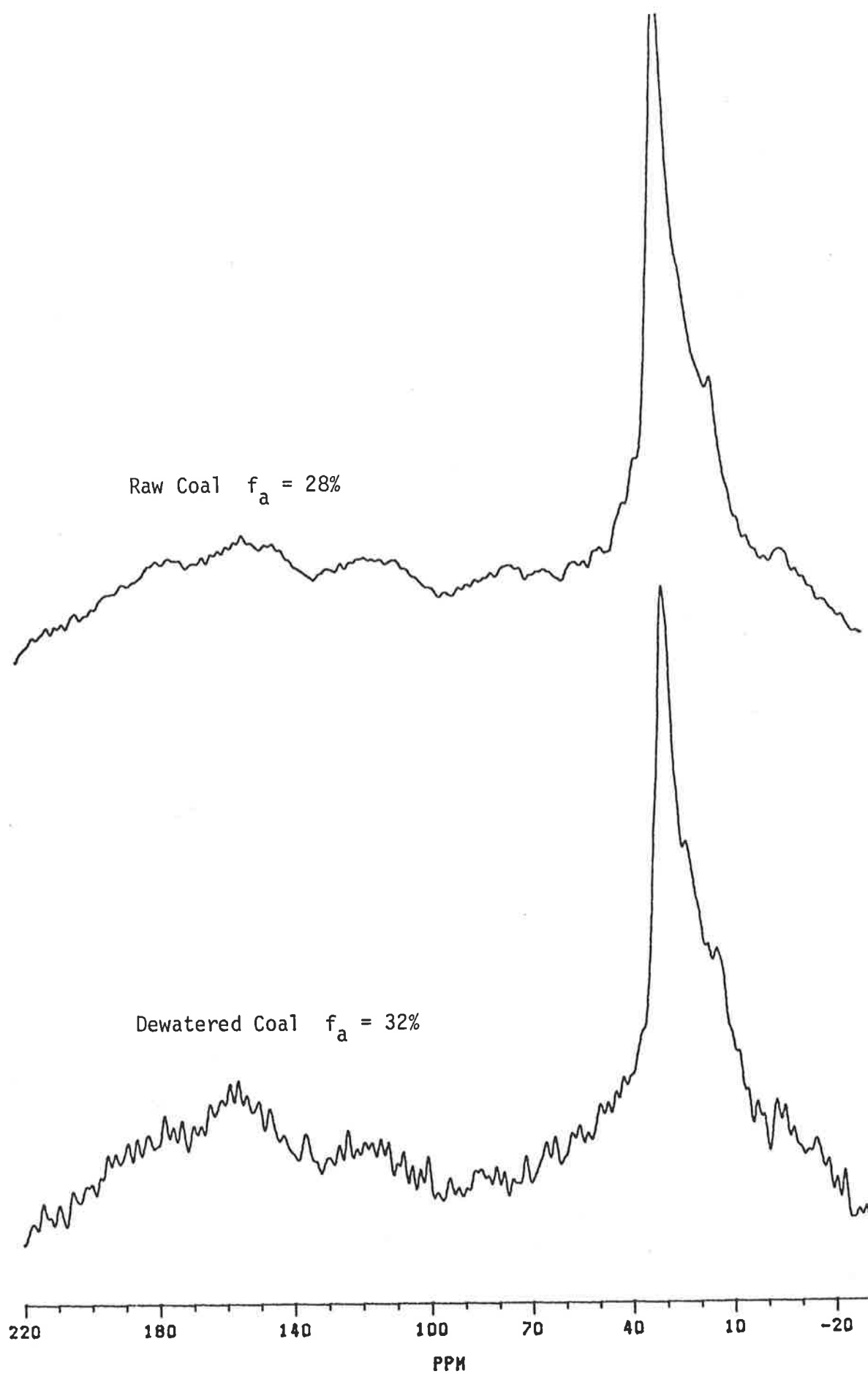
Dewatered Coal f_a = 32%

PPM

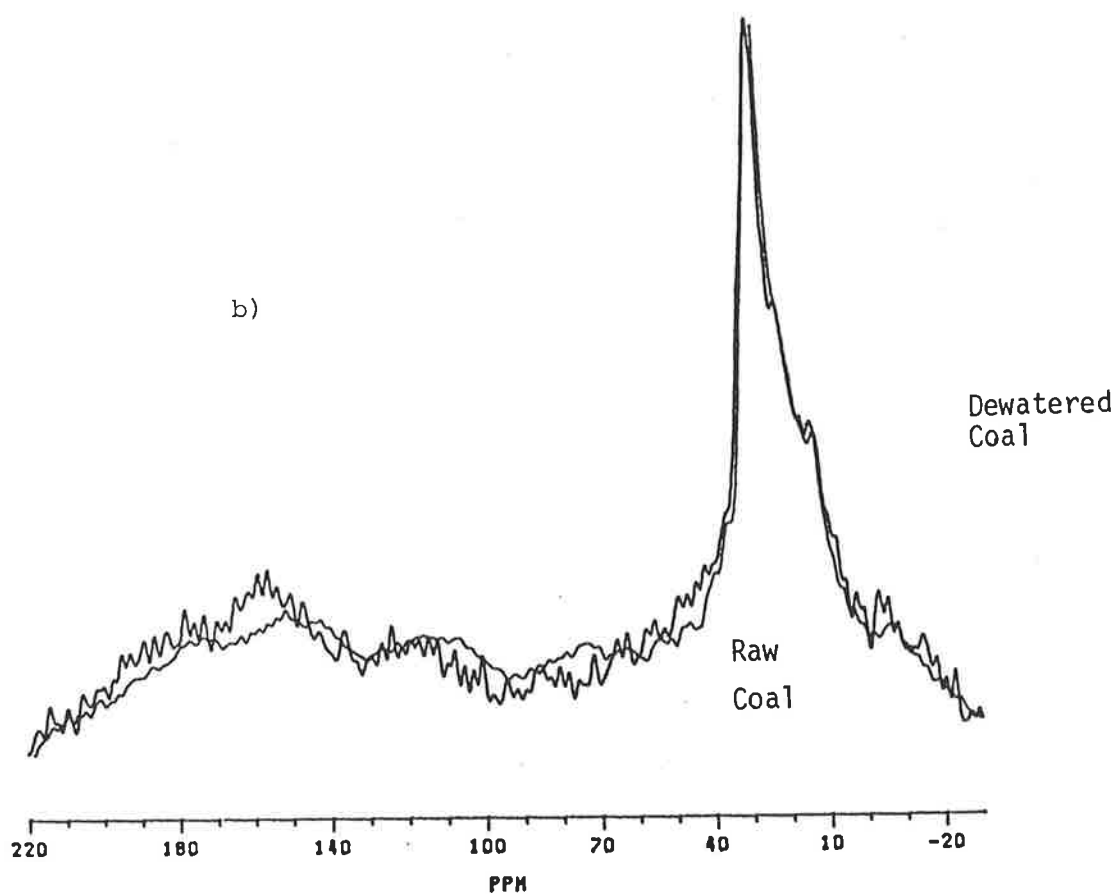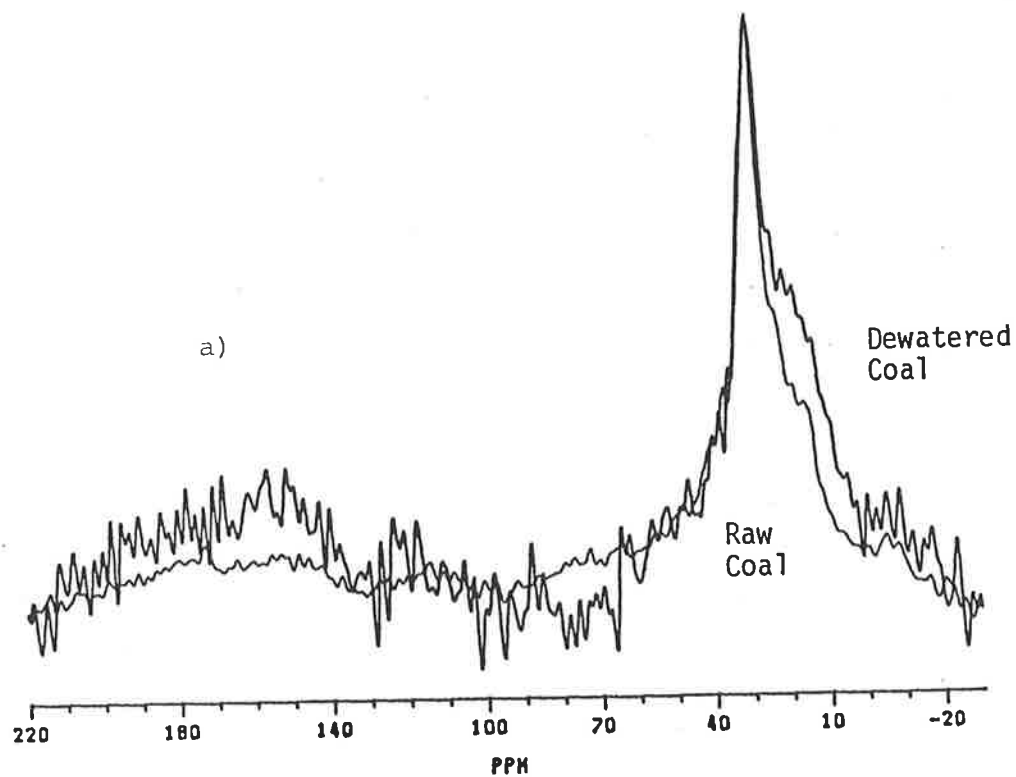Figure 7.20   Spectra of Raw, and Coal Dewatered at 325°C

Figure 7.21 Comparison between Coal and Dewatered Coal
a) Leached Coal followed by Dewatering
b) Raw and Dewatered Coal

7.4   SODIUM NUCLEAR MAGNETIC RESONANCE SPECTROSCOPY

7.4.1   Introduction

The forms of sodium and chlorine in lignite may influence the rate of moisture removal during high-temperature pre-treatment. This is because sodium is associated with carboxyl groups in coal, and the rate of destruction of these groups may effect the dewatering propensity of the coal. Therefore a method to quantitatively determine carboxylate functional groups in coal and their removal following treatment may prove invaluable. The use of sodium NMR with MAS techniques was suggested as a possible method to determine the sodium environments in coal. Although this method has not been extensively used, the difficulty experienced following the carboxylate reaction by infra-red or ^{13}C NMR methods prompted its use. The sodium is also thought to be associated with chlorine as well as the organic material in coal. This study was undertaken to determine all the sodium environments in coal, and whether they could be quantitatively calculated using sodium NMR techniques.

It has proved very difficult to determine the degree of association between sodium with chlorine in coal. Early investigators such as Edgecombe (1956) and Daybell (1967) used extraction techniques to compare the amount of sodium and chlorine removed. It was assumed from these tests that all soluble chlorine in the coal was combined with alkali cations, and particularly as sodium chloride. The main difficulty with this method is to match the extracted chlorine with a corresponding cation. The remaining sodium not matched to a chlorine ion was either assumed to be associated with another anion or present as organic sodium.

Other methods of analysis which have been used to elucidate the association of sodium with chlorine includes neutron activated analysis (Gluskoter and Ruch, 1971) and scanning electron microscopy with X-ray micro-analysis techniques (Saunders, 1980). From these

methods it has been determined that the chlorine in coal need not be directly associated with alkali cations, rather it is thought to be evenly distributed on the surface coal in a 'brine' solution. However, even by using these methods it has still proved difficult to determine a definite relationship between sodium and chlorine in coal.

Extensive leaching tests and analysis using scanning electron microscopy have been carried out on Bowmans coal by Readett et al. (1983,1984) and Allen (1981a,1981b). They found that up to 70% of the sodium and most of the chlorine could be extracted by water leaching in approximately equimolar quantities, while most of the sodium could be removed by leaching in acid solution. From their results it was concluded that up to 60% of the sodium was present as a chloride, 10% as sulphate and the remainder as organic humic acids. Figure 7.22 shows typical results obtained for the leaching of Bowmans coal in water and indicates the strong correlation between the rate of sodium and chlorine removal.

Work recently undertaken by Readett and Quast (1988) on Bowmans coal using mechanical dewatering techniques showed that sodium was extracted from coal at a different rate to chlorine when water was expressed from the coal under pressure. This was believed due to the sodium being adsorbed to the coal surface in the diffuse region of the double layer and in the Stern layer.

Recently, a study was undertaken by Howarth, Ratcliffe and Burchill (1987) using solid state sodium nuclear magnetic resonance on a number of English and one Australian brown coal. This work appears to show that little of the sodium precipitates as sodium chloride in dried coals, which may confirm the results obtained in this study. They found that the dried Australian brown coal produced no detectable shift which could be assigned as crystalline sodium chloride, while a broad band at -15.4 ppm was found which was lower than the known frequencies of carboxylates and phenoxides. This was thought to be organic in origin, due perhaps to the coordinative unsaturation of sodium in the presence of more than one carboxylate group in heavily oxygenated coal.

The objective of this study was to investigate the solid-state sodium nuclear magnetic resonance spectrum of Bowmans coal, and compare the result with the apparent state of sodium obtained from previous tests. By using sodium NMR it should be possible to make a direct quantitative determination of the forms of sodium in the lignite without the need to treat the coal by destructive means. It may then be possible to determine on which functional groups the sodium is attached, and would help establish which functional groups are destroyed during high-temperature pre-treatment.

7.4.2   Experimental

The solid state ^{23}Na NMR studies were carried out using a Bruker CXP 300 spectrophotometer at 7.05 Teslas with magic angle spinning rate of approximately 2,500 Hz. Typically about 10,000 scans were signal averaged using standard frequency of 79.398 MHz, a 90 RF pulse and a recycle time of 2 sec. About 0.3 grams of less than 495 μm coal was used in a boron nitride rotor.

A number of tests were carried out to determine the spectral characteristics of Bowmans lignite and to identify the chemical shifts of the known environments of sodium. Spectra were obtained of raw, water-leached and acid-leached coal, as well as coal spiked with various sodium compounds.

A study was initially made of the effect of moisture on the quality and type of spectra obtained, using raw coal and coal dried for 3 hours in nitrogen at 107°C. The general shapes of the spectra were very similar; however the high-moisture raw coal caused the magic angle spinning rotor to become unbalanced, and spectra required a large number of scans. The similar shapes of the spectra was probably caused by deposition of sodium as the coal dried in the rotor. Therefore all subsequent samples were dried for 1 hour at 107°C before being analysed by NMR.

The coal was leached using distilled water or 2M HCl in a 1:20 coal to liquor ratio for about 2 hours, and then separated in a buchner funnel. The leach liquor was analysed for sodium content using atomic absorption spectroscopy, while chlorine content was determined by Mohr titration.

Table 7.3 shows the extent of removal of sodium and chlorine from Bowmans lignite by water and acid leaching. The sodium removed by leaching in distilled water would be as dissociated sodium ions diffusing from the coal pores, while minor quantities would be removed as soluble humic acids. Acid leaching the coal would remove most of the sodium from the coal, including organic sodium by an ion exchange mechanism. However, slight quantities of residual sodium will remain in the coal after leaching, and sodium bound in mineral matter would not be removed.

An equivalent quantity of sodium in various forms was then reintroduced to the leached coal. The compounds used to spike the leached coal included sodium chloride, sulphate, silicate and carbonate. These compounds were added in concentrated solution to the leached coal and dried in an oven at 107°C until the surface moisture disappeared. It was then dried for a further hour. By reintroducing the sodium to the coal as a brine it was thought that the sodium would evenly disperse throughout the lignite during drying. The amount of sodium reintroduced to the coal after leaching is shown in table 7.4.

7.4.3   Results and Discussion

Figure 7.23 shows a ^{23}Na NMR resonance spectrum of raw coal dried in nitrogen for 1hr at 107°C. The two major peaks at 5.5 ppm and -15.8 ppm represent the environments of sodium present in the raw coal. The integrated areas under these peaks roughly indicate the proportion of each component present in the coal. From the relative sizes of the peaks in figure 7.23 it is obvious that there is much less sodium represented by the peak at 5.5 ppm.

Resonance structures of the large -15.8 ppm peak appear in the spectra at about 20ppm and -50ppm. The peak at -15.8 ppm is slightly asymmetric, and therefore shows at least two distinct types of sodium present. The shoulders present on the right portion of the peak indicate the less abundant component of sodium represented by this peak.

Figures 7.24 to 7.27 show ^{23}Na NMR spectra of coal following leaching, while figures 7.28 to 7.32 are spectra of leached coal which has been spiked with various forms of sodium. Note that the ordinate scale and the number of scans taken for each spectrum are dissimilar, so that a quantitative comparison of sodium content for each spectrum can not be undertaken easily. However rough calculation methods have shown that peak areas correspond to the quantity of sodium reintroduced to the coal.

A spectrum of coal leached in distilled water for 2 hrs is shown in figure 7.24, and shows that water leaching has removed most of the 5.5 ppm species. Although not obvious due to changes in scale and numbers of scans, much of the broad -15.8 ppm peak has also been removed leaving a smaller residual peak at -17 ppm. When the raw coal (figure 7.23) spectrum is superimposed on the water leached spectrum, figure 7.25, it it can be seen that the residual sodium corresponds roughly to the right shoulder of the broad peak in raw coal. Therefore it is apparent that the soluble sodium removed by water leaching is from the broad asymmetric peak between -15 ppm to -16 ppm and from the smaller peak at 5.5 ppm.

In this study it was found that the residual sodium from water leaching was ion exchangeable with various cations. Therefore the right shoulder in the broad peak in raw coal and the residual peak in water leached coal is likely to be organic carboxylate sodium. Note that the scales of the spectra compared in figure 7.25 are dissimilar to facilitate the study of the relative positions of the peaks. The quantity of sodium remaining in Bowmans coal after water leaching is only about 5% of the total sodium.

A spectrum of acid leached coal is shown in figure 7.26, and again is superimposed on a raw coal spectrum in figure 7.27. The spectrum of leached coal has been enlarged many times to compare differences between spectra, as only trace quantities of sodium remain in the coal after acid leaching. If a comparison of scale is made with the spectra of water leached coal (figure 7.24) the relative heights of the 5.5 ppm peak would be similar. From figure 7.27 it is apparent that most of the sodium represented by the peak at -17 ppm is removed, and that very little sodium remains in the coal.

Figures 7.28 and 7.29 show the spectra of water and acid leached coal which are spiked with sodium chloride in quantities similar to that removed by leaching. Both spectra show the peak at 5.5 ppm now as the major component in the coal. It was calculated that the area under this peak roughly correlates with the quantity of sodium reintroduced to the coal. Therefore the peak at 5.5 ppm must represent sodium chloride in coal. The small peak at 5.5 ppm in the raw coal spectrum (figure 7.23) strongly indicates there are only minor amounts of sodium chloride present in dried raw coal.

The identification of the larger soluble section in the broad peak at -15.8 ppm was undertaken by spiking the coal with a number of sodium compounds. They included sodium sulphate, silicate and carbonate; figures 7.30, 7.31 and 7.32 respectively. These compounds were chosen to get representative chemical shifts and shapes of the spectra for possible forms of sodium in coal. The most likely compound formed on drying the coal is sodium sulphate, as it was found in a study of the aqueous leaching characteristics of Bowmans coal (chapter 8) that significant quantities of soluble sulphate are present in the leach liquor. Sodium silicate was used because clay (silicate) minerals could contain sodium in their structure, and because a soluble form of silicon was detected in the lignite (Ruyter, van Raam and van der Poel, 1984; Allen, 1981) which was thought may associate with sodium on drying.

The spectra of spiked coal showed a similarly shaped broad peak to that found in spectra of raw coal at -15.8 ppm. Chemical shifts of these peaks were found to be about -13.7

ppm for sodium carbonate, -14.6 ppm for sodium silicate and -15.1 ppm for sodium sulphate. As these peaks are very similar it is difficult to determine any definite association between these compounds and raw coal. If the sodium was associated with a cation it would most likely be sodium sulphate. This is because it is the closest in chemical shift to the raw coal peak of -15.8 ppm and because there are large quantities of soluble sulphate present in raw coal. However this form of sodium may also be organic in origin, perhaps due to the co-ordinative unsaturation of sodium in the presence of carboxylate groups or due to sodium being absorbed on the coal surface.

The main advantage of this ^{23}Na NMR techniques is its ability to analyse some of the forms of sodium in coal by non-destructive methods. The quantity of sodium chloride present in dried Bowmans coal can be simply obtained by integrating the peak areas to get a ratio of sodium chloride to sodium in other forms. As organic sodium appears to be present at -17 ppm, and shoulders the right side of the major sodium peak, it should be possible to use spectral manipulation methods to quantitatively determine the size the peak. Therefore ^{23}Na NMR techniques may be used to find the quantity of sodium chloride and organic sodium in dried coal.

The use of ^{23}Na NMR techniques in coal dewatering studies are shown in figures 7.33 to 7.35. These figures show spectra of coal dewatered at 250, 300 and 350°C for 20 mins. Note that the scales of the dewatered coal spectra are not similar, and a quantitative comparison between samples can not be made. There appears to be two major mechanisms for removal of sodium from the coal during high-temperature pre-treatment. The first mechanism is leaching of soluble ions from the coal as the coal is slurried in water, and will be dependent on the time and temperature of dewatering, size of coal particle and coal/water ratio. The second is the release of sodium from the destruction of organic carboxylate groups under thermal treatment.

From figure 7.33 it is obvious that after pre-treatment at 250°C the leaching process has removed most of the dissociated sodium and chlorine ions which would associate as sodium

chloride when the coal is dried. The asymmetry of the large peak at -15.8 ppm also appears to have been substantially reduced; there is less organic sodium in the coal following dewatering. Similarly the spectrum of coal dewatered at 300°C in figure 7.34 shows that while most of the organic sodium appears to be removed, the unidentified sodium is still substantially present. There also appears to be more sodium chloride present in this sample than in figure 7.33. The spectrum of coal dewatered at 350°C does not show much residual sodium in the coal structure. No conclusions can be reached from this spectrum as the lack of any sodium present in this sample is probably due to the variable nature of Bowmans coal.

7.4.4   Conclusions

^{23}Na NMR of Bowmans coal showed that there are three major environments of sodium in dried coal. Two environments were tentatively identified as sodium chloride and organic sodium; there are only minor amounts of sodium chloride present in dried coal. The third and largest environment of sodium in Bowmans coal cannot be identified. However, it is likely to be either present as sodium loosely bound to the coal structure or as a complex salt. Spectra of dewatered coal samples show that most of the sodium chloride and organic sodium is no longer present in dried coal following dewatering.

TABLE 7.3

Moles of element removed from coal by leaching

Leachate	Sodium moles/100g dry coal	Chlorine moles/100g dry coal
Distilled water	0.056	0.043
2M HCl	0.059	-

TABLE 7.4

Moles of Compound used to Spike Leached Coal

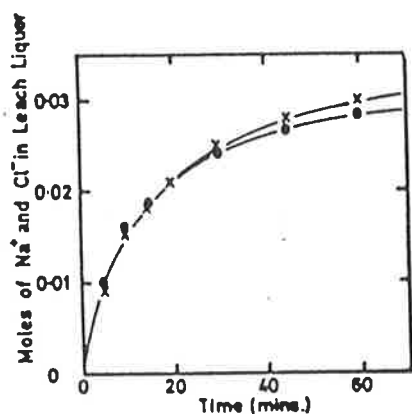| Compound	Liquor used to Leach Coal Sample	Moles of Sodium used to Spike Coal moles/100g dry coal
Sodium Chloride	Distilled Water	0.049
Sodium Chloride	2M HCl	0.045
Sodium Sulphate	2M HCl	0.033
Sodium Silicate	2M HCl	0.051
Sodium Carbonate	2M HCl	0.049

Figure 7.22 Leaching of Na and Cl
From Bowmans Coal ×Na •Cl
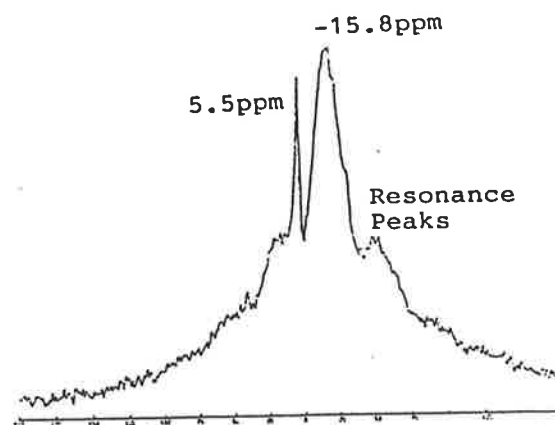(Readett et al. 1984)

Figure 7.23   Raw Coal

Figure 7.24   Water Leached Coal
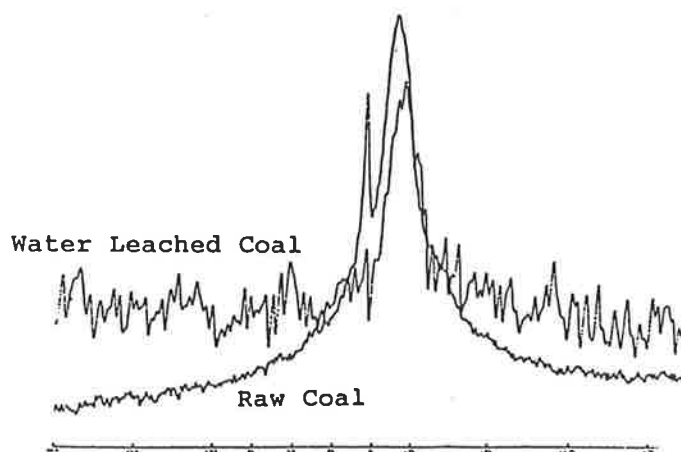
Figure 7.25   Comparison of Raw Coal
and Water Leached Coal
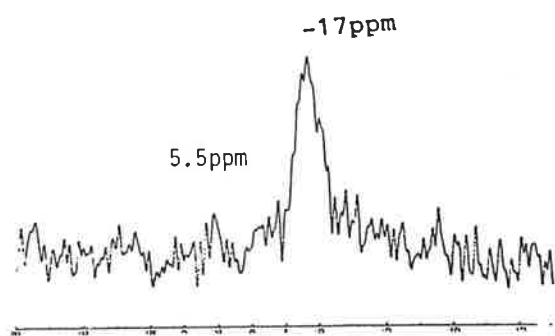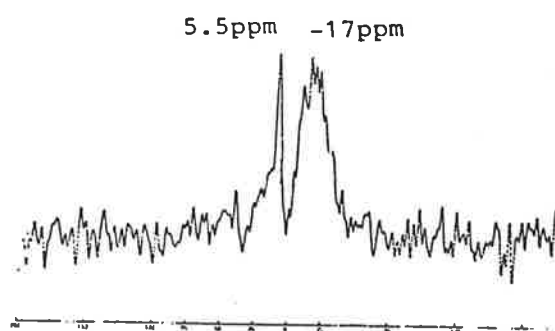

Figure 7.26   Acid Leached Coal
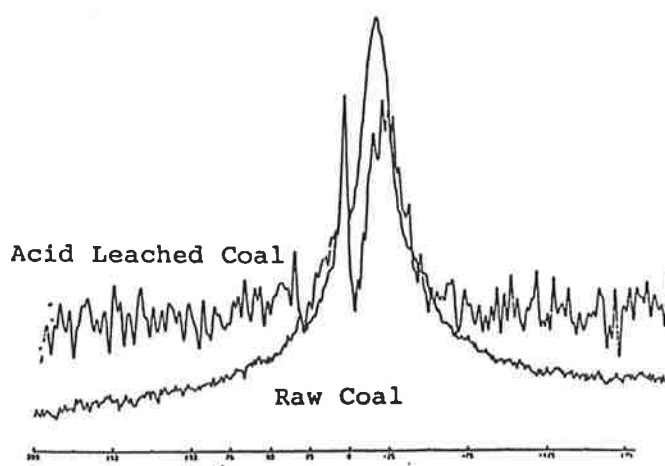
Figure 7.27   Comparison of Raw Coal
and Acid Leached Coal

Figure 7.28 Water Leached Coal
spiked with NaCl

Figure 7.29 Acid Leached Coal
spiked with NaCl

Figure 7.30 Water Leached Coal
spiked with Sodium Sulphate

Figure 7.31 Water Leached Coal
spiked with Sodium Silicate
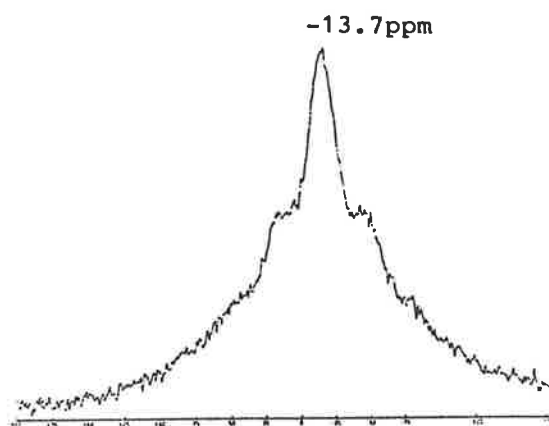
Figure 7.32 Water Leached Coal
spiked with Sodium Carbonate
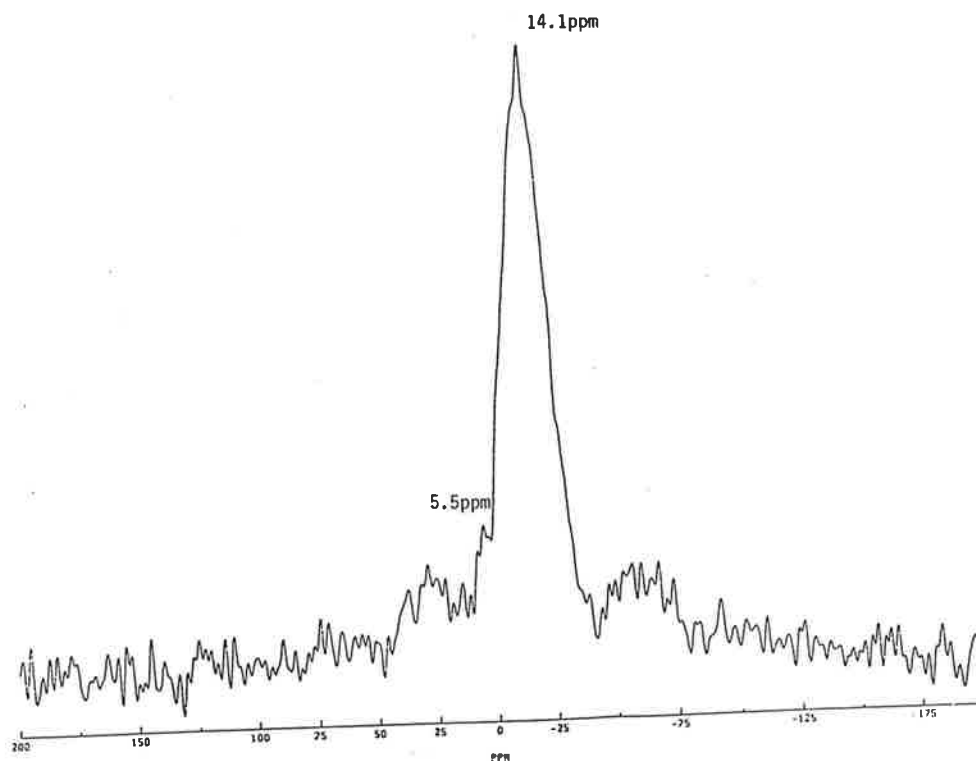
Figure 7.33 Coal Dewatered at 250°C
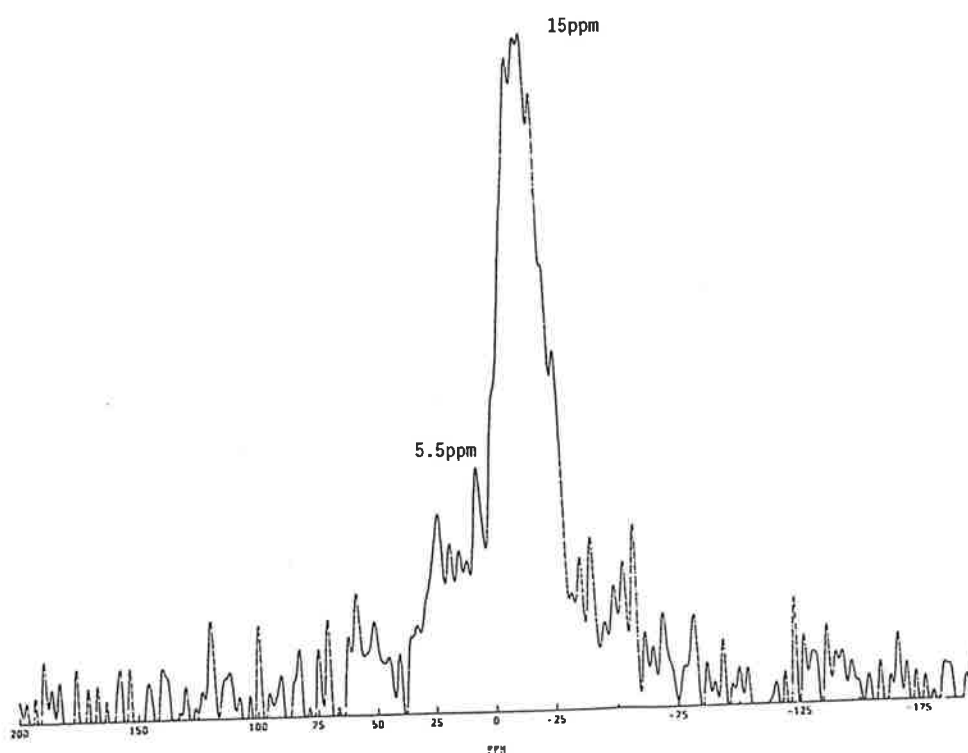
Figure 7.34 Coal Dewatered at 300°C
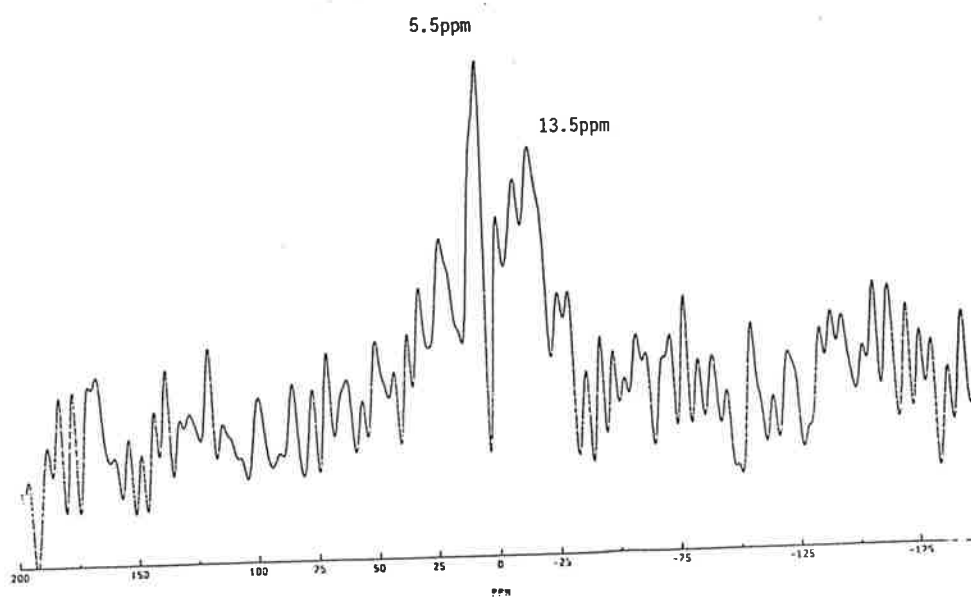
Figure 7.35   Coal Dewatered at 350°C

8. LEACHING CHARACTERISTICS

8.1   INTRODUCTION

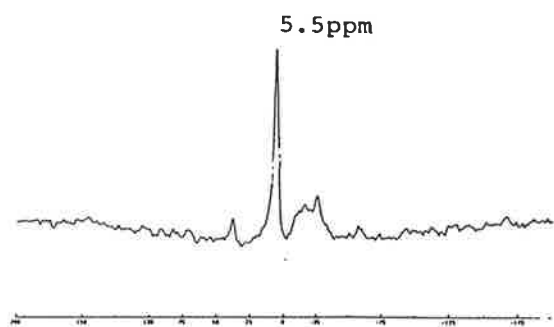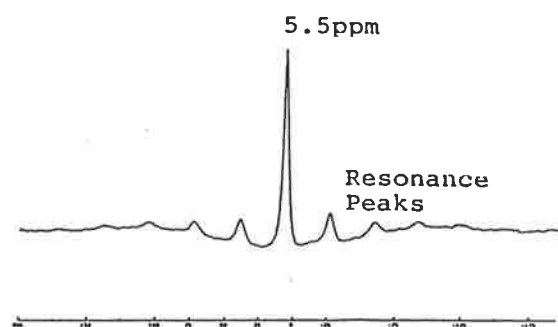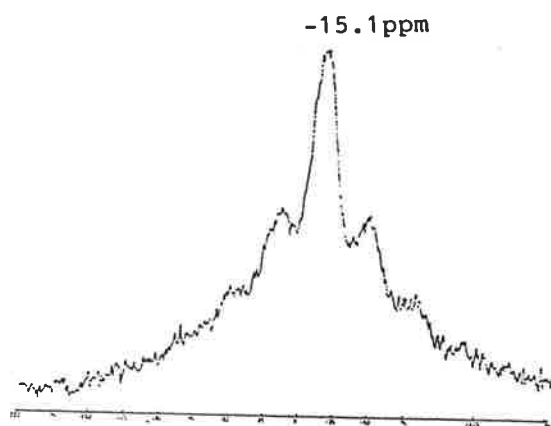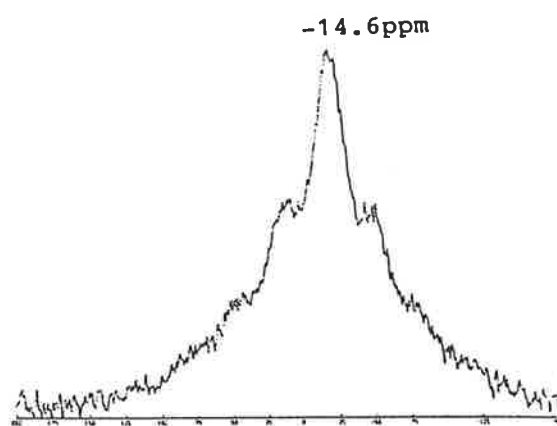To determine the kinetics of impurity removal during high-temperature pre-treatment is a difficult, if not impossible task. This is because low temperature aqueous leaching will occur as soon as the coal is slurried with water, which will mask the influence of other mechanisms which may take place during dewatering. Therefore to gain an insight into the possible mechanisms which will occur during the dewatering reaction, the leaching characteristics of the coal must first be known.

The major mechanisms for impurity removal during dewatering are likely to be: leaching of the coal when placed in the coal/water slurry, water displacement by pore volume shrinkage, and chemical reaction. Chlorine would be extracted mainly by water leaching and pore shrinkage, while additional removal of sodium and sulphur would be effected by decarboxylation and mild thermal cracking reactions. Boyd (1976) found that shrinkage reactions are very rapid for Morwell coal, while decarboxylation reactions are slower and appear to contribute less to water removal. Therefore a major rate limiting step for the removal of sodium, chlorine and sulphate from Bowmans coal is likely to be due to diffusion when the coal is slurried with water.

Separate batch studies were performed to study the diffusion of soluble electrolytes from the coal at temperatures up to 90°C. The results are represented using a model based on

the diffusion of dissociated ions from a sphere. This study forms a foundation for characterisation of soluble ion removal from small sample sizes of Bowmans coal, and assists in determining the relative benefits of various beneficiation processes.

Neavel, Nahas and Koh (1977) first modelled the water extraction of sodium from Illinios coal using a graphical solution to a model of diffusion from a well stirred solution of limited volume proposed by Crank (1957). This procedure relates the fractional extraction of solute (E) to extraction time (t) given by:

$$E = \phi \left(\frac{Dt}{a_{eff}^2} \right)$$

...(8.1)

where D is the diffusion coefficient and a_{eff} is the effective particle radius.

The effective particle radius a_{eff} was used to correct for nonspherical coal particles, pore size distribution and tortuosity. A diffusion coefficient for the leaching in a sodium chloride solution was used in the calculations. A less rigorous although similar approach was adopted by Bettelheim and Hann (1980) and Bettelheim, Hann and Saunders (1982) in their study of the leaching characteristics of chlorine from English coals.

Readett et al. (1984) modelled the removal of sodium chloride from Bowmans coal again using the graphical solution to the diffusion model, and an empirical model based on a two stage diffusion process. They found that the graphical solution to the diffusion problem did not adequately describe leaching from small coal particles, and concluded that the removal of sodium chloride can be adequately correlated by an empirical model. This model was also applied to sodium removal by ion exchange in 2M HCL solutions Readett et al. (1986).

Recently Chein et al. (1986) used a mathematical solution to the diffusional model of Crank, and an empirical model to study the removal of chlorine from Illinois coal. Although they were able to correlate chlorine removal using the diffusional model, they recommended the empirical approach because of the complex nature of the coal and the difficulty in evaluating key parameters such as effective diffusivity.

In this study, the diffusion of all soluble ions from the coal will be described rather than only one or two species. Diffusion coefficients for each ion were calculated from the theory of diffusion in solutions of mixed ions, and all other parameters were experimentally obtained. The more rigorous mathematical model of diffusion of solute from spheres in a solution of limited volume is given by

$$\frac{C_o - C}{C_o - C_\infty} = 1 + \sum_{n=1}^{\infty} \frac{6(1-\alpha)\exp(-Dq_n^2 t/a^2)}{9 + 9\alpha + q_n^2\alpha^2} \frac{a\,\sin(q_n r/a)}{r\,\sin q_n} \qquad ...(8.2)$$

where q_n's are the non-zero roots of the transcendental equation

$$\tan q_n = \frac{3q_n}{(3 + \alpha q_n^2)} \qquad ...(8.3)$$

the ratio of volumes of solution to sphere volume if there is a partition factor K is

$$\alpha = 3\frac{V}{4\pi a^3 K} \qquad ...(8.4)$$

which is expressed in terms of desorption into a well stirred solution is given by

$$3\frac{C_\infty}{4\pi a^3 C_o} = \frac{1}{1 + 1/\alpha} \qquad ...(8.5)$$

The model was used for correlating the rate of diffusion from the coal of all the soluble ions present in the coal. As there is some difficulty in experimentally calculating diffusion coefficients, these were estimated from theory of mixed ions in solution. For diffusion of electrolytes, electrical neutrality must be maintained; specifically the faster moving species may not move ahead of the slower moving partner. Previous experimental studies to model the leaching of electrolytes from coal failed to account for the effect of the presence of other ions. Therefore the Vinograd and McBain (1941) theory of diffusion of mixed ions was used to describe the diffusion of electrolytes within the coal. There are two equations, the first for the cation and then the anion.

$$D_+ G_+ = -\frac{rt\lambda_+}{F_a^2 n_+}\left(G_+ - n_+ c_+ \frac{\Sigma\lambda_+ G_+/n_+ - \Sigma\lambda_- G_-/n_-}{\Sigma\lambda_+ c_+ + \Sigma\lambda_- c_-}\right) \qquad ...(8.6a)$$

$$D_- G_- = -\frac{rt\lambda_-}{F_a^2 n_-}\left(G_- + n_- c_- \frac{\Sigma\lambda_+ G_+/n_+ - \Sigma\lambda_- G_-/n_-}{\Sigma\lambda_+ c_+ + \Sigma\lambda_- c_-}\right) \qquad ...(8.6b)$$

As this equation is a function of temperature, the effect of temperature on the leaching of ions from the coal can easily be included. These diffusion coefficients must relate to the effective diffusion in porous solids to allow for void fraction, tortuosity and varying pore section. This is given by:

$$D_{eff} = \frac{D}{\tau} \qquad ...(8.7)$$

8.2 EXPERIMENTAL

Experiments were performed using about 20 grams of Bowmans coal of particle sizes between 0-0.495, 1-2, and 2-4 mm. A known mass of coal was placed in a flask and water at leaching temperature was added in 1:1, 1:2 and 1:5 coal water ratios. Leaching was carried out at 20, 50 and 90°C; solutions were kept at this temperature for up to 24 hrs by placing the flask in a heated water bath. Evaporation of the water from the flask was minimized by placing a plastic film over the mouth of the vessel. A flask shaker was used to agitate the coal water mixtures, ensuring complete mixing. The mixture was then filtered off rapidly in a Buchner funnel and the liquor retained for analysis. The concentration of cations were determined using a atomic absorption spectrophotometer, while chloride and sulphate were analysed using Mohr titration and colorimetric methods respectively.

Further experiments were performed using much larger sample sizes to determine the equilibrium concentrations of ions in the liquor for each coal water ratio. A number of tests were also undertaken at leaching ratios of 1:25, as this gives an approximate value of the concentration of the ions in the coal. Results of these studies may be found in the Appendix.

Small batch tests for specific periods of time were undertaken rather than taking samples from a large slurry for two main reasons. Firstly, rapid liquor removal from the slurries could be achieved for tests of short residence time. Secondly the small sample size is consistent with the high-temperature pre-treatment experiments, and will enable the characterisation of small coal samples. To ensure results are representative of the coal used, each test was at least duplicated. However because of the variable nature of Bowmans coal it was difficult to model the leaching of low concentration elements such as Ca and Mg. Therefore a final leaching test was carried out using 500 grams of 2-4 mm coal slurried with 1 litre of distilled water; samples were taken from this slurry at specific time intervals and analysed for ion removal.

8.3   RESULTS AND DISCUSSION

Before applying the model for the removal of ions in coal a number of parameters must be found. These include the desorption constant, initial concentration of ions in coal, diffusivity coefficients and tortuosity. The values of desorption constant and initial concentration may be found experimentally using the equilibrium conditions of the leaching tests, while tortuosity was found by optimizing the leaching data.

Evaluating initial concentrations of soluble ions in the coal is hindered by the adsorption of these ions onto the coal surface. Although there may be some ions adsorbed to the coal surface, it is considered that most of the ions are removed from the coal by leaching in coal water ratios of 1:25. The partition factor gives a tool to measure the quantity of ions still adsorbed to the coal surface at various coal water ratios, and therefore a more accurate indication of the total amount of soluble ions present in the coal. A mass balance over the amount of ions present in the coal and in the leach liquor at equilibrium conditions is given by

$$VC_\infty + vKC_\infty = vC_o \qquad \qquad ...(8.8)$$

Note that v in this equation is the volume of water in the coal rather than the coal volume. Hence the calculations of initial concentrations are based on the water phase of coal particles, in Bowmans coal roughly about 50% of the total weight. The partition factor and initial concentration of electrolyte can be solved graphically by simple rearrangement of the formula.

$$\frac{VC_\infty}{v} + KC_\infty = C_o \qquad \qquad (8.9)$$

If VC_∞/v is plotted against C_∞, the slope of the graph is equal to the partition factor K, while the intercept is the initial concentration of soluble ions in the coal, C_o. A plot for

sodium removed from Bowmans coal is shown in Figure 8.1. Results of the equilibrium conditions were obtained from large scale leaching tests over 24 hrs, as well as kinetic data from long term batch leaching experiments. The linear fit of this plot indicates that there is indeed adsorption of sodium ions on the coal surface, the extent of which can be described in terms of a partition factor. A statistical analysis of this plot using a 95% confidence interval indicates that the partition factor is probably within 20% of its true value, while the initial concentration is within 5%. Partition factors and initial concentrations of soluble ions in Bowmans coal are shown in table 8.1, although the variability in equilibrium concentrations of calcium and chloride ions make it difficult to report the values of these parameters with the same degree of confidence.

The initial soluble ion concentrations calculated from these regressions were used in the diffusion equation to calculate coefficients for each ion. The diffusion equation modifies the diffusion coefficient of a single ion for the influence of mixed ions in the coal. Table 8.1 also shows values of single ion diffusivity, mixed ion diffusivity and effective diffusivity, as well as the values of ion conductances used in the diffusion equations. These values show that mixed ion diffusion coefficients for the cations have increased, while the anion coefficients have decreased to ensure electrical neutrality during leaching.

A tortuosity factor of 5 was used to change the value of mixed ion diffusivity to an effective diffusion coefficient. This parameter accounts for porosity, varying pore diameters, non spherical coal particles and 3 dimensional leaching in the diffusional model. The value was found by least squares optimization of the diffusion model with experimental data; generally this value is expected to lie between 3 to 6, therefore 5 is considered a reasonable estimation. As the optimization of diffusion coefficients was very sensitive to the initial concentration of free ions in the coal, estimating a more accurate value of this parameter proved to be difficult because of the variability in equilibrium concentrations of electrolytes in Bowmans coal.

In order to satisfactorily model the diffusion of electrolytes from the coal, an assumption must be made that the final concentration of ions in solution results not only from simple diffusion but also from other longer term physical and chemical mechanisms. Using the proposed model, diffusion of free ions would be expected to be completed within a few hours for coal of less than 4 mm in diameter, whereas in reality a steady state is still not reached after 3 days. These longer term effects result from interactions in the complex nature of coal and water, and it can be supposed that mechanisms such as adsorption, precipitation, ion exchange, oxidation/reduction and interaction with humic substances could play a part. The equilibrium concentration of soluble ions in the coal shows slightly more cations than anions can be extracted by water leaching. As there is also a slight brown coloration due a suspension of organic material, it is likely that the cations are associated with this material, probably as humic acids. Therefore the change in concentration cations in the leach liquor after long periods of time is probably due to the dissolution of humic material from coal. It has also been seen that the concentrations of sulphate and magnesium in the leach liquor appear to decrease after about 2 hrs. It has been noted during the dewatering experiments that these ions probably precipitate out of solution.

To model the leaching characteristics of ions from Bowmans coal would be a difficult task if all these mechanisms were taken into account. Fortunately the primary purpose of this study is to model impurity removal during high-temperature pre-treatment where process steps such as slurry forming and transport would require only short contact time between the coal and water. As mechanisms other than electrolytic diffusion appear to be much slower and exert less influence for impurity removal over short residence times, the dewatering process is adequately modelled.

Results of the diffusion model of sodium removal for various coal sizes in Bowmans coal are compared against experimental values in figure 8.2. The model prediction for sodium removal from Bowmans coal appears to correlate well with the experimental values. There is much difficulty of applying one value of initial concentration to all results, as each

series of tests generally exhibited varied equilibrium concentration of free ions. Therefore the plot of sodium removal is based on the equilibrium concentration measured for each particular series of tests. Results of leaching different coal particle sizes in various coal/ water ratios also appear to fit results well, albeit difficulty exists in getting reproducible results from small sample sizes.

Figure 8.3 shows the model predictions and experimental results for sodium removal as the coal/water ratio varies in coal of particle size between 2 to 4 mm. Again the model shows a good fit compared with experimental results.

Not shown in these figures are the results studying the effect temperature has on the extent of soluble ion removal. Although results appear to show progressively faster diffusion rates as temperature increases, the variable nature of Bowmans coal and the small overall change in diffusion rates makes it difficult to quantify the experimental results.

Model predictions for removal of other ions from Bowmans coal for particle size of 2-4 mm and for coal water ratio of 1:2 is shown in figure 8.4. These results are compared against the data obtained from the continuous leaching experiment. From these results it can be seen that the diffusion model appears to fit experimental data well. From these results it can be seen that the relative rates of each diffusing ion is predicted by theory; any discrepancy between the values of diffusion coefficient is probably due to difficulty in predicting the initial concentrations of free ions in the coal.

8.4   CONCLUSIONS

The kinetics of ion removal from Bowmans coal by aqueous leaching was studied to predict impurity removal from coal/water slurries during high-temperature pre-treatment. A mathematical model based on the diffusion of electrolytes from spherical particles in solutions

of limited volume was proposed. This model was found to adequately predict the leaching characteristics of sodium, chloride, magnesium, calcium and sulphate ions from coal up to 4 mm in size at temperatures up to 90°C.

Three parameters were needed in this model, a partition factor to account for ions absorbed to the coal surface, the initial concentrations of soluble ions, and a tortuosity factor to relate diffusion coefficients to porous coal particles. Diffusion coefficients were calculated from theoretical equations for diffusion of mixed electrolytes in solution.

TABLE 8.1

Concentrations, Partition Factors and Diffusion Coefficients
used in the Diffusion Model

| | Initial Conc in Coal liquor | Partition Factor | Ion Conductances | Diffusion Coefficients at 20°C $\times 10^5 \, cm^2 \, sec^{-1}$ | | |
				Single Ion	Mixed Ion	Effective
	ppm	K	λ			
Cations						
Na^+	11,800	1.5	50.1	1.33	1.47	0.29
Mg^{++}	3,200	1.0	53.1	0.71	0.87	0.17
Ca^{++}	1,700	1.4	59.5	0.79	0.97	0.19
Anions						
Cl^-	15,000	1.0	76.3	2.03	1.75	0.35
$SO_4^=$	21,000	1.5	79.2	1.06	0.79	0.16

Figure 8.1 Plot used to Determine Partition Factors and Initial Concentrations of Sodium
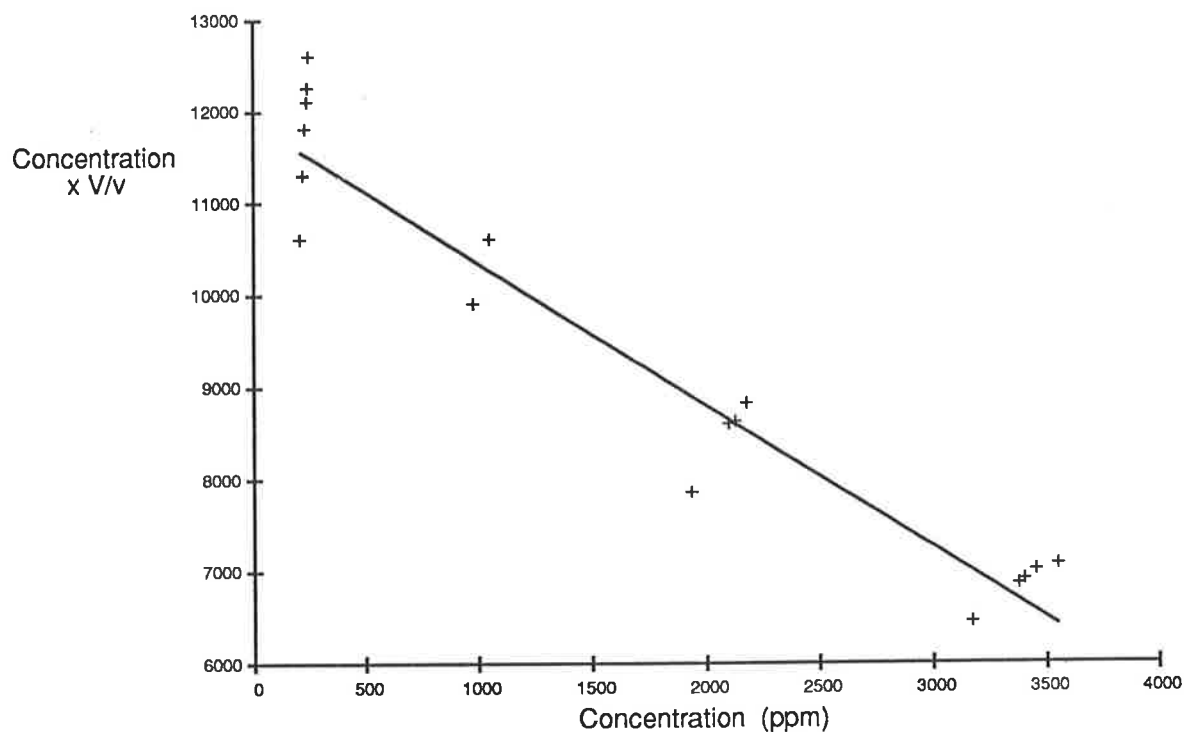
Figure 8.2 Percentage of Total Sodium Removed from Coal of Various Particle Sizes at a 1:1 Coal/Water Ratio and at 20 degC
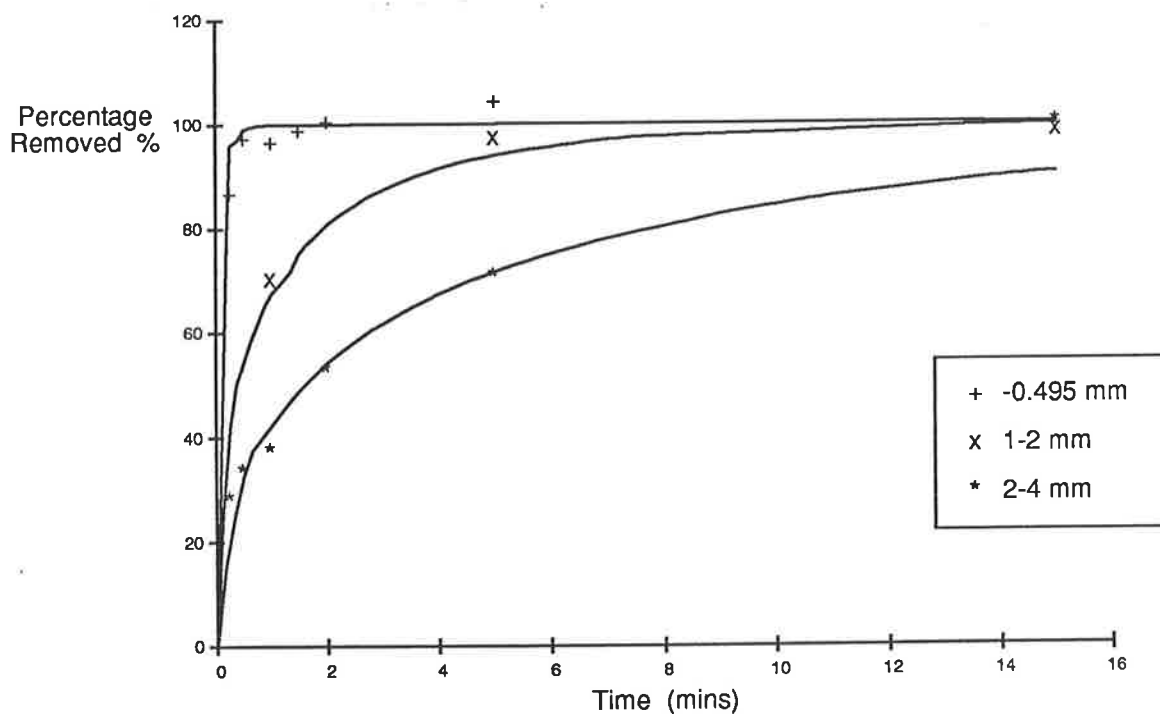
Figure 8.3 Concentration of Sodium in Leach Liquor
Effect of Changing the Coal/Water Ratio at 20 degC
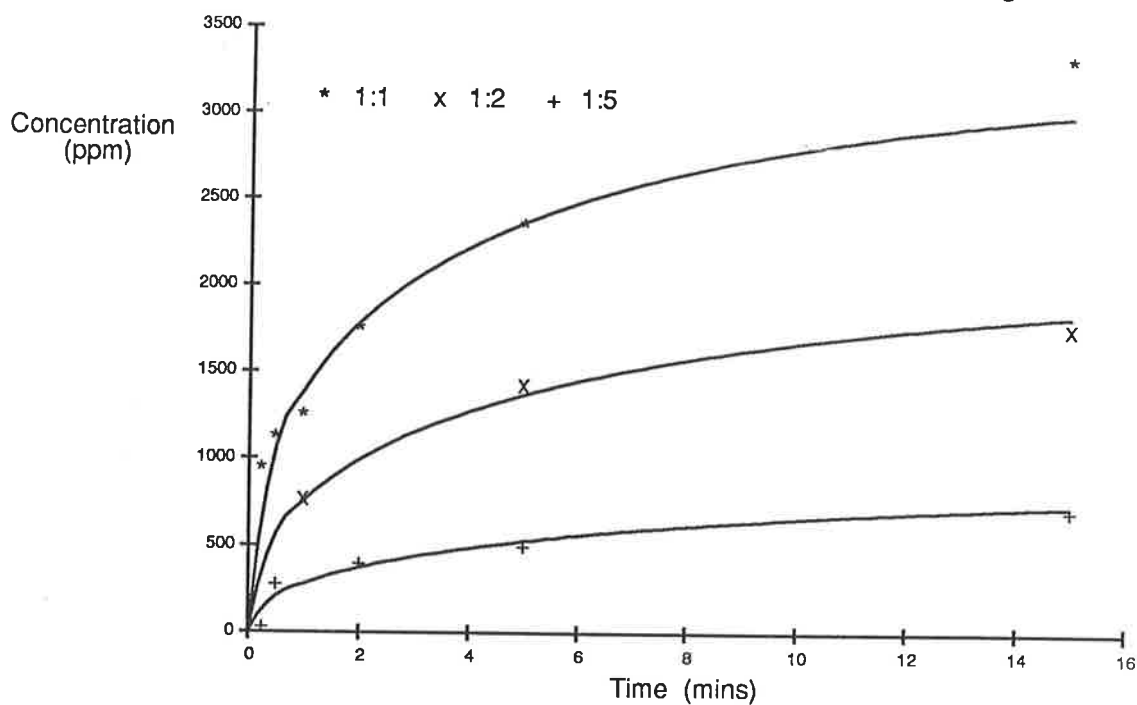
Figure 8.4 Concentration of Various Ions in Leach Liquor
Coal/Water Ratio 1:1, Coal Size 2-4 mm, Temp = 20 degC
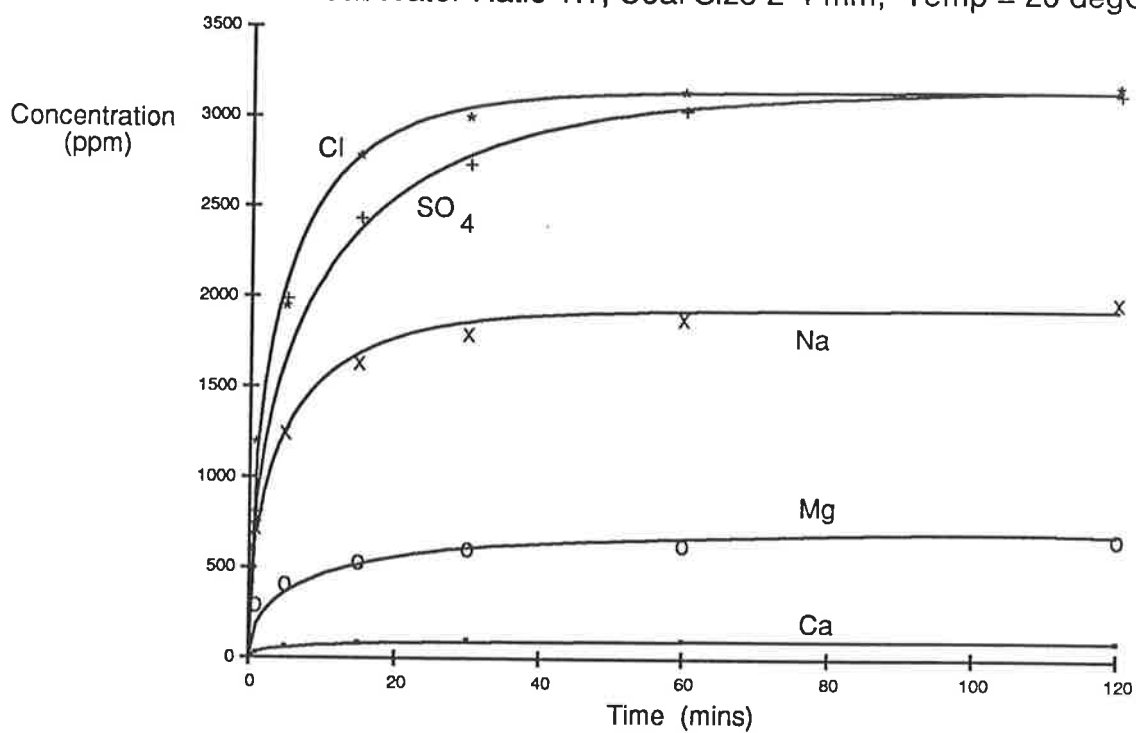
9. FILTRATION CHARACTERISTICS

9.1 INTRODUCTION

The filtration characteristics of raw and dewatered Bowmans coal were determined by small scale tests using a constant vacuum filtration cell. Tests were carried out to determine parameters necessary to calculate the filter design requirements for a high-temperature pre-treatment plant, and to forecast the likely filter performance.

Although large scale filtering tests are generally better for the design of filtration equipment, these tests were not possible with the small quantity of treated coal sample available. Therefore, while these tests should not be used as the sole basis for the design of processing plant, they are valuable in predicting the effects of changing process conditions on filter performance.

To interpret the results from the filtration cell, the design equation for filtration under constant pressure is used. It is given by

$$t = \frac{1}{\Delta P} \frac{\eta}{A} \left(\frac{\alpha m}{A} \left(\frac{B^2 - B_o^2}{2} \right) + \beta (B - B_o) \right) \qquad ...(9.1)$$

where alpha is the specific resistance of the cake and beta is the resistance of the filter medium. The variables in this equation can be determined from experimental data if a

constant pressure test is performed on a slurry. Figure 9.1 shows how the mass of filtrate is obtained over a corresponding time can be used to obtain values for the specific resistance of the filter cake and the resistance of the filter medium. The values can then be employed in the design of a pilot or processing plant to scale up from these small scale tests.

Figure 9.1

Typical Plot of Filtration Data

$$\frac{t}{B-B_o}$$

$$\text{Slope} = \frac{2A^2\Delta P}{\eta m}\alpha$$

$$\text{Intercept} = \frac{A\Delta P}{\eta}\beta$$

B_o = Volume at t=0

B
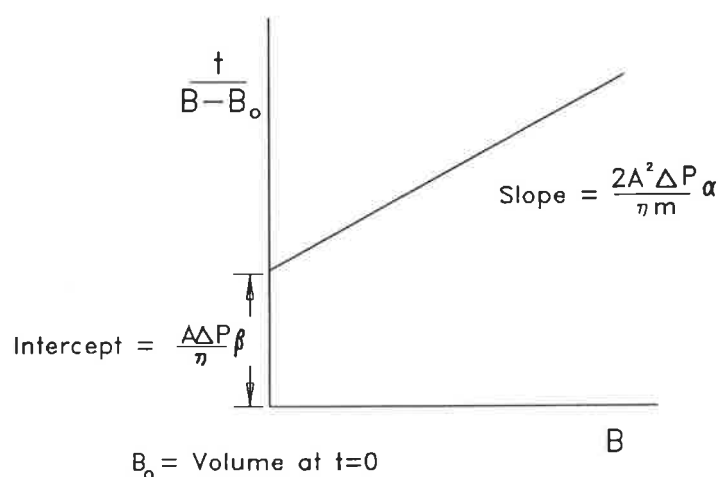
This figure shows that under constant pressure conditions alpha and beta can be calculated easily by plotting inverse rate of filtrate collected vs volume of filtrate. The slope of the plot can used to obtain specific resistance of the filter cake, and the intercept is used to find the resistance of the filter medium. Obviously, low values of the slope and intercept of these plots for a coal/water slurry indicates that the filtration characteristics are good. When the bulk water has drained from the coal the slope will increase, indicating that filtration of the slurry is completed. The rate of water thereafter removed from the coal indicates the dewatering characteristic of the solid on the filter.

9.2 EXPERIMENTAL

The experimental system used for this study is shown in figure 9.2. Coal of less than 1mm in size was slurried with water and left for 5 mins to equilibrate and leach. It was then quickly put into a Buchner funnel held under a vacuum of 10 ins of Hg. The amount of filtrate collected was recorded at regular time intervals for up to 6 minutes using a Mettler balance to measure the mass of water passing through the funnel. The coal was then collected and the moisture content determined in a nitrogen oven.

Tests were carried out for various coal to water ratios for raw coal, and on a number of dewatered coal samples. Also tested was the effect of using "fresh" coal samples (coal recently taken from a storage drum), and the use of methanol as a surfactant to improve dewatering ability of the coal. This type of test equipment simulates conditions similar to those found in belt filters, where the filter slurry is loaded quickly onto a continuous filter belt.

Figure 9.2

FILTRATION CELL
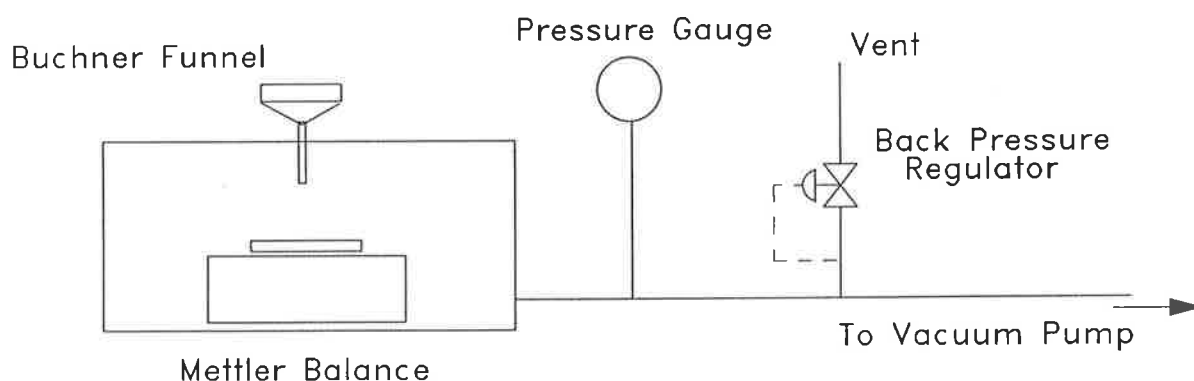
9.3 RESULTS AND DISCUSSION

Results of the filtration tests may be seen in table 9.1. This table shows the coal water ratio used in the slurry tests, the slope and intercept of the filtration plot. The plots of the filtration tests are in Appendix B. Three separate plots were obtained for each coal/water ratio, including graphs showing the rate of water collected and the dewatering characteristics after the coal is filtered.

It was observed that dewatered coal is much easier to filter than raw coal; the surface of the dewatered coal generally appeared drier, the filter cake more friable and it is easily removed from the filter paper. The improved filtering characteristics of dewatered coal were even more noticeable in earlier dewatering experiments when the coal was still fresh. It would be expected that the filtering characteristics of coal recently mined and thermally dewatered would be substantially better than that reported in these tests.

From table 9.1, results show that the specific resistance of both the cake and the filter medium have improved following thermal treatment. In past leaching studies of raw Bowmans coal it was found that variability of filtration rates during tests was probably due to cloth binding (AMDEL, 1983), and that this would probably be a problem in belt filters. Binding of the filter medium also appeared to occur when raw coal was used during these current tests. Cloth binding therefore may be a problem in design of a processing plant for leaching raw coal.

Dewatered coal, on the other hand, proved to filter well during all tests. The results show that the filtration characteristics of thermally treated coal are much improved over raw coal. The breakdown of functional water-binding groups in the coal would modify the surface characteristics of the coal markedly, making the coal more hydrophobic, a condition desirable in filtering solids. Thermal dewatering also appears to cause agglomeration of coal fines, which may also improve the filtering characteristics of the coal.

There was little improvement in the filtering characteristics of coal which had methanol added to slurry for either the dewatered or leached samples.

TABLE 9.1

Filtration Characteristics

COAL/WATER RATIO	MOISTURE CONTENT %	SLOPE $\dfrac{2A^2\Delta P}{\eta m}\alpha$	INTERCEPT $\dfrac{A\Delta P}{\eta}\beta$
Raw Coal			
5/5	62.4	1.88	11.53
5/10	60.3	0.28	9.15
5/25	66.4	0.49	6.51
10/20	61.0	0.25	6.52
10/20*	60.2	0.24	3.35
15/30	58.9	0.18	7.12
Dewatered			
7.7/13.4	39.7	0.14	5.03
8.7/16.6	43.8	0.05	3.38
8.8/17.3*	39.6	0.03	3.39
6.3/10.1*	34.8	0.11	2.18
1% Methanol			
Raw Coal			
10/20	60.2	0.27	3.71
dewatered			
8.8/17.4	38.7	0.11	2.18
7.2/15.1	37.2	0.02	2.63
10% Methanol			
Raw Coal			
10/20	59.3	0.27	5.47
dewatered			
10.0/16.8	42.8	0.09	6.32
7.7/15.5	39.7	0.00	5.41

* Fresh Sample taken from storage drum

10. WASTEWATER CHARACTERISATION

10.1 INTRODUCTION

High-temperature pre-treatment of Bowmans coal produces an upgraded coal which would be suitable for use in a conventional power station. However the process produces a significant amount of wastewater which would require treatment before being discharged from a process plant.

Effluent from the high-temperature pre-treatment process was analysed with the aim of providing data on the levels of impurities present. This information enables an insight into the wastewater treatment steps which would be incorporated into a processing plant.

10.2 EXPERIMENTAL

For this series of experiments Bowmans coal was dewatered in an enlarged tube bomb reactor to gain more product liquor to use for analysis. The tube bomb, while essentially the same as shown in figure 3.1, uses reactor tubing of 1" in diameter and is able to dewater up to 44g of coal in each experiment. To obtain the product liquor for analysis a 1:1 coal/water mixture was dewatered for 20 minutes at a temperature at $325^{\circ}C$.

The analysis of soluble ions in the product liquor have been described in chapter 4.4. The standard methods of analysis of B.O.D., C.O.D. and Humic Acids were obtained from

"Standard Methods for the Examination of Water and Wastewater", 14th Edition. Phenols were determined using a photometric method with 4-aminoantipyrine, as G.C. methods proved unsatisfactory. The biochemical oxygen demand was obtained with use of an acclimatized seed culture.

All determinations were performed on at least duplicate samples.

10.3 RESULTS AND DISCUSSION

The results from the analyses of the effluent from dewatering Bowmans coal are given in table 10.1. These are compared with the results from similar dewatering studies, which have been corrected to allow for the effect of dilution by make-up water or steam condensate. To facilitate this comparison Bowmans data have also been corrected.

The B.O.D. and C.O.D. values are an important measure of the degree of contamination of organic compounds. It can be seen that these values are relatively high for the product liquor from Bowmans coal and are similar to those found by Brown (1977) from the liquor obtained from Morwell coal. The ratio of B.O.D/C.O.D is high, indicating that a high proportion of organic pollutants is biodegradable; possibly due to the comparatively severe reaction conditions giving a greater extent of decomposition of large molecules.

The concentration of total phenolic compounds is comparable to that found by other studies. No phenolic groups were detected in the Morwell study. However, as it is difficult to effectively analyse these compounds, it is possible that some phenolic groups were present in Morwell wastewater. The quantity of phenolics evolved from the Bowmans coal during dewatering would not be expected to be very high, as NMR spectroscopic studies has shown that there is little aromatic material present in this coal.

The parameter which is significantly higher for Bowmans coal dewatering effluent is the total dissolved solids value (T.D.S.-which includes suspended solids). This is because of the high quantities of soluble inorganics present in the coal which can easily be removed in the wastewater.

The amount of hydrogen sulphide dissolved in the liquor will significantly change depending upon the conditions the liquor is subjected to before analysis. The aspiration of dissolved gases when the tube bomb reactor is opened, the use of vacuum filtration, and any agitation or aeration are all factors which would dramatically lower the concentration of hydrogen sulphide in the liquor. In order to have an idea of the possible concentration, the value of the amount of hydrogen sulphide in the gas (as measured by G.C.) was used to calculate the approximate level of dissolved hydrogen sulphide under equilibrium conditions. This was found to be 540 mg/l. A single analysis of a sample of filtered liquor gave a figure of 240 mg/l.

The liquor as taken from the tube bomb is a clear yellow solution, which rapidly darkens and a precipitate forms over a period of hours. This may have some consequence in the design of a treatment scheme. The discolouring of liquor is probably due to the oxidation of humic material in the waste water.

TABLE 10.1

Comparison of Wastewaters

mg/l	Bowmans 325°C	Bowmans corrected	Morwell 300°C (1)	Kosovo 235°C (2)	Motru 235°C (2)	Kolubara 300°C (2)	Koflach 235°C (2)
Na	3,500	14,400	1,140	226	296	59	-
Mg	200	820	530	23	26.2	27	-
Ca	300	1,230	990	100	226	110	-
K	50	210	970	5.7	12.8	17	-
Fe	4.0	16	4.0	1.3	3.2	2.1	-
SO_4	3,500	14,400	-	159	576	61	-
Cl	4,000	16,400	480	223	98.6	80	-
pH	5.1		5.25	7.6	7.3	6.0	-
BOD_s	3,900	16,000	14,300	1,000	813	1,700	1,500
COD	8,800	36,000	32,800	10,000	7,550	9,400	8,000
BOD_s/COD	0.44	0.44	0.44	0.1	0.11	0.18	0.17
TDS	13,300	54,500	20,850	14,000	20,000	11,000	9,000
Phenol	75	310	-	315	320	389	350
Humic Acids	500	2,000	-	572	560	598	5,500

(1) Brown (1977)

(2) Mitrovic (1968)

11. CONCEPTUAL DESIGN

11.1 OVERALL PROCESS DESIGN

A flow diagram showing the major stages of a continuous processing facility for Bowmans coal is presented in figure 11.1. This plant consists of four major areas

1) Slurry Preparation and Feeding

2) Dewatering Reactor

3) Solids Recovery

4) Wastewater Treatment.

Most of the technology required for the design of this processing plant can be obtained with little modification from established processes. Process equipment used in the design of this plant are generally "off the shelf" equipment items that are used in slurry transport or coal washing processes. However the design of the dewatering reactor will require detailed study to optimize performance.

11.2 SLURRY PREPARATION AND FEEDING

Figure 11.2 shows the equipment required for the preparation and feeding of the coal/water slurry to the reactor. The crushing equipment required for this process was based

on a study about washing Bowmans coal by AMDEL in 1984. A lock hopper pumping system has been used in the design to minimize possible difficulties in pumping a slurry of high solids loading and using coal of large particle size.

This design is based on utilizing dewatered coal for direct combustion in a power plant and assumes the coal/water mixture must be separated to remove the inorganic impurities. A coal particle size of 90% minus 4mm was used in this process, although the size which would be used in an actual processing plant would probably be determined by equipment constraints rather than process requirements. As the extent of dewatering does not appear to be affected by particle size the largest possible size should be used to minimize filtration costs. This should be balanced against the cost of pumping large particles and the effectiveness of ion removal. If it were desirable to increase the size of the coal particle above 4mm it would be necessary to allow the slurry to leach for a period of time in the mixing tank.

The are many pumping systems available which can be used to raise the slurry pressure to reaction conditions of about 13.0 MPa. Piston pumps are capable of delivering a coal/water slurry to this pressure but are generally limited to particle sizes finer than 3mm. However, to enable the use of large particles in the slurry a system of continuous lock hoppers were assumed in the process design. This system uses the principal of alternately filling and emptying chambers to pump the coal/water slurries to high pressure. As only water is pumped to high pressure large coal particle sizes can be used at high solids loading. However more plant equipment is required and the lock hoppers must be built to withstand high pressures. A similar technique which may be more efficient and less expensive is the use of Kamyr rotary lock hoppers. While they are capable of feeding large coal particles at rates of 500 ton/hour, they have only be used at pressures up to 10.4 MPa and may need modification for use in this process.

11.3 DEWATERING REACTOR/HEAT-EXCHANGE SYSTEM

While the kinetics of dewatering reactors can be modelled using tube bomb reactors, a number of additional factors must be taken into account to design an industrial scale continuous reactor. These factors include:

1) conventional shell and multiple tube heat exchangers may not be suitable for slurries of large particle size as dead spots may occur in the exchangers. They may therefore need to be modified to minimize these problems.

2) the exchanger would need to be designed to withstand high pressures.

3) coal may stick to the sides of the reactor causing fouling.

Shown in figure 11.3 is a conceptual design of a reactor/heat-exchange system. The design is based on using a multiple tube heat exchanger using a countercurrent heating medium in the shell side of the exchanger as the dewatering reactor. The heating medium would be used to recover energy from the product stream and would be heated externally to the required reaction temperature. The reactor tubes could be cleaned if surface fouling proved to be a problem and the heat exchange medium could be chosen to maximize heat transfer coefficients.

Other features may be incorporated into the design of the dewatering reactor to recover more energy and make the process more efficient. They include the more efficient use of counter current heat exchangers for the feed and product slurries, the use of turbines to recover energy from the high pressure gas, and the separation and use of product gases for combustion.

11.4   SOLIDS RECOVERY

A simple solids recovery system, figure 11.4, is proposed to recover the dewatered coal product from the slurry. The coal is initially screened to about 1mm in size; the large particles are then fed to a basket centrifuge while the fine solids in the slurry passes through the screen to the thickener.   The bottom product from the thicker is recycled through a hydrocyclone to the screen. The top product from the thickener is passed to a clarifier for final treatment. The clarifier must give a solids free effluent, and a vacuum filter recovers the fine solid components from the underflow.

The efficiency of solids recovery from this system is mainly dependent on the effectiveness of the clarifier. It is likely that a flocculant would be required to increase the rate of settling in the clarifier. However from the observations of the dewatered coal product it appeared that many fines in the slurry agglomerate during dewatering. This, in conjunction with the coal crushed to a reasonably large particle size, would mean that there would probably be very little solids in the effluent from the clarifier.

It was also noted that the filtration characteristics are of dewatered coal are very much improved compared with leached coal. Filtration requirements would not be as demanding as that required for water leached coal and less vacuum filters would be needed. This would significantly lower the cost of dewatering compared with comparable water leaching processes.

11.5   WASTEWATER TREATMENT

The effluent from the high-temperature pre-treatment process is not stable, and a period of equalisation may be necessary before wastewater treatment is undertaken. The precipitation of organics in the effluent has not been closely studied, but a significant

proportion of organic material may be precipitated over a period of hours to days. As part of the primary treatment of wastewater, it will probably be necessary to remove the settleable solids, possibly with the use of alum or other settling agents.

The wastewater will contain a relatively high amount of dissolved sulphide and possibly other dissolved gases which will inhibit or interfere with later operations. The removal of dissolved gases will probably be necessary, and may be achieved in a number of ways. Peroxide oxidation of sulphides with air oxidation using manganese sulphate as a catalyst would probably be necessary. Alternatively steam stripping could be used.

The pH of the wastewater will need to be adjusted to a range within which a biological or other oxidation operation may operate (normally 6-8). This step, using NaOH to neutralise the waste liquor, will probably raise the level of dissolved solids substantially.

Biochemical oxidation is an established technique for the decomposition of organic material in wastewater. Most of the organic compounds can be oxidised, typically 85-95% removal of total soluble organic carbon and total soluble C.O.D. Activated carbon can be used as a later step to remove the residual organics. It can also be added to the activated sludge to adsorb organic compounds in order to compensate for a shock load that would otherwise not be tolerated by the microorganisms. Biological treatment is an attractive process step to be considered, from an economic point of view as well as a practical one. The technology is proven, and is successfully used for the treatment of coal conversion wastewaters (Barnes et al., 1984).

Chemical oxidants such as chlorine or sodium hypochlorite can be used to oxidise organic pollutants but have cost disadvantages due to the large volumes which are required.

A potentially cheaper method is the use of oxygen from the atmosphere and the several processes available all have the advantage of virtually complete oxidation of pollutants. Wet-air oxidation is a process which mixes air into the wastewater stream under pressure at a temperature of 200-300°C. This process may have particular applicability for high-temperature process wastewater treatment and may be useful in conjunction with a biological treatment step. Also Aqueous-Phase-Catalytic Oxidation, which uses a packed bed catalytic reactor with lower temperatures and pressures than used by wet-air oxidation, may be used.

A study by Walker (1983) recommends the use of reverse osmosis for the treatment of wastewater produced from the washing of Bowmans coal. Similarly as the dewatering effluent from Bowmans coal is high in dissolved solids, reverse osmosis and/or vapour compression evaporation are the preferred processes for treating the product liquor.

As a preliminary study, a possible treatment scheme would consist of:

Pretreatment-Clarification

-dissolved gas stripping

-pH adjustment

Biological treatment with activated carbon

Reverse Osmosis

Evaporation Ponds

Coal Feed

Gas

Product
Coal

To Stage 4
Wastewater Treatment

Stage 1   Slurry Preparation
and Feeding

Stage 3   Recovery of Solids

Stage 2   Dewatering Reactor
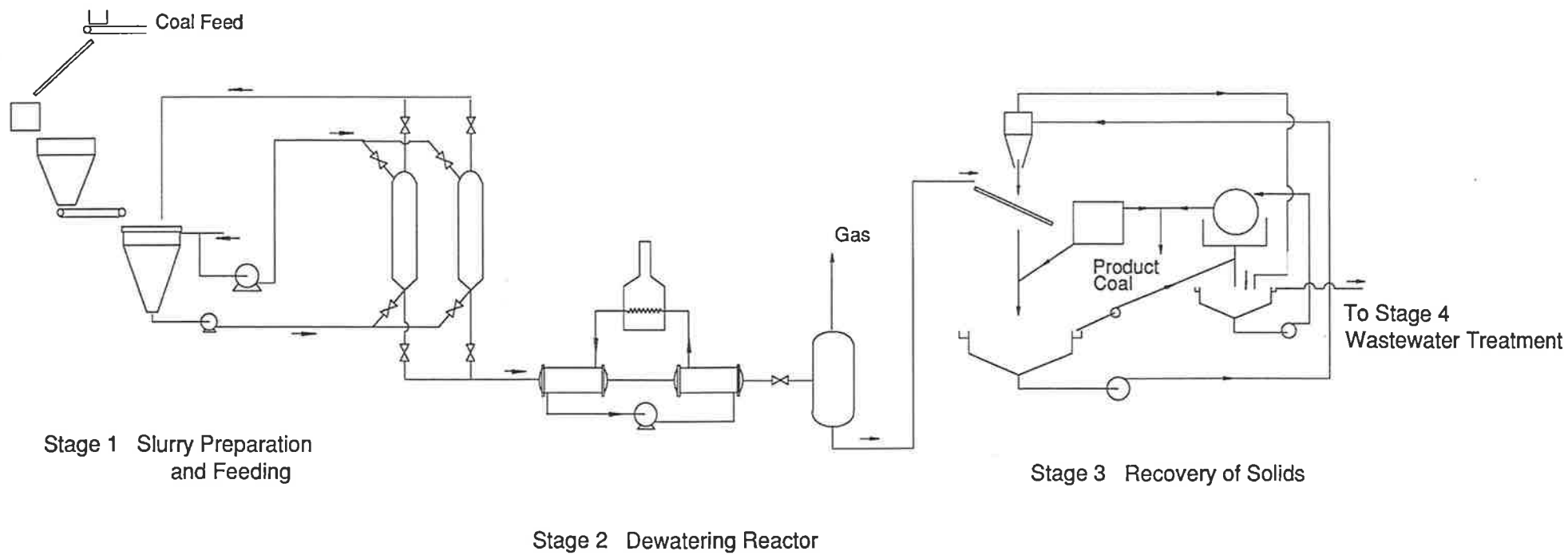
Figure 11.1   Conceptual Design of a Continuous Processing Plant
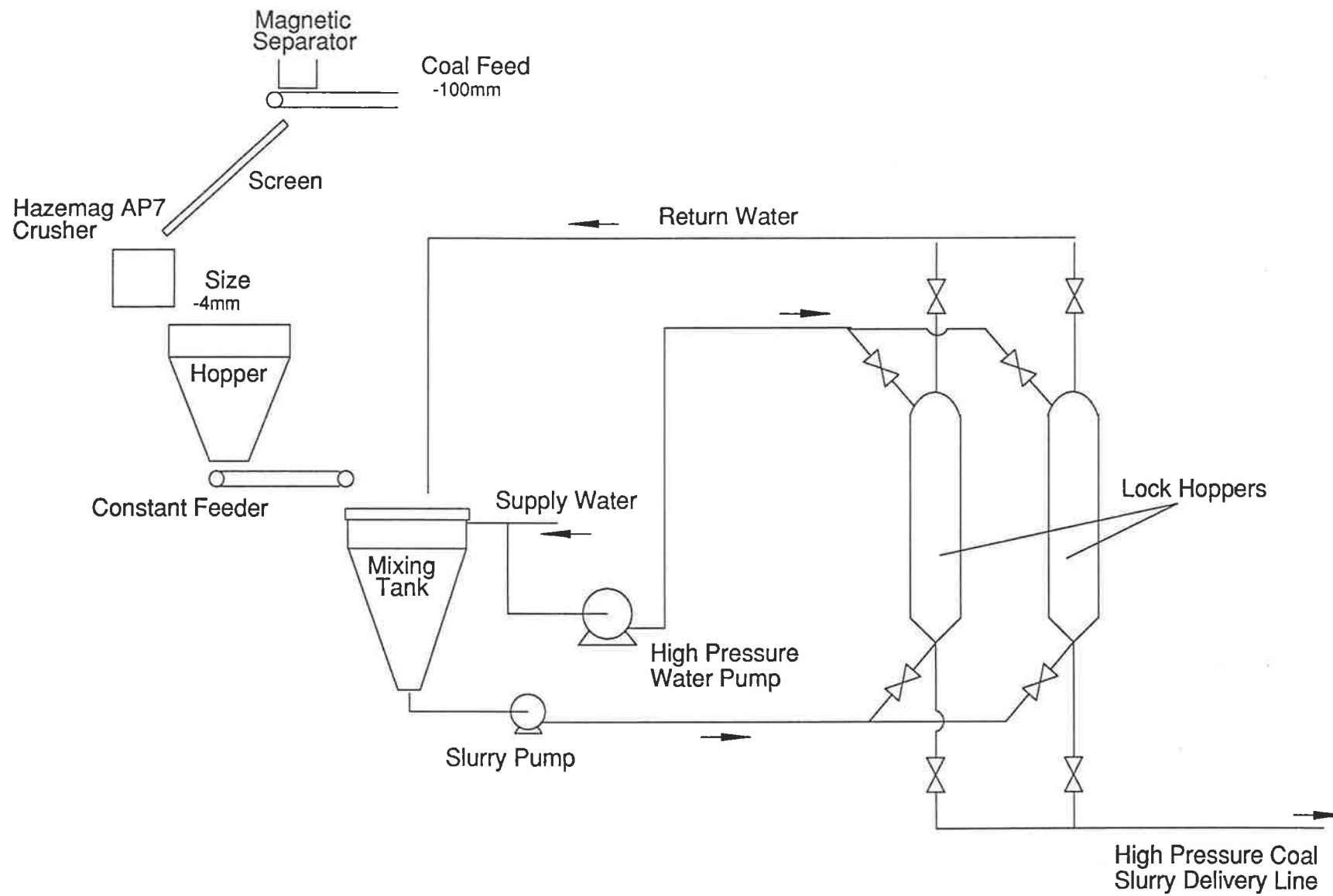
Figure 11.2 Slurry Preparation and Feeding System
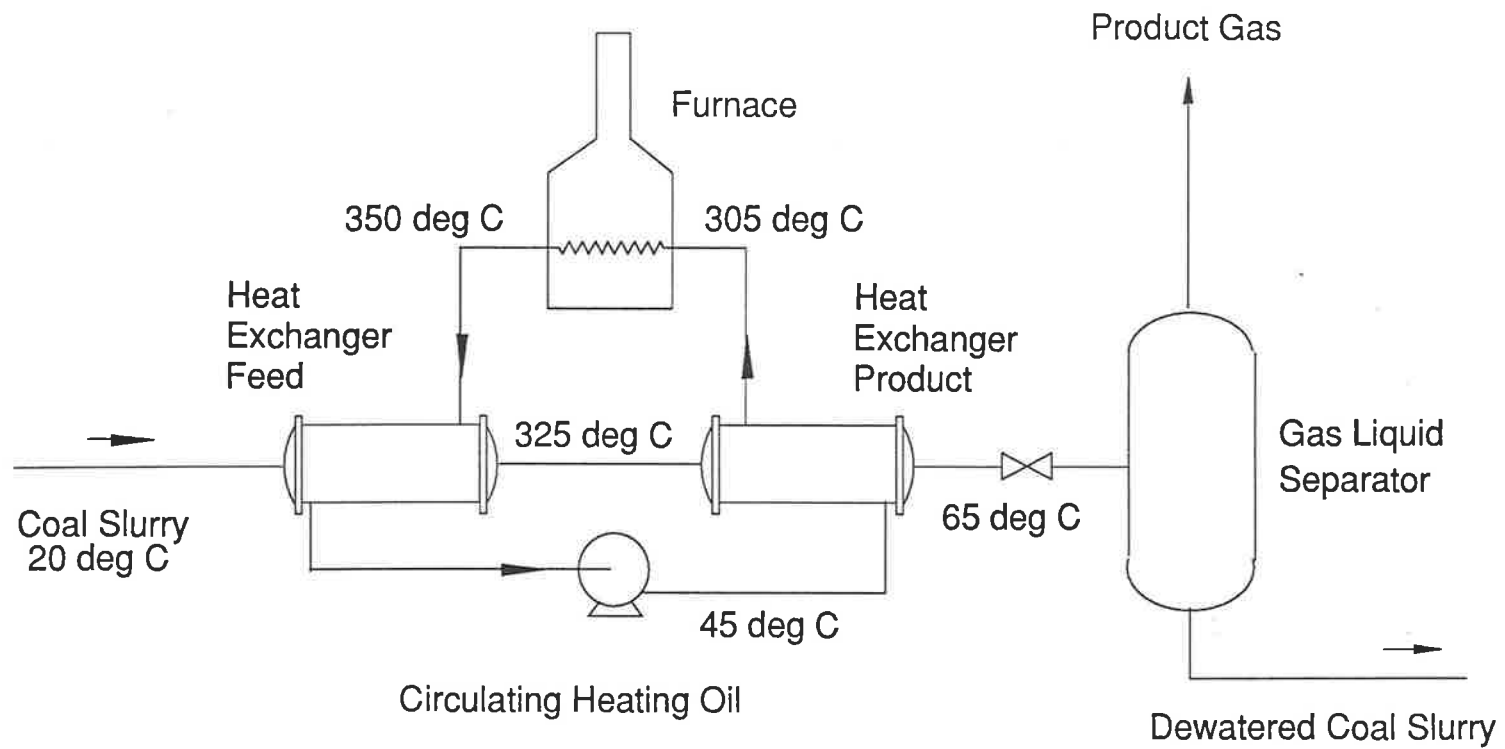
Figure 11.3 Dewatering Reactor and Energy Recovery System
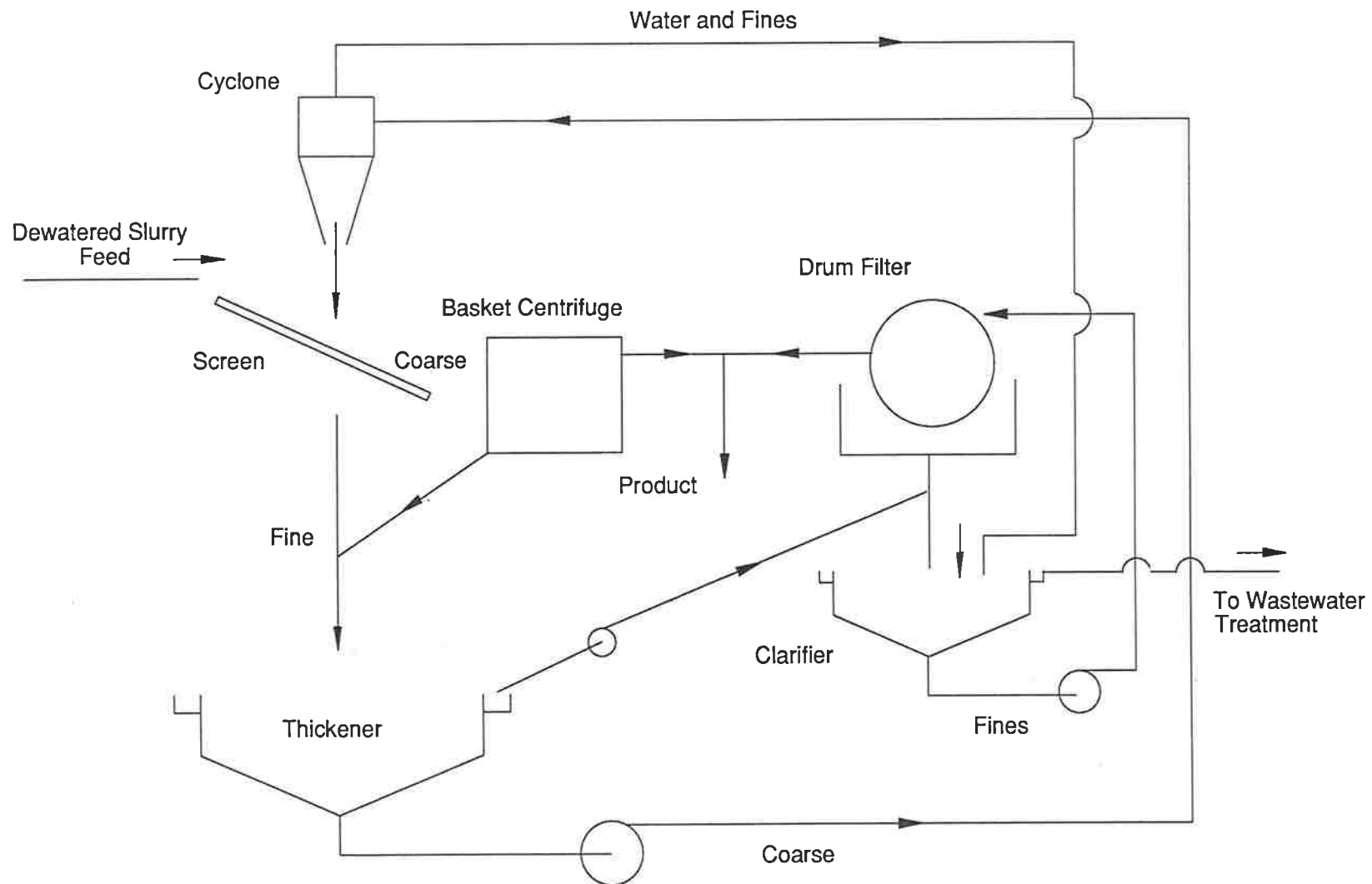
Figure 11.4 Solids Recovery System

11.6 MASS AND ENERGY BALANCES

Figures 11.5 and 11.6 show the mass and energy balances of the dewatering process. These diagrams present the overall balance of the dewatering process, and do not include the losses and inefficiencies which would be associated with an actual processing plant. More rigorous mass and energy balances would be required if detailed design and optimizaton of the major process equipment were undertaken.

The overall mass and energy balances were calculated based on a plant operating at $325^{O}C$ and 12.5 MPa. The ratio of coal to water in the feed was assumed to be 1:1, and all product coal was recovered following dewatering. The assumed analyses of the raw and product coal are shown in table 11.1.

TABLE 11.1

Assumed Analyses of Raw

and Dewatered Coal

	MOISTURE Total % in Coal	VOLATILE MATTER % d.b.	FIXED CARBON % d.b.	ASH % d.b.	HHV MJ/kg
RAW	57.0	50.0	38.0	12.0	24.0
$325^{O}C$	34.0	43.0	47.5	9.5	28.2

11.6.1 Mass Balance Calculations

The overall mass balance of the dewatering process is shown in figure 11.5. Calculations for this balance are based on the proximate analysis of raw and product coal.

Basis   100 tonne/hr raw coal

Feed Rate of Raw Coal (tonne/hr)

Volatile Matter	21.5
Fixed Carbon	16.3
Mineral Matter	5.2
Moisture	57.0
Total Feed Rate of Raw Coal	100.0 tonne/hr

Feed Rate of Water = 100 tonne/hr (1:1 coal to water ratio)

Yield of Product Coal (daf) = 82.4%
(Calculated by assuming the fixed carbon content of feed and product coal are equal)

Production Rate of Dewatered Coal

Volatile Matter	14.8
Fixed Carbon	16.3
Mineral Matter	3.3
Moisture	17.7
Total Production Rate of Dewatered Coal	52.1 tonne/hr

Rate of Moisture Removal from Coal = 39.3 tonne/hr

Total Rate of Water Leaving Process = 139.3 tonne/hr

Rate of Volatile Matter Removal (assume removed as a gas) = 6.7 tonne/hr

Rate of Mineral Matter Removal = 1.9 tonne/hr

11.6.2 Energy Balance Calculations

Figure 11.6 shows an overall energy balance of the thermal dewatering process. The energy required for heating and high pressure pumping have been calculated for the process conditions specified. However, the balance does not include energy required for filtering and wastewater treatment.

Basis   100 tonne/hr raw coal

Power Available from Combustion of :-

Raw Coal	252.0 MW
Product Coal	243.6 MW
Product Gas Removed	8.4 MW

Heat Requirements for Dewatering

Assume   Slurry to be heated from 20°C to 325°C
          Energy recovered from 320°C to 65°C.
          The Specific heat of coal 1.5 kJ/kg

Enthalpy Water   325°C = 1499 kJ/kg   Enthalpy Water   320°C = 1467 kJ/kg
   "   "   20°C = 83 kJ/kg   "   "   65°C = 283 kJ/kg

Energy Required to Heat Water $= \dot{m}\Delta H_{heating} - \dot{m}\Delta H_{recovery}$
                                 $= 10.18$ MW

Energy Required to Heat Coal $= \dot{m}C_p\Delta T$
                                 $= 0.84$ MW

Power Required to Pump Water to 12.5 MPa
     Volume of Water to be Pumped (density coal 1.2 kg/m^3) Q = 183 m^3/hr
     Power Required to Pump Fluid $= Q(P_2 - P_1)$
                                     $= 0.62$ MW

Assuming Efficiency of Power Generation is 32%
Actual Power Required to Pump Fluid = 1.89 MW

Total Power Required to Remove Water = 12.9 MW
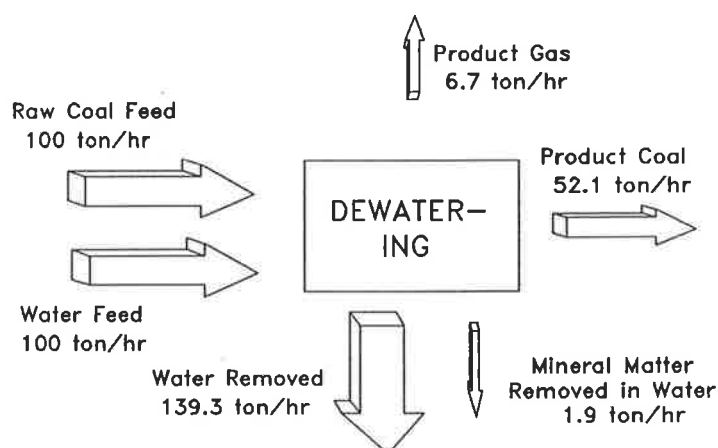
Figure 11.5 Mass Balance Diagram
Basis   100 ton/hr raw coal
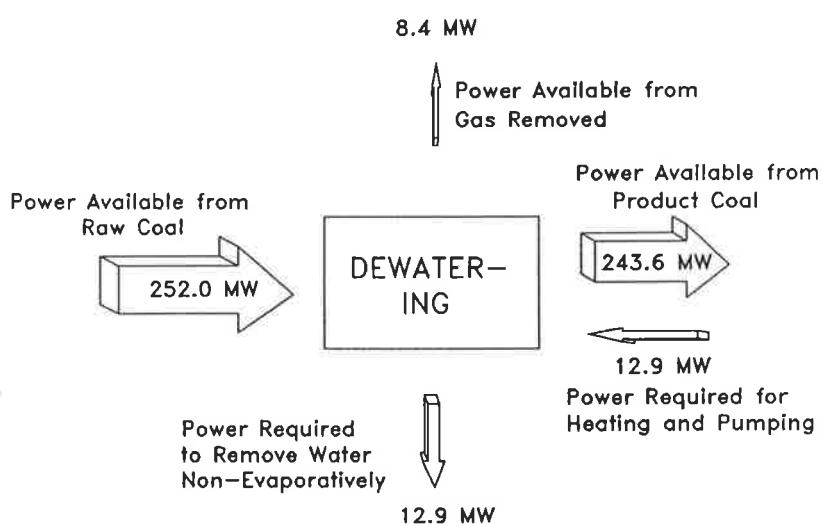
Figure 11.6 Energy Balance Diagram
Basis   100 ton/hr raw coal

CONCLUSIONS AND RECOMMENDATIONS

A detailed study of the characteristics of high-temperature pre-treatment was undertaken to investigate the reduction of impurities such as moisture, sodium, chlorine and sulphur. These impurities have an adverse effect during combustion in conventional pulverised fuel furnaces.

The kinetics of impurity removal were investigated at temperatures between 250°C to 350°C and for process times of up to 60 minutes. A substantial improvement in coal quality was achieved after only short reaction periods. Up to 80% moisture, 60% of both sodium and chlorine and 25% sulphur was removed during dewatering using coal to water ratios of 1:1.

The kinetics of devolatilization during dewatering was adequately modelled using time-temperature equivalence and distributed-activation-energy kinetic models. Moisture removal was modelled using a correlation between water removed from the coal during dewatering and devolatilization kinetics. The removal of individual gaseous species from coal during dewatering was also modelled using distributed activation energy kinetics.

Studies using ^{13}C NMR spectra of Bowmans coal show an unusually low carbon aromaticity which increases following dewatering. A general decrease in carboxyl and ether functional groups as a result of dewatering was observed using NMR and FT-IR

spectroscopic methods. Spectra of raw coal using ^{23}Na NMR shows that there is much less sodium present as sodium chloride in dried coal than would be expected from extraction analysis. It also indicates the presence of an unidentified sodium compound.

A marked reduction in the efficiency of dewatering in coal samples which were stored over the period of this research, about three years. This was attributed to oxidation of the coal surface.

The kinetics of aqueous leaching of ions from Bowmans coal was examined using a model based on the diffusion of electrolytes from spherical particles in solutions of limited volume. The leaching characteristics revealed insights into the removal of soluble inorganics during dewatering.

The filtration characteristics of dewatered coal slurries showed a marked improvement over untreated coal-water slurries. Cloth binding (apparent when filtering raw coal slurries) would no longer be a problem.

The aqueous effluent from high-temperature dewatering was found to contain high dissolved solids content and high sulphide content.

Preliminary engineering designs, based on the results obtained in this study, were presented to indicate the feasibility of a process to continuously upgrade Bowmans coal. However, various aspects of this proposal must be investigated at length before a more detailed design can be put forward.

Recommendations for further research include,

1) Large scale investigations to be carried out to determine the engineering aspects of the process and to determine the applicability of the kinetics obtained in this study for large scale plant design.

2) A feasibility study of the process economics be carried out.

3) Comprehensive studies be carried out on the treatment of product waste water from the process.

It was shown in this study that high-temperature pre-treatment significantly reduces some of the impurities in Bowmans coal. Because of the significance of this process to the utilization of low rank South Australian coals, it would be worthwhile to continue with this research.

NOMENCLATURE

a	particle radius, cm
a_{eff}	effective particle radius, cm
A	area, cm^2
B	constant, dimensionless
B	volume of filtrate collected, cm^3
B_o	volume at time t=0, cm^3
c	concentration of electrolytes, g equivalent/cm^3
C	constant, dimensionless
C	concentration of solute, g/cm^3
C_o	initial concentration of solute, g/cm^3
C_∞	concentration of solute after infinite time, g/cm^3
C_p	specific heat, cal g^{-1} $°C^{-1}$
D	diffusion coefficient, cm^2/sec
D_{eff}	effective diffusion coefficient, cm^2/sec
E	activation energy, kJ mol^{-1}
E	extent of extraction of soluble ions, dimensionless.
E_o	mean activation energy, kJ mol^{-1}
f	conversion of oxygen content during coalification, g/g coal
$f(E)$	Gaussian distribution function
F_a	Faraday constant, 96,500 coulombs/g equivalent
G	concentration gradients in direction of diffusion
h	heat transfer coefficient, cal s^{-1} cm^{-1} $°C^{-1}$
k_o	pre-exponential factor in Arrhenius rate Expression, s^{-1}
K	partition factor, dimensionless
m	mass of dry-cake solids per volume of filtrate, kg/cm^3
n	valences of electrolytes
P	pressure, kPa
R	gas constant, 8.314 J mol^{-1} K^{-1}
T	temperature, $°C$
T_o	initial temperature of coal, $°C$
T_R	reference temperature to achieve certain conversion, $°C$
T_∞	final temperature of coal, $°C$
t	time, s

t_R	reference time to achieve certain conversion, s
v	volume of water in coal, cm^3
V	volume, cm^3
V	volatiles evolved g/g coal
V_o	original volatile content g/g coal
V.M.	volatile matter removed from coal, g/g coal d.b.
x	chosen measure of conversion, g/g coal
x_R	reference measure of conversion, g/g coal
α	ratio of volumes of solution and sphere
α	specific resistance of filter cake,
β	resitance of filter medium, m/kg
λ	ion conductances, amp/(cm^2) (volt/cm) (g equivalent/cm^3)
σ	standard deviation in activation energy distribution function, kJ mol^{-1}
η	viscosity, kg/m s
τ	time constant, s
τ	tortuosity factor, dimensionless

BIBLIOGRAPHY

Allardice, D.J., (1970). A Preliminary Investigation of the Properties of Dewatered Coal. S.E.C.V., Scientific Division Report No. 217.

Allardice, D.J., (1973). A Review of the Fleissner Drying Process. S.E.C.V., Scientific Division Report No. 286.

Allardice, D.J., (1976). Brown Coal Dewatering: Summary of SECV Studies. S.E.C.V., Research and Development Department, Coal Science Section Report.

Allardice, D.J., and Evans, D.G., (1971). The Brown Coal/Water System: Part 1. The Effect of Temperature on the Evolution of Water from Brown Coal. Fuel, 50, 201.

Allardice, D.J. and Evans, D.J., (1971). The Brown Coal/Water System: Part 2. Water Sorption Isotherms on Bed-MOist Yallourn Brown Coal. Fuel, 50, 236.

American Public Health Association (APHA), (1976). "Standard Methods for the Examination of Water and Wastewater." 14th Edition.

Agarwal, P.K., (1984). Fluidized Bed Combustion of Low Rank Coals. PhD Thesis, University of Mississippi.

Allen, R.J., (1981a). Sodium Removal from Wakefield Coal. AMDEL Report 1408

Allen, R.J., (1981b). Sodium Removal from Wakefield Coal. AMDEL Report 1435.

Allen, R.J., (1981c). Pyrolysis of Wakefield Coal. AMDEL Report 1414.

Allen, R.J., (1982). Sodium Removal from Wakefield Coal. AMDEL Report 1435 (Appendix).

Anacreon, R.E., (1982). Applications of Diffuse Reflectance for Analysis of Coal Samples. Perkin-Elmer Infrared Bulletin, 92.

Anthony, D.B., Howard, J.B., Hottel, H.C. and Messner, M.P., (1975). Rapid Devoalatilizaton of Pulverised Coal. Fifteenth Symp. (Int) on Combustion, The Combustion Institute, Pittsburg. 103.

Aris, R., (1975). "Mathematical Theory of Diffusion and Reaction in Permeable Catalysis." Clarendon Press, Oxford, 25.

Bain, A.G. and Bonnigton, S.T., (1970). "Hydrolic Transport of Solids by Pipeline." Pergamon Press Ltd.

Bainbridge, J.R., (1947). Research into Fleissner Drying of South Australian Coal. Mining Review, NO 87, 46-61.

Bainbridge, J.R. and Satchwell, K., (1947). Experiments in Fleissner Drying Victorian Brown Coal. Fuel, Vol 26, 28-38.

Baker, P.J. and Jacobs, B.E.A., (1979). "A Guide to Slurry Pipeline Systems." BHRA Fluid Engineering, England.

Baria, D.N., Kube, W.R. and Paulson, L.E., (1982). Reduction in Ash Fouling Potential of Lignite by Ion Exchange. in "Recent Advances in Absorption and Ion Exchange", Ed. Ma Y.H., AIChE Symposium Series. 54-63.

Baria, D.N., Mass, D.J. and Paulson, L.E., (1983). Steam/Hot Water Drying of Lignite: Part 1. Activities of the Univesity of North Dakota. 12 Biennial Lignite Symposium, Grand Forks North Dakota, May 18-19.

Barnes, D., Forster, C.F. and Hrudey, S.E. (1984). "Surveys in Industrial Wastewater Treatment. Vol 2" Pitman Advanced Publishing Program.

Benson, S.W., (1968). "Thermochemical Kinetics." John Wiley & Sons, Inc.

Bettleheim, J. and Hann, W.W., (1980). An Investigation of Water Leaching of some British Coals. J. Inst. Energy, 53, 103-108.

Bettleheim J., Hann, W.W. and Saunders, K.G., (1982). The Interpretation of the Results of Extracting Chlorine and other Water Soluble Constituents from Coal in Relation to the Pore Structure of Coal. J. Inst. Energy, 55, 222-227.

Botto, R.E. and Winans, R.E., (1983). Characterization of whole coals by ^{13}C CP/MAS Spectroscopy at high field. Fuel, Vol 62, No.3., 271-273.

Boyd, A.R. (1976). Brown Coal Dewatering. Master of Engineering Science Thesis, University of Melbourne, 113p.

Brown, S.R., (1977). The Treatability of Brown Coal Effluent. M.Eng.Sc. Thesis, University of Melbourne.

Chemical Engineering, (1978). A Process for Beneficiating Lignite to a Heat Level of 12,000 Btu/lb. Vol 85, No. 5, Feb 27, 62.

Cooley, A.M.Jnr. and Lavine, I., (1933). Development of Dakota Lignite. VIII - Oil-Steam Atmosphere for Dehydrating Dakota Lignite. Ind. Eng. Chem., Vol 25, 221-224.

Crank, R.J., (1957). "Mathematics of Diffusion." Oxford Universsty Press, London.

Daybell, G.N., (1967). The relationship between sodium and chlorine in some British coals. Journal of the Institute of Fuel (now Energy), Vol 40, 3-6.

Daybell, G.N. and Pringle, W.J.S., (1958). The Mode of Occurence of Chlorine in Coal. Fuel, Vol 37, 283-292.

Davidson, R.M., (1980). Molecular Structure of Coal. IEA Coal Research Report No. ICTIS/TR 08.

Davy McKee Pacific, (1984). Comparison of Technologies for Brown Coal Drying for the VBCC. Study for the V.B.C.C.

Department of Mines and Energy, (1987). "Coal Deposits in South Australia." Mineral Information Series .

Drohan, P.J., (1977). Thermal Dewatering of Brown Coal Lithotypes. M. Eng. Sc. Thesis, University of Melbourne, 118p.

Dyrkacz, G.R., Bloomquist, C.A.A. and Solomon, P.R., (1984). Fourier Transform infra-red study of high purity maceral types. Fuel, Vol 63, 536-542.

Dudley, R.L. and Fyfe, C.A. (1982). Evaluation of the quantitative reliability of the ^{13}C CP/MAS technique for the analysis of Coals and related materials. Fuel, Vol 61, 651-657.

Dunne, D.J., Williams, E.H. and Agnew, J.B., (1985). Upgrading of low-grade low-rank South Australian Coals. CHEMECA '85, Perth. 59-63.

Dunne, D.J., Francis, I.L. and Agnew, J.B. (1987). The removal of impurities from Bowmans coal during Hot Water Dewatering. CHEMECA '87, Melbourne.

Dunne, D.J., Francis, I.L. and Agnew, J.B. (1988). Kinetics of Hot Water Dewatering. Australian Coal Science Conference, Adelaide.

Durie, R.A., (1961). Direct Determination of Sodium Content of Victorian Brown Coals. Fuel, Vol 30, 146-148.

Dybowolski, C., (1985). Solid-State investigations via NMR. Chem. Tech. March, 186-191.

Edgecome, L.J., (1956). State of Combination of Chlorine in Coal 1- Extraction of Coal with Water. Fuel, Vol 35, 38-48.

Eisenklam, P., (1947). Experimental Investigation into Direct Steam Drying of Brown Coals. M. Eng. Sci. Thesis, University of Melbourne, 157p.

Evans, D.G. and Siemon, S.R., (1968). Separation of Water from Solid Organic Materials. Commonwealth of Australia Patent 32,607/68 January 26.

Evans, D.G. and Siemon, S.R., (1970). Dewatering of Brown Coal before Combustion. Journal of the Institute of Fuel, 413-419.

Evans, D.G. and Siemon, S.R., (1971). Separation of Water from Solid Organic Materials. U.S. Patent 3,552,031 January 5.

Evans, D.G., Siemon, S.R. and Martin, W.R.B., (1974). Thermal Dewatering of Organic Materials. National Chemical Engineering Conference, Queensland, July 10-12, 412-419.

Farnum, S.A., Olson, E.S., Farnum, B.W., Miller, D.J., Bitzan, E.F. and Diehl, J.W., (1981). Characterization of Organics in Low-Rank Coal Processing. Proceedings of the Low Rank Coal Basic Coal Science Workshop, U.S. Dept. of Energy, Dec 8-9. CONF-811268 (DE 83002254) 92-111.

Fleissner, H. (1927). Drying Coal. U.S. Pat. 1,632,829, June 21.

Fleissner, H. (1928). Drying Coal and Other Fuels. U.S. Pat. 1,679,078, July 31.

Fuller, M.P., Hamadeh, I.M., Griffiths, P.R. and Lowenhaupt, D.E., (1982). Diffuse reflectance IR spectrometry of Powdered coals. Fuel, Vol 61, 529-536.

Furimsky, E. and Ripmeester, J., (1983). Characterization of Canadian Coals by N.M.R. Spectroscopy. Fuel Processing Technology, Vol 7, No. 3, 191-202.

Gerstein, B.C., Dubois, Murphy P. and Ryan, L.M., (1982). Aromaticity in Coal. in "Coal Structure", Ed. Meyers R.A., 87-129.

Gluskoter, H.J., (1967). Clay Minerals in Illinois Coals. Journal of Sedimentary Petrology, Vol 37, No. 1, 207-214.

Gluskoter, H.J. and Ruch, R.R., (1971). Chlorine and sodium in Illinios coals as determined by neutron activation analyses. Fuel, Vol 50, 65-76.

Harrington, L.C., Parry, V.F. and Koth, A., (1942). Technical and Economic Study of Drying Lignite and Subbituminous Coal by the Fleissner Process. BuMines Technical Paper 633, 84p.

Havens, J.R., Koenig, J.L. and Painter, P.C., (1982). Chemical Characterization of solid coals through magic angle ^{13}C NMR. Fuel, Vol 61, 393-396.

Havens, J.R., Koenig, J.L., Kuehn, D., Rhoads, C., Davis, A. and Painter, P.C., (1983). Characterization of Coals and Coal oxidation by magic-angle ^{13}C N.M.R. Spectroscopy. Fuel, Vol 62, No. 8, 936-941.

Higgins, R.S. and Allardice, D.J., (1973). The Development of Brown Coal Dewatering. S.E.C.V., Planning and Investigation Department, Scientific Division Report.

Howarth, O.W., Ratcliffe, G.S. and Burchill, P., (1987). Solid-State Nuclear Magnetic Resonance Studies of Sodium and Aluminium in Coal. Fuel, 66, 34-39

Jackson, W.R., Larkins, F.P. and Redlich, P.J., (1984). Australian Coal Science Conference, Churchill Victoria. Dec 3-5. p17-25.

Kamei, T., Ono, F., Komai, K., Wakabayashi, T. and Itoh, H., (1985). "Dewatering and Utilization of High Moisture Brown Coal." Drying '85, Ed Ryozo Toci and Arun S. Mujumdar, Hemisphere Publishing Corporation.

Kamyr Incorporated, (1983a). Application of Kamyr Technology for Hot Water Drying of Low Rank Coal.

Kamyr Incorporated, (1983b). Continuous feeding of Coal to Pressurised Systems." Chem. Eng. Progress, May, 37-41.

Klein, H., (1930). The Fleissner Method of Drying Lignites; its Underlying Chemical and Physical Principals. Braunkohle, Vol. 29, 1-10, 21-30.

Kube, W.R., (1957). Sorption of Water Vapour by Thermally Treated Lignite at Different Relative Humidities. Chem. and Eng. Data series, Vol 2, 46-51.

Kuehn, D.W., Snyder, R.W., Davis, A. and Painter, P.C., (1982). Characterization of vitrinite concentrates 1. Fourier Transform IR Studies. Fuel, Vol 61, 682-694.

Lavine, I., Gauger, A.W. and Mann, C.A., (1930). Studies in the Development of Dakota Lignite. III - Drying of Lignite Without Disintegration. Ind. Eng. Chem., Vol 22, 1437-1360.

Maa, P.S., Neavel, R.C. and Vernon, L.W., (1984). Tubing Bomb Coal Liquefaction Technique. Ind. Eng. Chem. Process Des. Dev. Vol 23, 242-250.

Maciel, G.E., Bartuska, V.J. and Miknis, F.P., (1979). Characterization of organic material in coal by proton-decoupled ^{13}C NMR with MAS. Fuel, Vol 58, 391-394.

Mitrovic, M., (1968). Characteristics of Wastewater Produced During the Drying of Younger Coals by the Fleissner Process. Bulletin of Mines Yugoslavia, Vol 7, No 2, 1-11.

Mourits, F.M. and Kybett, B.D. (1980). Thermal Dewatering of Lignite. Phase II. Saskatchewan Power Corp. Report, 4461-1980-2-Fuel, 169 p.

Murray, J.B. and Evans, D.G., (1972). The Brown Coal/Water System. Part 3: Thermal Dewatering of Brown Coal. Fuel, Vol 51, 290-296.

Murray, J.B. and Ireland, T.J.E., (1970). Thermal Dewatering of Morwell Brown Coal with Particular Reference to the Chemistry of the Process. S.E.C.V., Scientific Division Report No. MR-199.

Neavel, R.C., Nahas, N.C. and Koh, K.K., (1977). Removal of Sodium from Illinios Coal by Water Extraction. Trans. Soc. of Min. Eng., AIME, 262, 63-267.

Ohtsuka, Y., Nozawa, T., Tomita, A., Tomai, Y. and Hatano M., (1984). Application of high field, high resolution ^{13}C CP/MAS NMR Spectroscopy to the Structural Analysis of Yallourn Coal. Fuel, Vol 63, 1363-1366.

Oppelt, W.H., Ellman, R.C., Ongstad, O.C. and Kube, W.R., (1955). Experiments in Fleissner Drying of North Dakota Lignite. BuMines RI 5122, 23p.

Oppelt, W.H., Kube, W.R. and Kamps, T.W., (1959). Drying North Dakota Lignite to 1500 pounds pressure by the Fleissner Process. BuMines RI 5527, 30p.

Painter, P.C., Coleman, M.M., Jenkins, R.G. and Walker, P.L.Jnr., (1978). Fourier Transform infrared study of acid-demineralized coal. Fuel, Vol 57, 125-126.

Painter, P.C., Snyder, R.W., Starsnic, M., Coleman, M.M., Kuehn, D.W. and Davis, A., (1981). Concerning the application of FT-IR to the study of coal; A critical assesment of band assignments and the application of Spectral analysis Progams. Applied Spectroscopy, Vol 35, No.5, 475-485.

Painter, P.C., Snyder, R.W., Pearson, D.E. and Kwong, J., (1980). Fourier Transform infrared study of the variation in the oxidation of a Coking Coal. Fuel, Vol 59, 282-286.

Parkinson, G., (1970). How to Get Water out of Lignite, Wood and Peat. Chemical Engineering, Vol 85, No. 7, March 27, 77-78.

Paulson, L.E. and Wiltsee, G.A., (1982). A Process Concept for Producing High-Btu Coal/Water Slurries from Low Rank Coals, Employing 'Hot Water Drying'. Grand Forks Technology Center, GFETC/IR-6.

Phillips, R.C., Koppelman, E. and Murray, R.C., (1978). Upgrading Lignite by the Koppleman Process. International Coal Utilitzation Convention, Houston, Oct 17-19, Vol 2, 681-696.

Potas, T.A., Sears, R.E., Maas, D.J., Baker, G.G. and Willson, W.G., (1986). Prepartion of Hydrothermally Treated LRC/Water Fuel Slurries. Chem. Eng. Commun. Vol 44, 133-151.

Pugmire, R.J., Woolfenden, W.R., Mayne, C.L. and Grant, D.M., (1981). The use of Carbon-13 NMR CP/MAS Techniques in the study of Low Rank Coals. Proceedings of the Low-Rank coal basic Coal Science Workshop, U.S. Dept. of Energy, Dec 8-9, CONF-811268 (DE 83002254), 202-224.

Readett, D.J., (1983). Beneficiation of Wakefield Lignite: with particular reference to the Reduction of the Sodium Content. Report, South Australian Institute of Technology.

Readett, D.J., (1984). Beneficiation of Wakefield Lignite with particular reference to the Reduction of Sodium Content. Stage 2, Part 1. Report, South Australian Institute of Technology.

Readett, D.J. and Quast, K.B. (1988). Mechanical Dewatering of South Australian Brown Coals: Applications in Inorganics Characterisation. Australian Coal Science Conference, Adelaide, May 1988.

Readett, D.J., Quast, K.B., Mulcahy, D.E. and Ketteridge, I.B., (1984). Modelling the leaching of NaCl from Bowmans Lignite. Aus.I.M.M., Symposium on Extractive Metallurgy, Nov 1984.

Readett, D.J., Hall, S.F., Quast, K.B. and Ketteridge, I.B. (1986). CHEMECA 86, Adelaide, 325-329.

Renton, J.J., (1982). Mineral Matter in Coal. in "Coal Structure", Ed. Meyers R.A., 283-327.

Retcofsky, H.L., (1977). Investigation of the Chemical Structure of Coal by Nuclear Magnetic Resonance and Infrared Spectroscopy. Applied Spectroscopy, Vol 31, No 2, 116-121.

Riesser, B., Starsnic, M., Squires, E., Davis, A. and Painter, P.C., (1984). Determination of Aromatic and Aliphatic CH groups in coal by FT-ir. 2. Studies of coal and vitrinite concentrates. Fuel, Vol 63, 1253-1261.

Ruyter, H.P., (1982). Coalification Model. Fuel, 61, 1182-1187.

Ruyter, H.P., van Raam, L., and van der Poel, H., (1983). Upgrading Experiments on Brown Coal from South Australia. Shell International Research. AMER, 83.045.

Ruyter, H.P., van Raam, L., and van der Poel, H. (1984). Upgrading of Wakefield Brown Coal from South Australia. Fuel Processing Technology, Vol 9, 163-171.

Sampson, G. (1985). Investigations of the Fleissner Process for Upgrading Bowmans Coal. Internal Report, Chemical Engineering Department, University of Adelaide.

Saunders, K.G. (1982). Journal of the Institute of Energy. Vol 53, 109-115.

Schafer, H.N.S., (1972). Factors Affecting the Equilibrium Moisture Contents of Low-Rank Coals. Fuel, Vol 51, 4-9.

Schafer, H.N.S., (1979). Pyrolysis of Brown Coals: 1. Decomposition of acid groups in coals containing carboxyl groups in the acid and cation form. Fuel, Vol 58, 667-672.

Sears, R.E., Baker, G.G., Maas, D.J., Potas, T.A. and Patel, R., (1985). Production and Combustion of Hot-Water Dried Low-Rank Coal Slurries. 13th Biennial Lignite Symposium, Bismark North Dakota. May 21-23.

Solomon, P.R. and Carangelo, R.M., (1982). FT-IR analysis of coal 1. Techniques and determination of Hydroxyl concentrations. Fuel, Vol 61, 663-669.

Stanmore, B.R., Baria, D.N. and Paulson, L.E., (1982). Steam Drying of Lignite, A Review of Processes and Performance. Grand Forks Energy Technology Center, U.S. Dept. of Energy. DOE/GFETC/R1-82/1 (DE 82007849).

Stanmore, B.R. and Boyd, A.R., (1978). Removal of Water form Brown Coal by Treatment with Steam. Fuel Proc. Tech., Vol 1, 305-313.

Stanmore, B.R. and Boyd, A.R., (1976). Continuous Dewatering of Victorian Brown Coal. The Institution of Engineers Australia, 4th. National Conference on Chemical Engineering. The Effective use of Hydrocarbon Resources. Adelaide, August 25-26th, 76-79.

Starsinic, M., Otaka, Y., Walker, P.L.Jnr. and Painter, P.C., (1984). Application of FT-ir Spectroscopy to the determination of COOH groups in coal. Fuel, Vol 63, 1002-1006.

Steitz, J.T. and Balazs, C.F. (1968). Application of Time-Temperature Supersition Principle to Long Term Engineering Properties of Plastic Materials. Polymer Engineering and Science, 151-160.

Stewart, E.D.J., (1984). Advisory Committee on Future Energy Generation Options, Volume 3: Long Term Development Options for South Australian Coals. South Australian Government.

Szladow, A.J., Granatstein, D.L. and Champagne, P.J. (1984). Steam/hot Water Drying of Lignite Part II: Activities at Saskatchewan Power Corporation. Twelfth Biennial Lignite Symposium, Morgantown Energy Technology Center, Feb 1984.

Tooke, P.B. and Grant, A., (1982). Fourier Transform Infra-Red Studies of Coal. Fuel, Vol 62, No. 9, 1003-1008.

Verheyen, T.V., Johns, R.B., Bryson, R.L., Maciel, G.E. and Blackburn, D.T., (1984). A Spectroscopic investigation of the banding of lithotypes occuring in Victorian brown coal seams. Fuel, Vol 63, 1629-1635.

Vinograd, J.R. and McBain, J.W., (1941). J. Am. Chem. Soc., 63, 2008-2015.

Walker, W.M. (1983). Wakefield Coal Washing Design Study. AMDEL Report 1492.

Watson, V. (1984). Leaching of Lignite in South Australia. Internal Report, Chemical Engineering Department, University of Adelaide.

Williams, O.A., (1983). "Pneumatic and Hydrolic Conveying of Solids." Marcel Dekker, Inc., New York.

Wildegger-Gaissmaier, A.E., (1988). Fluidized Bed Utilization of South Australian Coals. PhD Thesis, University of Adelaide.

Willson W.G. (1985). Private Communication.

Yoshida, T.,Nakata, Y., Ueda, S., Kanda, N. and Maekawa, Y., (1982). Elucidation of Structural and Hydroliquefaction characteristics of Yallourn brown coal by ^{13}C CP/MAS NMR Spectroscopy. Fuel, Vol 61, 824-830.

APPENDIX A

LEACHING RESULTS

TABLE A1

LEACHING OF DISSOCIATED IONS FROM BOWMANS COAL

COAL PARTICLE SIZE   <0.495 mm
COAL WATER RATIO   1:1
TEMPERATURE   20°C

TIME mins	CONCENTRATION OF DISSOCIATED IONS IN LEACH LIQUOR ppm						
	Na^+	K^+	Mg^+	Ca^{++}	Fe^{+++}	$SO_4^=$	Cl^-
0.25	2870	23	825	90	0.4	4557	4800
0.5	3225	27	940	125	0.4	4830	5300
1.0	3200	28	1050	125	0.6	5418	5500
1.5	3275	29	1050	125	0.5	6930	5420
2.0	3350	40	1050	200	0.5	4935	5800
5.0	3450	37	1150	230	0.5	4810	5900
30	3550	40	1080	430	1.2	5990	6460
60	3170	26	1060	490	1.4	5730	5300
24hrs	3375	29	1070	525	1.4	6020	5100

TABLE A2

LEACHING OF DISSOCIATED IONS FROM BOWMANS COAL

COAL PARTICLE SIZE   1.0 - 2.0 mm
COAL WATER RATIO   1:1
TEMPERATURE   20°C

TIME mins	CONCENTRATION OF DISSOCIATED IONS IN LEACH LIQUOR ppm						
	Na^+	K^+	Mg^{++}	Ca^{++}	Fe^{+++}	$SO_4^=$	Cl^-
1.0	2440	21	557	230	1.5	2410	3920
5.0	3375	25	810	290	2.0	4110	5190
15	3413	25	910	280	1.7	3370	5310
30	3825	25	960	280	1.7	4234	5410

TABLE A3

LEACHING OF DISSOCIATED IONS FROM BOWMANS COAL

COAL PARTICLE SIZE   2.0 - 4.0 mm
COAL WATER RATIO   1:1
TEMPERATURE   20°C

TIME	CONCENTRATION OF DISSOCIATED IONS IN LEACH LIQUOR ppm						
mins	Na^+	K^+	Mg^{++}	Ca^{++}	Fe^{+++}	$SO_4^=$	Cl^-
0.25	932	10	200	113	0.5	880	1470
0.5	1110	14	238	107	0.9	1450	2340
1.0	1240	15	294	125	1.3	1650	2340
2.0	1740	17	426	157	2.0	1640	3040
5.0	2340	21	460	180	1.6	2820	3970
15.0	3300	25	620	230	1.7	4000	4990
30	3600	25	857	238	3.0	2800	5150
60	2940	25	910	250	1.7	3700	5186

TABLE A4

LEACHING OF DISSOCIATED IONS FROM BOWMANS COAL

COAL PARTICLE SIZE   <0.495 mm
COAL WATER RATIO   1:2
TEMPERATURE   20°C

TIME	CONCENTRATION OF DISSOCIATED IONS IN LEACH LIQUOR ppm						
mins	Na^+	K^+	Mg^{++}	Ca^{++}	Fe^{+++}	$SO_4^=$	Cl^-
0.25	2020	21	500	200	0.6	2700	2275
0.5	1990	20	480	195	0.4	2680	2910
1.0	2080	21	530	220	0.6	2670	2438
1.5	1900	20	545	225	0.5	2550	2600
2.0	1980	20	562	225	0.5	2675	3125
5.0	1938	28	575	263	0.6	2520	2200
15	2180	22	650	375	0.7	2700	2250
30	2130	24	731	444	0.7	2715	2500
24hrs	2130	18	638	310	0.9	3640	3100

TABLE A5

LEACHING OF DISSOCIATED IONS FROM BOWMANS COAL

COAL PARTICLE SIZE	2.0 - 4.0 mm
COAL WATER RATIO	1:2
TEMPERATURE	20°C

TIME mins	CONCENTRATION OF DISSOCIATED IONS IN LEACH LIQUOR ppm						
	Na^+	K^+	Mg^{++}	Ca^{++}	Fe^{+++}	$SO_4^=$	Cl^-
1.0	700	9	170	75	0.4	555	1280
5.0	1430	15	325	130	0.8	1300	2060
15.0	1760	16	410	140	0.8	1580	2910
30	1920	17	480	145	0.9	2200	3130

TABLE A6

LEACHING OF DISSOCIATED IONS FROM BOWMANS COAL

COAL PARTICLE SIZE   0 - 0.495 mm
COAL WATER RATIO   1:5
TEMPERATURE   20°C

TIME	CONCENTRATION OF DISSOCIATED IONS IN LEACH LIQUOR ppm						
mins	Na^+	K^+	Mg^{++}	Ca^{++}	Fe^{+++}	$SO_4^=$	Cl^-
1.0	340	5.4	94	32	0.2	247	720
5.0	730	7.2	140	50	0.4	560	1100
15	980	9.0	190	55	0.7	850	1380
30	1040	9.0	210	50	0.7	966	1420

TABLE A7

LEACHING OF DISSOCIATED IONS FROM BOWMANS COAL

COAL PARTICLE SIZE   2.0 - 2.36 mm
COAL WATER RATIO   1:5
TEMPERATURE   20°C

TIME mins	CONCENTRATION OF DISSOCIATED IONS IN LEACH LIQUOR ppm						
	Na^+	K^+	Mg^{++}	Ca^{++}	Fe^{+++}	$SO_4^=$	Cl^-
1.0	340	5.4	94	32	0.2	247	720
5.0	730	7.2	140	50	0.4	560	1100
15	980	9.0	190	55	0.7	850	1380
30	1040	9.0	210	50	0.7	966	1420

TABLE A8

LEACHING OF DISSOCIATED IONS FROM BOWMANS COAL

COAL PARTICLE SIZE   2.0 - 4.0 mm
COAL WATER RATIO   1:5
TEMPERATURE   20°C

TIME mins	CONCENTRATION OF DISSOCIATED IONS IN LEACH LIQUOR ppm						
	Na^+	K^+	Mg^{++}	Ca^{++}	Fe^{+++}	$SO_4^=$	Cl^-
0.25	44	2.9	82	9	0.2	330	120
0.5	290	3.3	200	13	0.1	440	190
2.0	410	3.9	270	32	0.3	770	340
5.0	510	6.0	300	38	0.6	780	440
15	720	8.1	360	50	0.7	1220	690
30	750	9.4	200	50	0.7	1300	1030

TABLE A9

LEACHING OF DISSOCIATED IONS FROM BOWMANS COAL

COAL PARTICLE SIZE   <0.495 mm
COAL WATER RATIO   1:1
TEMPERATURE   90°C

TIME mins	CONCENTRATION OF DISSOCIATED IONS IN LEACH LIQUOR ppm						
	Na^+	K^+	Mg^{++}	Ca^{++}	Fe^{+++}	$SO_4^=$	Cl^-
0.25	3350	29	825	150	5	5000	5300
0.5	3435	34	885	175	5	5600	5500
2.0	3600	34	988	210	10	6200	5500
6.0	3600	35	1000	225	26	6000	5500
30.0	3400	28	970	610	17	6900	4800

TABLE A10

LEACHING OF DISSOCIATED IONS FROM BOWMANS COAL

COAL PARTICLE SIZE 2.0 - 4.0 mm
COAL WATER RATIO 1:1
TEMPERATURE 50°C

TIME mins	CONCENTRATION OF DISSOCIATED IONS IN LEACH LIQUOR ppm						
	Na^+	K^+	Mg^{++}	Ca^{++}	Fe^{+++}	$SO_4^=$	Cl^-
1.0	1600	27	380	180	1.4	1750	2750
2.0	2130	34	475	230	2.2	5140	3680
15.0	3350	43	850	260	4.2	6860	5570
30	3320	43	900	260	4.6	7520	5420

TABLE A11

LEACHING OF DISSOCIATED IONS FROM BOWMANS COAL

COAL PARTICLE SIZE   2.0 - 4.0 mm
COAL WATER RATIO   1:1
TEMPERATURE   90°C

TIME mins	CONCENTRATION OF DISSOCIATED IONS IN LEACH LIQUOR ppm						
	Na^+	K^+	Mg^{++}	Ca^{++}	Fe^{+++}	$SO_4^=$	Cl^-
0.5	1350	15	300	150	0.7	1130	2340
1.0	1775	25	400	200	1.3	1800	3100
2.0	2710	30	625	250	3.0	2640	4473
5.0	3100	40	800	260	4.9	3400	5170
15	3410	10	840	275	0.2	3780	5670
30	3550	45	890	300	0.8	4230	5658

TABLE A12

LEACHING OF DISSOCIATED IONS FROM BOWMANS COAL

COAL PARTICLE SIZE   0.0 - 0.495 mm
COAL WATER RATIO   1:2
TEMPERATURE   90°C

TIME mins	CONCENTRATION OF DISSOCIATED IONS IN LEACH LIQUOR ppm						
	Na^+	K^+	Mg^{++}	Ca^{++}	Fe^{+++}	$SO_4^=$	Cl^-
0.25	2140	38	540	240	1.3	2880	2800
0.5	2040	24	550	255	1.4	2740	3000
2.0	2100	24	590	350	2.1	2770	3200
6.0	2100	24	590	490	3.9	2700	2700
30.0	2400	20	700	490	9.0	3500	5500

TABLE A13

LEACHING OF DISSOCIATED IONS FROM BOWMANS COAL

COAL PARTICLE SIZE   2.0 - 4.0 mm
COAL WATER RATIO   1:2
TEMPERATURE   90°C

TIME mins	CONCENTRATION OF DISSOCIATED IONS IN LEACH LIQUOR ppm						
	Na^+	K^+	Mg^{++}	Ca^{++}	Fe^{+++}	$SO_4^=$	Cl^-
1.0	1110	13	260	100	0.7	1090	1770
5.0	1960	23	420	160	4.8	1960	3040
15	2340	26	520	180	12	2570	3550
30	2300	26	500	180	16	2680	3450

TABLE A14

LEACHING OF DISSOCIATED IONS FROM BOWMANS COAL

Equilibrium Conditions

COAL PARTICLE SIZE   <0.495 mm
COAL WATER RATIO   1:25
TEMPERATURE   20°C, 90°C*

TIME	CONCENTRATION OF DISSOCIATED IONS IN LEACH LIQUOR ppm						
hours	Na^+	K^+	Mg^{++}	Ca^{++}	Fe^{+++}	$SO_4^=$	Cl^-
20#	250	2.5	150	38	0.2	420	909
44#	240	2.7	150	38	0.3	400	920
24	224	3.0	58	34	0.2	332	254
24	210	3.3	59	34	0.4	190	305
24*	234	4.3	67	47	10	397	263
24*	243	6.0	74	53	10	460	320

\# Samples taken of the same coal/water mixture at different times.

TABLE A15

LEACHING OF DISSOCIATED IONS FROM BOWMANS COAL

Equilibrium Conditions

COAL PARTICLE SIZE   0.0 - 0.495 mm
TIME   24 hrs
TEMPERATURE   20°C

Coal/ Water ratio	CONCENTRATION OF DISSOCIATED IONS IN LEACH LIQUOR ppm						
	Na^+	K^+	Mg^{++}	Ca^{++}	Fe^{+++}	$SO_4^=$	Cl^-
1:1	3375	29	1070	525	1.4	6020	5100
1:2	2130	18	638	310	0.9	3640	3100
1:5	980	9	250	110	0.4	1770	1320
1:25	230	3	62	33	0.2	410	300
1:25*	250	5.0	165	123	15	410	-

*Leached in 2M HCl

APPENDIX B

FILTRATION RESULTS

Figure B1

FILTRATION CHARACTERISTICS

5/10 gms Coal/Water at 10 ins Hg.
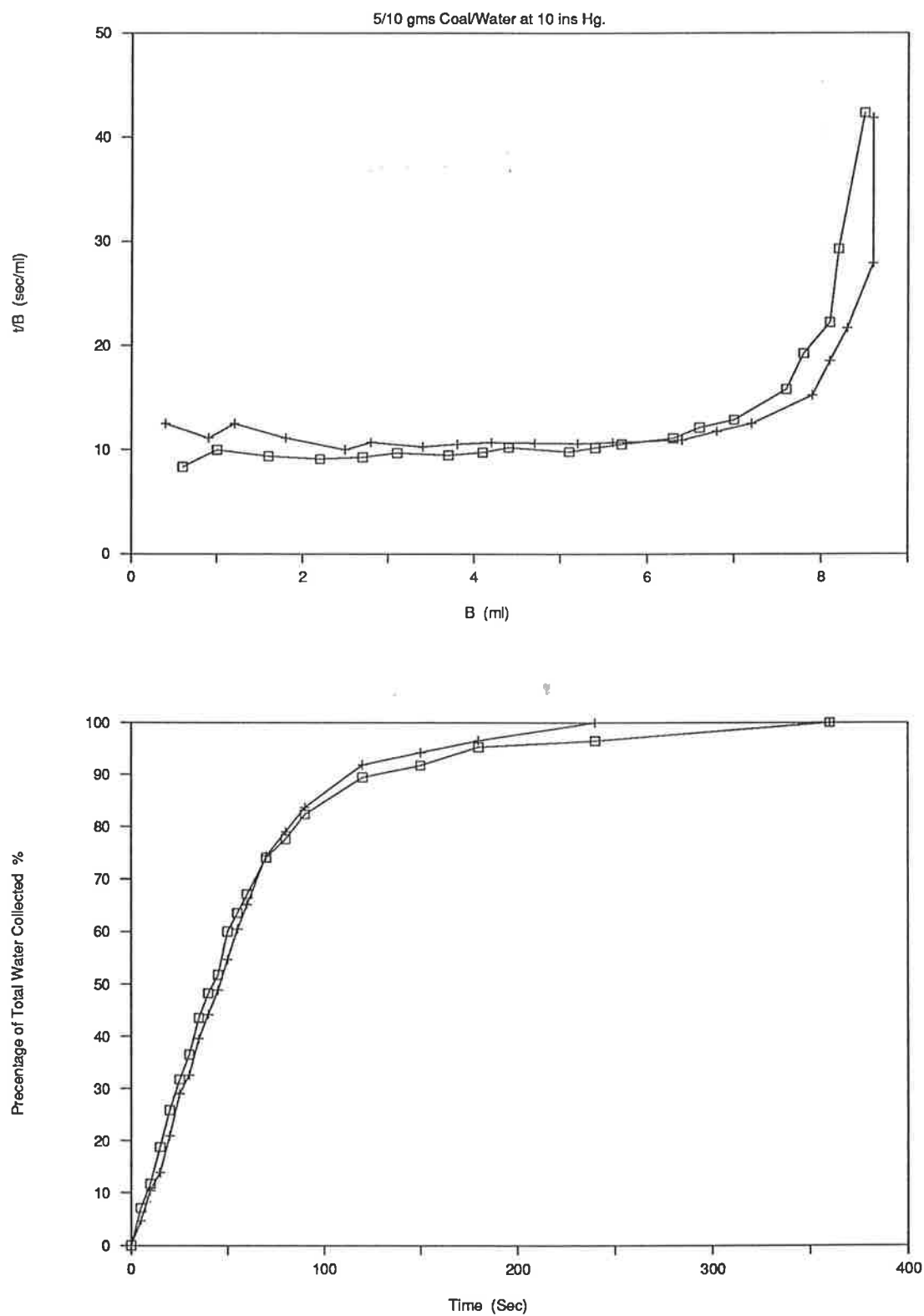
Figure B2

DEWATERING CHARACTERISTICS

5/10 gms Coal/Water at 10 ins Hg.
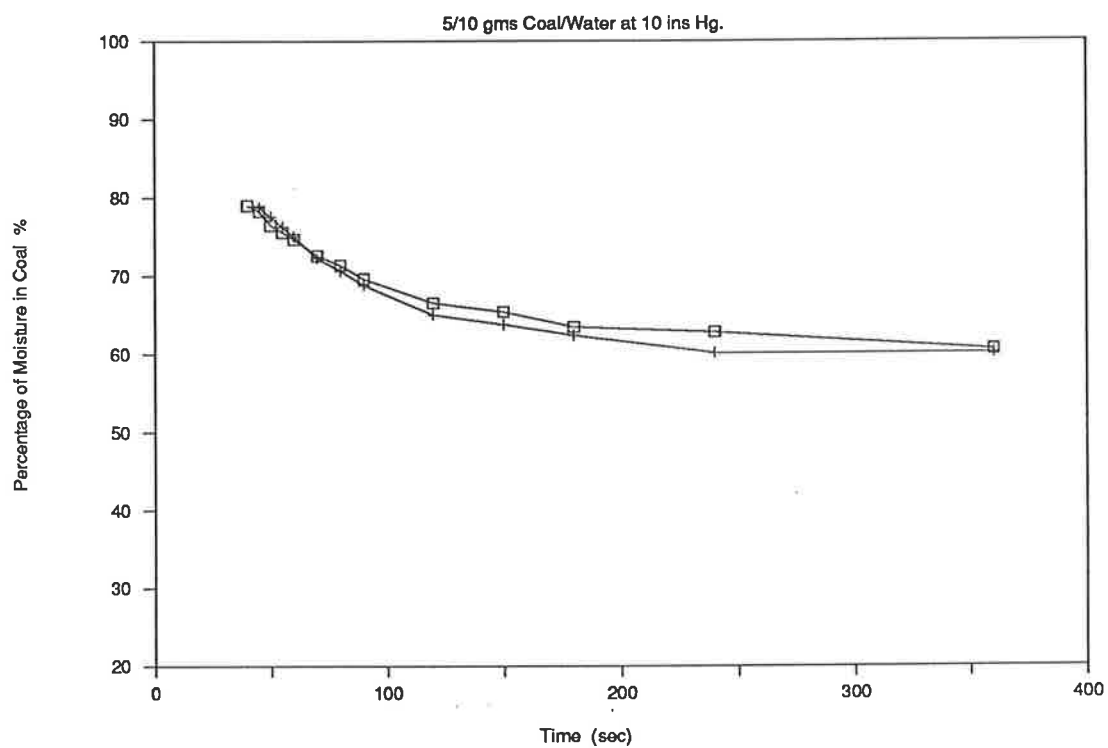
Figure B3

FILTRATION CHARACTERISTICS

10/20 gms Coal/Water at 10 ins Hg.
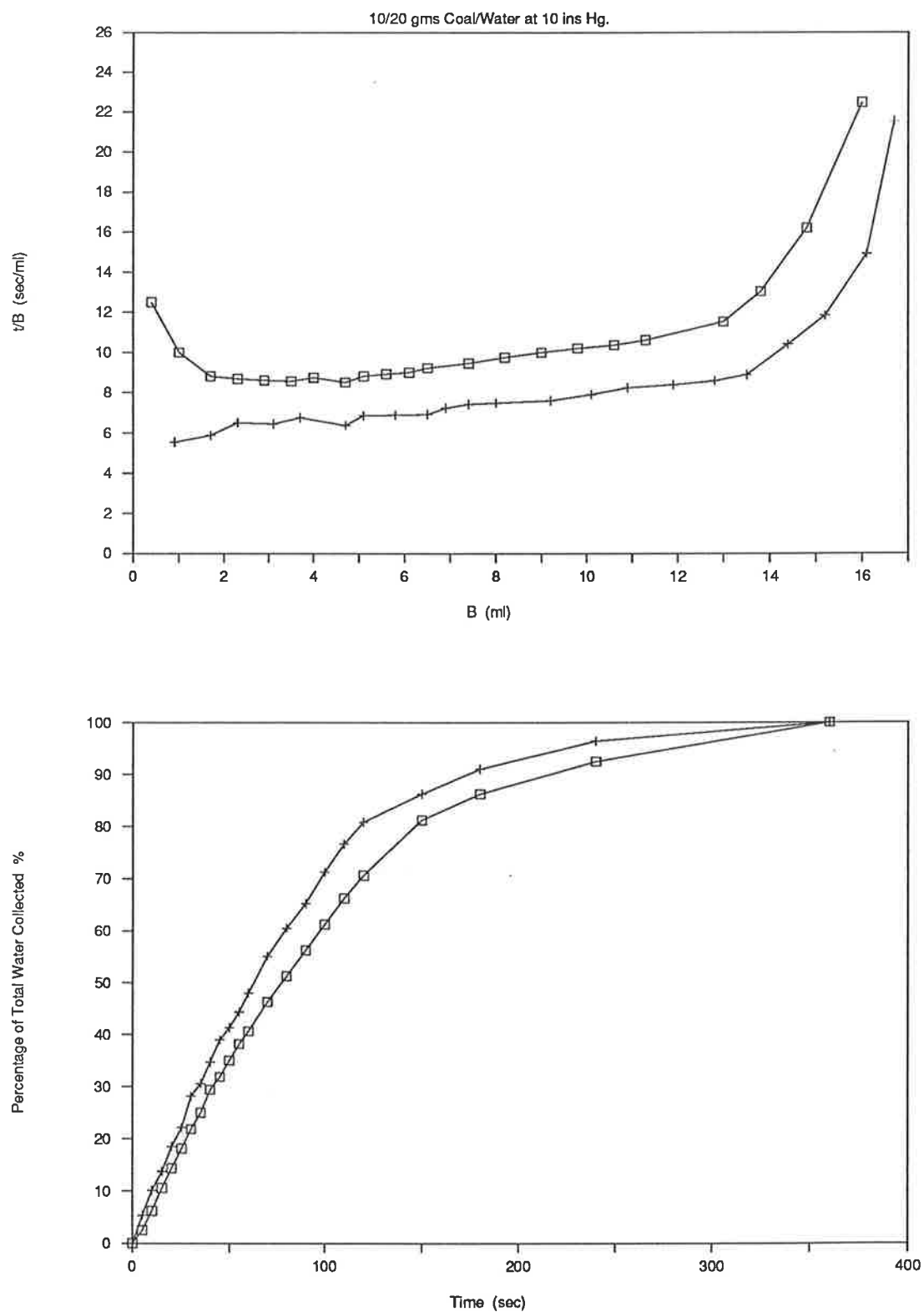
Figure B4

DEWATERING CHARACTERISTICS

10/20 gms Coal/Water at 10 ins Hg.
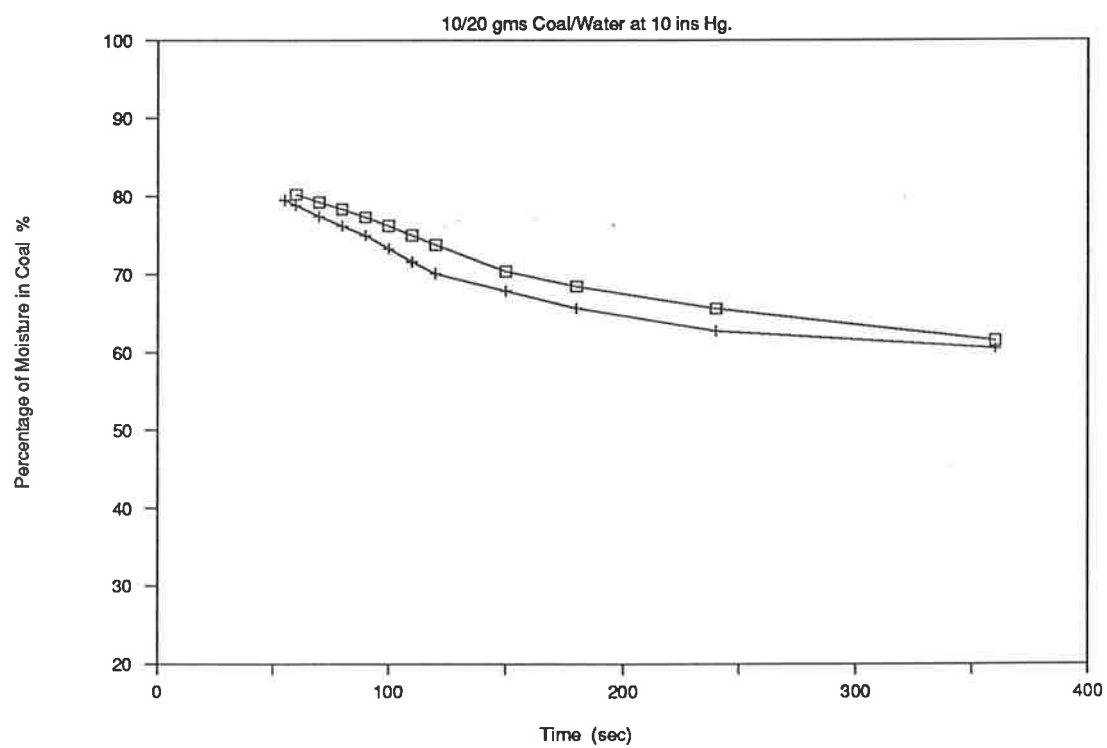
Figure B5

FILTRATION CHARACTERISTICS

15/30 gms Coal/Water at 10 ins Hg.
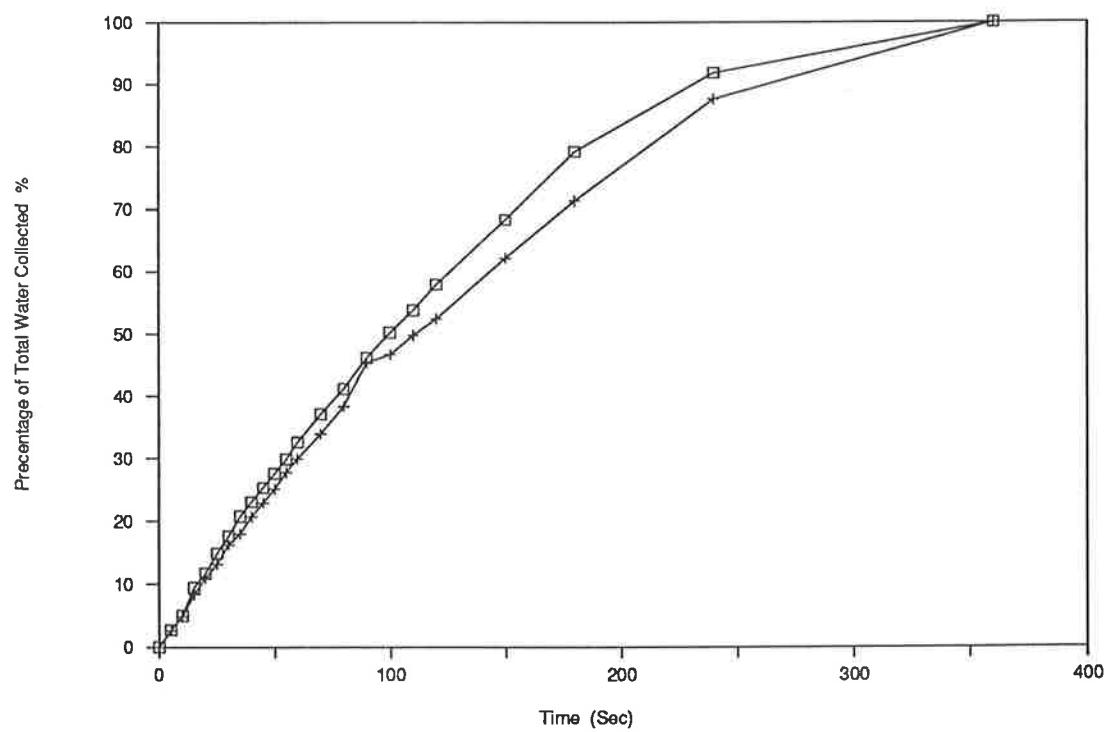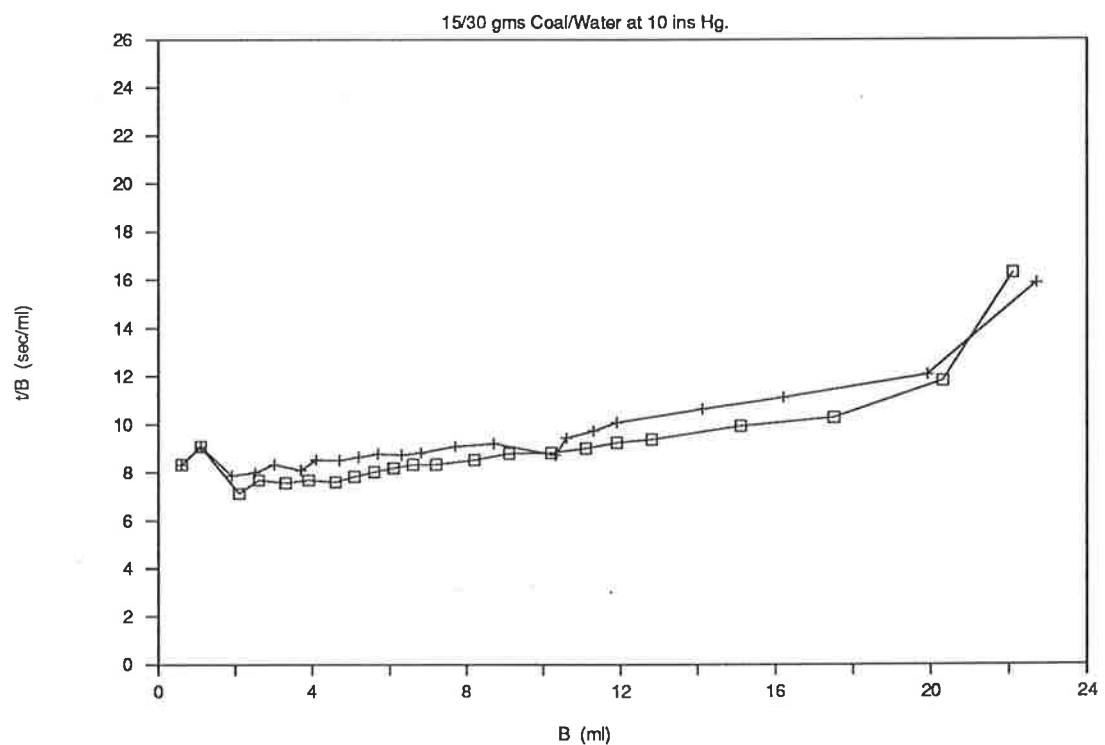
Figure B6

DEWATERING CHARACTERISTICS

15/30 gms Coal/Water at 10 ins Hg.
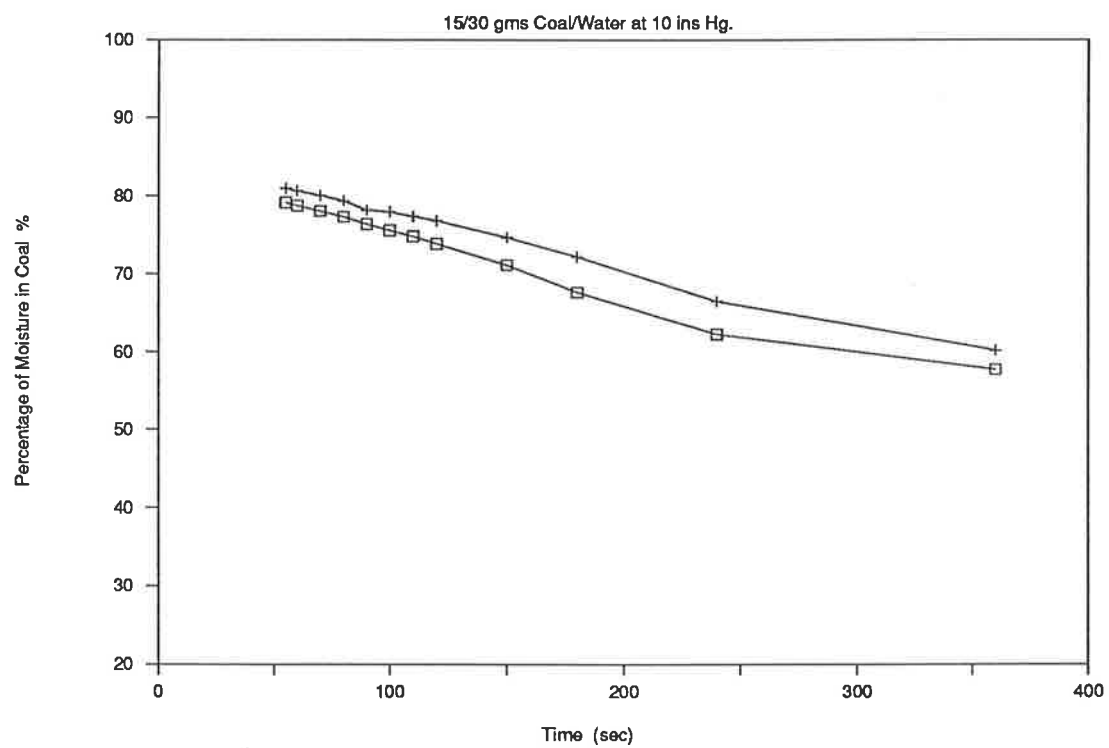
Figure B7

FILTRATION CHARACTERISTICS

5/25 gms Coal/Water at 10 ins Hg.
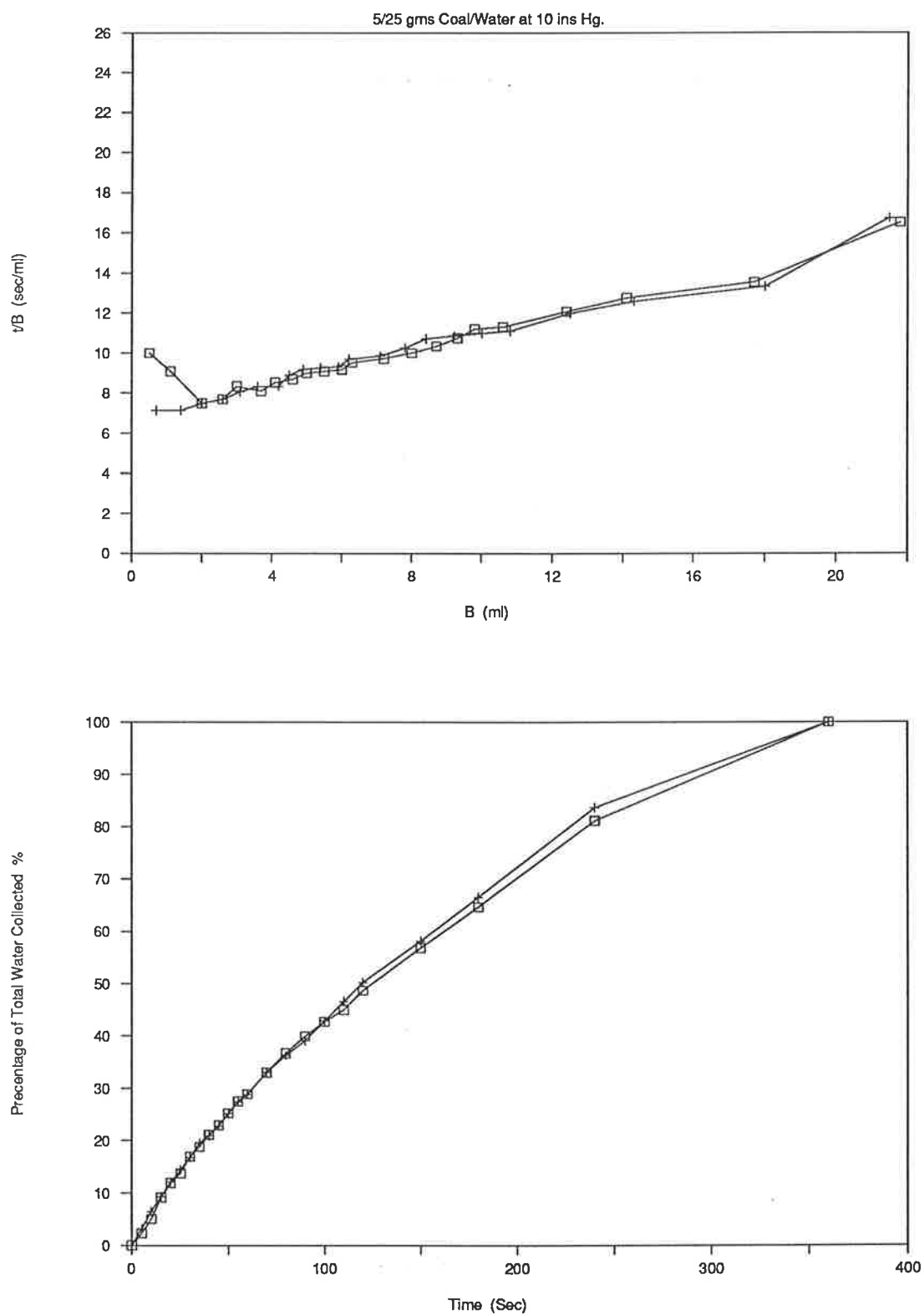
Figure B8

DEWATERING CHARACTERISTICS

5/25 gms Coal/Water at 10 ins Hg.
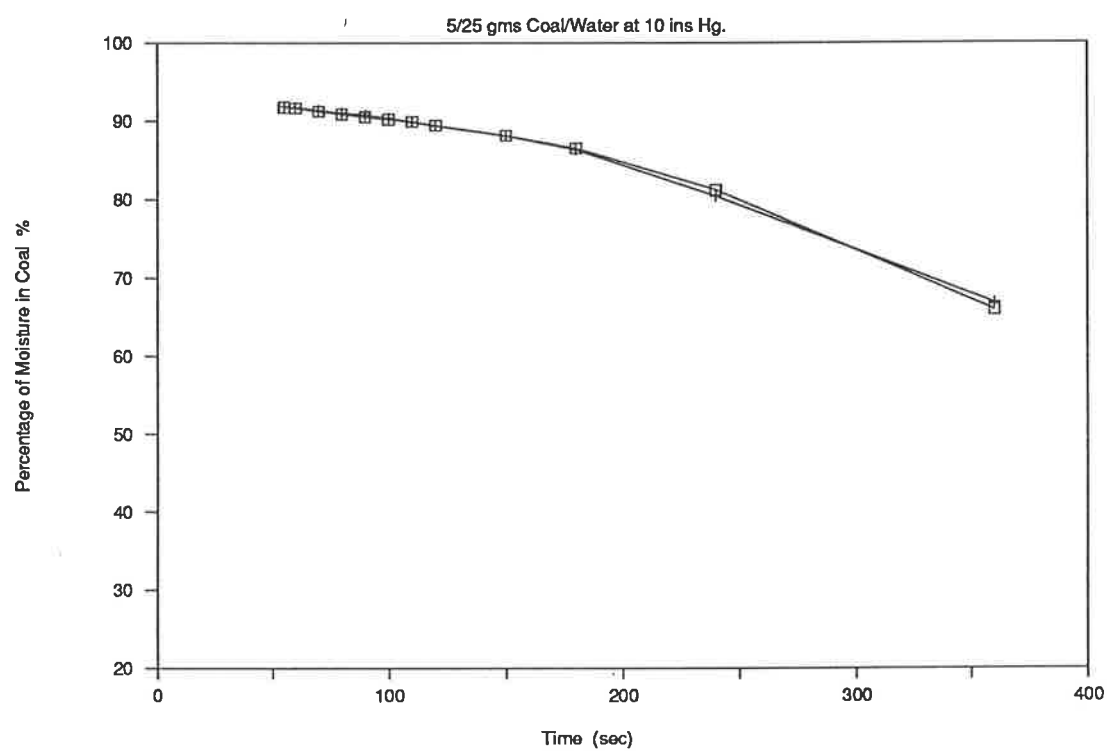
Figure B9

FILTRATION CHARACTERISTICS

5/5 gms Coal/Water at 10 ins Hg.
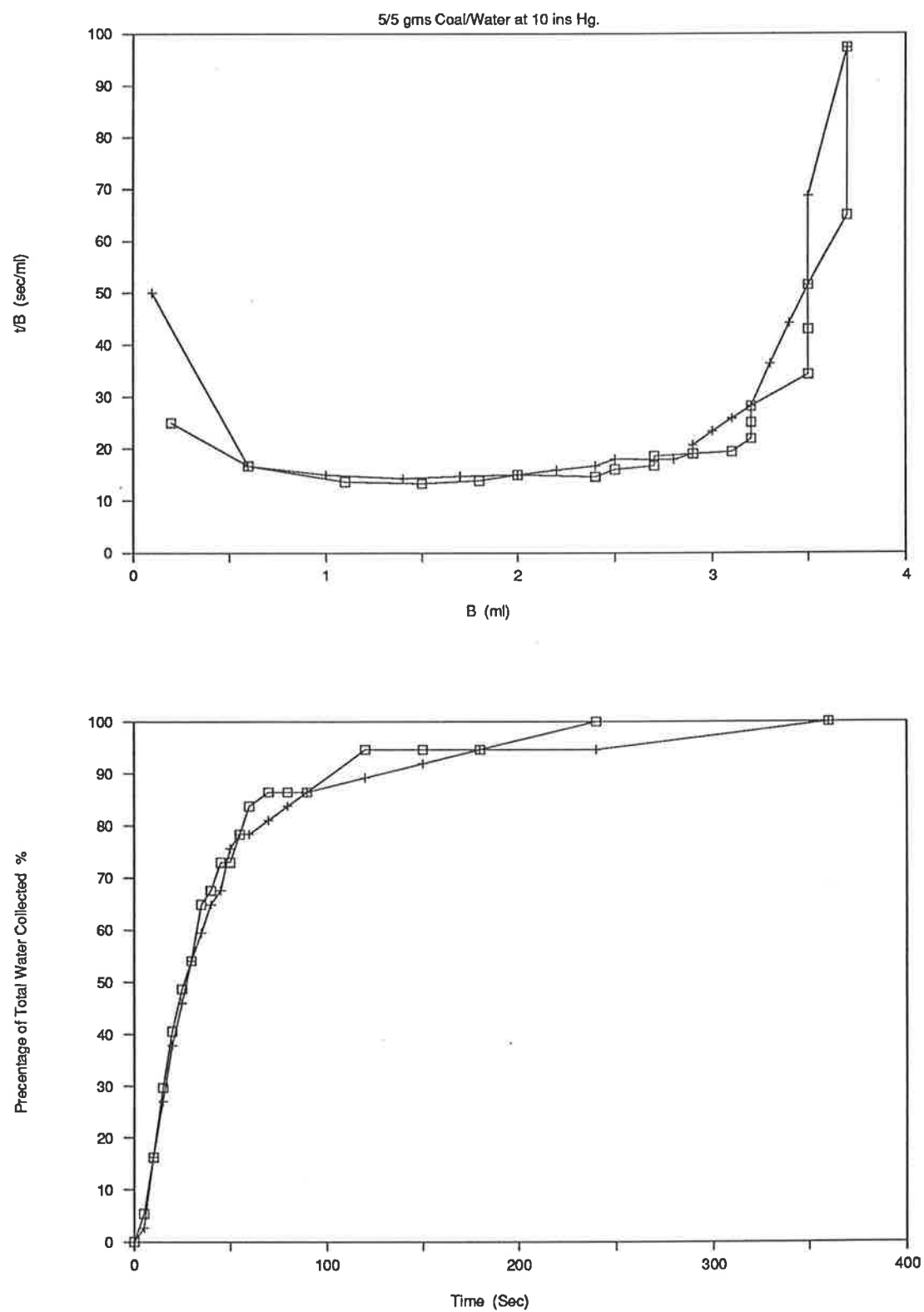
Figure B10

DEWATERING CHARACTERISTICS

5/5 gms Coal/Water at 10 ins Hg.
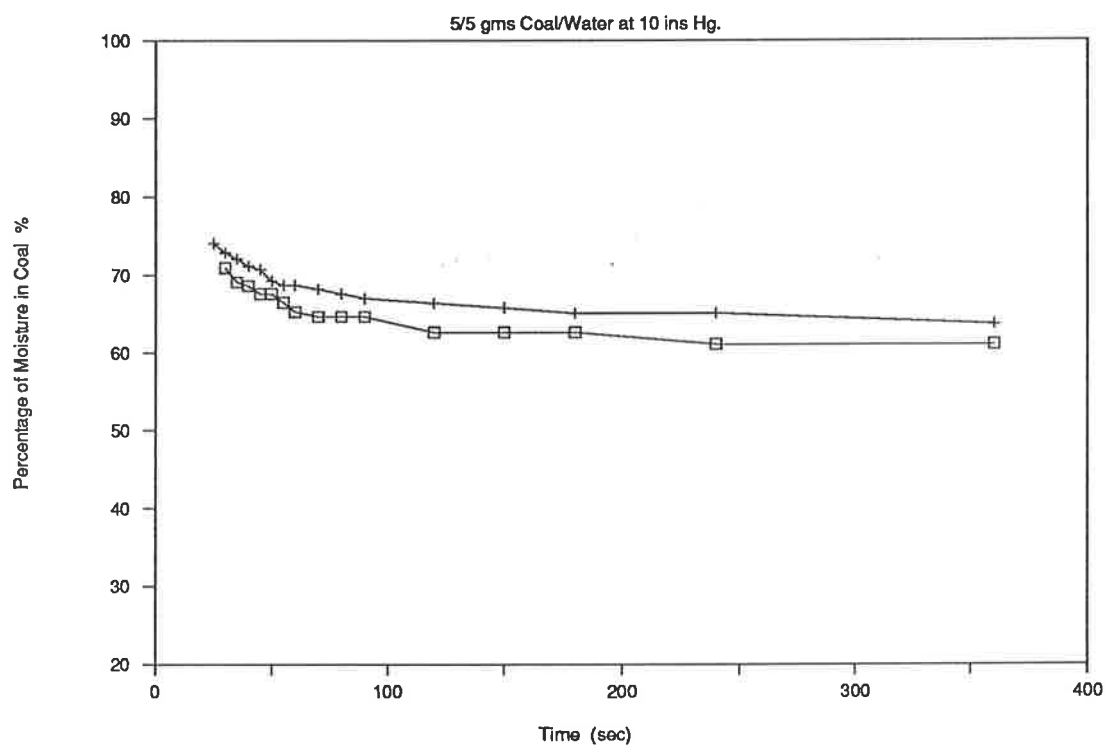
Figure B11

FILTRATION CHARACTERISTICS

Dewatered Coal: 20 mins at 325 deg C.

□   8/13 gms Coal/Water   +   9/17 gms Coal/Water
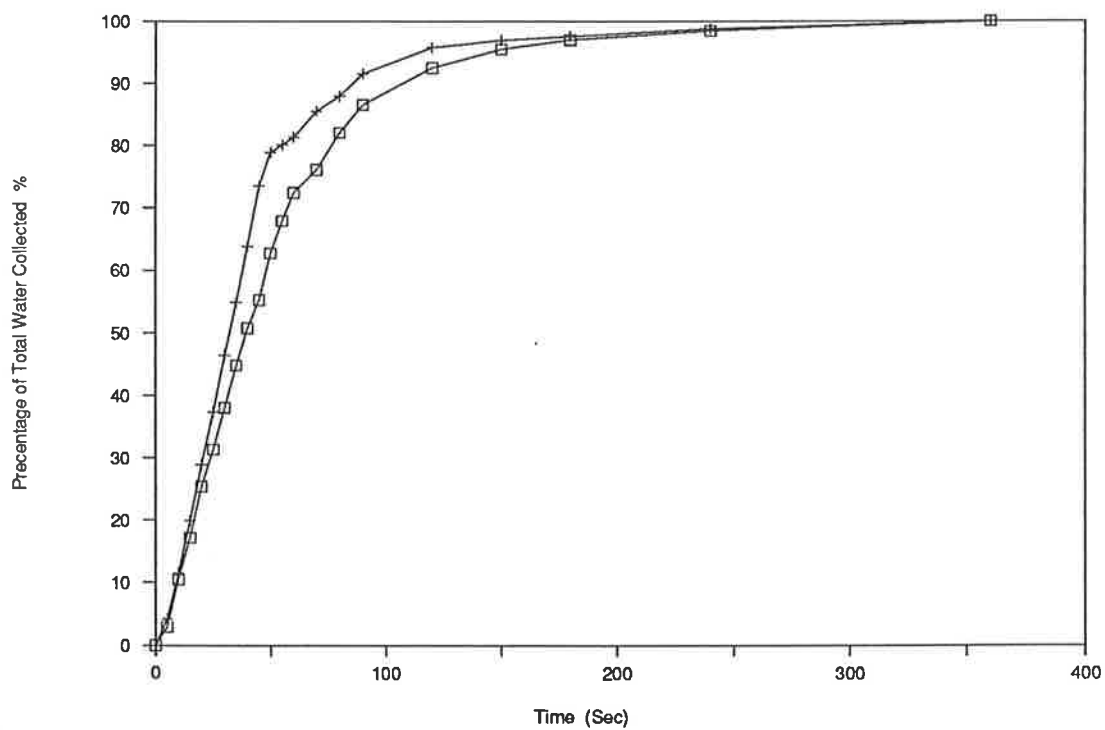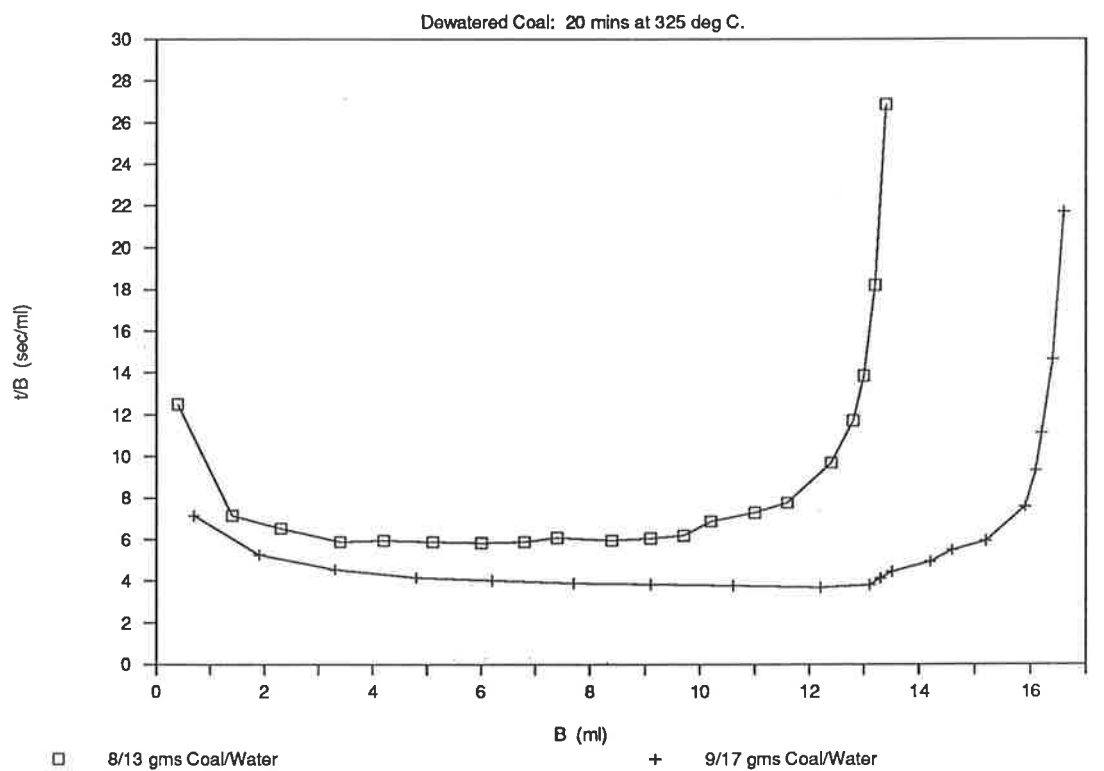
Figure B12

DEWATERING CHARACTERISTICS

Dewatered Coal: 20 mins at 325 degC.

□   8/13 gms Coal/Water   +   9/17 gms Coal/Water
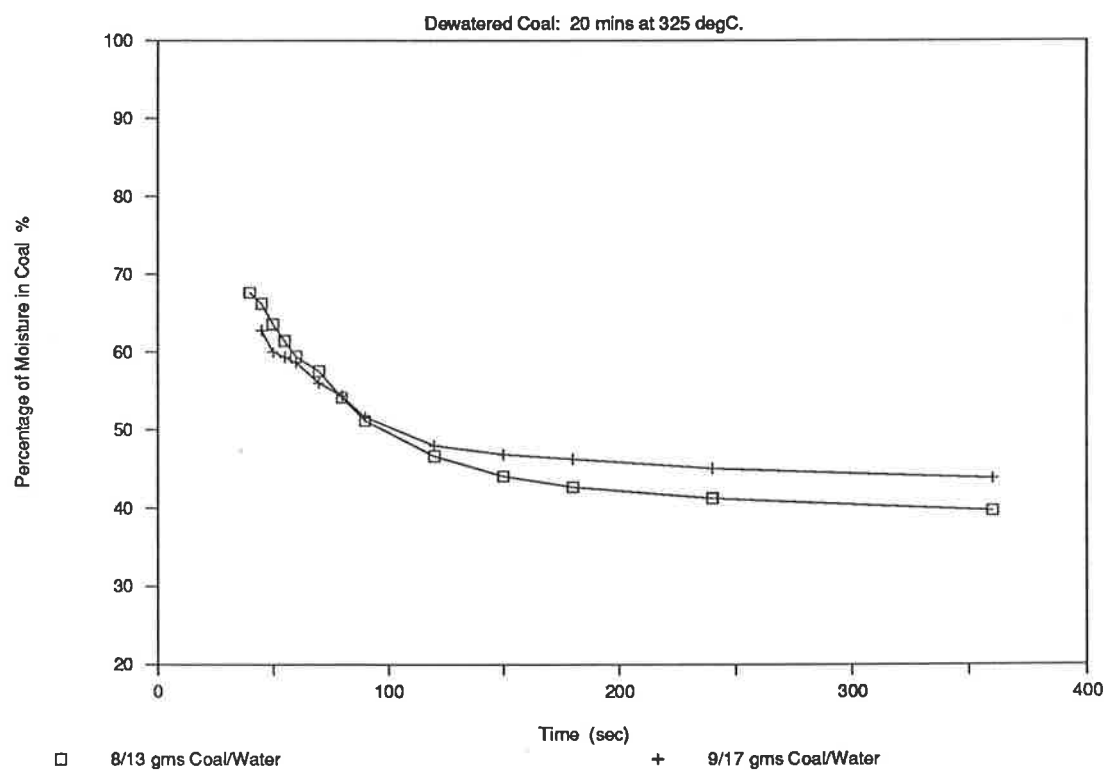
Figure B13

FILTRATION CHARACTERISTICS

Coal Recently Obtained from Drum.

10/20 gms Coal/Water at 10 in Hg.
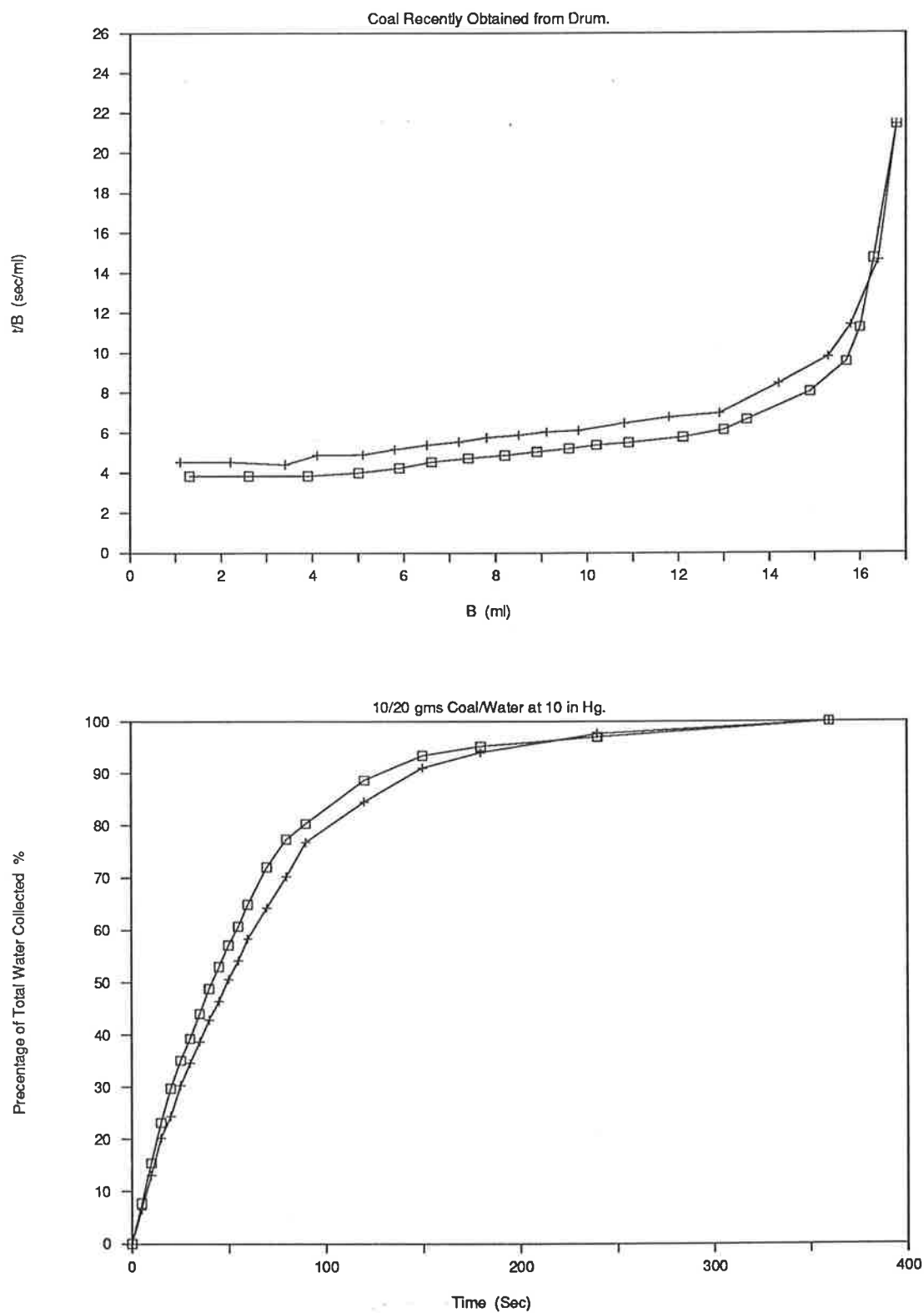
Figure B14

DEWATERING CHARACTERISTICS

Coal Recently Obtained from Drum.
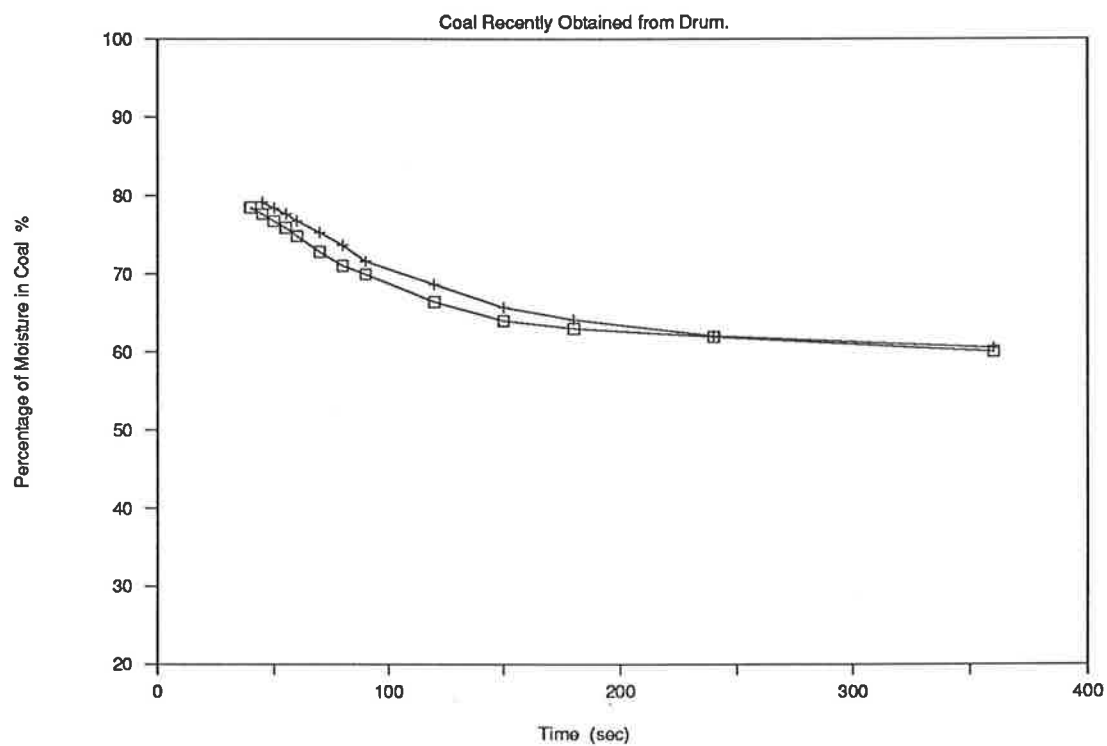
Figure B15

FILTRATION CHARACTERISTICS

Dewatered Coal, Fresh Feed Sample.

□ 9/17 gms Coal/Water   + 6/10 gms Coal/Water

Dewatered Coal: 20 mins at 325 deg C.
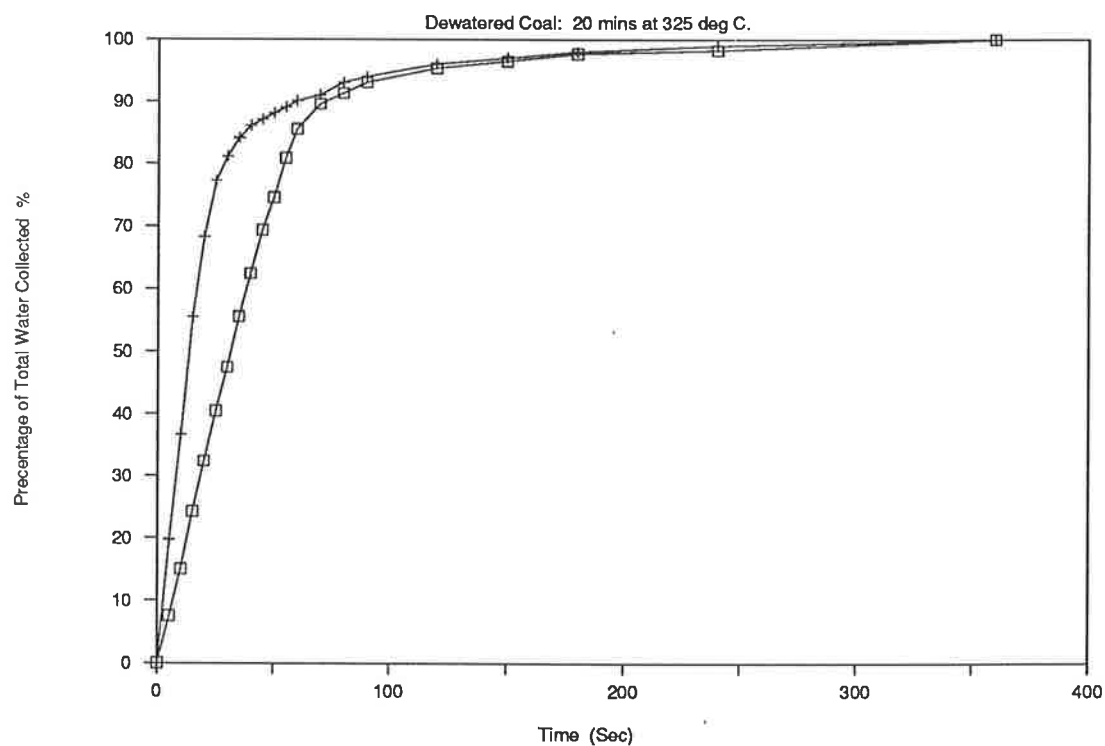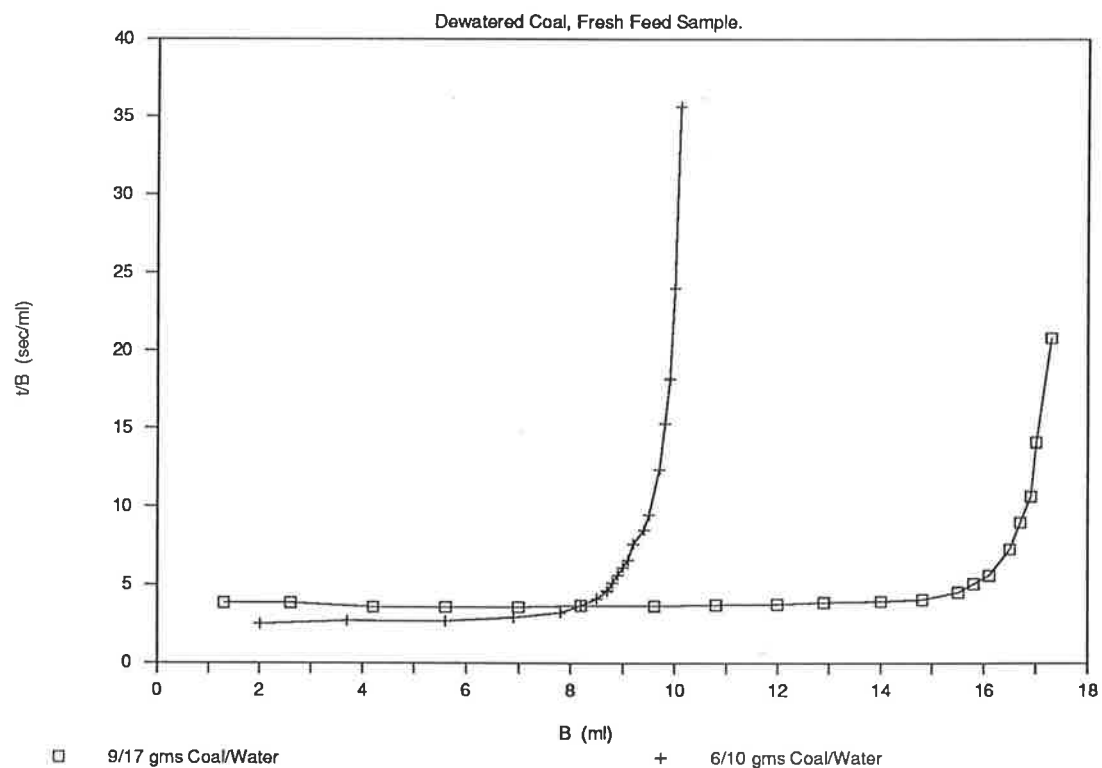
Figure B16

DEWATERING CHARACTERISTICS

Dewatered Coal, Fresh Feed Sample.

□ 9/17 gms Coal/Water   + 6/10 gms Coal/Water
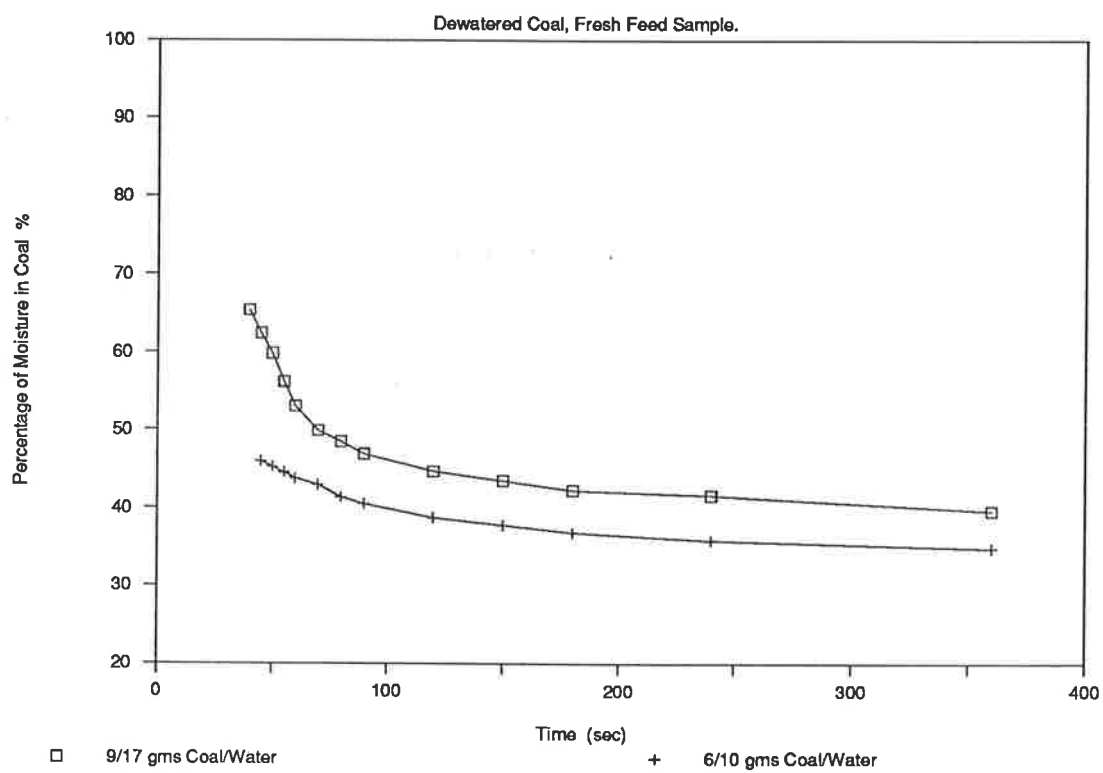
Figure B17

FILTRATION CHARACTERISTICS

10 gms Coal in 20 gms 1% Methanol.
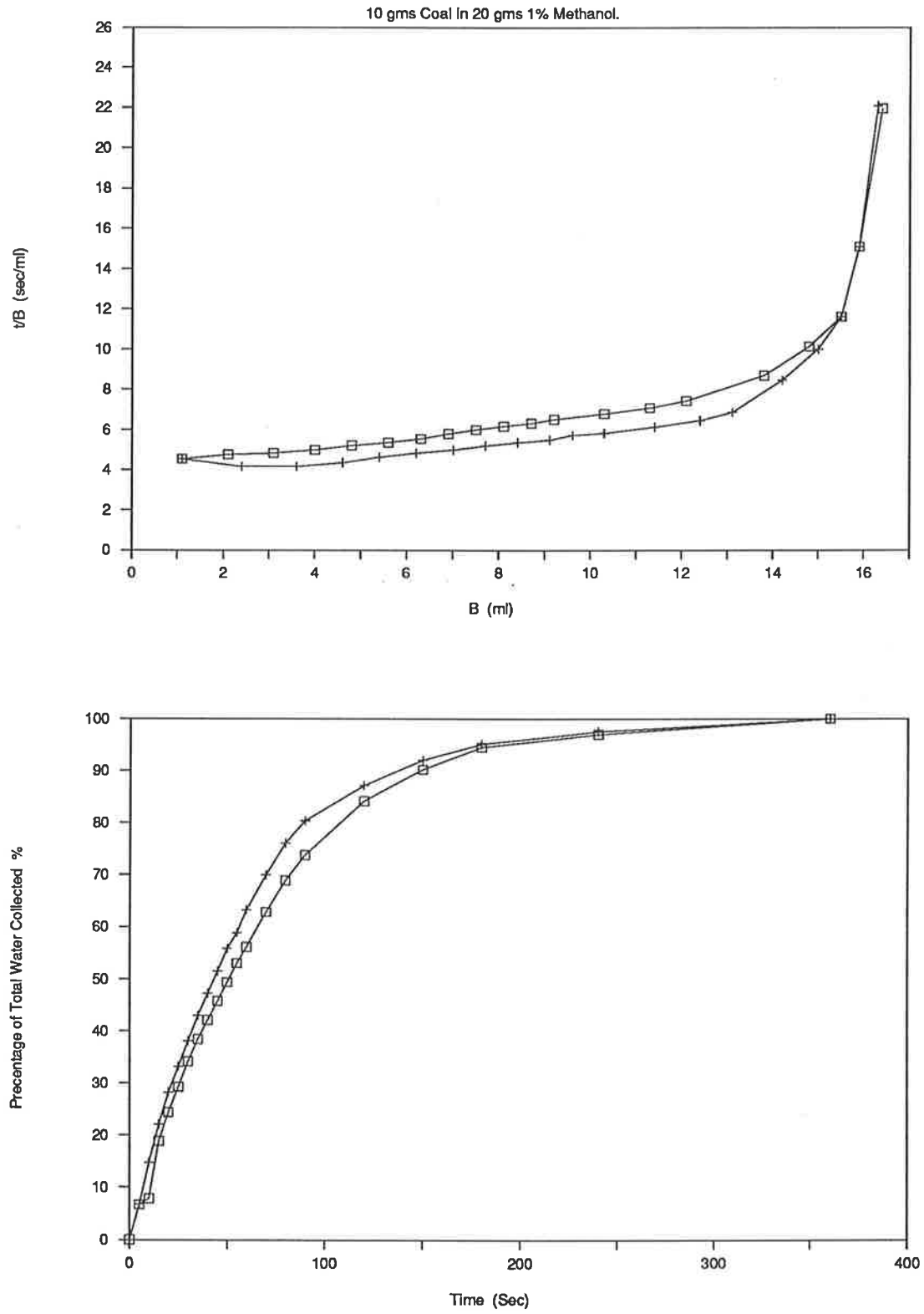
Figure B18

DEWATERING CHARACTERISTICS

10 gms Coal in 20 gms 1% Methanol.
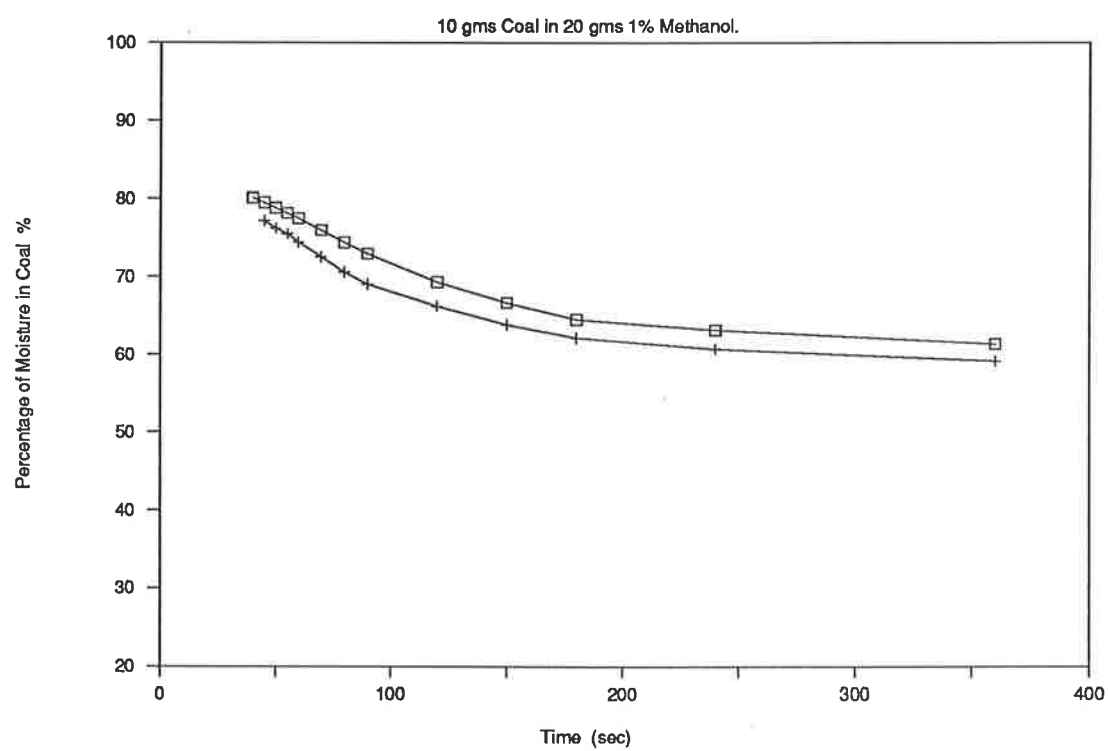
Figure B19

FILTRATION CHARACTERISTICS

Dewatered Coal, 1% Methanol.

□   9/17 gms Coal/Water   +   7/14 gms Coal/Water

Dewatered Coal: 20 mins at 325 deg C.
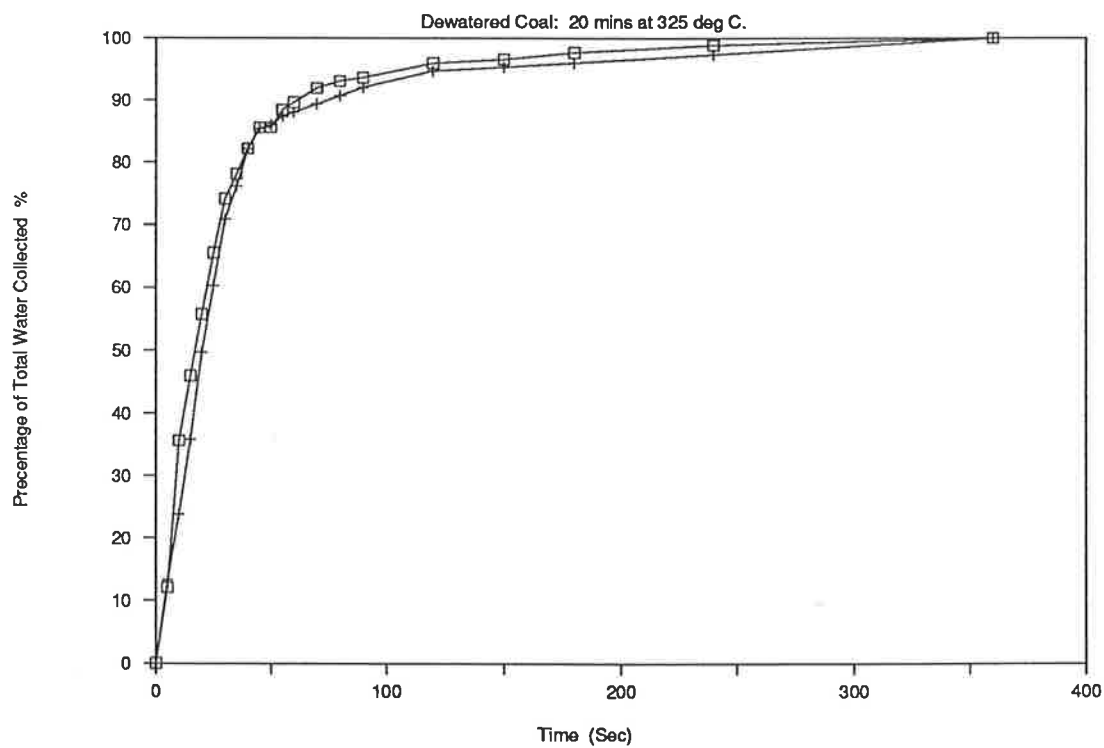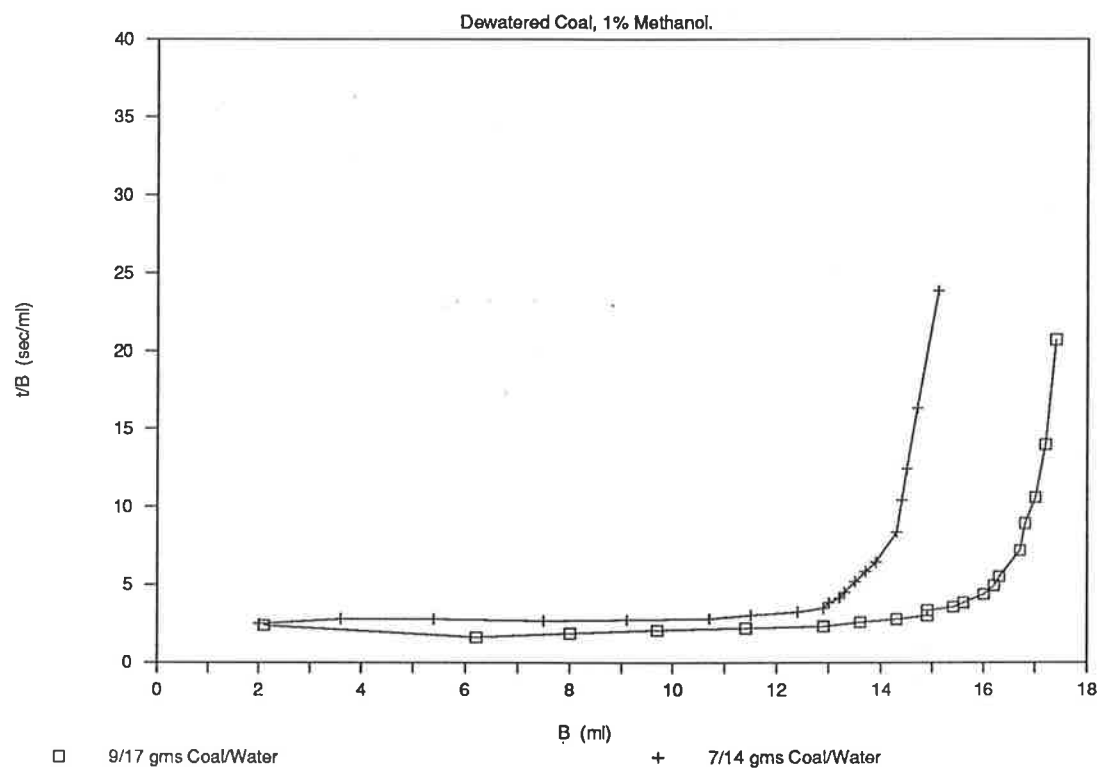
Figure B20

DEWATERING CHARACTERISTICS

Dewatered Coal, 1% Methanol.
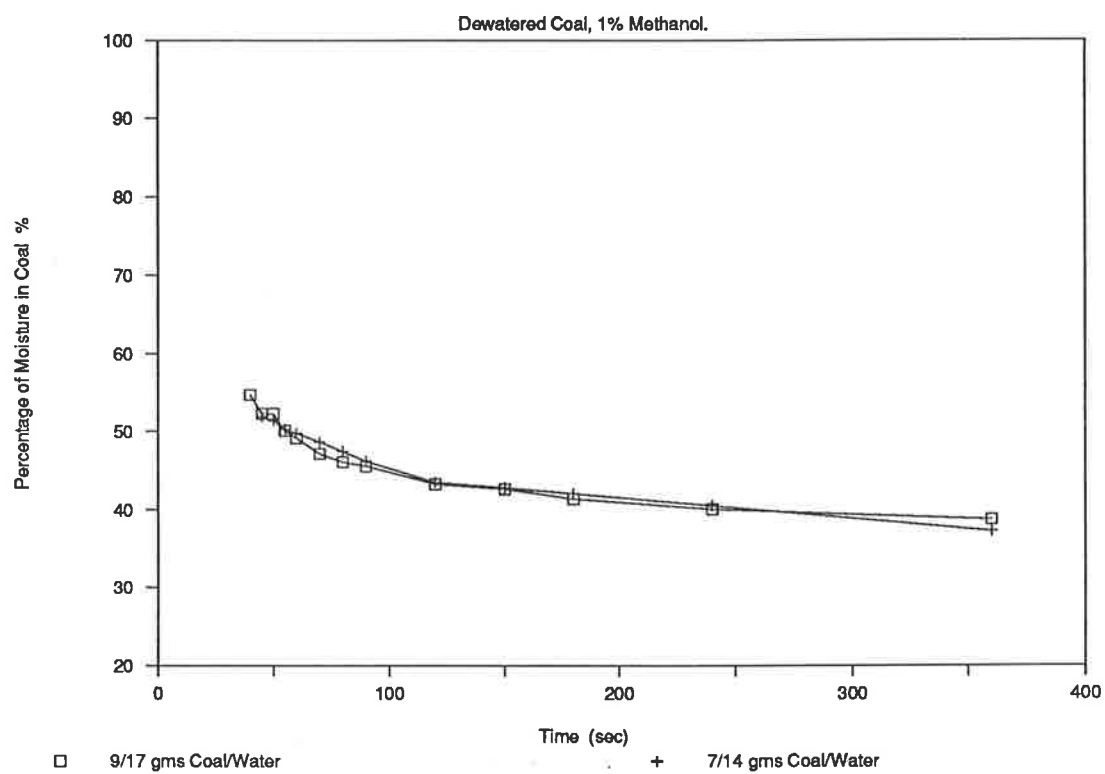
Figure B21

FILTRATION CHARACTERISTICS

10 gms Coal in 20 gms 10% Methanol.
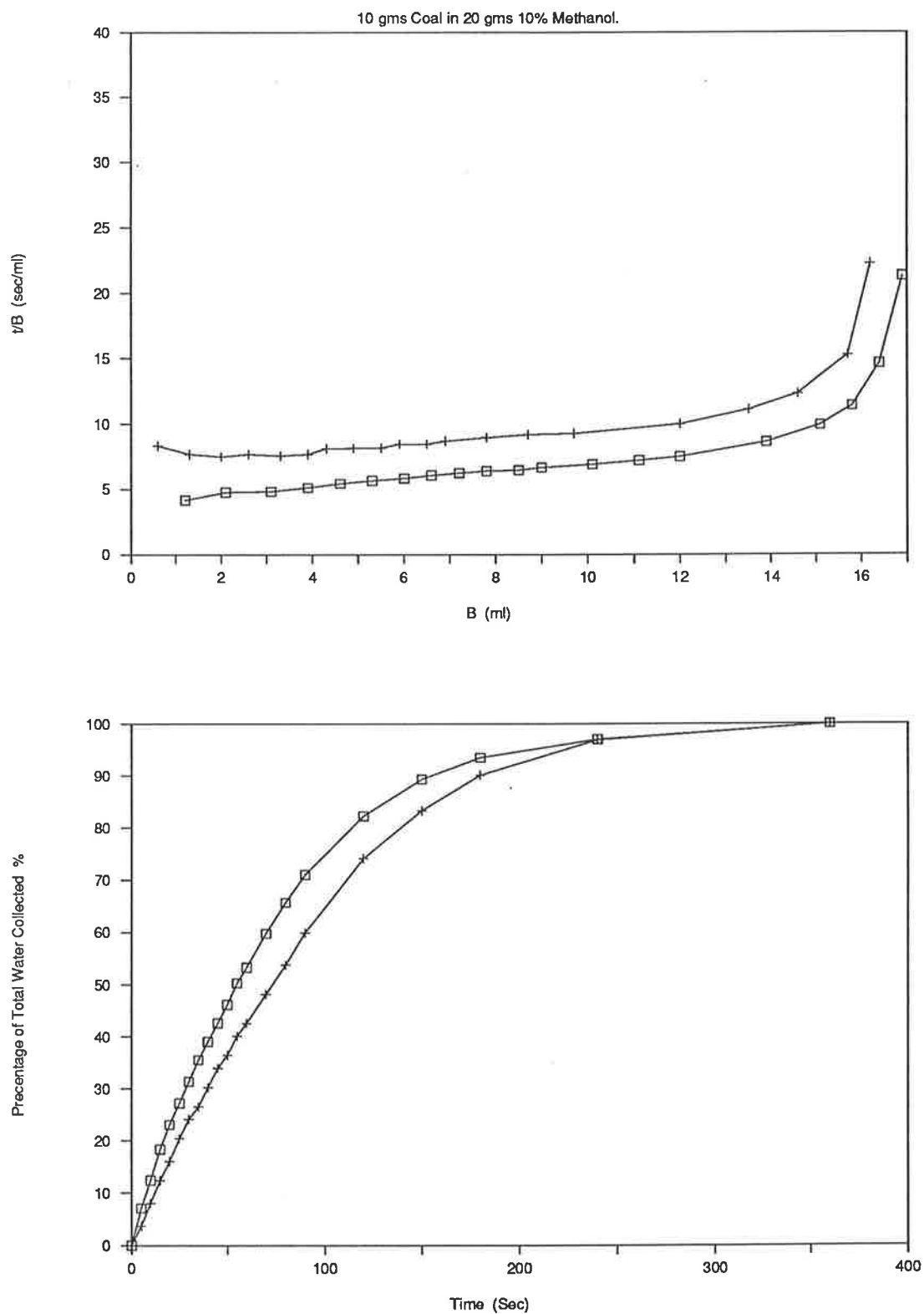
Figure B22

DEWATERING CHARACTERISTICS

10 gms Coal in 10% Methanol.
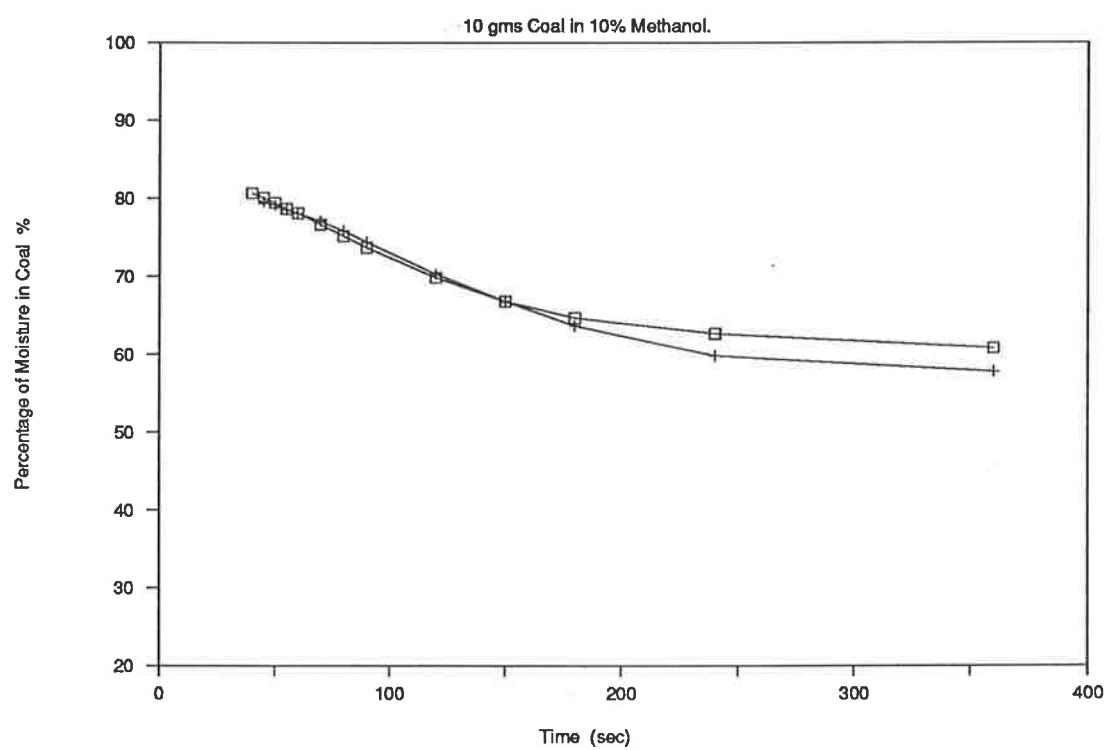
Figure B23

FILTRATION CHARACTERISTICS

Dewatered Coal, 10% Methanol.

□ 10/17gms Coal/Water + 8/16 gms Coal/Water

Dewatered Coal: 20 mins at 325 deg C.
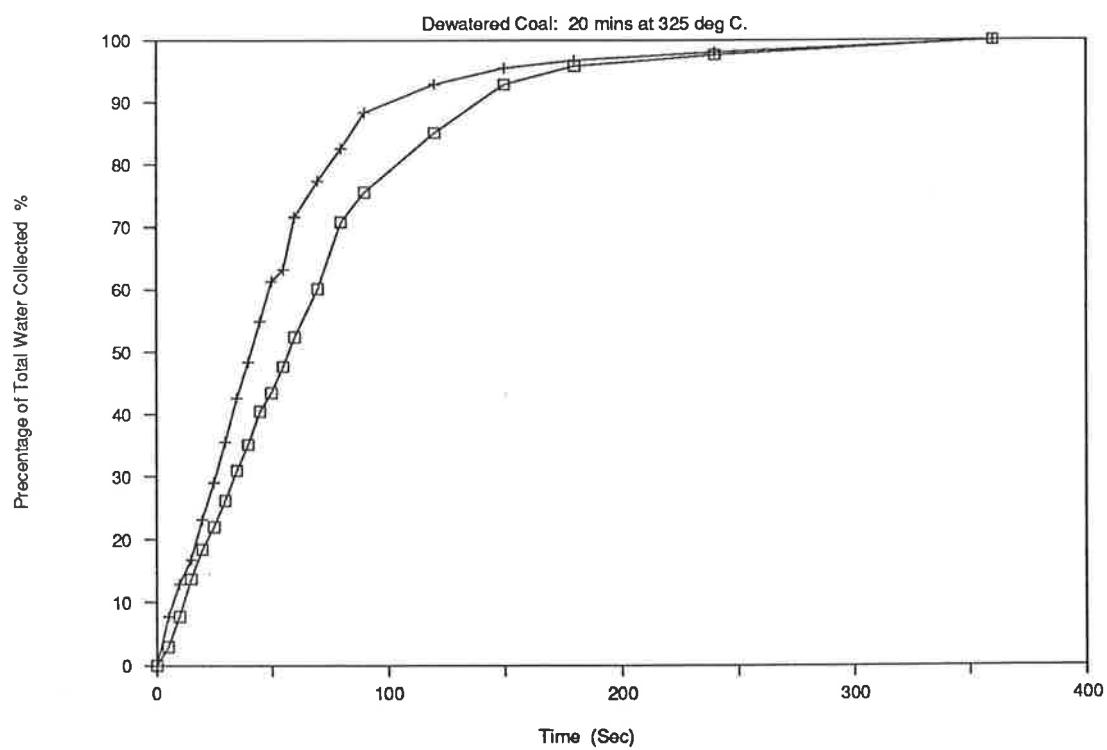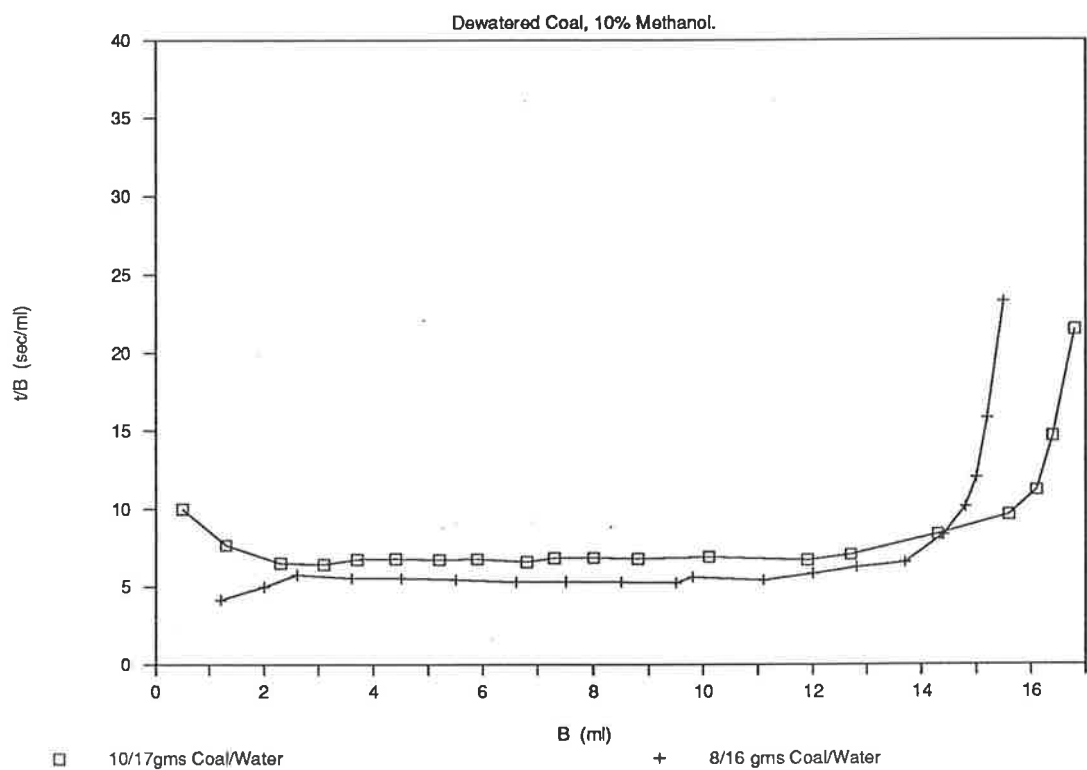
Figure B24

DEWATERING CHARACTERISTICS

Dewatered Coal, 10% Methanol.

□ 10/17gms Coal/Water   + 8/16 gms Coal/Water
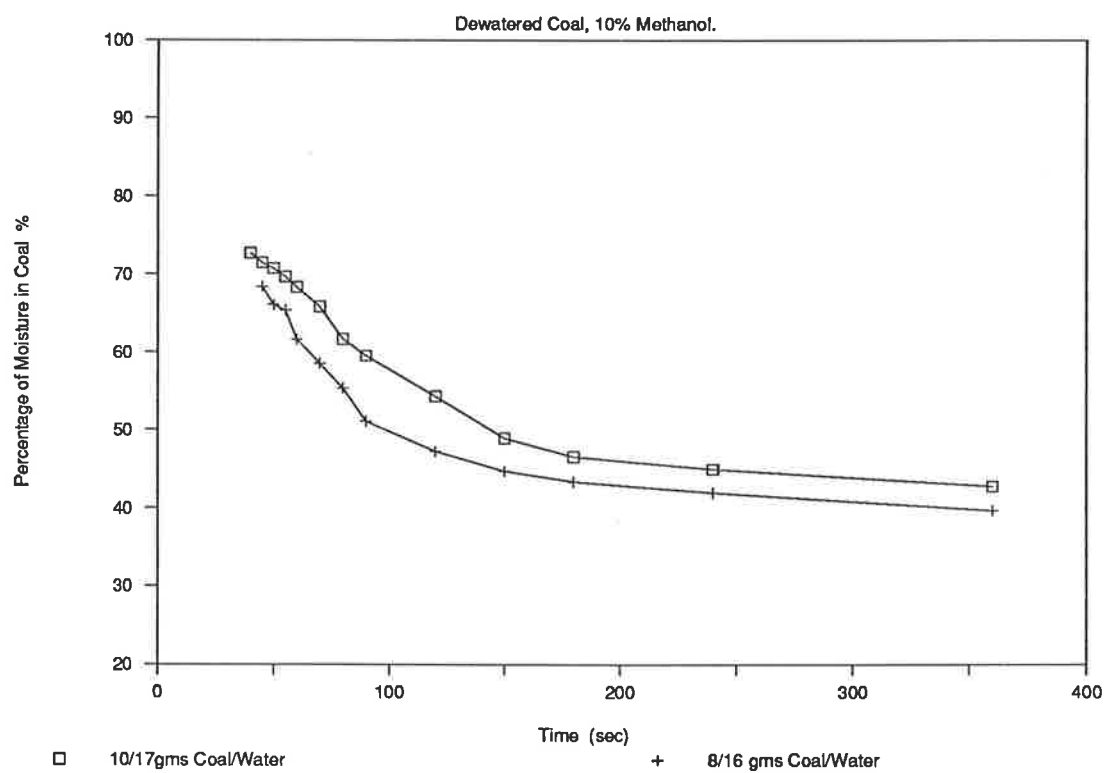
APPENDIX C

COMPUTER PROGRAMS

C1 Aqueous Leaching Diffusion Model

C2 Time-Temperature Equivalence Model

C3 Distributed-Activation-Energy Model

C1 PROGRAM USED TO CALCULATE THE KINETICS OF ION REMOVAL FROM BOWMANS COAL BY AQUEOUS LEACHING.

```
            PROGRAM LEACH
            DIMENSION Q10),DAT(20),TI(20),A(11),AD(11),CIN(20)
            REAL K,MOI
            CHARACTER ANS
    1       CONTINUE

    C       PROGRAM USED FOR KINETICS OF ION REMOVED FROM COAL BY
    C       AQUEOUS LEACHING USING CRANK'S MATHEMATICAL SOLUTION
    C       TO DIFFUSION IN A WELL STRIRRED SOLUTION IN LIMITED
    C       VOLUME

    C       TYPE IN THE PARAMETERS REQUIRED
            PRINT*, 'WHAT IS THE MAXIMUM DIAMETER OF THE COAL'
            PRINT*, 'PARTICLES? (mm)'
            READ(5,*) DIMAX

            PRINT*, 'WHAT IS THE MINIMUM DIAMETER OF THE COAL'
            PRINT*, 'PARTICLES? (mm)'
            READ(5,*) DIMIN

            PRINT*, 'WHAT IS THE DIFFUSION COEFFICIENT? (CM**2/SEC)'
            READ(5,*) DI

            PRINT*, 'PLEASE ENTER THE TEMPERATURE OF LEACHING. (deg C)'
            READ(5,*) TEMP

            PRINT*, 'PLEASE ENTER THE MASS OF WATER PER GM OF COAL'
            READ(5,*) VOL

            DIFF=DI*(273.+TEMP)/293.

    C       PRINT*, 'WHAT IS THE MOISTURE CONTENT OF COAL? (g/g )'
    C       READ(5,*) MOI
            MOI=0.5
```

```
PRINT*, 'WHAT IS THE VALUE OF THE DESORPTION CONSTANT'
READ(5,*) K


PRINT*, 'WHAT IS THE INITIAL CONCENTRATION IN COAL? (ppm)'
READ(5,*) CO
CEQM=CO/(VOL/MOI+K)

PRINT*, 'DO YOU WISH TO FIND THE CONCENTRATION OF AN'
PRINT*, 'ELEMENT AT A PARTICULAR TIME'
READ(5,11) ANS
IF (ANS.EQ.'Y'.OR.ANS.EQ.'y') GO TO 40


OPEN(UNIT=1,FILE='OPT.DAT',STATUS='OLD')
READ(1,*) I
DO 102 L=1,I
READ(1,*) DAT(L),TI(L)
102     CONTINUE

OPEN(UNIT=2,FILE='OUT.DAT',STATUS='OLD')
AX=0.0
WRITE(2,*) DAT(1), TI(1), AX,AX


PRINT*, 'HOW MANY SEGMENTS OF THE GRAPH ARE NEEDED TO'
PRINT*, 'SMOOTH THE RESULTS'
READ(5,*) M

ALP=VOL/(MOI*K)
D=(DIMAX-DIMIN)/10.

DO 15, MI=1,M
PRINT*, 'WHAT TIME INTERVAL DO YOU WANT'
READ(5,*) SEC
PRINT*, 'HOW MANY POINTS DO YOU WANT'
READ(5,*) IN

DO 200 J=1,IN
T=T+SEC

DO 60 L=1,11
```

```
        A(L)=(DIMIN+(FLOAT(L)-1.)*D)*.1/2.
        IF(A(L).EQ.0.0) A(L)=1.E-6
        QNI=3.0
        AD(L)=0.0

C       CALCULATE THE ION REMOVAL

        DO 50 N=1,6
        CALL PARAM(N,QNI,Q,ALP)
        ADD=6.0*ALP*(1.+ALP)*EXP(-1.*DIFF*(Q(N)**2)*T/
    +   (A(L)**2))/(9.0+9.0*ALP+(Q(N)*ALP)**2)
        AD(L)=ADD+AD(L)

50      CONTINUE
60      CONTINUE
        ACCUM=(AD(1)+AD(11)+4.*(AD(2)+AD(4)+AD(6)+AD(8)+
    +   AD(10))+2.*(AD(3)+AD(5)+AD(7)+AD(9)))/30.

        CONC=(1.0-ACCUM)*CEQM
        PRINT*, T,CONC
        IF (J.GT.I) THEN
        WRITE(2,*) DAT(1),TI(1),CONC,T
        ELSE
        WRITE(2,*) DAT(J),TI(J),CONC,T
        END IF

200     CONTINUE
15      CONTINUE
        GO TO 300

40      CONTINUE
        PRINT*, 'WHAT TIME DO YOU WANT?'
        READ(5,*) T


        DO 65 L=1,11

        A(L)=(DIMIN+(FLOAT(L)-1.)*D)*.1/2.
        IF(A(L).EQ.0.0) A(L)=1.E-6
        QNI=3.0
        AD(L)=0.0
```

```
C           CALCULATE THE REMOVAL OF IONS FOR ONLY ONE TIME INTERVAL
            DO 55 N=1,6
            CALL PARAM(N,QNI,Q,ALP)
            ADD=6.0*ALP*(1.+ALP)*EXP(-1.*DIFF*(Q(N)**2)*T/
     +      (A(L)**2))/(9.0+9.0*ALP+(Q(N)*ALP)**2)
            AD(L)=ADD+AD(L)

55          CONTINUE
65          CONTINUE
            ACCUM=(AD(1)+AD(11)+4.*(AD(2)+AD(4)+AD(6)+AD(8)+
     +      AD(10))+2.*(AD(3)+AD(5)+AD(7)+AD(9)))/30.

            CONC=(1.0-ACCUM)*CEQM
            PRINT*, T,CONC

300         CONTINUE
            PRINT*, 'DO YOU WISH TO RUN AGAIN?'
            READ (5,11) ANS
11          FORMAT (A)
            IF (ANS.EQ.'Y'.OR.ANS.EQ.'y') GO TO 1


            END



            SUBROUTINE PARAM(I,QNO,QN,ALPHA)
            DIMENSION QN(100)
C           CALCULATION OF THE NON-XERO ROOTS OF THE TRANSCENDEN-
C           TAL
            EQUATION
            X=3.

10          CONTINUE

            EQN=3.0*TAN(QNO)+ALPHA*(QNO**2)*TAN(QNO)-3.0*QNO

            DEQN=3.0/((COS(QNO))**2)+ALPHA*(QNO**2/((COS(QNO))**2)+2.0*
     +      QNO*TAN(QNO))-3.0
```

```
        IF (ABS(EQN/DEQN).GT.0.01) THEN
        IF (EQN/DEQN)5,5,15
5       QNO=QNO+0.001
        GO TO 25
15      QNO=QNO-0.001
        GO TO 25
        END IF
        QNO=QNO-EQN/DEQN
25      CONTINUE

        IF (ABS(EQN/DEQN).GT.1.0E-4) GO TO 10
        IF (QNO.LT.0.1) GO TO 20
        IF (I.EQ.1) GO TO 30

20      IF (QNO-QN(I-1).LT.0.1) THEN
        X=X+0.01
        QNO=QNO+X
        GO TO 10
        END IF

30      CONTINUE
        QN(I)=QNO

        END
```

C2 PROGRAM USED TO CALCULATE THE KINETICS OF DEVOLATILIZATION DURING HIGH-TEMPERATURE PRE-TREATMENT BY THE TIME TEMPERATURE EQUIVALENCE MODEL.

```
        PROGRAM KINETICS
        DIMENSION TIME(2),F(2),B(3)

C       THIS PROGRAM IS USED TO FIND THE KINETICS OF
C       DEVOLATILIZATON OF COAL USING THE PRINCIPLE
C       OF TIME-TEMPERATURE EQUIVALENCE.

C       INPUT THE INITIAL PARAMETERS

        DO 50 I=1,3
        WRITE(5,25) I
25      FORMAT(' WHAT IS THE CONSTANT',I2,/)
        READ(6,*) B(I)
50      CONTINUE
        WRITE(5,*)' WHAT IS THE REACTION TEMPERATURE?  '
        READ(6,*) TFINAL

        TINIT=15.0
        TIME(1)=0.0
        FADD=0.0
        CONST=10.0
        NUM=1

150     CONTINUE
        TIME(2)=TIME(1)+CONST

C       CALCULATE THE TEMPERATURE OF THE TUBE BOMBS AND
C       THEN PUT INTO KINETIC MODEL

        DO 200 I=1,2
        TEMP=273+TFINAL+(TINIT-TFINAL)*EXP((-2.38E-2+3.0E-5*TFINAL)
```

```fortran
     +        *(TIME(I)+CONST/2.0))
              F(I)=B(1)*(TIME(I)**B(2))*EXP(-B(3)/TEMP)
200           CONTINUE

              DELTF=F(2)-F(1)
              FADD=FADD+DELTF
              IF(TIME(2)/100.EQ.NUM) THEN
              OPEN(UNIT=12,FILE='MODOUT.DAT',STATUS='OLD')
              WRITE(12,*) TIME(2), FADD
              NUM=NUM+1
              ENDIF

              IF (TIME(2).EQ.3600.0) GOTO 15

              TIME(1)=TIME(2)
              GOTO 150

15            CONTINUE
              END
```

C3 PROGRAM USED TO CALCULATE THE DEVOLATILIZATION AND GASEOUS SPECIES REMOVAL DURING HIGH-TEMPERATURE PRE-TREATMENT BY USING DISTRIBUTED ACTIVATION KINETICS

```
        PROGRAM KINETICS

C       THIS PROGRAM CALCULATES THE KINETICS OF VOLATILE MATTER
C       REMOVAL BY USING ACTIVATION KINETICS

        IMPLICIT DOUBLE PRECISION (A-H,O-Z)
        REAL*8 KO
        DIMENSION ANS(200)

        COMMON/F1/ TINIT,TFINAL,KO
        COMMON/F2/ X1,X2,NVAL,EO,SIGMA
        EXTERNAL FUNC2

C       READ IN THE PARAMETERS TO EVALUATE THE DATA
        OPEN(UNIT=1,FILE='COMP.DAT',STATUS='OLD')
        READ(1,*) A,B,EO,SIGMA,TINIT,KO,TI,ITIME,NVAL
        X1=0.0
        X2=0.0
        WRITE(6,*) ' WHAT IS THE FINAL TEMPERATURE?'
        READ(5,*) TFINAL
        DO 100 I=1,ITIME
        X2=X2+TI

C       CALL THE SECOND INTEGRAL TO CALCULATE THE
C       GAUSSIAN DISTRIBUTION
        CALL CGQB(FUNC2,A,B,NVAL,SS1)
        ANS(I)=1.0-SS1

        WRITE(5,13) I,X2,ANS(I)

13      FORMAT(10X,' ITERATION No ',I4,/,1X,' TIME ',F7.0,5X,
     *          ' CONVERSION ',F7.6,/)
```

```
C       WRITE THE CALCULATED DATA TO AN OUTPUT FILE
        OPEN(UNIT=2,FILE='COMPOUT.DAT',STATUS='OLD')
        ANS(I)=ANS(I)
        WRITE(2,14) X2,ANS(I)
14      FORMAT(5X,F7.0,5X,F7.6)

100     CONTINUE
        END


        FUNCTION FUNC1(Y)
        IMPLICIT DOUBLE PRECISION (A-H,O-Z)
        REAL*8 KO
        COMMON/F21/ E,T
        COMMON/F1/ TINIT,TFINAL,KO
        R=0.008314

        T=273+TFINAL+(TINIT-TFINAL)*EXP((-2.38E-2+3.0E-5*TFINAL)
*        *Y)

        AVAL=E/(R*T)
        IF (AVAL.LT.120) THEN
        FUNC1=KO*DEXP(-AVAL)
        ELSE
        FUNC1=0.0
        ENDIF

        RETURN
        END


        FUNCTION FUNC2(X)
        IMPLICIT DOUBLE PRECISION (A-H,O-Z)

        COMMON/F2/ X1,X2,NVAL,EO,SIGMA
        COMMON/F21/ E,T
        EXTERNAL FUNC1
```

```
      PI=3.14519
      E=X


C     CALL THE FIRST INTEGRAL IN THE MODEL TO CALCULATE
C     THE ARRHENIUS RATE EXPRESSION

      CALL CGQA(FUNC1,X1,X2,NVAL,SS2)

      FEA=(SIGMA*SQRT(2*PI))
      FEB=((X-EO)**2)/(2*(SIGMA**2))
      IF (FEB.LT.120) THEN
      FE=(FEA**(-1.0))*DEXP(-FEB)
      ELSE
      FE=0.0
      ENDIF

      IF(SS2.LT.60) THEN
      FUNC2=DEXP(-SS2)*FE
      ELSE
      FUNC2=0.0
      ENDIF

      RETURN
      END



C     FIRST INTEGRAL IN THE KINETIC MODEL

      SUBROUTINE CGQA(CF,XL,XU,N,CVAL)
      IMPLICIT DOUBLE PRECISION (A-H,O-Z)
C        PERFORMS INTEGRATION OF A FUNCTION OF A SINGLE VARIABLE
C        BY GAUSSIAN QUADRATURE.
C
C        N = ORDER OF GUASSIAN QUADRATURE APPROXIMATION. VALUE
C     MAY BE ON
C           (1,2,4,8,10,12,16,32).  IF N=1, CGQA PERFORMS A ONE-POINT
C           RECTANGULAR RULE INTEGRATION.
C        CF = EXTERNALLY SUPPLIED FUNCTION....MUST BE FUNCTION OF
C     ONE
C           VARIABLE FOR CQG1.
```

```
C          XL = LOWER BOUND OF VARIABLE
C          XU = UPPER BOUND OF VARIABLE
C          CVAL = RESULTING VALUE OF THE INTEGRATION
C
C          NOTE:  CF MUST BE LISTED IN AN EXTERNAL STATEMENT IN THE
                  CALLING ROUTINE

           EXTERNAL CF

           DIMENSION Q1(52),Q2(24),Q3(32),NQ(8),NS(8),QG(108)
     $     EQUIVALENCE (Q1(1),QG(1)),(Q2(1),QG(53)),(Q3(1),QG(77))
     $     DATA Q1
     $           /.288675134594812882E0,0.5E0,.43056815579702629E0,
     $     .17392742256872693E0,.16999052179242813E0,.32607257743127307E0,
     $     0.48014492824876812E0,.50614268145188130E-1,.39833323870681337E0,
     $     .11119051722668724E0,.26276620495816449E0,.15685332293894364E0,
     $     .9171732124782490E-1,.18134189168918099E0,.48695326425858586E0,
     $     .3333567215434407E-1,.43253168334449225E0,.7472567457752903E-1,
     $     .3397047841496122E0,.10954318125799102E0,.21669769706462360E0,
     $     .13463335965499818E0,.74437169490815605E-1,.14776211235737644E0,
     $     0.49078031712335963E0,.23587668193255914E-1,.45205862818523743E0,
     $     .53469662997659215E-1,.38495133709715234E0,.80039164427167311E-1,
     $     .29365897714330872E0,.10158371336153296E0,.18391574949909010E0,
     $     .11674626826917740E0,.62616704255734458E-1,.12457352290670139E0,
     $     .49470046749582497E0,.13576229705877047E-1,.47228751153661629E0,
     $     .31126761969323946E-1,.43281560119391587E0,.47579255841246392E-1,
     $     .37770220417750152E0,.62314485627766936E-1,.30893812220132187E0,
     $     .74797994408288837E-1,.22900838882861369E0,.8457825969750127E-1,
     $     .14080177538962946E0,.9130170752246179E-1,.47506254918818720E-1,
     $     .9472530522753425E-1 /
     *     DATA Q2
     *           / 0.49759360999851068E+0 ,0.61706148999935998E-2 ,
     *           0.48736427798565475E+0  ,  0.14265694314466832E-1 ,
     *           0.46913727600136638E+0  ,  0.22138719408709903E-1 ,
     *           0.44320776350220052E+0  ,  0.29649292457718890E-1 ,
     *           0.41000099298695146E+0  ,  0.36673240705540153E-1 ,
     *           0.37006209578927718E+0  ,  0.43095080765976638E-1 ,
     *           0.32404682596848778E+0  ,  0.48809326052056944E-1 ,
     *           0.27271073569441977E+0  ,  0.53722135057982817E-1 ,
     *           0.21689675381302257E+0  ,  0.57752834026862801E-1 ,
```

```
*          0.15752133984808169E+0  ,   0.60835236463901696E-1 ,
           0.95559433736808150E-1  ,   0.62918728173414148E-1 ,
$          0.32028446431302813E-1  ,   0.63969097673376078E-1 /
*      DATA Q3
*          /0.49863193092474078E+0 ,  0.35093050047350483E-2 ,
*          0.49280575577263417E+0  ,   0.81371973654528350E-2 ,
*          0.48238112779375322E+0  ,   0.126960326546 31030E-1 ,
*          0.46745303796886984E+0  ,   0.171369314565 10717E-1 ,
*          0.44816057788302606E+0  ,   0.21417949011113340E-1 ,
*          0.42468380686628499E+0  ,   0.25499029631188088E-1 ,
*          0.39724189798397120E+0  ,   0.29342046739267774E-1 ,
*          0.36609105937014484E+0  ,   0.32911111388180923E-1 ,
*          0.33152213346510760E+0  ,   0.36172897054424253E-1 ,
*          0.29385787862038116E+0  ,   0.39096947893535153E-1 ,
*          0.25344995446611470E+0  ,   0.41655962113473378E-1 ,
*          0.21067563806531767E+0  ,   0.43826046502201906E-1 ,
*          0.16593430114106382E+0  ,   0.45586939347881942E-1 ,
*          0.11964368112606854E+0  ,   0.46922199540402283E-1 ,
$          0.72235980791398250E-1  ,   0.478193600 39637430E-1 ,
$          0.24153832843869158E-1  ,   0.48270044257363900E-1 /
          ,NQ/2,4,8,10,12,16,24,32/,
          NS/1,3,7,15,25,37,53,77/
          IF(N .EQ. 1) GO TO 200
300       DO 300 L=1,8
9001      IF(N.EQ.NQ(L)) GO TO 301
905       CONTINUE
          WRITE(5,905) N
200       FORMAT('0 CALLING  PARAMETER  =',I5,'  INTEGRATION  NOT  POSSI-
          BLE'//)
          RETURN
301       AX=0.5*(XU+XL)
          CVAL=CF(AX)*(XU-XL)
          RETURN
          CONTINUE
          NP=NS(L)
          NE=NP+N-1
          AX=0.5*(XU+XL)
          BX=XU-XL
          CVAL=0.
350       DO 350 J=NP,NE,2
```

```
      DX=QG(J)*BX
      CVAL=CVAL+QG(J+1)*(CF(AX+DX)+CF(AX-DX))
      CONTINUE
      CVAL=CVAL*BX
      RETURN
      END
```

C   SECOND INTEGRAL IN KINETIC MODEL

```
      SUBROUTINE CGQB(CF,XL,XU,N,CVAL)
      IMPLICIT DOUBLE PRECISION (A-H,O-Z)
```
C   PERFORMS INTEGRATION OF A FUNCTION OF A SINGLE VARIABLE
C   BY GAUSSIAN QUADRATURE.
C
C   N = ORDER OF GUASSIAN QUADRATURE APPROXIMATION. VALUE
C   MAY BE ON
C   (1,2,4,8,10,12,16,32). IF N=1, CGQA PERFORMS A ONE-POINT
C   RECTANGULAR RULE INTEGRATION.
C   CF = EXTERNALLY SUPPLIED FUNCTION....MUST BE FUNCTION OF
C   ONE
C   VARIABLE FOR CQG1.
C   XL = LOWER BOUND OF VARIABLE
C   XU = UPPER BOUND OF VARIABLE
C   CVAL = RESULTING VALUE OF THE INTEGRATION
C
C   NOTE: CF MUST BE LISTED IN AN EXTERNAL STATEMENT IN THE
C   CALLING ROUTINE

      EXTERNAL CF

      DIMENSION Q1(52),Q2(24),Q3(32),NQ(8),NS(8),QG(108)
     $ EQUIVALENCE (Q1(1),QG(1)),(Q2(1),QG(53)),(Q3(1),QG(77))
     $ DATA Q1
     $ /.288675134594812882E0,0.5E0,.43056815579702629E0,
     $ .17392742256872693E0,.16999052179242813E0,.326072577743127307E0,
     $ 0.480144928248768l2E0,.50614268145188130E-1,.39833323870681337E0,
     $ .11119051722668724E0,.26276620495816449E0,.15685332293894364E0,
     $ .9171732124782490E-1,.18134189168918099E0,.48695326425858586E0,
```

$ .3333567215434407E-1,.43253168334449225E0,.7472567457529O3E-1,

$ .3397047841496122E0,.10954318125799102E0,.2166976970646236E0,

$ .13463335965499818E0,.74437169490815605E-1,.14776211235737644E0,

$ 0.49078031712335963E0,.23587668193255914E-1,.45205862818523743E0,

$ .53469662997659215E-1,.38495133709715234E0,.80039164271673 11E-1,

$ .29365897714330872E0,.10158371336153296E0,.18391574949909010E0,

$ .11674626826917740E0,.62616704255734458E-1,.12457352290670139E0,

$ .49470046749582497E0,.13576229705877047E-1,.47228751153661629E0,

$ .31126761969323946E-1,.43281560119391587E0,.47579255841246392E-1,

$ .37770220417750152E0,.62314485627766936E-1,.30893812220132187E0,

$ .74797994408288 37E-1,.22900838882861369E0,.84578259697501 27E-1,

    .14080177538962946E0,.91301707522461 79E-1,.47506254918818720E-1,

$ .9472530522753425E-1 /

* DATA Q2

*         / 0.49759360999851068E+0  ,0.61706148999935998E-2 ,

*         0.48736427798565475E+0  ,  0.14265694314466832E-1 ,

*         0.46913727600136638E+0  ,  0.22138719408709903E-1 ,

*         0.44320776350220052E+0  ,  0.29649292457718890E-1 ,

*         0.41000099298695146E+0  ,  0.36673240705540153E-1 ,

*         0.37006209578927718E+0  ,  0.43095080765976638E-1 ,

*         0.32404682596848778E+0  ,  0.48809326052056944E-1 ,

*         0.27271073569441977E+0  ,  0.53722135057982817E-1 ,

*         0.21689675381302257E+0  ,  0.57752834026862801E-1 ,

*         0.15752133984808169E+0  ,  0.60835236463901696E-1 ,

          0.95559433736808150E-1 ,  0.62918728173414148E-1 ,

$         0.32028446431302813E-1 ,  0.63969097673376078E-1 /

* DATA Q3

*         /0.49863193092474078E+0 ,  0.35093050047350483E-2 ,

*         0.49280575577263417E+0 ,  0.81371973654528350E-2 ,

*         0.48238112779375322E+0 ,  0.12696032654631030E-1 ,

*         0.46745303796886984E+0 ,  0.17136931456510717E-1 ,

*         0.44816057788302606E+0 ,  0.21417949011113340E-1 ,

*         0.42468380686628499E+0 ,  0.25499029631188088E-1 ,

*         0.39724189798397120E+0 ,  0.29342046739267774E-1 ,

*         0.36609105937014484E+0 ,  0.32911111388180923E-1 ,

*         0.33152213346510760E+0 ,  0.36172897054424253E-1 ,

*         0.29385787862038116E+0 ,  0.39096947893535153E-1 ,

*         0.25344995446611470E+0 ,  0.41655962113473378E-1 ,

*         0.21067563806531767E+0 ,  0.43826046502201906E-1 ,

*         0.16593430114106382E+0 ,  0.45586939347881942E-1 ,

```
*           0.11964368112606854E+0  ,  0.46922199540402283E-1 ,
$           0.72235980791398250E-1  ,  0.47819360039637430E-1 ,
$           0.24153832843869158E-1  ,  0.48270044257363900E-1 /
          ,NQ/2,4,8,10,12,16,24,32/,
           NS/1,3,7,15,25,37,53,77/
           IF(N .EQ. 1) GO TO 200
300        DO 300 L=1,8
9001       IF(N.EQ.NQ(L)) GO TO 301
905        CONTINUE
           WRITE(5,905) N
200        FORMAT('0 CALLING PARAMETER =',I5,' INTEGRATION NOT POSSI-
           BLE'//)
           RETURN
301        AX=0.5*(XU+XL)
           CVAL=CF(AX)*(XU-XL)
           RETURN
           CONTINUE
           NP=NS(L)
           NE=NP+N-1
           AX=0.5*(XU+XL)
           BX=XU-XL
           CVAL=0.
350        DO 350 J=NP,NE,2
           DX=QG(J)*BX
           CVAL=CVAL+QG(J+1)*(CF(AX+DX)+CF(AX-DX))
           CONTINUE
           CVAL=CVAL*BX
           RETURN
           END
```